

PERFORMANCE OF SHEAR STUD CLUSTERS
FOR PRECAST CONCRETE BRIDGE DECK PANELS

by

KENT EVAN LAROSE

Dipl. Eng., Saskatchewan Institute of Applied Science and Technology, 1995
B. Eng., Lakehead University, 1999

A THESIS SUBMITTED IN PARTIAL FULFILLMENT OF
THE REQUIREMENTS FOR THE DEGREE OF

MASTER OF APPLIED SCIENCE

in

THE FACULTY OF GRADUATE STUDIES

THE UNIVERSITY OF BRITISH COLUMBIA

December 2006

© Kent Evan LaRose, 2006

ABSTRACT

The current edition of the Canadian Highway Bridge Design Code (CHBDC), CAN/CSA-S6-00 provides limited guidance for the design of composite bridges with precast concrete deck panels and steel girders. The shear connection is critical in determining the overall performance of the composite superstructure and is commonly achieved with a grout breakout in a precast concrete deck panel, which accepts a cluster of tightly spaced steel shear studs. No specific equations are found in the CHBDC for the design of shear studs used in this system. Furthermore, the current longitudinal spacing limitation of 600 mm for shear studs in the CHBDC is not conducive to the construction of precast concrete decks where an increased spacing of the stud cluster is desirable.

An experimental testing regime was completed using push-test specimens constructed with precast concrete panels connected to steel flanges with steel studs within a circular grout pocket. Specimens were tested to failure to determine the ultimate capacity of a stud cluster and to investigate the reduction in ultimate strength after exposure to a number of loading cycles.

A 36 m simple span composite superstructure was designed to the CHBDC. A parametric study was conducted on the spacing of stud clusters to investigate the serviceability limit state of the composite superstructure using data captured from the push test specimens.

Experiments show that clustered shear studs embedded in high strength grout for construction using precast deck panels meet CHBDC strength requirements and that exceeding the code maximum stud spacing of 600 mm by a factor of two will not result in excessive displacements.

TABLE OF CONTENTS

ABSTRACT.....	ii
TABLE OF CONTENTS.....	iii
LIST OF TABLES.....	vi
LIST OF FIGURES	vii
ACKNOWLEDGMENTS	ix
1.0 Introduction.....	1
1.1 General.....	1
1.2 Definition of Terms.....	1
1.3 Project Background and Research Objectives	2
1.4 Relevance to Current Practice.....	3
1.5 Typical Construction Procedures.....	4
1.6 Thesis Organization	5
2.0 Literature Review.....	7
2.1 General.....	7
2.2 Historical Perspective	7
2.3 Canadian Highway Bridge Design Code	8
2.3.1 Precast Concrete Deck Panels.....	8
2.3.2 General Design of Shear Connectors.....	10
2.3.3 Material Properties of Shear Studs	10
2.3.4 Geometry Requirements of Shear Studs.....	10
2.3.5 Ultimate Limit State Design of Shear Studs.....	11
2.3.6 Fatigue Limit State of Shear Studs	13
2.4 Comprehensive Research Reports	15
2.4.1 NCHRP Report 407 “Rapid Replacement of Bridge Decks” (1998).....	16
2.4.2 “Experimental Evaluation of Full Depth Precast / Prestressed Concrete Bridge Deck Panels” (2002)	16
2.5 Durability	17
2.6 Push Tests for Ultimate Limit States	18
2.7 Deterioration of Stud Strength.....	24
2.8 Superstructure Testing	26

2.9 Grout Selection	28
2.10 Bedding Layer.....	29
2.11 Finite Element Analysis.....	30
2.12 Literature Review Summary.....	31
2.13 References.....	33
3.0 Performance of Shear Stud Clusters for Precast Concrete Bridge Deck Panels.....	35
3.1 Introduction.....	35
3.2 Push Test Experiments.....	37
3.2.1 Push Test Background	37
3.2.2 Push Test Design and Construction	38
3.2.3 Push Test Configuration	40
3.2.4 Loading Routine.....	41
3.2.5 Instrumentation	42
3.2.6 Push Test Regime	42
3.3 Stud Cluster Performance	44
3.3.1 Qualitative Observations from Push Tests.....	45
3.3.2 Ultimate Strength	45
3.3.3 Residual Strength	48
3.3.4 Stud Cluster Failure Mechanism.....	51
3.4 Parametric Bridge Study	52
3.4.1 Bridge Design	53
3.4.2 Finite Element Model	53
3.5 Conclusions.....	57
3.6 References.....	58
4.0 ConclusionS and Recommendations for Future Research.....	59
4.1 Summary and Conclusions	59
4.2 Recommendations for Future Research	60
APPENDIX A Push Test Program	62
APPENDIX B Component Material Testing.....	72
APPENDIX C Monotonic and Cyclic Push Test Data	88
APPENDIX D Bridge Analysis and Design.....	107

APPENDIX E Parametric Bridge Study.....	142
APPENDIX F Drawings.....	146

LIST OF TABLES

Table 2-1	Push Test Summary	24
Table 2-2	Bridge Model Summary.....	28
Table 3-1	Push Test Specimen Summary.....	43
Table 3-2	Monotonic Push Test Summary.....	45
Table 3-3	Residual Strength Summary	49
Table 3-4	Comparison of Residual Strengths.....	51
Table 3-5	Finite Element Mechanical Properties.....	54
Table 3-6	Static Deflections at Midspan of Exterior Girder (mm)	55
Table 3-7	First Flexure Frequencies (Hz)	55
Table B-1	Concrete Cylinder Test Results	72
Table B-2	CAN/CSA-S6-00 Minimum Stud Material Properties	74
Table B-3	Results of Tensile Testing Used in Monotonic Tests	75
Table B-4	Grout Testing Results for Monotonic Tests.....	78
Table B-5	Grout Testing Results for Cyclic Tests.....	83
Table C-1	Monotonic Push Test Specimen Schedule.....	88
Table C-2	Monotonic Push Test Data Summary	89
Table C-3	Cyclic Push Test Specimen Schedule.....	100
Table C-4	Cyclic Push Test Data Summary	100
Table E-1	Finite Element Mechanical Properties.....	142

LIST OF FIGURES

Figure 1-1	Thesis Development Flow Chart	3
Figure 1-2	Powerline Creek Bridge Deck Construction.....	4
Figure 2-1	Shear Stud Strength Equation used in CHBDC - Barker & Pucket (1997).....	12
Figure 2-2	Shear Stud Fatigue Data used in CHDBC – Barker & Puckett (1997).....	14
Figure 2-3	Typical Push Test Specimen.....	19
Figure 2-4	Fatigue of Precast Concrete Push Test Specimens – Shim et al. (2001)	22
Figure 2-5	Shear Stud Strength CIP vs. Precast Concrete – Shim et al. (2001).....	23
Figure 2-6	Illustrative Residual Strength Failure Envelope (Seracino R., Oehlers, D.J., and Yeo M.F., August 1999)	25
Figure 2-7	Interaction Between Strength and Endurance (Oehler, December 1990).....	26
Figure 3-1	Powerline Creek Bridge.....	36
Figure 3-2	Typical Push Test Configuration	38
Figure 3-3	Stud Cluster Geometry.....	39
Figure 3-4	Concrete Panel and Steel Plate for Push Test Specimens.....	40
Figure 3-5	Unsymmetrical Test Setup Front	41
Figure 3-6	Unsymmetrical Test Setup Back.....	41
Figure 3-7	Unidirectional Cyclic Loading.....	41
Figure 3-8	Schematic Push Test Plot.....	44
Figure 3-9	Combined Ultimate Strength of Monotonic Push Tests	46
Figure 3-10	Ultimate Strength Comparison	48
Figure 3-11	Residual Strength 6 Stud.....	50
Figure 3-12	Residual Strength 10 Stud.....	50
Figure 3-13	Residual Strength vs. No. Cycles.....	50
Figure 3-14	Stud Deformation for Specimen 6B.....	52

Figure 3-15	Grout Pocket Damage	52
Figure 3-16	Superstructure Cross Section	53
Figure 3-17	Finite Element Model	54
Figure 3-18	Deflections for Stud Clusters with Experimental Stiffness	56
Figure 3-19	Deflections for Stud Clusters with 0.5X Experimental Stiffness	57
Figure A-1	Studs Welded on Plate	63
Figure A-2	Form Construction	65
Figure A-3	Troweling Concrete Panels	65
Figure A-4	Typical Bend Test	66
Figure A-5	Precast Concrete Panel on Steel Plate 9A	67
Figure A-6	Grout Being Placed and Consolidated for Test Specimen 9A	67
Figure A-7	Wave Form Generator	69
Figure A-8	Data Acquisition Box	69
Figure A-9	LVDT for Actuator Control	70
Figure A-10	LVDT for Interface Slip	70
Figure A-11	Permissible Range of Interface Shear of 16mm Steel Studs vs. No. Cycles	71
Figure C-1	Shear Studs on Plate After Removal from Grout from Specimen 9B	99
Figure D-1	Bridge Cross Section	108
Figure E-1	Typical Finite Element Bridge Model	143
Figure E-2	Typical Finite Element Model Perspective from Above the Desk	144
Figure E-3	Typical Finite Element Model Perspective from Below the Soffit	144
Figure E-4	Finite Element Model Two Lanes Loaded	145
Figure E-5	Finite Element Model Three Lanes Loaded	145

ACKNOWLEDGMENTS

I am genuinely grateful for the many gifts bestowed upon me through my association with a number of great people in my life. First and foremost is my wife Katherine, since this thesis would have never been completed if not for her sacrifice, faith, and encouragement.

I am deeply indebted to Dr. Kenneth Elwood for his input over the years. I am certain that the insight and patience I observed during the production of this thesis will serve him well in his academic career.

Ron Mathieson and Kevin Baskin of the Ministry of Transportation are to be commended for the vision required to initiate this project and for also facilitating the financing for the project.

Many thanks go to Glen Furtado, a good friend and talented colleague, for his assistance in the laboratory and for convincing me to undertake this thesis.

Canadian Stud Welding generously provided the headed shear studs and welding of the steel studs. Rock Solid Steel provided the steel plate and fabrication services as part of their commitment to the Canadian Institute of Steel Construction.

The coursework and thesis in support of this degree were completed while being employed full-time as a bridge engineer for McElhanney Consulting Services Ltd.. My heartfelt thanks go to the management at McElhanney for their support and understanding required to complete this undertaking. Victoria Nowell graciously provided the expertise to format the document.

December 21, 2006

Vancouver, BC

1.0 INTRODUCTION

1.1 General

This thesis is focused on the performance of a shear connection between a steel girder and precast full depth concrete deck panel. The headed shear studs are grouped into a tight cluster and placed in a grout pocket to accommodate the construction of precast concrete decks on steel girders.

The results of experimental physical tests on shear stud clusters have been incorporated into a parametric study of a 36 meter simply supported composite superstructure using this system to investigate the effect that stud group spacing exceeding the prescribed code maximum has on the serviceability limit states of the superstructure.

This document will add to the body of knowledge in the discipline of bridge engineering and serve as an aid for engineers involved in the design of composite superstructures using precast concrete bridge deck panels.

1.2 Definition of Terms

A number of specific terms are used throughout this document. Precise descriptions of these terms are critical to the understanding of this work and are presented below.

Failure Load in Push Test: This is defined as the peak load that the specimen can withstand to under displacement control testing.

Grout Pocket: A void in a precast concrete component that accommodates a group of studs and is filled with grout to connect a steel element to the precast concrete element

Interface Slip: This is the displacement measured between the concrete and steel and represents the movement of the stud base relative to the concrete.

Leading Edge: This is the side of the stud that is bearing against the grout and is opposite to the side of the applied load.

Residual Strength: This is the strength of the shear stud group after it has been subjected to cyclic loading. The strength determined after cyclic loading is defined as the peak load that the specimen can withstand to under displacement control testing.

Stud Cluster: A group of headed shear studs arranged in a tight configuration that is inserted into a grout pocket

Stud Cluster Linear Stiffness: This is the mathematical relationship of force divided by displacement. This is defined as 7% of the Failure Load divided by the Interface Slip at 7% of the Failure Load.

Trailing Edge: This is the side of the stud that is pulling away from the grout and is on the same side as the applied load.

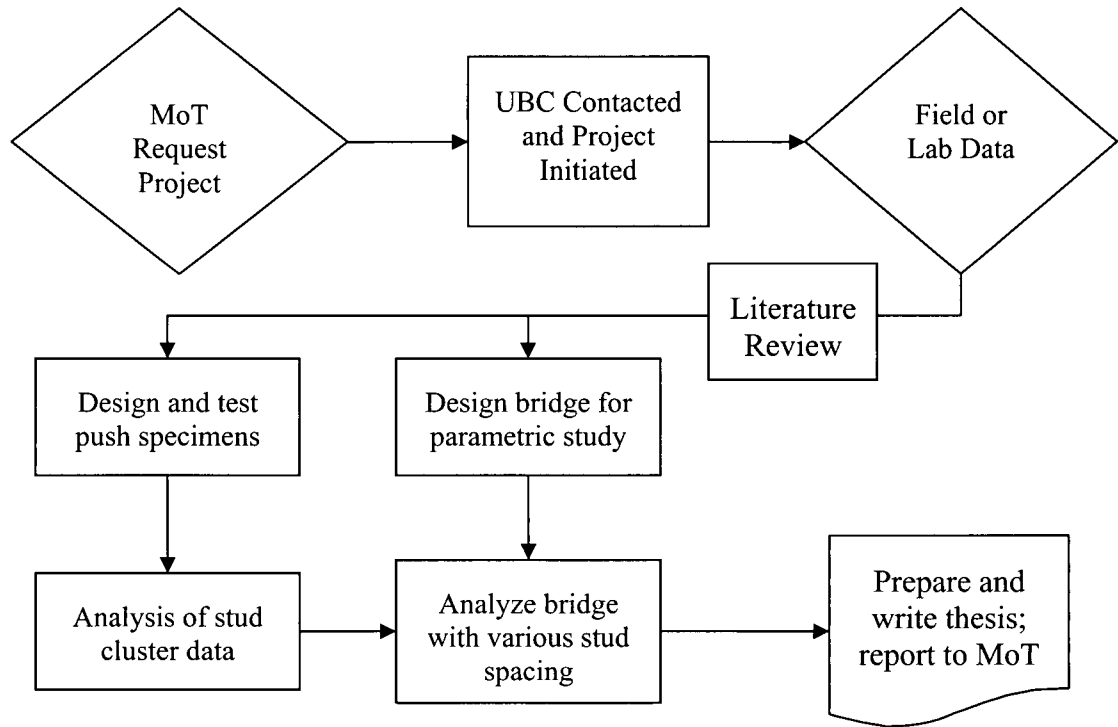
1.3 Project Background and Research Objectives

This project was initiated by the British Columbia's Provincial Ministry of Transportation (MoT) in response to recent bridge design submissions employing precast concrete deck panels. This system is new to MoT and, as such, the personnel responsible for reviewing the designs had numerous questions and concerns. This curiosity has stimulated MoT to compile a technical document that addresses these concerns.

The objectives underwent an evolutionary process of refinement as knowledge was gained and synthesized. The initial contemplation was to instrument a newly constructed bridge, but the available sites under construction at the onset of the project were too remote to effectively monitor. It was decided that it would be beneficial to first develop an understanding of the shear connection through laboratory experiments prior to undertaking any field instrumentation.

To accomplish these objectives, a research program was developed using a total of 16 physical specimens. These specimens would be used to capture the response of stud groups under static and cyclic load conditions, with the key variable being the number of studs in a grout pocket. This data would subsequently be used in a parametric study of stud group spacing for a range of bridge spans and this affect on the serviceability limit states of the superstructure system. The results of the parametric study would be used to assess the current the design procedures in the CAN/CSA-S6-00 and provide guidance to the reviews and designers of this system in British Columbia. A flow chart illustrating the scope development of the thesis is provided in Figure 1.1.

Figure 1-1 Thesis Development Flow Chart

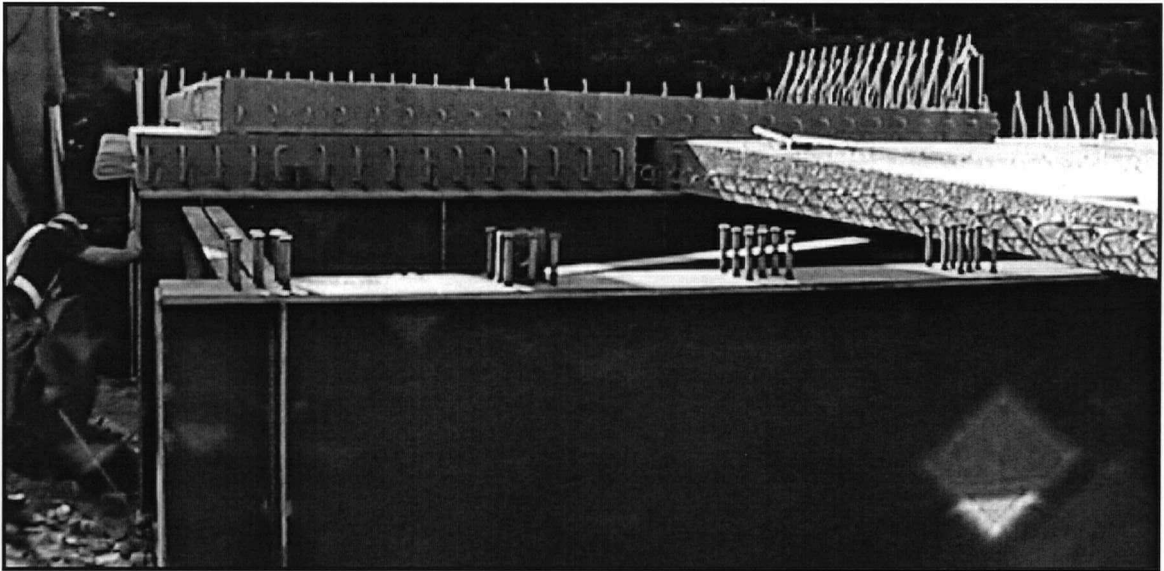


1.4 Relevance to Current Practice

Precast concrete deck panels have been used for bridge deck rehabilitation and new bridge construction since the 1970s. The speed with which bridge decks can be reconstructed without implementing a complete road closure has been the catalyst for recent research into this bridge deck system, given the large number of deficient concrete bridge decks in North America. The current state of research for precast concrete decks includes the refinement of the deck design, further investigation into shear connection behaviour and innovative ideas to increase the construction speed of the deck system.

Numerous bridges have been constructed using full-depth precast concrete in various regions of North America, including British Columbia. Hundreds of examples of local composite bridges utilizing precast concrete bridges can be found on the vast expanse of the British Columbia's industrial resource roads. Figure 1.2 shows the deck system being constructed on Highway 37, near Kitimat, BC.

Figure 1-2 Powerline Creek Bridge Deck Construction



Precast concrete deck panels provide many advantages over the more common cast-in-place concrete deck including:

1. Increased construction speed;
2. Minimal interference with traffic during deck replacements;
3. Applicable to all girder configurations; and
4. Decreased shrinkage in the deck.

One key advantage that was overlooked in the literature is that precast panels are very suitable for remote construction sites where producing quality concrete is difficult and expensive. Historically in British Columbia, this type of superstructure has been an economical choice for industrial road applications, where the distances to ready mix plants is too far and construction schedules are short. This is a very relevant concern in many regions of Canada.

1.5 Typical Construction Procedures

Issa et al. (1995) prepared a State-of-the-Art paper that was the compilation of an extensive questionnaire survey sent to 53 Departments of Transportation (DOTs); there were 51 responses with 13 DOTs using the precast concrete deck system. The paper concluded that the deck system has been used for numerous bridge types with various

geometric configurations, but that consistent design and construction guidelines need to be developed.

The typical spacing of shear stud pockets in the precast concrete panels is ~600 mm, but it has been suggested that more research is required to verify this typical spacing (Issa et al., 1995). Local construction practice has seen spacing in excess of 600 mm.

The construction sequence to remove and replace a concrete bridge deck is as follows:

1. A rubber strip is glued to the outside edges the top flange of the steel bridge girders to accommodate the required haunch;
2. Precast panels are placed on the supporting girders;
3. The precast concrete panels are levelled with embedded threaded bolts;
4. Longitudinal post-tensioning tendons are installed;
5. Transverse joints are filled with non-shrink grout;
6. Headed shear studs are welded to the steel girder at the grout pockets (alternatively, the studs can be shop welded prior to shipping the girders);
7. Longitudinal post-tensioning is applied after the transverse joint grout has reached specified strength and the ducts are then grouted;
8. Shear pockets and haunches are filled with non-shrink grout; and
9. Closure pours at the ends of the deck are cast with high-early strength concrete.

1.6 Thesis Organization

This is a manuscript-based thesis, organized into 4 chapters and 5 appendices. The appendices contain the bulk of the raw data captured during the experiments and the design of the bridges used in the parametric study. This allows the document to focus on discussing the results while providing a writing style that flows and is simple for the reader to digest.

Chapter 1 contains the background material of the project and also provides an introduction to the thesis.

Chapter 2 presents a literature review.

Chapter 3 contains the journal paper for this manuscript-based thesis, providing a thorough presentation of the test results and analytical study. This manuscript will be submitted to the Journal of Bridge Engineering.

Chapter 4 provides conclusions, recommendations, and suggestions for future research.

2.0 LITERATURE REVIEW

2.1 General

Previous research, including field performance reviews, finite element models, and laboratory tests, have generally focused on the following components of the deck system:

1. Shear connection between the deck and the girder and the grout material;
2. Fatigue of the deck shear connection and system components;
3. Effect of the bedding haunch on shear connection;
4. Transverse joint configuration and grout material; and
5. Post-tensioning in the longitudinal direction to maintain the transverse joints in compression.

The bulk of this literature review has focus on the shear connection used for precast concrete panels. Background information on the deck system has also been provided to identify possible effects that other components of the deck system may have on the performance of the steel stud connection. A historical perspective on the stud connection is also provided, in addition to a summary of relevant design standards in Canada.

There are three main academic institutions currently involved in the research and development of this bridge deck system:

1. University of Illinois at Chicago;
2. University of Nebraska-Lincoln; and
3. Seoul National University.

The majority of these papers are driven by the need for quick bridge deck replacement in high traffic volume areas where long term lane closures associated with conventional cast-in-place (CIP) concrete decks is undesirable to the motoring public.

2.2 Historical Perspective

Composite bridges using cast-in-place concrete decks on steel beams have been used for over seventy years, with Viest (1996) reporting that a continuous composite bridge was constructed in the 1930s.

The initial use of precast concrete decks occurred during the early 1970s in the United States as part of deck replacement projects (Issa et al., 2002). The bulk of these decks were non-composite. As the deck system development and experience was gained, the use of composite decks increased due to the recognition that the connection between the deck slab and the steel girders controlled the superstructure response.

2.3 Canadian Highway Bridge Design Code

The current Canadian Highway Bridge Design Code (CAN/CSA-S6-00) has provisions for the design and construction of full-depth precast concrete bridge deck panels. The composite section is designed to resist a wide variety of load types to satisfy serviceability, fatigue and ultimate limit states, while meeting durability requirements. The composite section is typically composed of a steel girder and concrete deck that are mechanically connected to allow a transfer of forces between the two materials.

The Slutter and Fisher (1967) paper is the basis for the code prescribed maximum spacing of 600 mm, *“The spacing of connectors should never exceed 24 in. because connectors also perform the necessary function of holding the concrete slab in contact with the steel beam”*, which is somewhat subjective and was not supported by experimental data. This maximum spacing of shear studs is the driving force behind the development of this thesis. Further information on the paper is presented in Section 2.6.

2.3.1 Precast Concrete Deck Panels

The design of full-depth precast panels is prescribed in cl. 8.18.4.4. Structural design of the slab can be completed with the empirical design of cl. 8.18.4 if the following conditions are met:

1. Panels are the full-width of the deck;
2. Minimum panel depth is 190 mm;
3. Transverse deck joints are grouted key ways, longitudinally post-tensioned to an effective stress of 1.7 MPa;
4. Ducts for the post-tensioning are located at mid-depth;

5. Block outs provided where panels are connected to beams for composite action;
6. Initially panels are supported on the beams by temporary levelling devices with grouting of the block outs and haunches completed after the longitudinal post-tensioning; and
7. Grout used in the shear keys has a minimum strength of 35 MPa at 24 hours.

The above design requirements were derived from the work of Issa et al. (1995a), Issa et al. (1995b) and Gulyas et al. (1995). If the empirical design method is not used to design the deck, then the above conditions do not apply, as the deck could be designed by other methods.

Issa et al. (1995) completed a finite element analysis of a bridge deck with grouted transverse key way joint to determine the minimum prestress required to keep the join in compression for the full depth of the deck, as it was felt that this was required for durability. Longitudinal post-tensioning provided in the deck; though this appears to be the most significant condition, it is not commonly done on bridges in BC. Also theoretically a simply supported bridge should have the top portion of the deck always in compression, and deck soffit potentially in tension under live loads, for which crack control steel across the joint can be provided.

The requirement for fit up between the precast deck modules and top flange is not addressed in the CHBDC. This is a potential issues when dealing with full width decks that span over more than two girders, since the opportunity to have the deck soffit not fully rest on all the girders, which would create a gap between the deck and flange. To overcome this problem a grout bedding layer can be used between the deck and flange, for which the deck requires temporary support and the ability to make fine geometric adjustments in the vertical direction. Verbal discussions with MoT field personnel exposed that this has been completed on highway bridges in the Province with some success. The bridges constructed on industrial roads do not have a bedding layer requirement because the are usually single lane roads with a two girder system.

2.3.2 General Design of Shear Connectors

The design of mechanical shear connectors to resist the vertical and horizontal movements between the concrete deck and the steel girder is prescribed in clause 10.11.8. These mechanical connectors force the steel and concrete to act as a monolithic member and are designed for strength and fatigue. It is obvious that the connection between the two materials plays an integral part in the overall response and performance of the composite superstructure. No calculations are required for the vertical tensile force present in the shear stud connection to keep the concrete in contact with the flange.

2.3.3 Material Properties of Shear Studs

Shear connectors designed following the CHBDC must conform to ASTM Standard A (Grades 1015, 1018, or 1020) and have the following typical mechanical properties:

Minimum tensile strength	410 MPa;
Minimum yield strength, by 0.2% offset method	350 MPa;
Minimum elongation in 50mm	20%;
Minimum reduction of area	50%.

2.3.4 Geometry Requirements of Shear Studs

Designers may choose the longitudinal spacing of the studs to be uniform or according to the variation of interface shear. The maximum longitudinal spacing of studs is not to exceed 600mm except for fatigue requirements, as prescribed in Clause 10.11.8.2. Slutter and Fisher (1967) reported that the maximum spacing of the studs was not to exceed 600mm, but they provided no technical justification, other than to eliminate vertical separation of the two materials. This 1967 study appears to be the source for the 600mm spacing requirement. S6-00 provides no minimum spacing between studs, conversely AASHTO (1996) has a minimum pitch of six stud diameters and six stud diameters transverse to the longitudinal axis of the supporting member.

Other geometric requirements include:

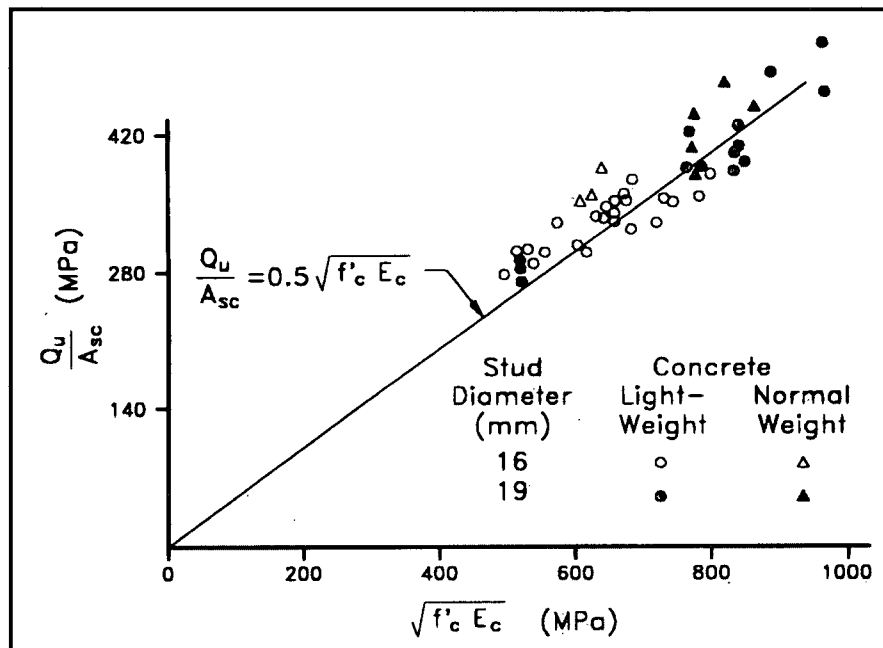
- The minimum height to diameter ratio is 4.
- Minimum clear edge distance from the flange edge to stud shank is 25mm.
- There are no special requirements for concrete covers.
- The underside of the head to the top of the bottom transverse reinforcement or, when the slab is haunched, to the top of the transverse reinforcement in the slab haunch is not less than 25mm.

2.3.5 Ultimate Limit State Design of Shear Studs

The design of the studs at ultimate limit state is based on experimental tests conducted on 48 test specimens and analysed by Ollgaard et al. (1971). The push test specimens were single headed stud shear connectors embedded in solid concrete slabs. Variables considered in the experiment included stud diameter, type of aggregate, number of connections per slab, concrete compressive strength, concrete split tensile strength, concrete modulus of elasticity, and concrete density.

The test results showed that no sudden failure occurred and significant inelastic deformation was recorded. Failure mechanisms included a shearing off of the steel stud with the stud remaining in the concrete or the concrete failed and the stud pulled out of the concrete with a wedge of concrete. The regression analysis equation was rounded off to provide a reasonable estimate of the shear stud connector strength used in the current code. The plot of the original work and the current design equation is presented in Figure 2-1.

Figure 2-1 Shear Stud Strength Equation used in CHBDC -
Barker & Pucket (1997)



The tensile capacity of the steel stud is used as an upper bound, consistent with the observed pull out failure mechanism for the current code equation in cl. 10.11.8.3, which is presented in Equation 2-1.

$$q_r = 0.5 \phi_{sc} A_{sc} \sqrt{f'_c E_c} \leq \phi_{sc} F_u A_{sc} \quad (2-1)$$

where q_r is the shear stud resistance, ϕ_{sc} is the resistance factor for the shear connectors, A_{sc} is the area of the shear stud, f'_c is the specified compressive strength of the concrete, E_c is the modulus of elasticity of the concrete and F_u is the minimum tensile strength of the steel stud.

The required number of studs between the point of zero moment and maximum moment in a span, N , is found through application of the following equation:

$$N = P / q_r \quad (2-2)$$

where P is the factored force to be transferred by the shear connectors as determined by the following expressions:

(a) for positive moment

(i) when the plastic neutral axis is in the concrete slab

$$P = \phi_s A_s F_y \quad (2-3)$$

(ii) when the plastic neutral axis is in the steel section

$$P = 0.85\phi_c f_c' b_e t_c + \phi_r A_r f_y \quad (2-4)$$

(b) for negative moment

$$P = \phi_r A_r f_y \quad (2-5)$$

where ϕ_s is the resistance factor for steel, A_s is the area of steel section, F_y is the specified minimum yield stress of the steel girder, ϕ_c is the resistance factor for concrete, b_e is the effective width of the concrete slab, t_c is the thickness of concrete slab, ϕ_r is the resistance factor for reinforcement, A_r is the area of reinforcement within the effective slab width, and f_y is the specified minimum yield strength of reinforced steel in the deck.

It is interesting to note that AASHTO LRFD uses the nominal strength of the concrete slab or the steel girder to determine the force to be transferred to the shear connectors. The current edition of the CHBDC reduces the force to be transferred by the appropriate material resistance factor. The philosophy behind the reduction of the design forces for the shear connectors in the CHBDC is unknown at this time.

2.3.6 Fatigue Limit State of Shear Studs

As a vehicle moves across the superstructure it develops both positive and negative shear, effectively reversing the load direction. The elastic range of shear that must be designed for is from the maximum to minimum values of the shear diagram. A typical simply supported superstructure produces an almost constant range of shear over the length of the bridge, thereby allowing designers to utilize

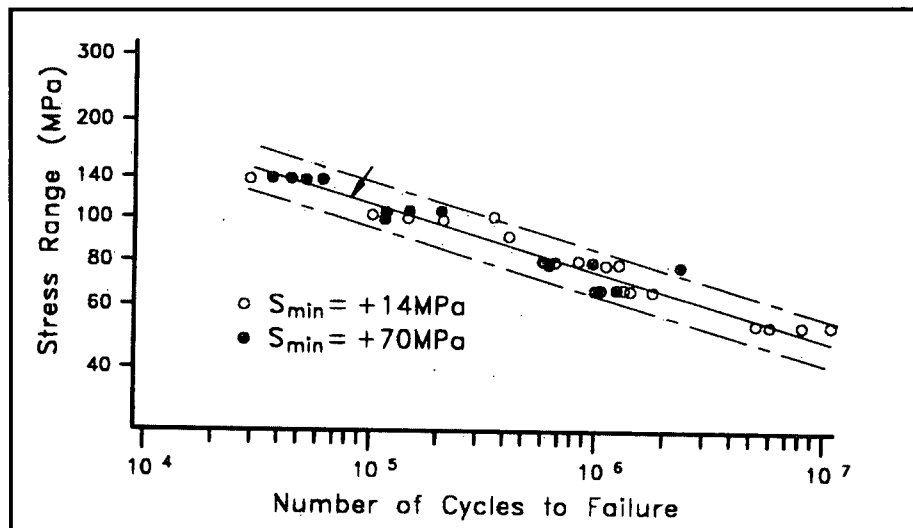
a constant spacing of the shear studs. Both the base metal at the weld connection and the shear stud itself determine fatigue resistance of the connection.

The CHBDC makes reference to the experimental work conducted on push test specimens by Slutter and Fisher (1967). Parameters that were deemed important in this study included concrete compressive strength, concrete age, connector size, minimum stress and stress range. It was determined through regression analysis that the stress range was the principal variable and could be used as a reliable predictor of the fatigue life of the connection. The allowable stress range of the shear connector is related to the number of cycles through the application of Equation 2-6.

$$Sr = 1065N^{-0.19} \quad (2-6)$$

where Sr is the stress range in MPa and N is the number of cycles. Figure 2.2 presents a plot of the data captured from the original experiments. It should be noted that no endurance limit was observed during the study.

Figure 2-2 Shear Stud Fatigue Data used in CHBDC – Barker & Puckett (1997)



Since the fatigue of the shear connector is a function of the stress range, the allowable shear force for one shear connector can be calculated using Equation 2-7. It is noted that there is an error in the CHBDC in clause 10.17.2.6; it should read as below (Errata Letter, Canadian Institute of Steel Construction, 26

February 2003), for which the permissible range of interface shear of an individual stud shear connector is

$$Z_{sr} = (238 - 29.5 \log N_c) d^2 \geq \frac{38d^2}{2} \quad (2-7)$$

where N_c is the number of cycles, and d is the stud diameter. The shear connectors are designed for a range of interface shear as defined by

$$q_{sr} = 0.52 \frac{V_{sr} Q}{I_t} \bullet \frac{s}{n} \quad (2-8)$$

where V_{sr} is the range of interface shear resulting from the passage of one CL truck, Q moment of area about the neutral axis of the composite member, I_t is the moment of inertia of the transformed member, s is the center to center spacing of stud groups, and n is the number of studs in a stud group.

In some situations a designer may choose not place any shear studs in the negative moment region to reduce the fatigue effect on the top flange. In this scenario, an additional number of shear connectors are provided at each point of counterflexure, within a distance equal to one-third the effective slab width on each side of the point of counterflexure, as determined by

$$N_a = \frac{A_r F_{sr}}{Z_{sr}} \quad (2-9)$$

where A_r is the area of reinforcing steel within the effective width of the slab, and F_{sr} is the calculated fatigue stress range at the detail from the passage of one CL-W truck.

2.4 Comprehensive Research Reports

Two significant reports have recently been completed on the subject of full-depth precast concrete bridge deck panels. A brief summary of each report is provided below.

2.4.1 NCHRP Report 407 “Rapid Replacement of Bridge Decks” (1998)

This comprehensive report was completed by the University of Nebraska and focused on evaluating the existing methods for rapid deck replacement and developing improved methods for future rapid deck replacement. A comprehensive literature review was conducted, numerous Departments of Transportation as well as Japanese engineers were surveyed, focusing on both partial- and full-depth precast concrete deck panels.

The report identified three main aspects for rapid deck replacement considering steel and concrete girders:

1. The demolition process for existing concrete decks;
2. The deck system; and
3. The deck to girder connection.

The researchers developed a 32mm diameter stud for the steel girder to precast concrete deck. The testing program included 28 push tests divided into five groups and a full-scale test using the 32mm diameter studs. Results of the testing indicated that the 32mm diameter studs could be shop or field welded, the weld quality inspected and designed all using standard procedures.

2.4.2 “Experimental Evaluation of Full Depth Precast / Prestressed Concrete Bridge Deck Panels” (2002)

This comprehensive report was completed for the Illinois Transportation Research Center by the University of Illinois at Chicago. The report was the culmination of numerous papers that were completed on the subject during the last decade. The objectives of this report were to:

1. Conduct scaled and full scale testing of the shear connections under static loading;
2. Conduct scaled and full-scale testing for the transverse panel joint under positive and negative moments;

3. Test a full scale superstructure under various loadings patterns; and
4. Provide design and construction procedures for inclusion in future bridge codes.

The investigators looked at all major components of the deck system including grout type, transverse joints, and the shear connection. The shear connection testing was evaluated with push testing of 12 quarter-scale and 14 full-scale specimens to investigate the effects of varying the number of shear studs within one panel, 1 to 4 inclusive, in addition to varying the number of pockets within one panel, 1 to 4 inclusive. The largest component of this project included the construction and testing of a full-scale two-span bridge, 5.48 metres wide by 24.99 metres long. The deck was longitudinally post-tensioned. The bridge was tested under service loading, overloads at two times the service load and ultimate loads, for both positive and negative moments. It was reported that this bridge resisted 7.9 times the service loading with only hairline cracking in the deck. No cracks were found at service load levels.

The report concluded that the precast concrete deck system could achieve full composite behaviour and exhibits exceptional behaviour when the maximum load in the jacks was reached. Results of the push tests indicated a couple of key observations. There is an apparent size effect that over predicts the strength of the shear connectors from results of $\frac{1}{4}$ scale test specimens to full size specimens. It was also observed from push test specimens that the configuration and number of specimens with the same number of studs per pocket but extra pockets, hence more stud per specimen, did not exhibit a lineal relationship for the strength of the panel. For example, doubling the number of studs did not necessarily double the ultimate strength of the connection.

2.5 Durability

A two-year inspection program of bridges utilizing precast concrete deck panels in various regions of the United States and Canada was completed by Issa et al. (1995). The inspections consisted of visual inspections, review of the as-built drawings, and a review of the historic construction procedures. The results of the inspection were that the precast

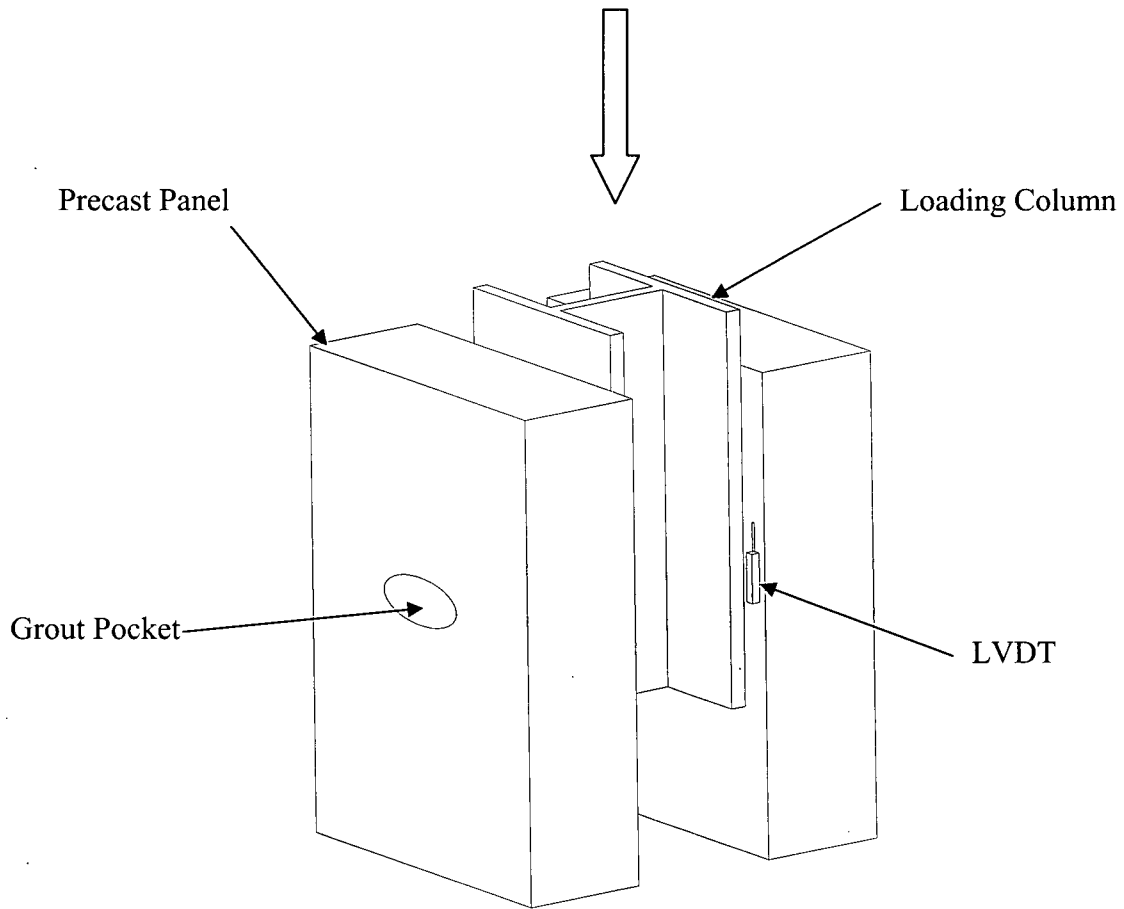
concrete panel provides excellent performance, with the majority of problems being the result of poor workmanship, unconventional design of the shear connection (i.e. using spring clips), design of the transverse shear key, lack of longitudinal post-tensioning, and improper specification of materials. The study concluded that:

1. Headed shear studs could be used for composite connection;
2. The panels should be post-tensioned longitudinally to control cracking at the transverse joints;
3. An overlay is required to provide a smooth ride (typical overlays are latex modified concrete and silica fume concrete);
4. The transverse shear key at the panel joint requires careful detailing, including grout selection; and
5. Haunches must be provided for geometric irregularities.

2.6 Push Tests for Ultimate Limit States

Given the wide variety of mechanical connectors available on the market, in combination with differing grout pocket configurations, unknowns surrounding dowel action, material nonlinearities in the grout and concrete, and residual stresses due to welding require that the ductility and strength of each shear connection be determined experimentally. These experiments load the shear connections directly to determine the applied load and slip between the concrete and steel. Figure 2-3 provides an isometric schematic of a typical push test specimen.

Figure 2-3 Typical Push Test Specimen



As noted in Section 2.3.5, Ollgaard et al. (1971) pioneered the current equations used for the ultimate limit states design of shear studs in cast-in-place concrete in North American loads. Variables for the push tests included stud diameter, type of concrete, number of connectors per slab, and concrete properties. The following equation was derived through statistical analysis of 48 test specimens that did not fail by splitting of the concrete, shear or embedment.

$$Q_u = 1.106 A_h f'_c{}^{0.3} E_c{}^{0.44} \quad (2-10)$$

which was then simplified for the purposes of design to

$$Q_u = 0.5 A_h \sqrt{f'_c} E_c \quad (2-11)$$

where Q_u is the ultimate strength, A_s is the area of shear stud, f_c is the compressive strength of the concrete, and E_c is the modulus of elasticity of the concrete.

Ollgaard 's original work on the ultimate strength of shear studs was then expanded by Oehlers et al. (1995) to account for variation of material properties. Data was gathered from various push tests and a statistical analysis was performed. The following equation can be used for analysis purposes to predict the strength of a shear stud connector in push tests:

$$(D_{\max})_{push} = \left(5.3 - \frac{1.3}{\sqrt{n}} \right) A_{sh} f_u^{0.65} f'_c{}^{0.35} \left(\frac{E_c}{E_s} \right) \quad (2-12)$$

where $(D_{\max})_{push}$ is the shear strength of a connector in a push test, n is the number of shear connectors, A_{sh} is the cross-sectional area of the shear stud, f_u is the ultimate tensile strength of the stud, f'_c is the compressive cylinder strength of the concrete, E_c is the concrete modulus of elasticity, E_s is the steel modulus of elasticity. Equation 2-12 is only valid for the range of $430 < f_u < 640 \text{ N/mm}^2$; $10,000 < E_c < 33,000 \text{ N/mm}^2$; and $24 < f'_c < 81 \text{ N/mm}^2$. Stud heights exceed 4 times the stud diameter and the weld collar height was an average of 31 percent of the stud diameter. Since the shear studs exhibit a plastic ductility region, the characteristic strength of the stud can be used since the studs will fail as a group. Since the geometric configuration of the push test induces compression into the specimen not present in a composite beam, it tends to over predict the strength in a composite beam by approximately 21%. Consequently, the following equation should be used when predicting the ultimate strength of the shear studs used in a composite beam.

$$(D_{\max})_{push} = \left(4.3 - \frac{1.3}{\sqrt{n}} \right) A_{sh} f_u^{0.65} f'_c{}^{0.35} \left(\frac{E_c}{E_s} \right) \quad (2-13)$$

Slutter and Fisher (1967) conducted fatigue testing using 44 push test specimens constructed from 19 mm and 22 mm diameters shear studs in cast-in-place concrete. A mathematical equation was developed that expresses the fatigue life of the stud as a function of the stress range given in Equation 2-14.

$$Z_r = \alpha d_s^2 \quad (2-14)$$

where Z_r is the allowable range of shear force per stud in pounds, d_s is the diameter of the stud in inches and $\alpha = 13,800$ for 100,000 cycles, 10,600 for 500,000 cycles and 7,850 for 2,000,000 cycles. The paper provides a design methodology for composite beams, which CHBDC is based upon. Furthermore, the results of the push tests were found to conform to the lower bound of the experimental composite beam data prepared by Torpac (1965).

Shim et al. (2002) conducted push tests on 24 specimens. Parameters for the push tests included the cross-sectional area of the stud shank, the compressive strength of the pocket grout and the thickness of the grout bedding layer. The authors developed an empirical relationship to account for the degradation of the ultimate strength of the connection and the increased slip as the depth of the bedding layer increased. It was concluded that using the tensile strength of a connection ($A_{sh}f_{su}$) typically used by design codes to determine the upper bound strength of the connection is un-conservative for the design of full-depth precast concrete deck slabs with a bedding layer. The results of the push tests had tensile strengths ranging from 75% to 101% for specimens with a 20mm thick bedding layer.

$$\begin{aligned} Q_u &= \alpha(0.36A_{sh} + 18.71) \\ \alpha &= 1 - 0.086(B_h - 20) \end{aligned} \quad (2-15)$$

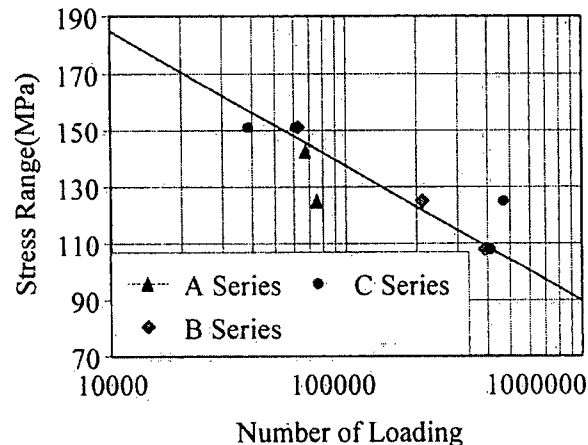
where Q_u is the ultimate strength of a single shear stud, kN, α is a reduction factor for the bedding thickness (1.0 for no bedding), A_{sh} is the cross sectional area of the shear stud shank mm^2 , and B_h is the bedding layer thickness, mm.

Shim et al. (2001) completed fatigue testing on specimens with a bedding layer of 20mm. Friction forces between the panel and the girder were observed to prolong the fatigue life of the connector. Once the chemical bond at the panel/girder interface and the friction was overcome, the flexural stiffness of the composite section was reduced by approximately 14%. The measured strains showed that there was very little load on the studs until the friction capacity was exceeded, thereby extending the fatigue life of the connection over mathematical models that ignore the time effect of the reduction of friction. The line in Figure 2-4 references the following equation

$$\log_{10} N = 7.8869 - 0.021\sigma_r \quad (2-16)$$

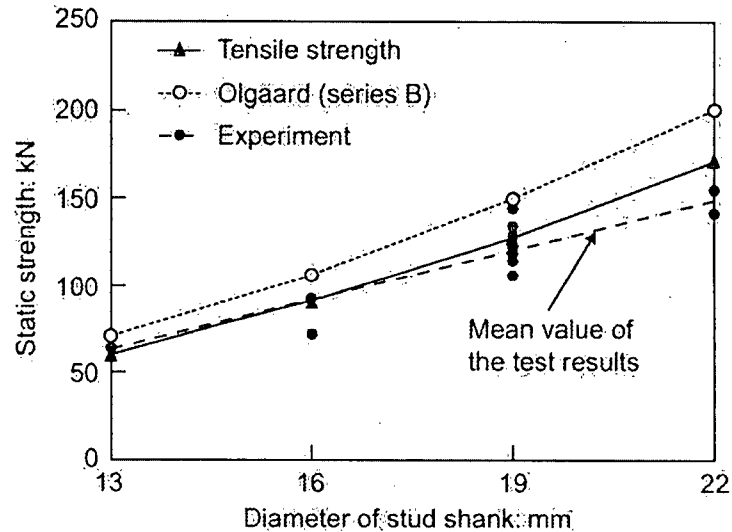
where N is the number of cycles and σ_r is the allowable stress range.

Figure 2-4 Fatigue of Precast Concrete Push Test Specimens – Shim et al. (2001)



Shim et al. (2000) conducted static and fatigue push tests on 18 specimens. The strength, stiffness, slip capacity and fatigue were investigated for shear connection of full-depth precast concrete deck panels. Push tests were conducted with variations of the stud shank diameter and compressive strength of the mortar. The results show that if the grout used in the panel pocket has a higher strength than 55MPa, then the grout has no effect on the ultimate strength of the composite section. The fatigue testing showed that the friction between the steel and grout bedding increased the fatigue life. The authors suggested that experimental parameter studies on the thickness of the bedding layer would be useful to evaluate the shear connector strength, slip and stiffness. The shear stud strength predicted from the results of the cast-in-place push testing completed by Ollgaard (1971) and subsequently used in the CHBDC, and precast concrete testing by Shim et al. (2001) is shown in Figure 2-5. The tensile strength of the studs used by Shim et al. is also provided. The concrete used for the precast concrete decks was similar to Ollgaard. The precast concrete specimens had a 20mm thick grout layer that contributed to the consistently lower ultimate strengths.

Figure 2-5 Shear Stud Strength CIP vs. Precast Concrete – Shim et al. (2001)



Tadros et al. (2002) prepared and tested 20 push specimens to determine the ultimate strength. The test compared the 22mm diameter stud to the 32mm diameter stud, investigated the effect of residual stresses by reusing the beams from the 22mm diameter stud for the 32mm diameter stud tests, used head studs in conjunction with headless studs and used steel ties around the stud group. The results showed that both the 22mm diameter and the 32mm diameter studs fail at their tensile capacity and that the larger studs had 30% less slip. It was concluded that the ultimate strength of the 32mm diameter stud could safely be determined using the AASHTO LRDF bridge design specifications (1998). The study concluded that 31.8mm headed studs are feasible for construction, but that further research is warranted for the use of 31.8mm headless studs.

Issa et al. (2002) prepared and tested 12 quarter scale (9.5 mm diameter) and 14 full scale (25 mm diameter) specimens. The parameters investigated included varying the number of pockets within the panel and also the number of studs per pocket using 2, 3 and 4 studs per pocket. Slip deflections and strains were measured. A size effect was observed when the predicted strength of the full scale specimens based on the quarter scale specimens under predicted the experimental value. No equations were provided in the study, but the average ultimate strength of the full scale stud is 142.1 kN and the quarter scale stud is 12.2 kN. It was reported that the arrangement of the studs was critical in the performance of the studs and that the load capacity increased linearly with the number of studs.

The following table summarizes the tests and the associated parameters considered by each of the studies.

Table 2-1 Push Test Summary

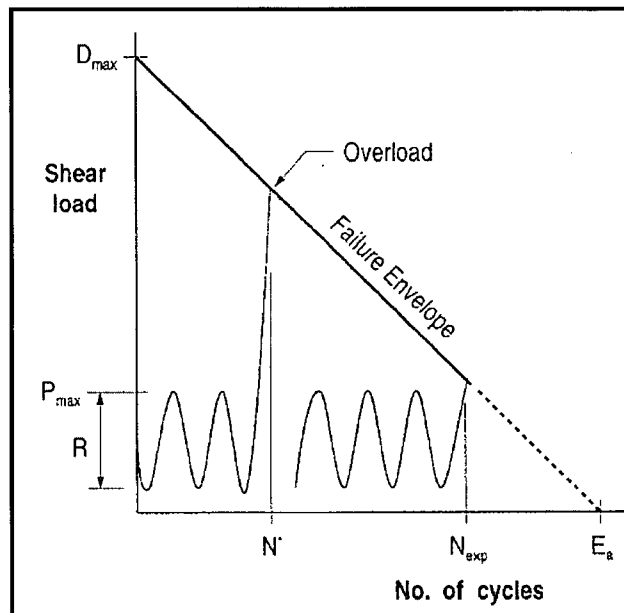
	Researchers						
	Ollgaard et al.	Slutter and Fisher	Shim et al.	Shim et al.	Shim et al.	Tadros et al.	Issa et al.
Year	1971	1967	2000	2001	2002	2002	2002
Diameter of Stud (mm)	15.9 and 19.1	19.1 and 22.2	13, 16, 19, and 22	13, 16, 19, and 22	13, 16, 19, and 22	22 and 32	9.5 (1/4 scale) 25 (full size)
Pitch of Studs (mm)	305	355	300	300	Not reported	152.4	Varied
No. Studs per Pocket	n/a	n/a	1	1	1	n/a	1, 2, 3 and 4
Thickness of Bedding Layer (mm)	n/a	n/a	20	0, 20, and 40	0, 20, and 40	n/a	9.5
Compressive Strength of Pocket Grout (MPa)	n/a	n/a	54.88, 61.09, 71.38	54.88, 61.09, 71.38	54.88, 61.09, 71.38	n/a	Not reported
Compressive Strength of Concrete Slab (MPa)	Varied	Varied	35.5	42	35.8	varied	42.8
Comments	Not precast panels, strength testing	Not precast panels, fatigue testing	Higher grout strengths had no increase in ultimate strength	Fatigue tested on 20mm bedding layer only	No fatigue testing conducted	Not precast panels, large studs	No fatigue testing conducted

2.7 Deterioration of Stud Strength

Experimental research has shown that the static strength of the shear stud is reduced after being subjected to cyclic loading (Oehlers 1995). The current design method for shear

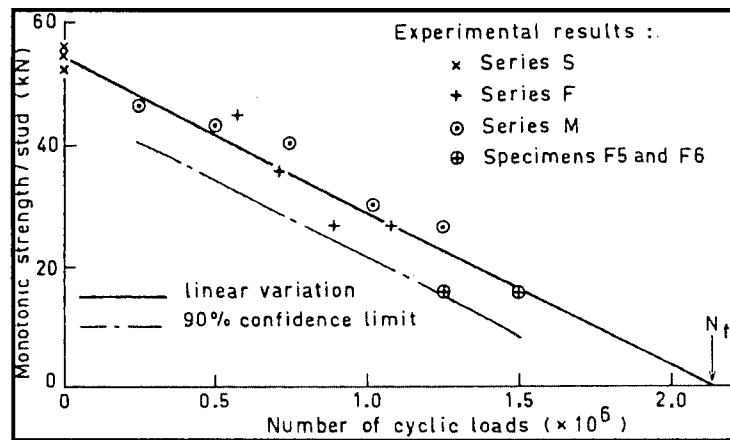
studs considers the strength of the connection independent of the fatigue capacity. This implies that the strength of the stud connection is a constant over the service life of the structure. The fatigue capacity is based on the endurance of the stud for a given stress level and the predicated number of cycles based on the average annual daily truck traffic (AADT) for the bridge site. Figure 2-6 provides a schematic plot of the deterioration of the stud strength as a function of the number of applied cycles.

Figure 2-6 Illustrative Residual Strength Failure Envelope
(Seracino R., Oehlers, D.J., and Yeo M.F., August 1999)



This new approach to the design and evaluation of shear connections provides an improved understanding of the connection over the current code equations, since the strength of the connection is modeled as a function of time. Oehlers (1995) constructed 14 push test specimens with cast-in-place concrete and two rows of studs. A series of three tests were conducted on these push test specimens. Three were used to determine the static strength of the shear studs monotonically, six were tested cyclically at a load equal to 25% of the static strength until failure of the studs, and the remaining five were loaded cyclically with a stress range equal to 25% of the static strength and then loaded monotonically before the endurance limit was reached. From analysis of the data, a linear regression line was produced to represent the deterioration of the stud strength and a plot of this work is presented in Figure 2-7.

Figure 2-7 Interaction Between Strength and Endurance
(Oehler, December 1990)



The equation relating to the linear regression is:

$$N_e = N_f \cdot \left(1 - \frac{P_m}{P_s}\right) \quad (2-17)$$

where N_e is the number of cycles to reduce P_s to P_m , N_f is the number of cycles to reach endurance limit, P_m is the static strength after N_e cycles (kN) and P_s is the static strength (kN) of the shear stud.

2.8 Superstructure Testing

Shim et al. (2000) conducted experimental testing on an eight meter simply supported composite beam under fatigue and static loading. The deck, comprised of seven 200mm thick precast concrete panels, was longitudinally post-tensioned. Shear connection was provided with three 19mm diameter headed shear studs placed in grout pockets spaced at 400mm on centre. It was observed that the weaker studs will shed load to the stiffer studs, allowing a uniform spacing of the studs. Shear load on the studs was found to be negligible until the chemical bonding and friction between the panels and the girders is overcome.

Tadros et al. (2002) conducted testing on a 12200mm composite beam, with a cast-in-place concrete deck under fatigue and static loading. The results of the testing showed that current ASSTHO fatigue criteria, which the CHBDC is calibrated against, were conservative and that the 32mm diameter studs had approximately twice the capacity of

equivalent 22mm diameter studs. A three span continuous demonstration bridge was constructed for the Nebraska Department of Roads as a result of this study.

Issa (2002) constructed and tested a full-scale, two-lane, two-span continuous bridge. The superstructure was 5.5m wide with two 12.19m spans consisting of three W18x86 steel girders and 11 precast concrete panels. The deck was longitudinally post-tensioned after the transverse joints were grouted. Instrumentation included numerous strain gauges on the steel girders. Linear variable displacement transducers were used to measure the vertical deflection and slip at the panel to girder interface. Crack displacement transducers were used to monitor the behaviour of the transverse joint. The specimen was subject to loading patterns to simulate truck loading, including 30% for impact. The maximum load applied was 7.9 times the service load. This load was limited by the capacity of the hydraulic jacks; therefore, the ultimate load capacity was not determined. Only small cracks in the deck were observed.

Torpac (1965) conducted endurance based fatigue experiments on seven simply supported 24WF68 steel beams made composite with a 6 inch thick cast-in-place concrete slab using 3/4 inch diameter shear studs. The beams were 36' feet long with a 6' wide concrete slab. Strain gauges were applied to a number of studs, but were found through testing to effective only in determining relative comparisons and not absolute values. Pairs of shear studs were spaced at ranges that varied from 8 inches to 14 inches. The product of the study was S-N fatigue curves that were subsequently used by Slutter and Fisher (1967) to confirm the results of their fatigue based push test regime. Torpac reported that the stud failure is progressive in nature and that measuring the slip at the end span is insensitive to individual stud failures as it was observed that numerous instrumented studs failed prior to end slip or increased deflections.

Table 2-2 Bridge Model Summary

Parameters	Researchers				
	Torpac	Shim et al.	Shim et al.	Tadros et al.	Issa et al.
Year	1967	2000	2001	2002	2002
Span (mm)	10972	8000	8000	12200	40000-40000
Deck Type	Cast-in-Place	Precast	Precast	Cast-in-Place	Precast
Diameter of Stud (mm)	19	19	19	32	22
Pitch of Studs	200 - 350	400	400	152.4	600
No. Studs per Pocket	n/a	3	3	n/a	3
Thickness of Bedding Layer (mm)	n/a	15	0, 20, and 40	n/a	25
Compressive Strength of Precast Slab (MPa)	28.6 – 39.5	35.5	42	CIP, not reported	Not reported
Compressive Strength of Pocket Grout (MPa)	n/a	53.3	33	n/a	Not reported
Longitudinal Post-tensioning	No	Yes, but no reported stress level	Yes, but no reported stress level	No	Yes
Compressive Strength of Transverse Joint Grout (MPa)	n/a	53.3	30	n/a	Not reported
Comments	Not precast panels 7 beams tested	Precast panel with a bedding layer	Precast panel with three bedding layer thickness'	Not precast panels	Two span

2.9 Grout Selection

Gulyas et al. (1995) evaluated the grout used in the longitudinal keyway for precast concrete bridges through tensile and shear tests. The results of the testing showed that a

bond failure of the carbonated surface on the concrete and that material testing of the grout doesn't provide a representative indication of the actual performance. A variety of grouts were tested under varying environmental conditions. Set 45 grout was determined to be slightly advantageous during hot weather installations. Recommendations included:

1. Grit blasting all faces exposed to grout; and
2. Specifying a non-shrink grout is not acceptable as bond strength was found to be a paramount parameter for durability.

Shim et al. (2001) conducted push tests to investigate the effect of the grout material of the panel pockets and the bedding layer located between the steel girder and the precast concrete panel. The ultimate strength and fatigue endurance were estimated from the experiments. No effect on the ultimate strength of the composite section was observed if grout 28 day compressive strength exceeded 55MPa.

2.10 Bedding Layer

When matching full deck width precast concrete deck panels on girder systems with more than two girders, there is the possibility that a good match will not be made and that the panel will rock on the girders. This, in turn, could drive additional compression into the shear stud group when loaded with traffic, since full bearing support is not provided by the flange. To overcome this field fit-up problem, some designs use a grout bedding layer between the top of the top flange and the soffit of the concrete panel. This bedding layer is constructed with a flowable grout that is pumped into a void between the top of the flange and the soffit of the panel. Foam strips are glued to the edges of the flange to contain the grout.

Shim et al. (2001) evaluated the effect of the bedding layer thickness through experimental push tests. The tests showed that the ultimate strength of the connection decreases as the thickness of the bedding layer increases as shown previously in Section 2.6. It was observed that the grout used in the bedding layer cracks at low load levels and the studs used with the precast panels show greater deformation capacity than those used with the CIP decks. The behaviour of the shear connector needs to be verified at the ultimate limit state through additional experiments and fatigue tests on push specimens considering various bedding thickness should be conducted.

Shim et al. (2000) found that the depth of the bedding layer has a significant influence on the strength and stiffness of the shear stud connector. The studs were found to exhibit a bi-linear force deformation relationship that is attributed to the degradation and tensile cracking of the bedding layer during cyclic loading. In addition, it was found that the shear stud connection for the precast concrete panel is more flexible than a comparable CIP concrete slab, and therefore exhibits an increase in ultimate slip allowing a uniform spacing of shear studs. The authors concluded that parameter studies on the thickness of the bedding layer through experimentation were needed to evaluate the effects of the shear connection on strength, slip and stiffness. Further research on the shear connections considering the characteristics of the filling material, non-shrink mortar and bedding layer was also suggested.

2.11 Finite Element Analysis

Shim et al. (2000) prepared finite element analysis of their push test specimens to determine the initial stress distribution of the shear stud connector to confirm the experimental results. The model showed a concentration of stresses at the top of the grouted bedding layer. Cracking of the grout bed was predicted to occur at approximately 3% of the static strength of the shear stud, which contributes to the greater flexural deformation of the stud over the traditional cast-in-place concrete deck or decks without a bedding layer.

Shim et. al. (2001) prepared a finite element model of the composite bridge that they had tested in the lab using partial interaction theory considering the shear stiffness of the shear studs from push tests. They found that the shear stiffness of the finite element analysis was within 10% of the push test data. Based on this study, they concluded that the studs could be spaced uniformly along the girders, because of stud ductility.

Issa, et al. (1998) completed an analytical study using the ALGOR finite element software package to determine the required amount of post-tensioning stress to have the transverse panel joints remain in compression. Both simply supported and continuous bridges were analyzed. The results of the study showed that a minimum prestress level of 1.38MPa was required for simply supported and the midspan of continuous bridges and 3.1MPa for continuous superstructures to keep the transverse joint in compression. It

was also found that the stress in the grout for the transverse joints was higher than the deck panels, since the grout is substantially stiffer than the precast concrete.

2.12 Literature Review Summary

Composite bridge construction has been in use in North America for over seventy years, with experience using precast concrete panels dating back to the early 1970's. During this time there have been numerous methods of mechanical shear connectors developed, with the headed shear stud becoming the most commonly used because of the development automated stud gun welding process. There are also a wide variety of grout pockets that are used by precast concrete deck manufactures. Within the shear stud pocket there are unknowns surrounding dowel action, material nonlinearities in the grout and concrete, and residual stresses due to welding require that the ductility, strength and fatigue characteristics of each unique shear connection be determined experimentally.

The CHBDC, CAN/CSA-S6-00 provides some guidance on the design of precast concrete decks, but the code prescribed stud spacing limitation of 600 mm, is not conducive to the design and construction of this deck system. An increase of the grout pocket spacing with many studs per pocket is desirable for the following reasons;

- Constructability: where there are less stud pockets there is more room on the flange for workers to walk and reduced risk of fit up conflicts;
- Improved durability: reducing the number of grout pockets reduces the number of potential sources for ingress of chloride laden water; and
- Deck strength: a reduction of the number of opening in the deck allows for more transverse reinforcement, which is necessary for moment demand due to impact of the barrier system and any deck cantilever.

A gap in the research literature exists when one questions the applicability of the code prescribed stud spacing limitation of 600 mm. The only reference found was the Slutter and Fisher (1967) paper which stated the following, "*The spacing of connectors should never exceed 24 in. because connectors also perform the necessary function of holding the concrete slab in contact with the steel beam*", which was not found to be supported by experimental data. At the time the study was conducted, only cast-in-place decks were

constructed, so this would have been a logic limit to place on the stud spacing, since there is no warrant to group the studs into discrete locations along the girder flange.

2.13 References

- AASHTO LRFD. 1996 *Bridge Design Specifications*. American Association of State and Highway Transportation Officials, Washington, D.C.
- AASHTO. *Standard Specifications for Highway Bridges, and Interim Specifications DATE*, 15th Edition. American Association of State and Highway Transportation Officials, Washington, D.C.
- Badie S.S., Tadros M.K., Kakish H.F., Splittgerber D.L., and Baishya M.C. 2002 "Large Shear Studs for Composite Action in Steel Bridge Girders." *ASCE Journal of Bridge Engineering*, Vol. 7, No. 3, pp. 195-203.
- Barker R.M. and Pucket J.A., 1997, "Design of Highway Bridges." *John Wiley and Sons, Inc.*
- Byfield M.P., 2002, "Analysis Of Composite Beams With Widely Spaced Shear Connectors." *The Structural Engineer*, Vol 80, No. 13, pp. 31-33.
- CSA. 2000. *Canadian Highway Bridge Design Code*. CAN/CSA-S6-00, Canadian Standards Association, Rexdale, Ontario, Canada.
- Gulyas R.J., Wirthlin G.J., and Champa J.T. 1995 "Evaluation of Keyway Grout Test Methods for Precast Concrete Bridges." *PCI Journal*, Vol. 40, No. 1, pp. 44-57.
- Issa M.A. 2002 *Experimental Evaluation of Full Depth Precast/Prestressed Concrete Bridge Deck Panels*. Report No. ITRC FR 98-5, Illinois Transportation Research Center, Edwardsville, Illinois.
- Issa M.A., Yousif A.A., and Issa M.A. 2000 "Experimental Behaviour of Full-Depth Precast Concrete Panels for Bridge Rehabilitation." *ACI Structural Journal*, Vol. 97, No. 3, pp 397-407.
- Issa M.A., Yousif A.A., Issa M.A., Kaspar I.I., and Khayyat S.Y. 1998 "Analysis of Full-Depth Precast Concrete Panels." *PCI Journal*, Vol. 43, No. 1, pp. 74-85.
- Issa M.A., Idriss A.T., Kaspar I.I., and Khayyat S.Y. 1995a "Full-Depth Precast and Prestressed Concrete Bridge Deck Panels." *PCI Journal*, Vol. 40, No. 1, pp. 59-80.
- Issa M.A., Yousif A.A., Issa M.A., Kaspar I.I., and Khayyat S.Y. 1995b "Field Performance of Full-Depth Precast Concrete Panels in Bridge Deck Construction." *PCI Journal*, Vol. 40, No. 3, pp. 82-108.
- Issa M.A., Yousif A.A., and Issa M.A. 1995 "Construction Procedures for Rapid Replacement of Bridge Decks." *Concrete International*, Vol. 17, No. 2, pp. 49-52.
- Kim J.H., Shim C.S., Matsui S., and Chang S.P. 2002. "The Effect of Bedding Layer on the Strength of Shear Connection in Full-Depth Precast Deck." *Engineering Journal*, Third Quarter, pp. 127-135.
- Oehlers D.J., and Brandford, M.A. 1995 "Composite Steel and Concrete Structural Members: Fundamental Behaviour." Elsevier Science Ltd., New York
- Oehlers D.J., 1995, "Design and Assessment of Shear Connectors in Composite Bridge Beams." *Journal of Structural Engineering*, February, pp. 214-224.

- Oehlers D.J., Seracino R., and Yeo M.F., 2000, "Fatigue Behaviour of Composite Steel and Concrete Beams with Stud Shear Connections." *Prog. Struct. Engng. Mater.*, Vol 2, pp. 187-195.
- OHBD. 1991. *Ontario Highway Bridge Design Code*. Ministry of Transportation of Ontario, Downsview, Ontario.
- Ollgaard J.G., Slutter R.G., and Fisher J.W., 1971 "Shear Strength of Stud Connectors in Lightweight and Normal-Weight Concrete." *AISC Engineering Journal*, April, pp. 55-64.
- Picard A. and Beaulieu D., 1993 "Factored Moment Resistance of Composite Bridge Girders with Singly Symmetric Non-compact Steel Sections", *Canadian Journal of Civil Engineering*, 20(5), pp. 828-833.
- Seracino R., Oehlers, D.J., and Yeo M.F., August 1999 "Reverse-Cyclic Fatigue Tests on Stud Shear Connectors." Research Report No. R 165, The University of Adelaide, Australia
- Shim C.S., Lee P.G., and Chang S.P., 2001. "Design of Shear Connection in Composite Steel and Concrete Bridges with Precast Decks." *Journal of Constructional Steel Research*, Vol. 57, No. 3, March pp. 203-219.
- Shim C.S., Kim J.H., Chang S.P. and Chung C.H. 2000. "The Behaviour of Shear Connection in a Composite Beam with a Full-Depth Precast Slab." *Proc. Instn Civ. Engrs Structs & Bldgs*, Vol. 140, pp.101-110.
- Slutter R.J., and Fisher J.W., 1967, "Fatigue Strength of Shear Connectors." Highway Research Record No. 147. Highway Research Report, Washington D.C.
- Tadros M.K., and Mantu M.C. 1998 *Rapid Replacement of Bridge Decks*. NCHRP Report 407. Transportation Research Board, Washington, D.C.
- Toprac A.A., 1965, "Fatigue Strength of 3/4 -Inch Stud Shear Connectors." Highway Research Record 103, pp. 53-77.
- Veist I.M., 1996, "Studies of Composite Construction at Illinios and Lehigh, 1940-1978", *Composite Construction in Steel and Concrete III*, C.D. Buckner and B.M. Shahirooz ed., pp. 1-14.
- Yamane T., Tadros M.K., Badie S.S., and Baishya M.C. 1998 "Full Depth Precast, Prestressed Concrete Bridge Deck System." *PCI Journal*, Vol. 43, No. 3, pp. 50-66.

3.0 PERFORMANCE OF SHEAR STUD CLUSTERS FOR PRECAST CONCRETE BRIDGE DECK PANELS¹

3.1 Introduction

Composite bridge construction has been in use in North America for over seventy years, with experience using precast concrete panels dating back to the early 1970s. Many examples of bridges utilizing full depth precast concrete bridge deck panels exist in service today. The system is particularly popular for bridge deck rehabilitation projects, where a rapid construction technique is required to minimize traffic disruptions during construction, Issa (2000) and Tadros (1998). Another advantage of this deck system is found on the many remote construction sites, where quality cast-in-place concrete can be difficult to produce.

The Canadian Highway Bridge Design Code (CHBDC), CAN/CSA-S6-00, has provisions to allow for the design of full depth precast concrete deck panels made composite with steel girders, but questions surrounding the shear stud connection linger. Current code equations for determining the ultimate limit strength of the shear stud were empirically derived from push tests conducted by Ollgaard et al. (1971) on cast-in-place concrete specimens. The fundamental differences of shear studs used for the precast concrete deck system are that the shear studs are tightly packed into clusters at discrete locations along the girder and the studs are embedded in grout that transfers load to the precast concrete panel. The limiting longitudinal spacing of 600mm was originally suggested by Slutter and Fisher (1967) to keep the concrete and steel in contact, but it is desired to relax this requirement for the precast concrete panel system to improve constructability.

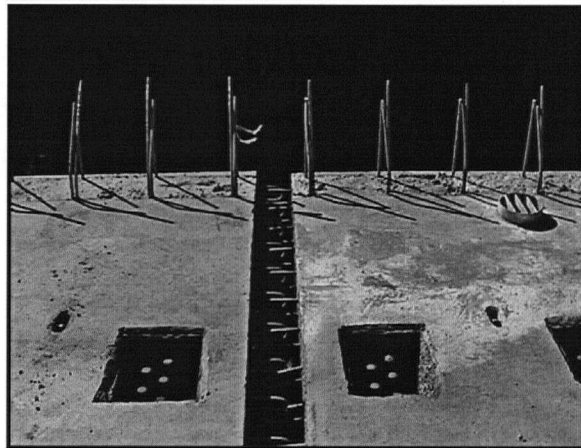
The CHBDC requires two independent calculations for the design of shear studs; a check of the stud strength for ultimate limit strength and a check of the endurance limit for

¹ A version of this chapter will be submitted for publication. La Rose, K.E., Elwood, K.J. Performance of Shear Stud Clusters for Precast Concrete Bridge Deck Panels.

fatigue limit states. Oehlers et al. (1995) showed that there is a reduction of the monotonic strength of the shear stud connection exposed to repeated loads. This potential for stud failure due to overload prior to reaching the fatigue endurance limit deserves attention since the stud clusters cannot be visually inspected for fatigue damage.

Figure 3-1 illustrates an example of this superstructure system used on the Powerline Creek Bridge, Highway 37, near Terrace British Columbia, Canada, constructed in 2004, using the design/build delivery method. The bridge is a 35 meter long simple span composite bridge with three girders. The concrete panels are not full width of the deck, but rather span from girder to

Figure 3-1 Powerline Creek Bridge



girder with a longitudinal deck joint over the interior girder, neglecting the need for a grout bedding layer to accommodate any fit up issues between the girder and the deck. The stud cluster spacing is limited to 600mm per CHBDC and the deck was not longitudinally post-tensioned. The square grout pockets used on the exterior girders were designed to accommodate the deck suppliers existing equipment. A waterproof membrane and asphalt were subsequently placed.

The CHBDC, CAN/CSA-S6-00 provides some guidance on the design of precast concrete decks based on the work of Issa et al. (1995a & 1995b) and Gulyas (1995), but the code prescribed stud spacing limitation of 600 mm, is not conducive to the design and construction of this deck system. An increase of the grout pocket spacing with many studs per pocket is desirable for the following reasons;

- Constructability: where there are less stud pockets there is more room on the flange for workers to walk and reduced risk of fit up conflicts;
- Improved durability: reducing the number of grout pockets reduces the number of potential sources for ingress of chloride laden water; and

- Deck strength: a reduction of the number of opening in the deck allows for more transverse reinforcement, which is necessary for moment demand due to impact of the barrier system and any deck cantilever.

A gap in the research literature was identified when one questions the applicability of the code prescribed stud spacing limitation of 600 mm. The only reference found was the Slutter and Fisher (1967) paper which stated the following, “*The spacing of connectors should never exceed 24 in. because connectors also perform the necessary function of holding the concrete slab in contact with the steel beam*”, which was not found to be supported by experimental data. At the time the study was conducted, only cast-in-place decks were constructed, so this would have been a logic limit to place on the stud spacing, since there is no warrant to group the studs into discrete locations along the girder flange.

To address these issues an experimental testing regime was conducted on push test specimens with the key variable being the number of shear studs in a grout pocket. A parametric study was then completed using data from the push tests to investigate the response of a 36 meter span, simply supported composite superstructure, by varying the longitudinal spacing of the stud clusters.

3.2 Push Test Experiments

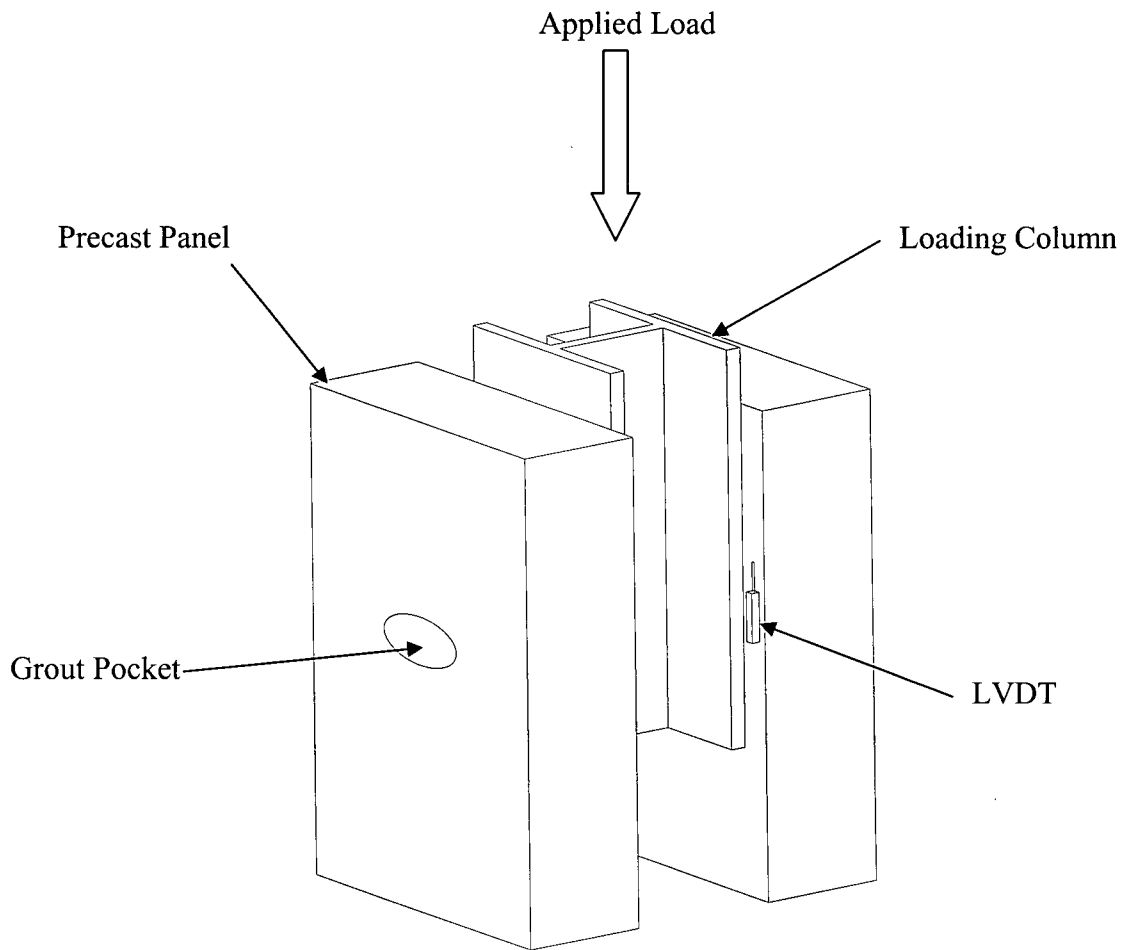
During the development of composite construction there have been numerous methods of mechanical shear connectors developed, with the headed shear stud becoming the most commonly used because of the development automated stud gun welding process. There are also a wide variety of grout pockets that are used by precast concrete deck manufactures. Within the shear stud pocket there are unknowns surrounding dowel action, material nonlinearities in the grout and concrete, and residual stresses due to welding require that the ductility, strength and fatigue characteristics of each unique shear connection be determined experimentally.

3.2.1 Push Test Background

A push test is the industry standard practice used to determine the response of a shear stud, although the test is not formalized in any North American standards or codes. This

is a direct load test that sees the shear studs placed within a concrete panel. The shear studs are welded to a steel plate that is connected to a hydraulic actuator. Instrumentation consists of a load cell and linear variable transducers to measure slip between the concrete and steel plate, in addition to out of plane movements of the concrete panels. Figure 3-2 shows an isometric schematic of a typical push test specimen.

Figure 3-2 Typical Push Test Configuration



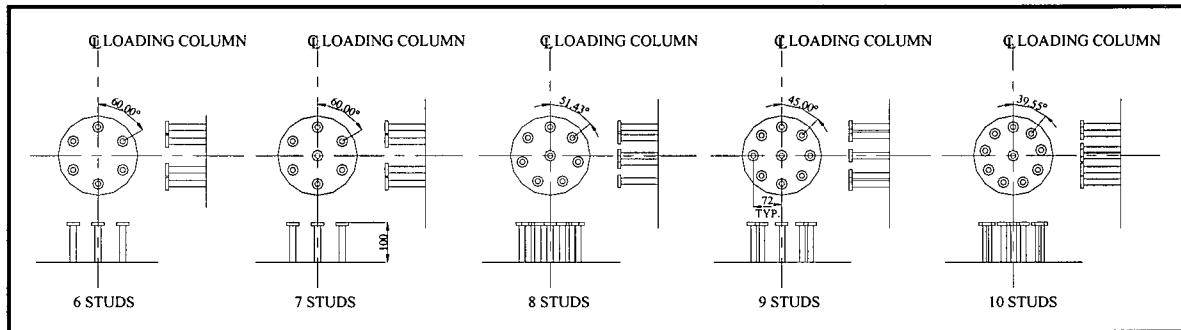
3.2.2 Push Test Design and Construction

Push test specimens were constructed to determine the shear stud cluster behaviour. Headed steel shear studs were welded to a 32 mm thick steel plate. The numbers of studs

in a cluster ranged from six to ten inclusively and were laid out in a 72 mm radius circle, as shown in Figure 3-3. The 16mm steel studs used in the experiments represent a scale factor of 0.73 for 22mm diameter studs commonly used in bridge construction.

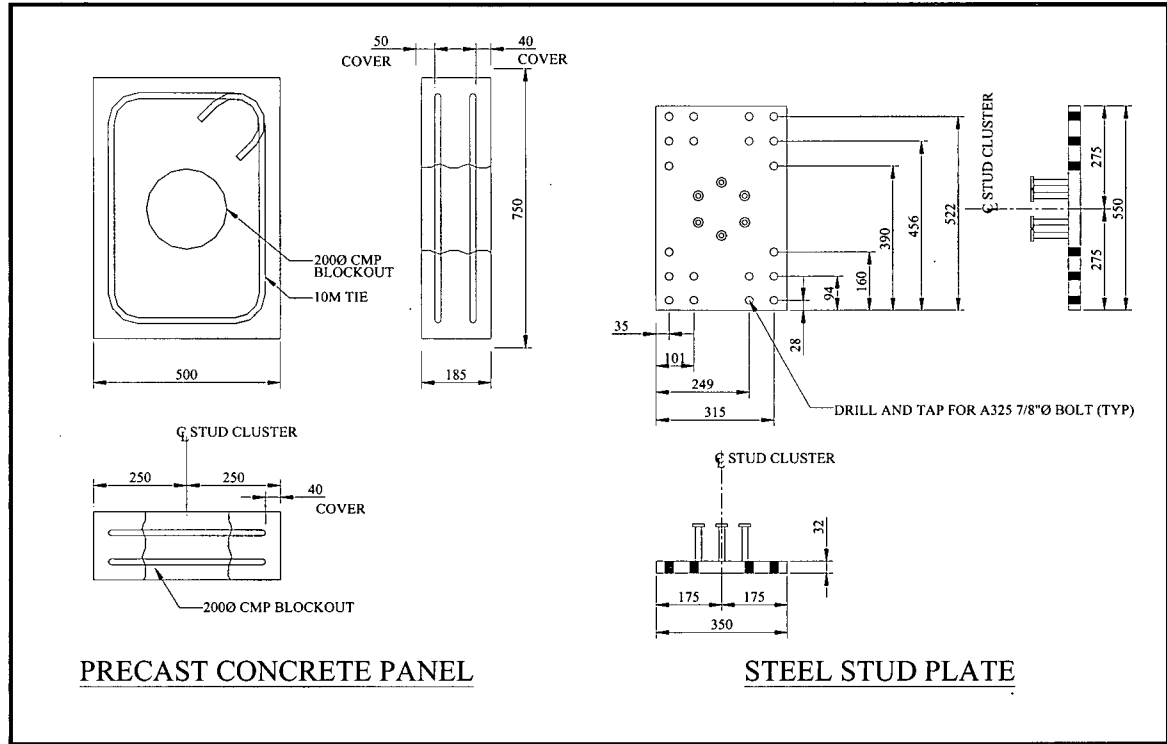
Consequently, the push test specimen components were scaled to 73% to reproduce the geometry of a typical full-scale stud cluster.

Figure 3-3 Stud Cluster Geometry



The stud clusters were welded to 350AT steel plates which were laid horizontally and the precast concrete panels placed on the steel plates. The precast panels were all cast at the same time using the same concrete mix. The stud cluster configuration chosen is similar to those used in bridge construction. This allowed the shear stud clusters to be grouted to the precast concrete panels in the horizontal position simulating construction techniques and using the same grout mix for similar specimens. To isolate the performance of the shear studs, petroleum jelly was spread over the top surface of the plate to remove friction and inhibit the chemical bond between the grout and the steel. The plates were bolted to a loading column, consisting of a custom fabricated welded steel wide flange beam that was bolted to the hydraulic actuator. This eliminated the need for expensive and time consuming welding and required only ten plates since they were reused, after the monotonic testing was completed, by welding new stud groups onto the opposite face of the plates. The grout pocket diameter was chosen to suit the scaled down specimens resulting in the selection of a 200mm diameter corrugated steel pipe with a wall thickness of 1.6mm.

Figure 3-4 Concrete Panel and Steel Plate for Push Test Specimens



3.2.3 Push Test Configuration

The push tests had two physical setups: unsymmetrical (one precast panel) for monotonic loading and symmetrical (two precast panels) for cyclic loading. The unsymmetrical configuration illustrated in Figures 3.5 and 3.6 was adopted for the monotonic push tests to determine the ultimate and residual strength of the stud cluster. Contrary to the test procedures of other researchers, the testing of one panel at a time was chosen to maintain system stability at failure and ensure complete failure of each panel. This also allowed data to be collected for the full range of the loading for each concrete panel tested without having to make assumptions regarding the distribution of load and reduced demands on the hydraulic system. The symmetrical setup was chosen for the cyclic load system to reduce the testing time requirements. The base of the precast concrete specimens was uneven and required a smooth bearing surface to ensure even distribution of pressure from the floor reaction and to provide a specimen that was plumb. This was accomplished by placing the concrete panel in a mortar bed of Hydro-Stone®, a gypsum cement produced by the United States Gypsum Company.

Figure 3-5 Unsymmetrical Test Setup Front

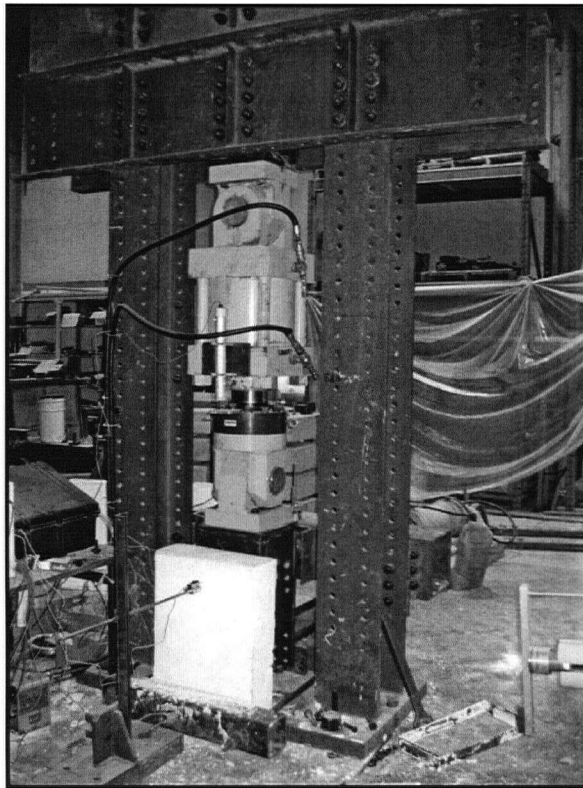
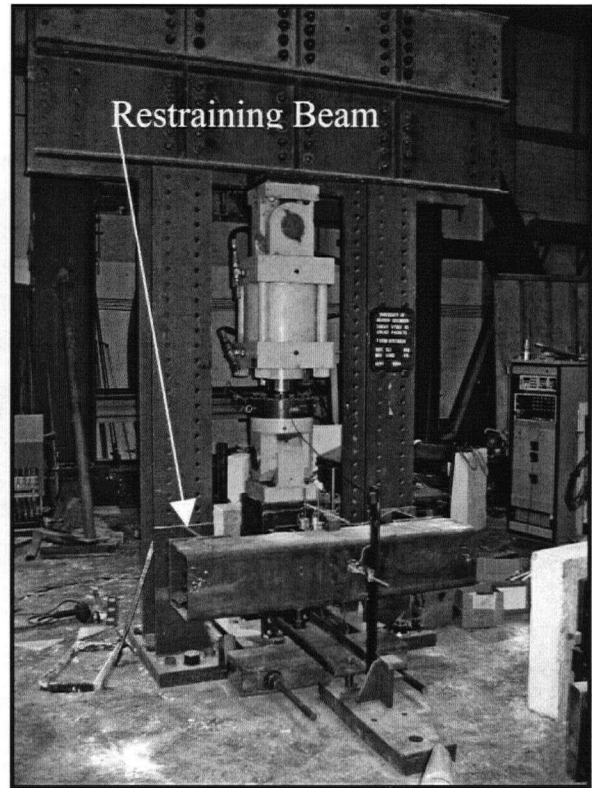


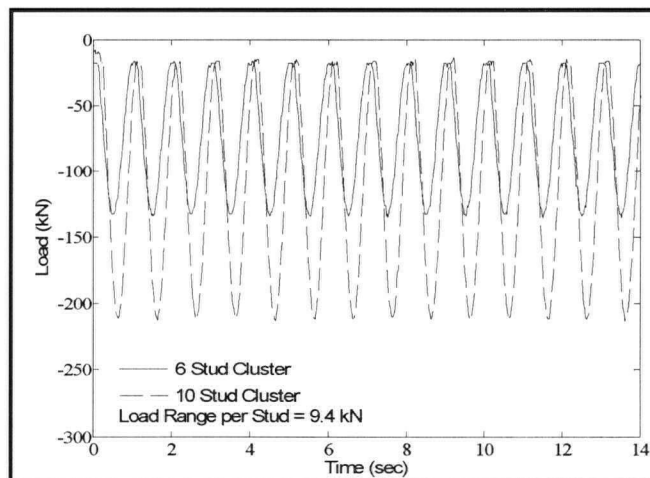
Figure 3-6 Unsymmetrical Test Setup Back



3.2.4 Loading Routine

The monotonic loading was conducted under displacement control until failure of the stud cluster was observed. The cyclic loading, shown in Figure 3-7 was a unidirectional sinusoidal wave, conducted under load control conditions at a frequency of 1 Hz for a predetermined number of

Figure 3-7 Unidirectional Cyclic Loading



cycles, namely 250,000, 500,000, and 750,000. The two panels were loaded for 250,000 cycles, then one panel removed and a new panel bolted to the loading column for another

500,000 cycles, resulting in 250,000, 500,000 and 750,000 cycles. A nominal load of 15 kN was kept on the panel to ensure stability during testing. For the cyclic loading, it is assumed that the load was shared equally between each panel. The stress range used for loading during the cyclic testing conforms to the permissible range of interface shear found in clause 10.17.2.6 in the CHBDC for a Class C highway. A class C highway has an Average Daily Truck Traffic (ADTT) of 250, providing 5.8 million fatigue cycles in 75 years for two design lanes. The CHBDC allowable stress range for fatigue of a 16 mm diameter shear stud translated to a load of 9.4 kN per stud. The more heavily traveled highways, i.e. class B and A, have permissible range of shear that equates the endurance limit for fatigue. To determine the residual strength of the shear stud group, the monotonic load procedure previously described was used, testing one panel at a time.

3.2.5 Instrumentation

For the monotonic loading instrumentation, a set of nine linear variable displacement transducers (LVDT) and 2 load cells were used. A LVDT was positioned on both sides of and at the center of the stud cluster to record the relative slip between the steel plate and the concrete panel. Additional LVDTs were used to record the out of plane displacement of the concrete panels and two measured displacement of the restraining beams any displacement of the load cell mounted on the restraining beam and to measure the stroke of the hydraulic actuator. Load cells were used to measure the applied load from the hydraulic actuator and the induced load on the restraining beam.

3.2.6 Push Test Regime

The experimental push test program included 15 push test specimens. Nine of the specimens were loaded monotonically to determine the ultimate strength of 5 different stud cluster groups, with the remaining 6 used to determine the residual ultimate strength after being exposed to cyclic loading.

Six studs were machined and tested to determine the average yield strength at 0.2% offset of 428.3 MPa and an average tensile strength of 536.0 MPa. The average compressive stress of nine 300mm x 150mm concrete cylinders cast for the concrete slab was found to be 41.8 MPa. Target Traffic Patch Coarse Mix, a shrink compensated, steel fibre

reinforced, high early strength premixed grout was used in the grout pockets to attach the concrete panels to the steel plates. The selected grout is commonly used for precast deck panel construction in British Columbia. Both the grout and the concrete were allowed to cure for a minimum of 100 days prior to testing the cylinders and push test specimens to mimic in-service conditions. Average cylinder strengths for the grout ranged from 48.7 MPa to 68.9 MPa.

Table 3-1 provides the labelling convention for the push test specimens and the loading condition.

Table 3-1 Push Test Specimen Summary

Panel No.	Studs per Cluster	Test Type*	Monotonic Setup**	Cyclic Setup**	No. of Load Cycles	Grout Comp. Strength (MPa)
6A	6	M	A	-	-	45.6
6B	6	M	A	-	-	45.6
6C	6	C/M	A	S	250,000	59.9
6D	6	C/M	A	S	500,000	59.9
6E	6	C/M	A	S	750,000	59.9
7C	7	M	A	-	-	59.9
8A	8	M	A	-	-	63.1
8B	8	M	A	-	-	63.1
9A	9	M	A	-	-	53.7
9B	9	M	A	-	-	53.7
10A	10	M	A	-	-	60.9
10B	10	M	A	-	-	60.9
10C	10	C/M	A	S	250,000	66.4
10D	10	C/M	A	S	500,000	66.4
10E	10	C/M	A	S	750,000	66.4

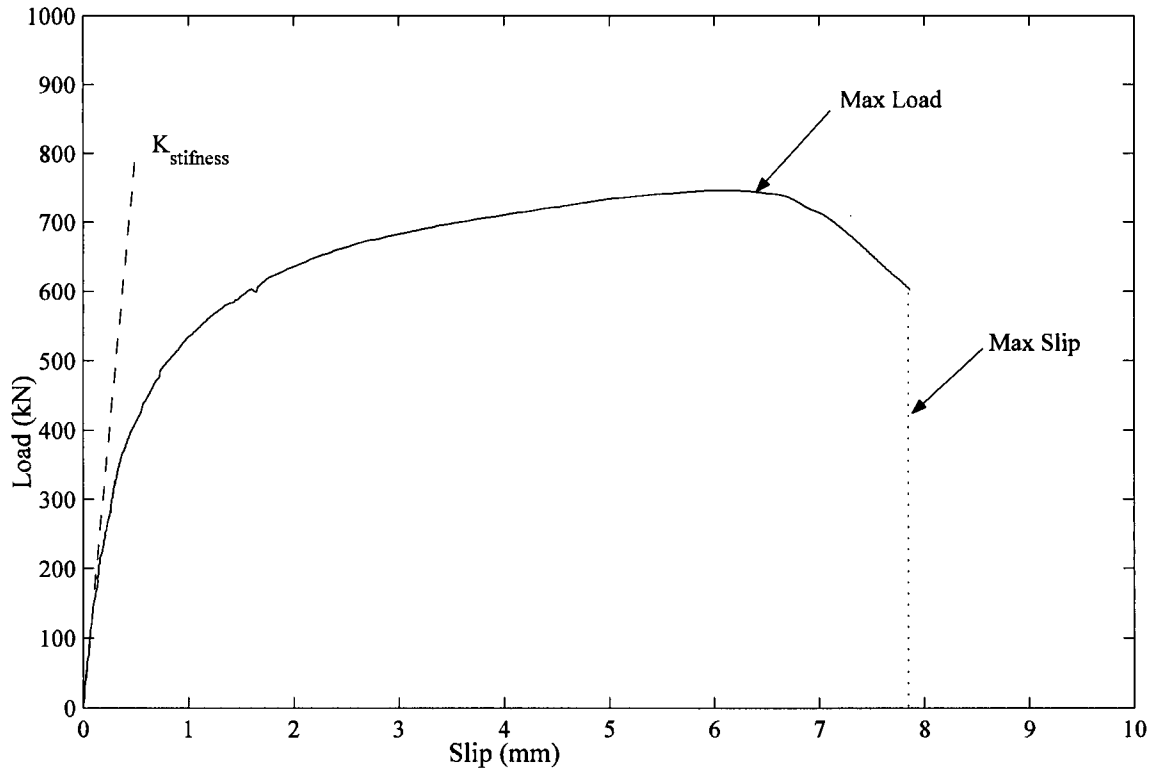
* M = Monotonic Loading, C = Cyclic Loading

** S = Symmetrical, A = Asymmetrical

3.3 Stud Cluster Performance

Observations during the testing and of the failure mode of the stud cluster are provided and comparisons made to the code equations provided in CAN/CSA-S6-00 and to the results of research completed by others. The schematically illustrated load vs. slip plot for a push test, along with stiffness is further defined in Figure 3-8.

Figure 3-8 Schematic Push Test Plot



The maximum slip, $Slip_{max}$, was taken at the point where the first substantial drop in load occurred. The load level used to determine the stud cluster stiffness was chosen to be 7% of the maximum load, since this closely corresponds to the stress range associated with a Class C highway, and is representative of in-service loading conditions. The stiffness of a stud cluster is defined in Equation 3-1.

$$k = \frac{P_{0.7max}}{Slip_{0.7}} \quad (3-1)$$

Ductility has been defined as per Equation 3-2.

$$Ductility = \frac{Slip_{max}}{\left(\frac{P_{max}}{k}\right)} \quad (3-2)$$

3.3.1 Qualitative Observations from Push Tests

Cracking of the precast concrete panel was observed at higher load levels, typically first occurring at approximately 200 kN; this is collateral damage as a result of the grout pocket bearing against the concrete. The cracking pattern was found to be consistent between specimens. Cracking was for the full depth of the panel with, in some instances, a vertical crack occurring above the grout pocket at about the 1000 kN load range, attributed to the effect of the grout pocket expanding horizontally. Due to the location of instrumentation, cracking of the concrete panels did not influence the slip data reported here.

3.3.2 Ultimate Strength

Table 3-2 provides a summary of the test results and the derived properties for the monotonically loaded push tests.

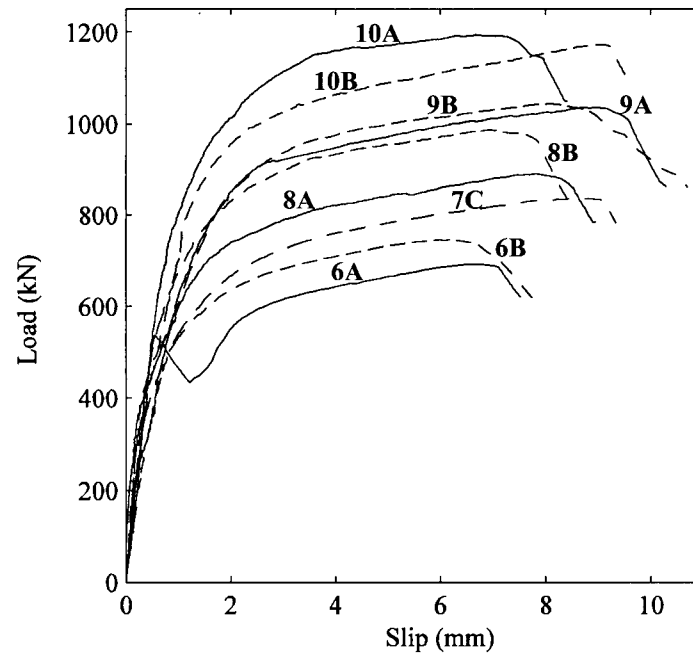
Table 3-2 Monotonic Push Test Summary

Panel No.	P _{max} (kN)	Slip _{max} (mm)	P _{0.7max} (kN)	Slip _{0.7} (mm)	k (kN/mm)	Ductility
6A	693.2	7.5	48.5	0.0444	1092.3	11.82
6B	746.0	7.9	52.2	0.0341	1527.7	16.17
7C	836.1	9.3	58.5	0.0643	909.7	10.12
8A	890.6	9.0	62.3	0.0488	1280.4	12.94
8B	987.4	8.5	69.1	0.0650	1213.9	10.45
9A	1036.1	10.3	72.5	0.0485	1493.6	14.85
9B	1043.9	10.7	73.1	0.0549	1329.8	13.63
10A	1194.3	8.4	83.6	0.0808	1033.5	7.27
10B	1173.5	9.6	82.1	0.0637	1288.4	10.54

Figure 3-9 provides a combined plot of the load slip characteristics for the monotonic load tests. The initial stiffness of the studs is similar and is fairly consistent, showing that

additional studs provide no appreciable increase in stiffness. There is also a trend of increased plastic deformation with an increase in the number of studs. All the test specimens exhibited ductility, which is a required characteristic to allow load sharing among stud groups throughout the length of the superstructure. The premature failure of one stud is believed to have resulted in the sharp drop in capacity for Specimen 6A at a slip of 0.5 mm.

Figure 3-9 Combined Ultimate Strength of Monotonic Push Tests



Shim et al. (2002) proposed the following equation for the ultimate strength of a shear connector in a precast concrete panel.

$$Q_u = \alpha(0.36A_{sh} + 18.71) \quad (3-3)$$

$$\alpha = 1 - 0.086(B_h - 20)$$

Where Q_u is the ultimate strength of a single shear stud in kN, α is the reduction factor for the bedding thickness (1.0 for no bedding), A_{sh} is the cross sectional area of the shear stud shank mm^2 , and B_h is the bedding layer thickness mm.

Equation 3-3 was deemed to be suitable for predicting the ultimate strength of a shear connector, accounting for a grout bedding layer between the concrete panel and steel plate, provided that the grout is greater than 55 MPa.

Ollgaard et al.'s (1971) original work on the ultimate strength of shear studs was then expanded by Oehlers et al. (1995) to account for variation of material properties. Data was gathered from various push tests and a statistical analysis was performed. The following equation can be used for analysis purposes to predict the strength of a shear stud connector in cast-in-place concrete push tests:

$$(D_{\max})_{push} = \left(5.3 - \frac{1.3}{\sqrt{n}} \right) A_{sh} f_u^{0.65} f'_c{}^{0.35} \left(\frac{E_c}{E_s} \right) \quad (3-4)$$

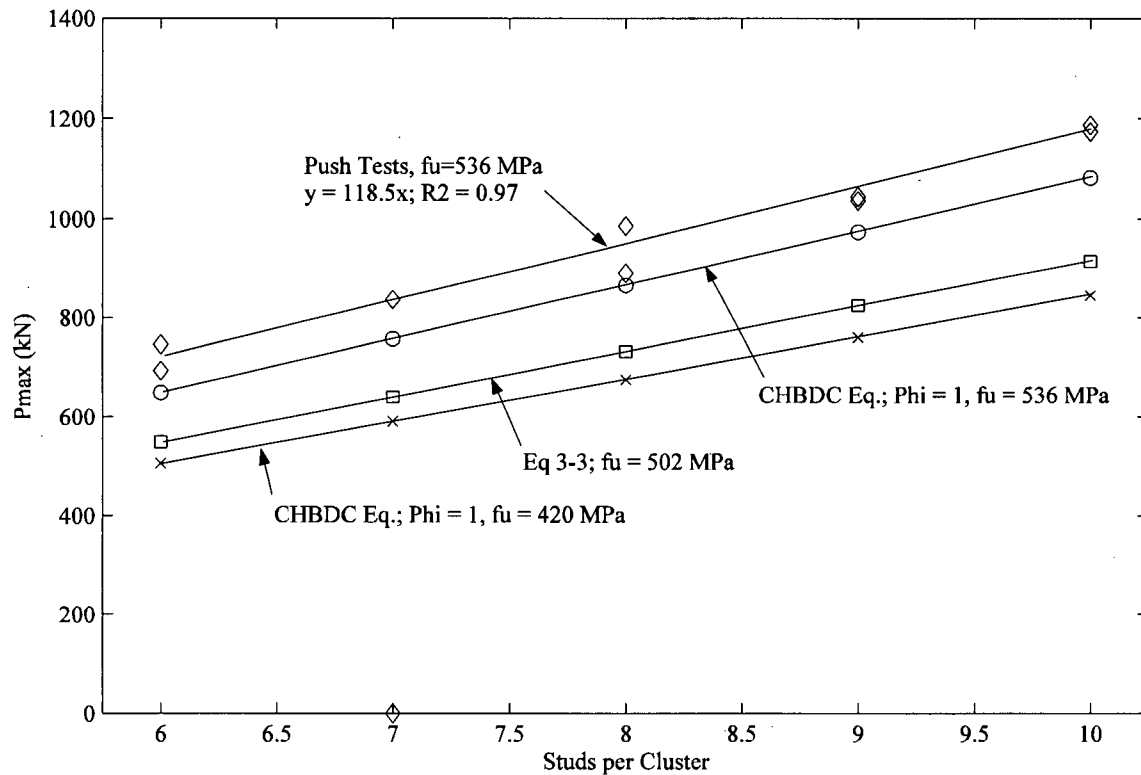
where $(D_{\max})_{push}$ is the shear strength of a connector in a push test, n is the number of shear connectors, A_{sh} is the cross-sectional area of the shear stud, f_u is the ultimate tensile strength of the stud, f'_c is the compressive cylinder strength of the concrete, E_c is the concrete modulus of elasticity, E_s is the steel modulus of elasticity.

Figure 3-10 compares the ultimate strength observed in the monotonic push tests and the strength predicted by Equation 3-3, Equation 3-4 and the CHBDC requirements. The tensile capacity of the steel stud is used as an upper bound, consistent with the observed pull out failure mechanism for the current code equation in cl. 10.11.8.3, which is presented in Equation 3-5.

$$q_r = 0.5\phi_{sc} A_{sc} \sqrt{f'_c E_c} \leq \phi_{sc} F_u A_{sc} \quad (3-5)$$

where q_r is the shear stud resistance, ϕ_{sc} is the resistance factor for the shear connectors, A_{sc} is the area of the shear stud, f'_c is the specified compressive strength of the concrete, E_c is the modulus of elasticity of the concrete and F_u is the minimum tensile strength of the steel stud.

Figure 3-10 Ultimate Strength Comparison



Based on the test data, the ultimate strength of the stud cluster scales linearly with the number of studs and the CHBDC equation provides a lower bound to the measured monotonic strength. Linear regression line returns a value of 118.5 kN per stud with a correlation coefficient value of 0.97 for the monotonic push tests. The equation of Shim et al. (2002) predicts a value of 91.5kN per stud, approximately 93 percent of the tensile strength of the studs used in this experiment. Shim's equation was based on the best data fit with the studs used in the experiment having a tensile strength of 502 MPa.

3.3.3 Residual Strength

The CHBDC assumes that the ultimate strength of a shear stud is independent of the loading history, and only experiences fatigue failure upon reaching its endurance limit. Oehlers et al. (1995) showed that there is a reduction of the ultimate strength of a shear stud embedded in cast-in-place concrete panels exposed to cyclic loading (referred to here as the residual strength) as result of crack propagation and that there is a linear relation between the residual stud strength and the number of cycles. This suggests that it

is possible that a shear stud could fail prior to reaching its fatigue endurance limit if exposed to overload. Since the shear studs are not accessible for inspection during the service life of the bridge, the fatigue design is critical in the performance of the superstructure. The equation used to predict the reduction in stud strength is:

$$N_e = N_f \cdot \left(1 - \frac{P_m}{P_s}\right) \quad (3-6)$$

where N_e is the number of cycles to reduce P_s to P_m , N_f is the number of cycles to reach endurance limit, P_m is the static strength after N_e cycles (kN) and P_s is the static strength (kN) of the shear stud.

Table 3-3 provides a summary of the residual strength testing. The residual strength of both the 6 and 10 stud cluster groups shows a modest reduction in the ultimate strength as a result of being exposed to cyclic loading. The damage accumulated from the cyclic loading also tends to reduce the deformation capacity, particularly for 750,000 cycles.

Table 3-3 Residual Strength Summary

Panel No.	No. of Load Cycles	$P_{\max\text{res}}$ (kN)	$\text{Slip}_{\max\text{res}}$ (mm)	$P_{0.7\max}$ (kN)	$\text{Slip}_{0.7}$ (mm)	k (kN/mm)	Ductility
6E	250,000	682.6	7.2	47.7	0.0376	1270.2	13.40
6C	500,000	650.7	9.0	45.5	0.0382	1190.2	16.46
6D	750,000	621.2	5.9	43.5	0.0650	668.2	6.35
10D	250,000	1113.2	16.7	77.9	0.0886	879.3	13.19
10C	500,000	1125.6	9.5	78.8	0.1014	777.0	6.56
10E	750,000	1087.0	8.2	76.1	0.1138	668.5	5.04

Figure 3-11 Residual Strength 6 Stud

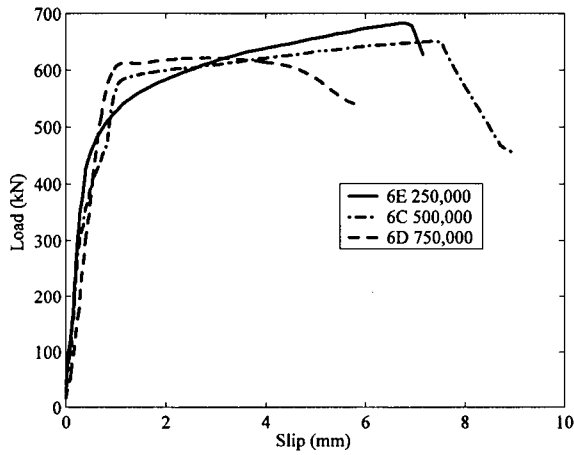


Figure 3-12 Residual Strength 10 Stud

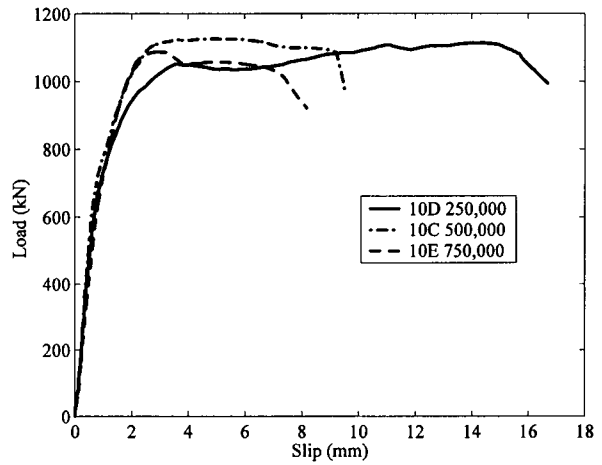
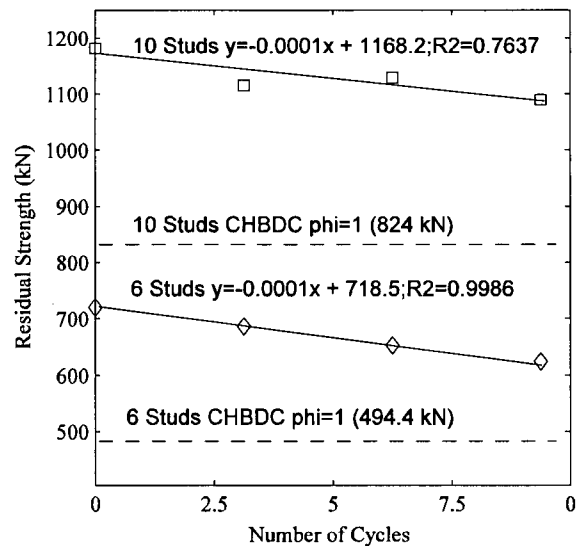


Figure 3-13 provides a plot of the residual strength of the 6 and 10 stud clusters versus the number of cycles. As witnessed by Oehlers (1995), after cyclic loading the shear stud connections experienced a reduction of the ultimate (residual) strength of the shear stud connections. The 6 stud cluster group shows exceptional fit with linear regression, with the 10 stud cluster also presenting a linear trend.

Figure 3-13 Residual Strength vs. No. Cycles



The data points corresponding to the “zero” cycles is the average of the two monotonic test results.

Using Equation 3-6, and assuming that N_f is 5.8 million cycles which is the endurance limit for a shear stud in CHBDC and is also the cyclic load range that the push tests were subjected too, the residual strength P_m is predicted for the given number of loads and compared to the strength from the push tests.

Table 3-4 Comparison of Residual Strengths

No. of Load Cycles	6 Studs		10 Studs	
	P_{maxres} (kN)	P_m (kN)	P_{maxres} (kN)	P_m (kN)
250,000	682.6	688.6	1113.2	1132.9
500,000	650.7	657.6	1125.6	1081.8
750,000	621.2	626.5	1087.0	1030.8

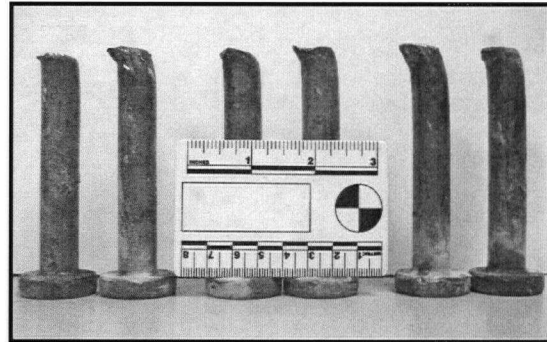
Observation of Table 3-4 that there is a strong correlation and since the equation is linear, interpolation yields that the code strength prediction would be eclipsed at approximately 1.8 million cycles, or about one third of the bridges design service life. This is considered to be a un-conservative approach to the design of the shear stud connection, bearing in mind that the studs can not be visually inspected for fatigue damage. Additional data on the full range of fatigue properties needs to be collected to confirm the assumptions and hypothesis, prior to implementing in design.

3.3.4 Stud Cluster Failure Mechanism

The studs failed near the base of the stud for all monotonic loading tests. There were three distinct zones of failure observed among the different specimens: at the plate; at the top of the weld collar; or along a secondary shear plane approximately 6mm to 8mm above the base of the plate (or approximately 0.6 times the diameter of the stud). Contrary to the observations of Ollgaard et al. (1971), where the stud was deformed in bending over the full height, the studs deformed mainly in shear for only the first 6-8 mm, with the upper portion of the stud remaining undeformed. In some instances, some portions of the weld collar were also sheared from the plate. The lack of deformation along the stud was likely due to the high strength of the grout and additional confining pressures provided by the CMP blockout. Figure 3-14 shows the typical deformation of the studs after removal from the grout pocket. Note the concentration of deformation at the base of the stud, which is similar to that reported by Shim et al. (2000).

Regardless of the number of studs, there were no indications of overlapping zones of influence between two studs in the same cluster. No other damage was observed in the grout pocket. As noted above, the steel corrugated metal pipe grout pocket provides a confining force for the grout pocket, minimizing damage to the grout medium.

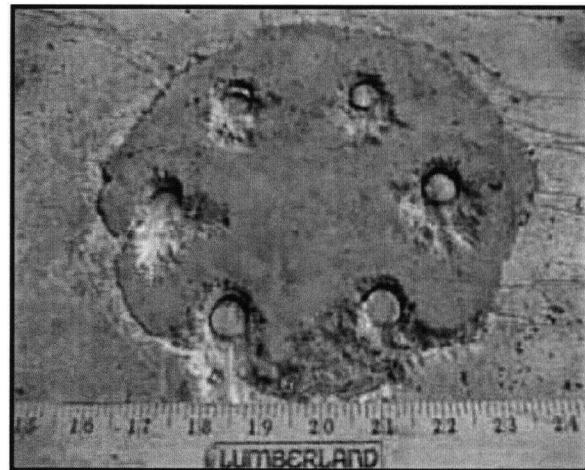
Figure 3-14 Stud Deformation for Specimen 6B



After all the data was collected from the specimens, the studs were removed from the grout pockets of a select number of specimens with a concrete rotary drill and jackhammer

Crushing and powdering of the grout was observed for a depth of approximately 8mm to 10mm at the leading edge of the studs, as they bore against the grout (Figure 3-15). The trailing edge of the studs pulled away from the grout, leaving a gap consistent with the slip reading from the LVDTs. Localized crushing of the concrete panel was also observed at the leading edge of the grout pocket.

Figure 3-15 Grout Pocket Damage



3.4 Parametric Bridge Study

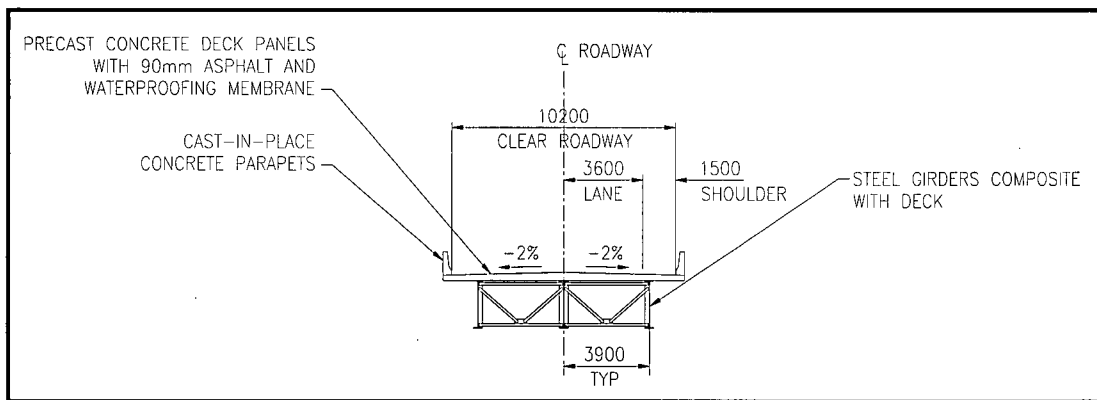
A 36 meter span composite superstructure was designed using the conventional methods provided in CAN/CSA-S6-00. The superstructure was subsequently modeled with three dimensional finite elements using the commercially available STAAD.Pro 2005™ to investigate the effect of varying the longitudinal stud spacing of the shear stud clusters has on the deflection and the first frequency of vibration. The spacing considered include

300 mm, 600 mm, 1200 mm and 2400 mm. A total of 10 models were created and considered a total of four stud cluster stiffness'; infinitely rigid, experimental, half of the experimental and infinitely flexible.

3.4.1 Bridge Design

The superstructure has a 10.98m wide deck providing a 10.2m wide driving surface (Figure 3-16). The deck was designed as a variable depth precast concrete panel system to provide deck crossfall, incorporating standard 810mm high cast-in-place concrete parapets complete with a steel railing. An allowance was included in the design for a 90mm thick asphalt wearing surface. A three girder superstructure system was chosen, providing 3.9m center to center of girders and a 1.59m deck cantilever.

Figure 3-16 Superstructure Cross Section



The superstructure was designed to maximize the flexibility, since this would have the largest impact on the serviceability limit states. The superstructure design was completed using the "simplified methods of analysis" in CAN/CSA-S6-00 and finite element plate models generated from the design to check the serviceability limit states using the commercially available analysis package STAAD.Pro 2005™.

3.4.2 Finite Element Model

Details of typical superstructure design not contributing to the stiffness of the superstructure system, such as girder splices and stiffener plates, were specifically not included. The model used four node plate elements to represent the deck and plate girder web. Beam elements were used for the top and bottom flanges, in addition to the

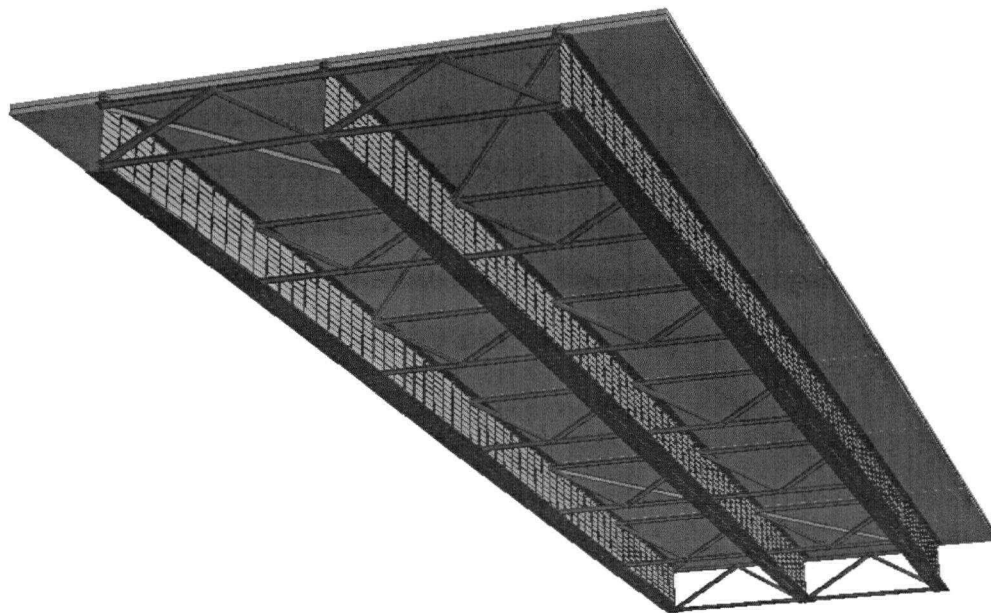
diaphragms and plan bracing. The connections of the diaphragms and plan bracing were modeled with an offset from the flanges to represent a typical connection detail. The shear connection of the stud cluster was modeled with a rigid beam element between the top flange and the, and a spring was used at the top flange to model the stud cluster stiffness. Since the model with the stud clusters spaced greater 300 mm had more elements than the other models, these elements were provided with no density so as not to affect the frequency calculations. The number of plates in all the models was 4200, and the minimum number of beam elements totalling 1522. The boundary conditions were assumed to be the classic pinned-roller supports. The isotropic material properties used in the model are consistent with CAN/CSA-S6-00 and are summarised below.

Table 3-5 Finite Element Mechanical Properties

	Elasticity (MPa)	Possion Ratio	Density (kN/m³)
Steel	200000	0.3	77
Concrete	24648	0.2	24

Figure 3-17 shows the typical finite element model layout from the soffit of the superstructure.

Figure 3-17 Finite Element Model



The following longitudinal stud cluster spacings were considered: 300mm, 600mm, 1200mm and 2400mm. Two stud cluster stiffness' were considered: the average stiffness value from the push tests (1100 kN/mm), half of the average stiffness value from the push tests (550 kN/mm), in addition to the upper and lower bounds of the cases where rigid and flexible connections are considered. The deflection of a superstructure with an infinitely rigid and no shear connection were also calculated at the midspan for the exterior girder and are 38.7 mm and 109.9 mm respectively. The span to deflection ratios varied from 913 to 807 and the absolute values of the deflections are summarized in Table 3-6 for the CHBDC Serviceability Limit States.

Table 3-6 Static Deflections at Midspan of Exterior Girder (mm)

	Longitudinal Cluster Spacing			
	300 mm	600 mm	1200 mm	2400 mm
Experimental Shear Stiffness	39.4	39.4	40.3	42.0
0.5X Experimental Shear Stiffness	40.1	40.1	41.8	44.6

The fundamental frequency of the superstructure was also calculated using modal analysis and the results are presented in Table 3-7. The fundamental frequency of the superstructure with infinitely rigid connection is 2.536 Hz and the superstructure with no shear connection has a frequency of 1.282 Hz.

Table 3-7 First Flexure Frequencies (Hz)

	Longitudinal Cluster Spacing			
	300 mm	600 mm	1200 mm	2400 mm
Experimental Shear Stiffness	2.516	2.516	2.490	2.441
0.5X Experimental Shear Stiffness	2.494	2.494	2.451	2.377

The allowable deflections from CAN/CSA-S6-00 are related to the first flexural frequency of the superstructure, which provides for a larger deflection for more flexible systems. Hence the calculated and allowable deflections parallel each other since

increasing the spacing of the shear stud clusters tends to increase the flexural frequencies. The allowable deflection corresponding with the infinitely rigid connection is a pragmatic choice as a limit for deflection of this system, since it is the typical assumption made in design, provides a conservative limit and is consistent with the level of sophistication typically used in the design of these structures.

Two plots of the deflection data are provided, corresponding to the two connection stiffness', to compare the calculated deflection against the allowable static deflections. In both cases all the four stud cluster spacing meets the code requirements for deflections, but would not be constructible at the 2400 mm spacing, since the number of studs per cluster is 26, which will not fit in a grout pocket. The 1200 mm spacing required up to 13 studs, considered to be within the range of extrapolation from the push test data.

Figure 3-18 Deflections for Stud Clusters with Experimental Stiffness

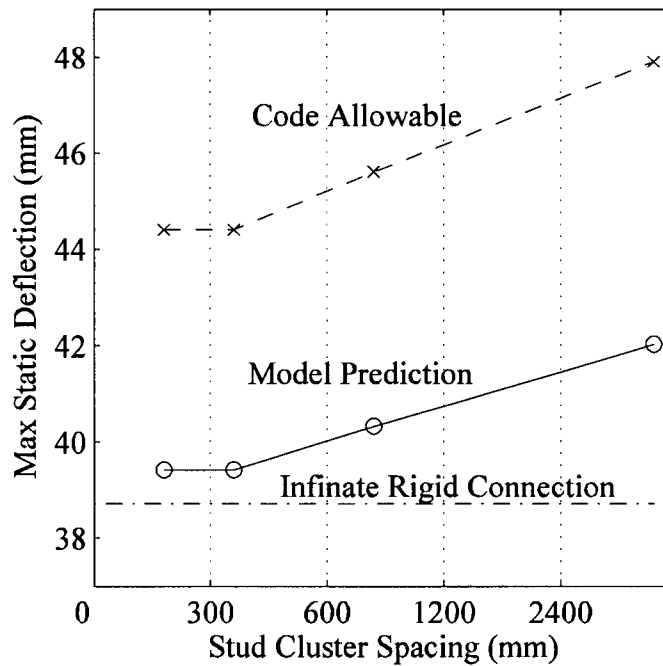
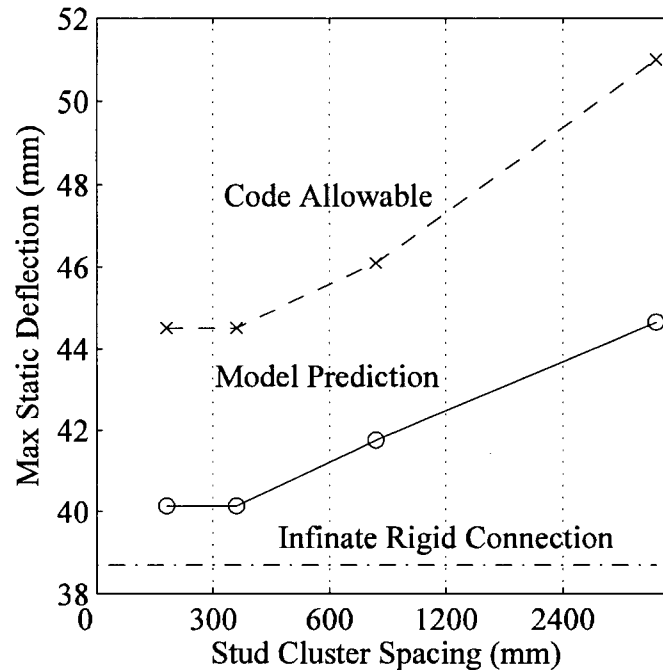


Figure 3-19 Deflections for Stud Clusters with 0.5X Experimental Stiffness



3.5 Conclusions

Based on the push test experiment results and preliminary analysis of the finite element models, the findings from this study suggest that the CHBDC prescribed maximum 600mm spacing of shear studs can be exceeded for shear stud groups if using a grout pocket similar to that used in the experiments. Since the majority of precast concrete deck panels are in the range of 3 metres in length because of lifting, shipping and handling considerations, the 1200 mm spacing is a pragmatic choice to limit stud cluster spacing, with only a minor increase in the deflections from the rigid case with 300 mm spacing.

The push tests also confirm that the CHBDC equations provide a lower bound to ultimate strength of a stud cluster. An immediate reduction of the monotonic shear strength was observed with increased number of cycles but further study is required to predict the residual strength of the stud clusters over the full range of stress and number of cycles used in design. It is recommended that other potential grout pocket / stud cluster configurations be push tested to confirm their performance in order to extend the conclusions of this study to other configurations.

3.6 References

- CSA. 2000. *Canadian Highway Bridge Design Code*. CAN/CSA-S6-00, Canadian Standards Association, Rexdale, Ontario, Canada.
- Gulyas R.J., Wirthlin G.J., and Champa J.T. 1995 "Evaluation of Keyway Grout Test Methods for Precast Concrete Bridges." *PCI Journal*, Vol. 40, No. 1, pp. 44-57.
- Issa M.A., Idriss A.T., Kaspar I.I., and Khayyat S.Y. 1995a "Full-Depth Precast and Prestressed Concrete Bridge Deck Panels." *PCI Journal*, Vol. 40, No. 1, pp. 59-80.
- Issa M.A., Yousif A.A., Issa M.A., Kaspar I.I., and Khayyat S.Y. 1995b "Field Performance of Full-Depth Precast Concrete Panels in Bridge Deck Construction." *PCI Journal*, Vol. 40, No. 3, pp. 82-108.
- Issa M.A., Yousif A.A., and Issa M.A. 1995 "Construction Procedures for Rapid Replacement of Bridge Decks." *Concrete International*, Vol. 17, No. 2, pp. 49-52.
- Kim J.H., Shim C.S., Matsui S., and Chang S.P. 2002. "The Effect of Bedding Layer on the Strength of Shear Connection in Full-Depth Precast Deck." *Engineering Journal*, Third Quarter, pp. 127-135.
- Oehlers D.J. and Bradford M.A., 1995, "Composite Steel and Concrete Structural Members Fundamental Behaviour." *Elsevier Science Ltd*.
- Oehlers D.J., Ghosh A., and Wahab M., 1995, "Residual Strength Approach to Fatigue Design and Analysis", *Journal of Structural Engineering*, September, pp. 1271-1279.
- Oehlers D.J., 1995, "Design and Assessment of Shear Connectors in Composite Bridge Beams." *Journal of Structural Engineering*, February, pp. 214-224.
- Ollgaard J.G., Slutter R.G., and Fisher J.W., 1971 "Shear Strength of Stud Connectors in Lightweight and Normal-Weight Concrete." *AISC Engineering Journal*, April, pp. 55-64.
- Slutter R.J., and Fisher J.W., 1967, "Fatigue Strength of Shear Connectors." *Highway Research Record No. 147*. Highway Research Report, Washington D.C.
- STAAD.Pro 2005, 2005 "STAAD.Pro 2005 Getting Started and Tutorials", Software Users Manual, Research Engineers International, Yorba Linda, California
- Tadros M.K., and Mantu M.C. 1998 *Rapid Replacement of Bridge Decks*. NCHRP Report 407. Transportation Research Board, Washington, D.C.

4.0 CONCLUSIONS AND RECOMMENDATIONS FOR FUTURE RESEARCH

4.1 Summary and Conclusions

The work for the thesis consisted of a literature review on for the design and construction of shear studs used in composite construction that consider a steel girder in combination with a precast or cast-in-place concrete decks. Following in the footsteps of previous researchers, push test specimens were designed and constructed to experimentally determine the performance of headed shear stud clusters grouted to precast concrete panels, with the main variable being the number of studs within one cluster. A 36.0 meter simply supported composite bridge was designed and subsequently used in a parametric study. The parametric study used a three dimensional finite element model to determine the fundamental frequency and maximum static deflection for various longitudinal spacing of stud clusters.

The findings from this study suggest that the CHBDC prescribed maximum 600 mm spacing of shear studs can be exceeded, without compromising the response of the structure, following conventional design methods. This is applicable for shear stud clusters if using a grout pocket similar to those used in the experiments. Without further studies, it is suggested that a pragmatic limit of 1200 mm be adopted for the longitudinal spacing of stud clusters.

The push tests also confirm that the CHBDC equations provide a lower bound to ultimate strength of a shear stud cluster in high strength grout. Given the limited zone of damage at the base of the studs, and the linear relationship between the number of studs and the ultimate strength, it is suspected that increasing the number of studs to say 13 or 14 would not be unreasonable.

A modest reduction of the monotonic shear strength was observed with increased number of load cycles but, while the CHBDC requirements for ultimate strength appears to provide sufficient conservatism for the number of cycles considered in this study, not enough data was gathered to provide design guidance for cycles beyond 750,000. Further push test experiments are required to quantify the potential for stud failure due to

overload prior to reaching the endurance limit. It is recommended that other potential grout pocket / stud cluster configurations be push tested to confirm their performance in order to extend the conclusions of this study to other configurations.

4.2 Recommendations for Future Research

As identified from the literature and from observation of current construction and design practices, there are numerous issues related to the response of full-depth precast deck panel systems that require further research. The current edition of the CHBDC explicitly allows for the design and construction of full depth precast concrete deck panels, but still bases the design of the shear studs on research conducted on cast-in-place concrete decks.

Some directions that could be taken to research the shear connection include:

- Conduct additional monotonic push tests with more than 10 studs per cluster;
- Conduct additional push tests with various stress ranges and number of cycles up to the endurance limit of the studs;
- Conduct push tests on other grout pocket styles currently in use;
- Conduct cyclic and monotonic push tests with specimens that use a grout bedding layer;
- Perform visual condition survey of existing bridges constructed with full-depth precast deck panels;
- Use full instrumentation of in-service bridges constructed with this deck system to monitor field performance and durability; and
- Investigate the effect that post-tensioning of precast concrete deck has on stud response and durability.

The instrumentation and analysis of an in-service bridge that utilizes the precast deck system is of prime interest. A number of factors must be considered in selecting the bridge for instrumentation, such as power supply, data capture and transmission, adequate volume of traffic. The data to be measured would be the slip at the interface between the concrete deck and the steel girders. This could be accomplished with the use of linear

variable differential transformer sensors placed at the deck soffit to capture both horizontal and vertical displacements. The slip data would need to be captured over a period of years to provide data on the degradation of the stud clusters. Other instrumentation would include the incorporation of strain gauges on the steel girders and, ideally, the shear studs at the top of the grout bedding layer. Accelerometers would most likely be included and could be used to record vibrations induced by traffic and to track any degradation of the superstructures stiffness and provide valuable data after seismic events.

APPENDIX A Push Test Program

The design of the test specimens was initially completed to satisfy the symmetric test setup and was driven by the capacity of the hydraulic actuator using the symmetric test setup and the strength of the reaction frame and its components. A sixteen millimetre diameter stud was chosen for the studs, allowing up to ten studs per pocket, which was felt was a reasonable number of studs for current construction practices. The bulk of studs used in the design and construction of superstructures are 22mm diameter, yielding a scaled down test specimen of approximately 73%. The ability to cast the concrete panels and subsequently grout the concrete panels to the steel plates in the horizontal position and using the same mix was a critical constraint that needed to be observed during the design phase of the testing.

A.1 Precast Concrete Slab

The concrete slab dimensions was chosen to be 185mm deep, following the scale value determined from the stud diameter would represent a concrete deck slab thickness of approximately 255mm, which is common for this system. The width of the slab was sized to fit the opening left between the columns of the reaction frame. The height determined based on longitudinal shear demands that would be expected in the test specimens. Both the width and the height were then optimized to suit available dimensional lumber lengths that would later be used to construct the concrete formwork. Two 10M rebar ties were provided at the top and bottom of the concrete slab to contain the concrete and assist in resisting the tendency to split the concrete in the longitudinal direction. The rebar also provides a tension tie at the base of the concrete slab.

A.2 Shear Studs and Steel Plate

A total of five distinct stud groups were designed and included groups with six, seven, eight, nine and ten studs. Each group was geometrically designed to provide a circular configuration with a radius of 72 mm. The shear stud selected for construction were manufactured by Nelson™ that were supplied by Canadian Stud Welding Associates Inc. of Delta, BC.

The stud groups were welded to ten 550x350x32 350AT steel plates. The weathering steel plates were chosen since a majority of the steel girders designed use this steel for the girders in British Columbia. Only ten plates were fabricated because they could be reused after the monotonic testing was completed, by welding new stud groups onto the opposite of the plates.

The plates were designed to be bolted to a loading column, consisting of a custom fabricated welded steel wide flange beam that was bolted to the hydraulic actuator. Figure A-1 depicts the plate with the drilled and tapped holes and stud group constructed for specimen 9A. The plates were designed and

Figure A-1 Studs Welded on Plate



constructed to allow grout to be placed in to horizontal position, from the same mix, excluding the need for expensive and time consuming welding.

A.3 Grout Pocket

The grout pocket diameter was chosen to suit the scaled down specimens resulting in the selection of a 200mm diameter corrugated steel pipe, with a corrugation profile of 38 x 6.5 and a wall thickness of 1.6 mm. This was one of the first known methods used to construct the grout pockets for precast concrete bridge deck panels in British Columbia and is easily available. Discussions with industry personnel revealed that there are other methods, such as tapered rectangular forms of steel or plywood and rubber forms which are reusable. In all instances the grout pocket is geometrically designed to resist any tensile force that is induced into the connection by shear in the precast concrete panel. The corrugations of the pipe used in the design of the test specimen meets this requirement through shear resistance provided by the varying diameter of the grout pocket and the steel ring also provides confinement for the grout pocket. Target Traffic Patch Course Mix was selected for the grout. This product is a shrink compensated, steel

fibre reinforced, high early strength premixed grout that is commonly used by contractors for grout pockets in local construction.

A.4 Push-Test Specimen Construction

A total of twenty individual concrete panels and ten steel panels were constructed for the experimental portion of this research project. The following sections document the construction of the push test specimens for both monotonic and cyclic loading.

A set of timber forms was built to place the concrete. This consisted of 38 mm x 185 mm dimensional lumber that was notched to form two rows of five panels. The dimensional lumber forms were then connected to a bed of plywood, to provide a level casting surface. A sheet of poly was placed on the top of the plywood to form as a bond breaker. The forms were oiled and joints sealed with an outdoor silicone. The corrugated steel pipes used for the grout pockets were located in the center of the panel and secured with screws to the plywood base to maintain their proper position curing casing. The bottom rebar stirrup was placed on PVC chairs, with the top stirrup being inserted into the wet concrete to the appropriate depth and position by hand after placing the concrete.

The concrete for the precast panels was hand placed and consolidated. A wood trowel was used to screed the concrete and a steel trowel and edger were used to finish the concrete top face. The concrete was cast outside and moist cured for seven days under a poly sheet. The nine 150mmx300mm concrete cylinders, C-1 to C-9, used for determining the material properties were also cured under the same conditions.

Drawings of the push test specimens are found in Appendix F.

Figure A-2 Form Construction

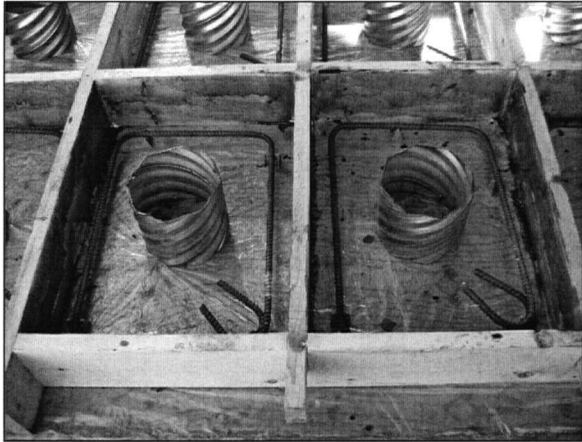
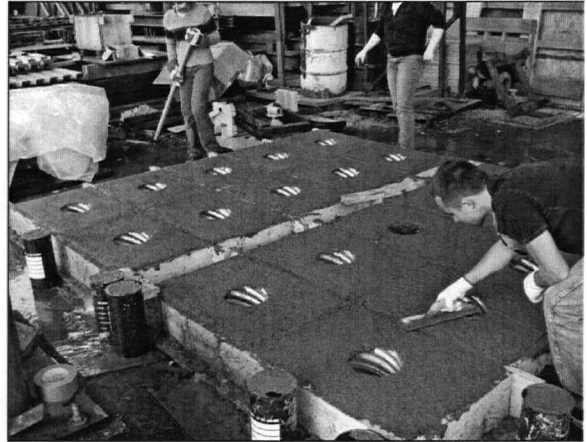


Figure A-3 Troweling Concrete Panels

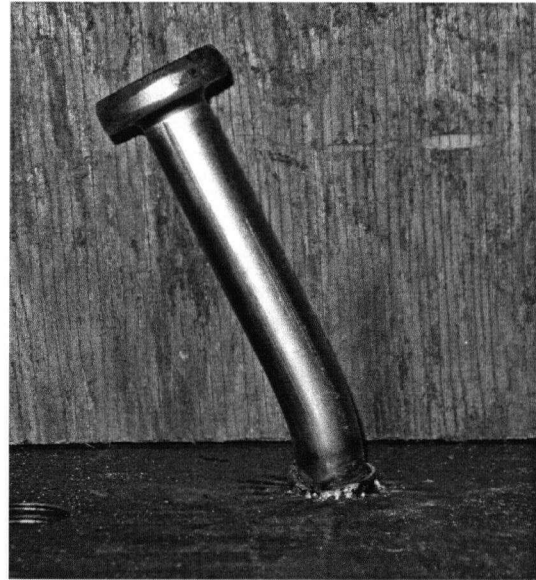


After the concrete was cured, the forms were stripped and the panels moved to the laboratory. The concrete cylinders were also stripped and kept indoors, near the panels, to provide a similar environment. The concrete panels were later painted white to assist in defining the crack pattern.

A total of 10 550 x 350 x 32 350AT steel plates were provided to weld the stud groups onto. The plates were provided with a total of 20, 22 mm diameter drilled holes in a predetermined arrangement. The Nelson™ studs were welded onto the steel plates by a local fabricator for the monotonic tests and at Canadian Stud Welding Accessories Inc. for the cyclic tests and monotonic test 7C. An extra stud was welded onto the plates used for the cyclic tests and was stuck with a sledge hammer. The purpose of this bend test was to quickly assess the weld quality of the studs.

All nine studs were bent similarly to that shown in Figure A.4 without breakage or cracking of the weld or the stud. It is also interesting to observe the weld collar at the base of the stud and the blue coloured heat affected zone immediately above the base of the stud. The plates were brought back to the laboratory and these holes were subsequently tapped on the rotary drill in the laboratory to accept 22 mm diameter A325 bolts. These bolts would transfer the force between the loading

Figure A-4 Typical Bend Test



column attached to the actuator to the steel plate and then into the stud group. It was later determined, when the plates were to be bolted to the load column, that a form had not been used and that not all the bolts could be inserted into the loading column. This was rectified by removing the loading column from the actuator and reaming the bolt holes over. Hardened steel threaded inserts with 22 mm outside diameter and 16 mm inside diameter were ordered and screwed into some of the tapped holes in the steel plates to accommodate the misaligned holes.

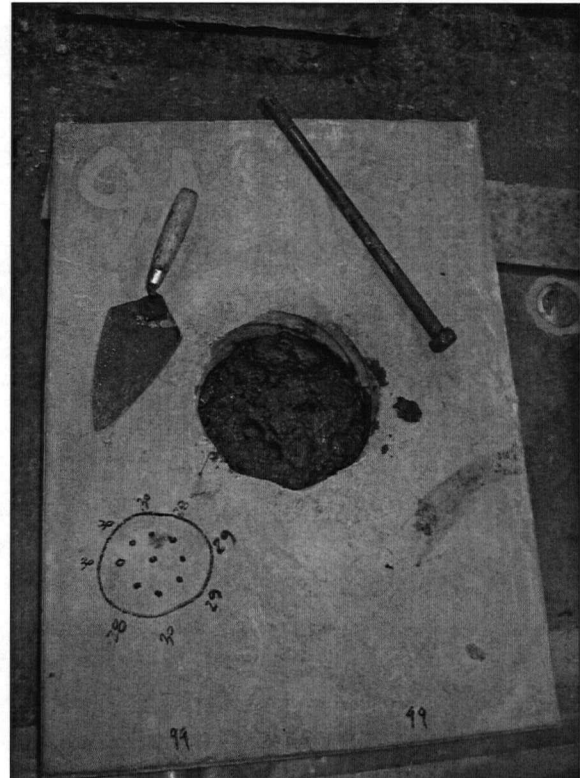
After the plates with the Nelson™ stud groups had been tapped, they were laid out on the floor and the top of the plates greased with petroleum jelly. This jelly provides a bond breaker between the panel and the plate, thereby validating the assumption that there is no friction. The concrete panels were placed and aligned on the steel plates. The Target™ traffic patch course mix grout was prepared in the pan mixer located in the materials laboratory and then transported by wheelbarrow to the structures laboratory, where it was placed and the specimens cured. The size of the mixing pan limited the volume of grout that could be mixed at one time. It was decided that for the monotonic specimens that two 25kg bags would fill two grout pockets and some 100mmx200mm cylinders. This allowed each stud group to be constructed from the same grout mix. A total of three 25kg bags were used to grout the cyclic tests, since there are three specimens with the same

number of studs in the stud group. This resulted in a separate mix for each of the five different stud groups. Figure A-5 depicts how the concrete panel mounts to the steel plate and Figure A-6 shows the grout being placed and tools used to consolidate the grout.

Figure A-5 Precast Concrete Panel On Steel Plate 9A



Figure A-6 Grout Being Placed And Consolidated For Test Specimen 9A



A.5 Push Test Geometry

The geometry of the push test components that are included in the experiment are provided in drawings in Appendix F. The drawings illustrate the assembly of the concrete panels to the loading columns and how these components integrate with the reaction frame for both the symmetrical and unsymmetrical loading configurations.

A.6 Boundary Conditions

The base of the precast concrete specimens was uneven and required a smooth bearing surface to ensure even distribution of pressure from the floor reaction and to provide a specimen that was plumb. This was accomplished by placing the concrete panel in a bed

of mortar. Hydro-Stone®, a gypsum cement produced by the United States Gypsum Company, was chosen for this purpose. It is highly fluid mixture that is self-levelling, sets and cures quickly and provides a reported 1 hour compressive strength of 27 MPa when mechanically mixed following the manufactures recommended proportions. It did not bond well with the concrete floor, making clean up a simple task. Cold water should be mixed with the cement, since even room temperature water was observed to greatly reduce the set time.

For the symmetric test configuration, both panels were plumbed and placed into wet beds of Hydro-Stone®. The boundary configuration for this setup was considered to be fixed at the base, with friction providing the horizontal force component to resist the overturning. The unsymmetrical test configuration was also considered to be fixed at the base, relying on friction and an external restraint in the form of two 28 mm diameter DWYDAG™ thread bars connected to an HSS section bolted to the strong floor and a section HSS section bearing against the panel. The interface between the base of the concrete panel and the HSS beam was also grouted with Hydro-Stone® to provide even bearing surface.

A.7 Reaction Frame, Experiment Procedures and Data Acquisition

One of the existing standard steel reaction frames located in the structures laboratory was used to mount the Team Corp 400kip hydraulic actuator. A total of four steel channels, two on each side of the columns, were mounted to a custom fabricated steel wide flange column to support the hydraulic actuator. A total of six cap head machine screws were used to secure the hydraulic actuator to the custom steel wide flange column. All connections on the reaction frame used A325, 22 mm diameter, high strength bolts installed with the air impact wrench. The reaction frame was mounted to the floor with a total of four laboratory standard steel threaded rods.

A 400kip (1800kN) capacity TEAM Corporation hydraulic actuator was used to load the push test specimens. The stroke of the actuator is 300 mm and is double acting. A servo valve was used to control the direction and pressure from the hydraulic pump.

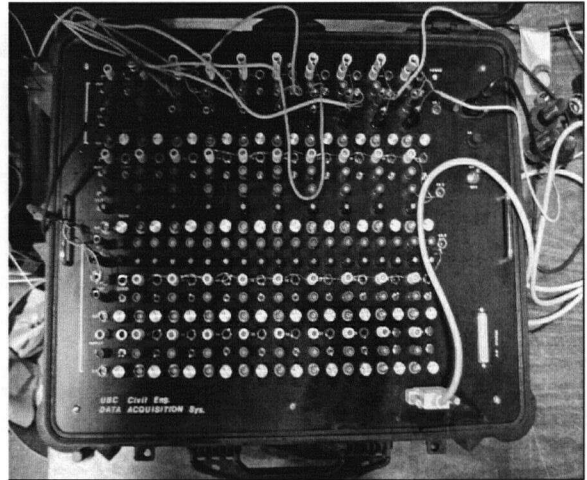
Two custom steel loading columns were fabricated for allow connection of the concrete panels to the hydraulic actuator and the actuator to the reaction frame.

The portable MTS controller and waveform generator in the structures laboratory were used for the signal generation for the cyclic loading and monotonic loading of the push tests.

Figure A-7 Wave Form Generator



Figure A-8 Data Acquisition Box



The software used for the data acquisition is Notebook™ running on MSDos™ operating system. The instrument sampling rates were 1Hz for the monotonic tests and 50Hz for the cyclic tests.

A set of 9 linear variable displacement transducers and 2 load cells were used in the push tests. Four Novotechnik™ were used to record the slip between the steel plate and the concrete panel. These LVDT instruments were attached to custom fabricated steel blocks that were tack welded to the steel plate, slightly offset below the center of the stud group. The LVDTs were positioned below the center of the stud group so that they would be moving away from the aluminum HSS section that was glued to the concrete panel with 5ton epoxy. These instruments would read the relative slip between the stud group and the concrete panel. Refer to figures A-9 and A-10 for photos of the instrument setup. Four Novotechnik™ TR was used to record the out of plane displacement of the concrete panels.

A Sensotec™ load cell is integral with the Team Corp hydraulic actuator and measures the direct load applied. A BLH Electronics load cell was used to measure the horizontal component of the resisting moment and is attached to the 305x305x12.5 HSS beam. The Sensotec™ load cell was removed from the hydraulic actuator and calibrated in the Baldwin universal testing machine located in the structures laboratory. The BLH Electronics load cell was calibrated against the Sensotec™ load cell once it was reattached to the actuator.

Figure A-9 LVDT for Actuator Control

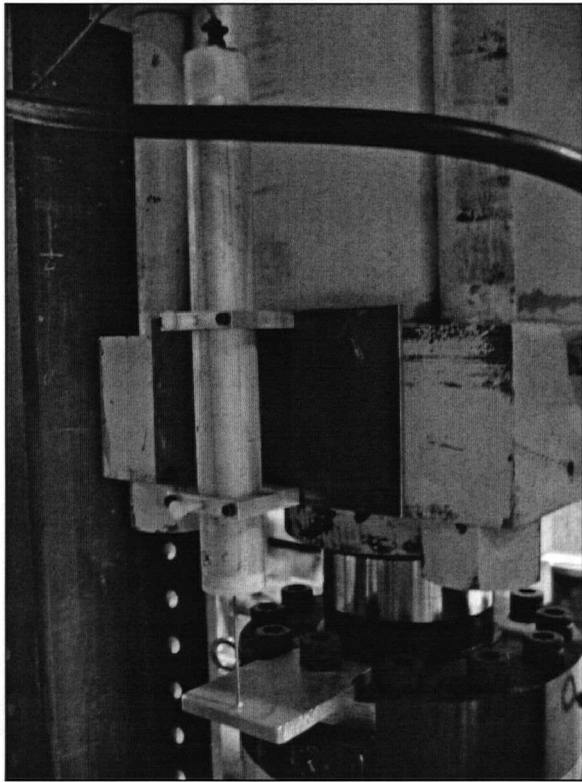
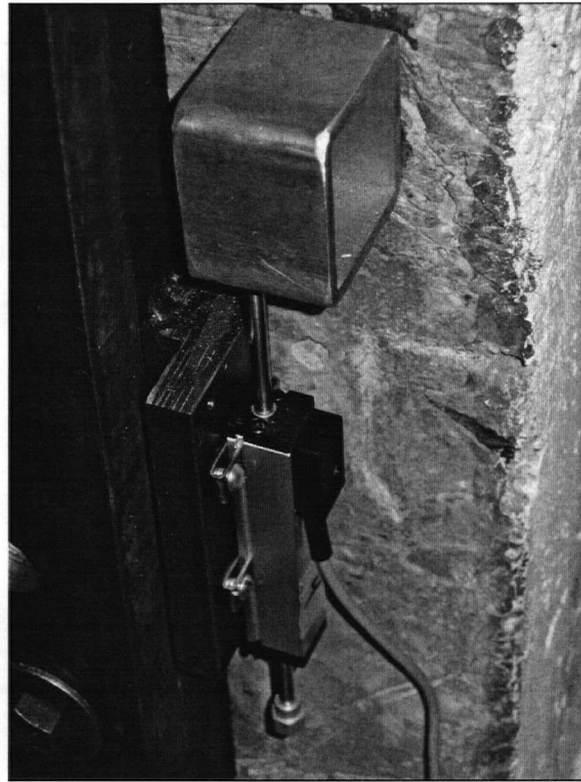


Figure A-10 LVDT for Interface Slip



A.8 Loading Protocol

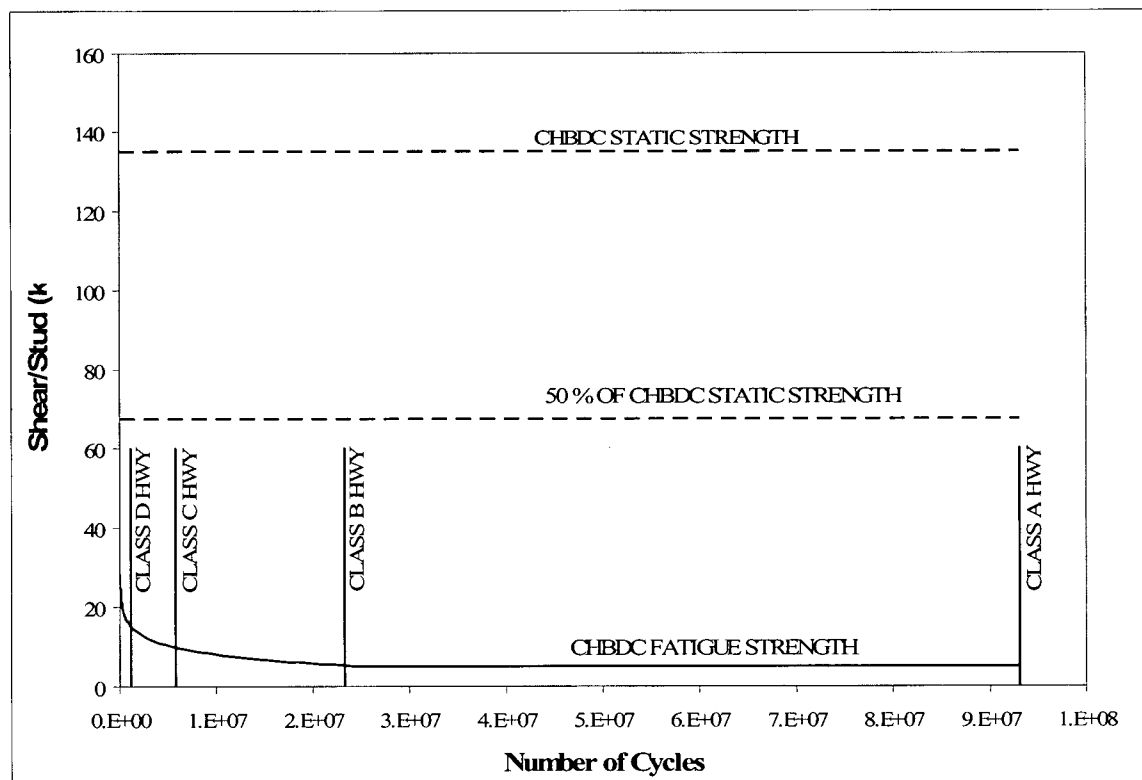
The monotonic loading for the push tests was conducted under displacement control, with the loading rate never exceeding 0.5 mm/min. The MTS controller was used to establish the loading rate using the DC error to determine the displacement rates. The loading continued until all the shear studs fractured.

The cyclic test was accomplished using load control at a frequency of 1Hz. A sinusoidal wave was generated using the wave form generator and was routed to the servo valve via

the controller the regulate pressure in the hydraulic system. The peak load was controlled with the gain on the MTS controller and the span to control the lower load level. The DC error was set one unit on the positive side as a safety measure, since the wave form generator was running inversely, causing the system to unload in the event of a breakdown. To determine the residual strength of the shear stud group, the monotonic load procedure previously described was used.

The stress range used for loading during the cyclic testing conforms to the permissible range of interface shear found in clause 10.17.2.6 in S6-00 for a Class C highway. A class C highway has an Average Daily Truck Traffic (ADTT) of 250, providing 5.8 million fatigue cycles in 75 years for two design lanes. The more heavily traveled highways, i.e. class B and A, have permissible range of shear that equates the endurance limit for fatigue. The vertical lines represent the number of cycles over a 75 year design life for the four highway classes.

Figure A-11 Permissible Range of Interface Shear of 16mm Steel Studs vs. No. Cycles



APPENDIX B Component Material Testing

Material properties for the concrete, steel studs and grout were obtained following standardized testing procedures. The results of this component testing are presented in the following headings.

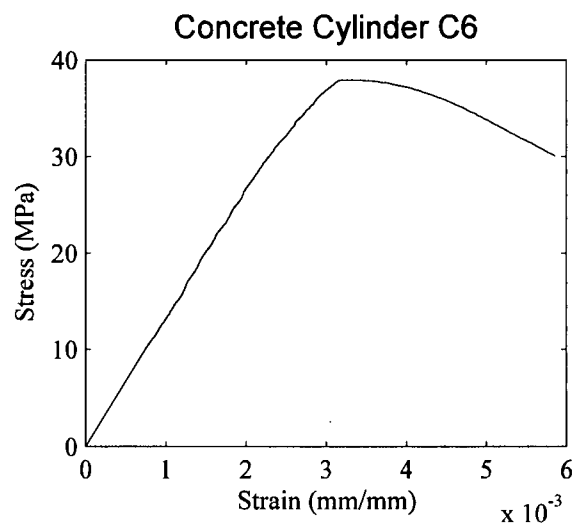
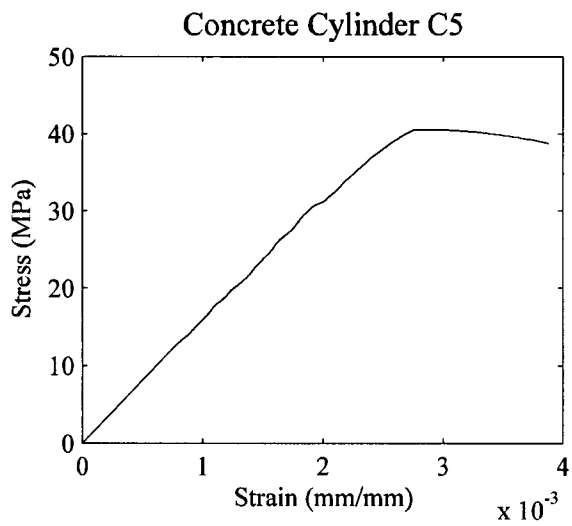
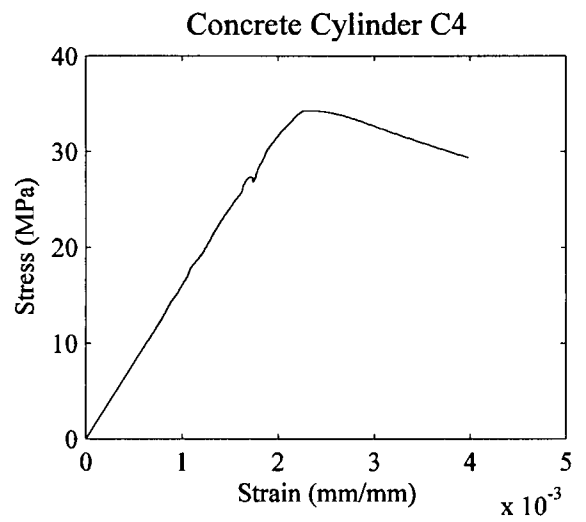
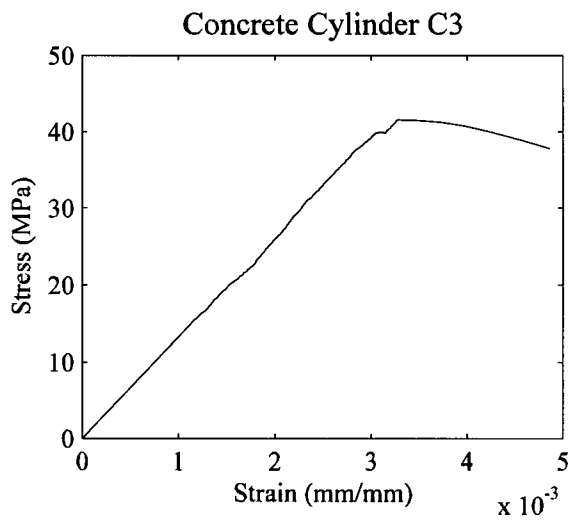
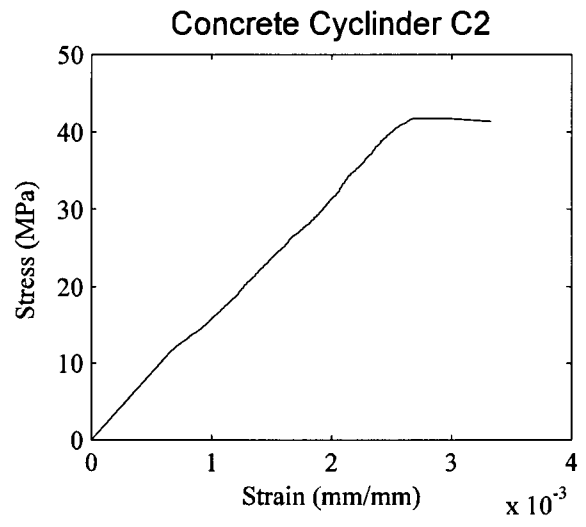
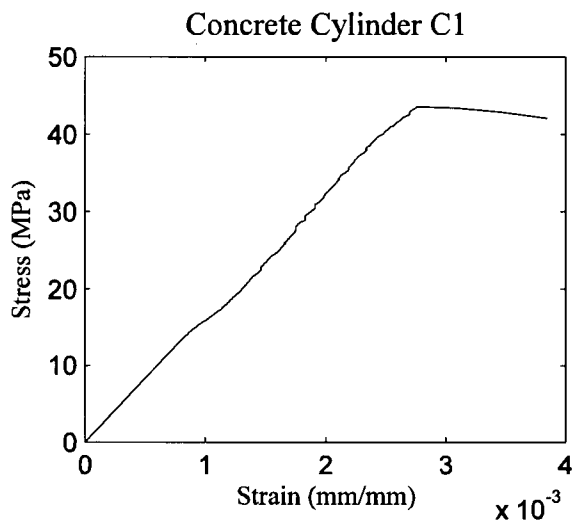
B.1 Concrete

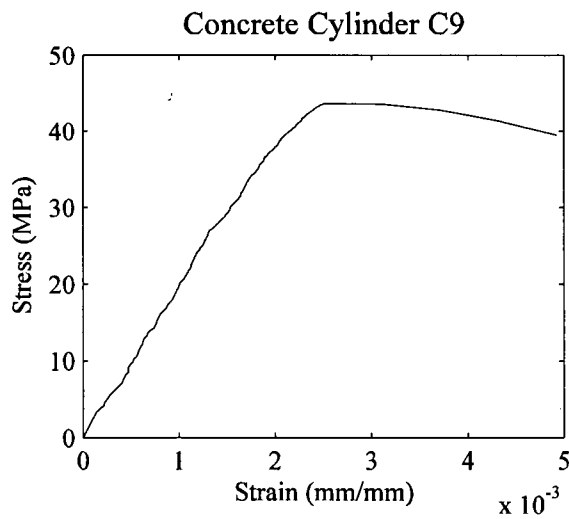
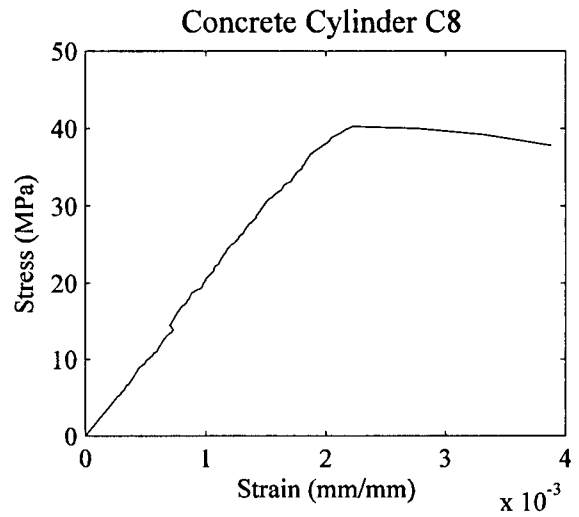
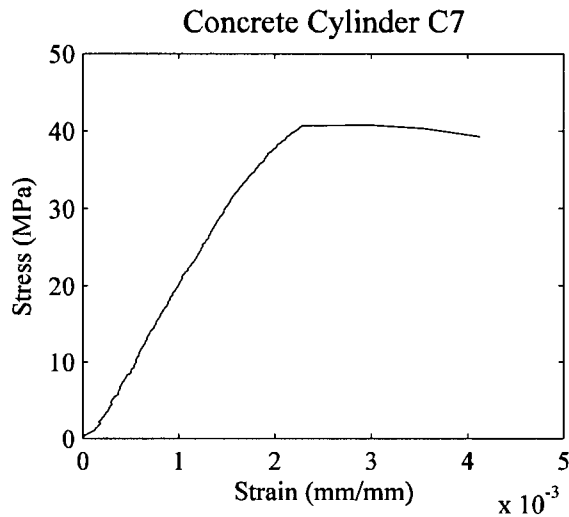
The concrete used to cast the concrete panels was supplied by Yard-at-a-Time, a ready mix plant in Delta, BC. The concrete was ordered to have a 28 day compressive strength of 35MPa, with a maximum aggregate size of 19mm and 5-7% air. The concrete panels and cylinders were cast on February 12, 2004 outside of the structures laboratory. A set of nine concrete cylinders were used to determine the material properties over the duration of the testing schedule. Table B-1 provides the results from the compressive tests conducted on the concrete cylinders.

Table B-1 Concrete Cylinder Test Results

Cylinder #	Max Compressive Stress (MPa)	Average Max Compressive Stress (MPa)	Concrete Age (days)
C-1	44.4	42.6	217
C-2	41.7		217
C-3	41.6		217
C-4	34.3	37.6	414
C-5	40.5		414
C-6	37.9		414
C-7	40.8	41.6	719
C-8	40.2		719
C-9	43.7		719

The following two pages contain the stress strain plots for the concrete cylinders.





B.2 Steel Shear Studs

“Nelson” mild steel headed shear stud anchors were used for the push tests. Table B-2 provides the minimum CHBDC requirements for the material properties of shear studs.

Table B-2 CAN/CSA-S6-00 Minimum Stud Material Properties

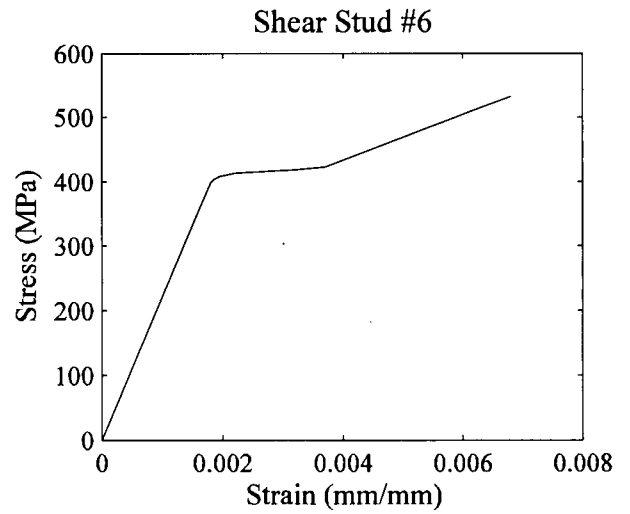
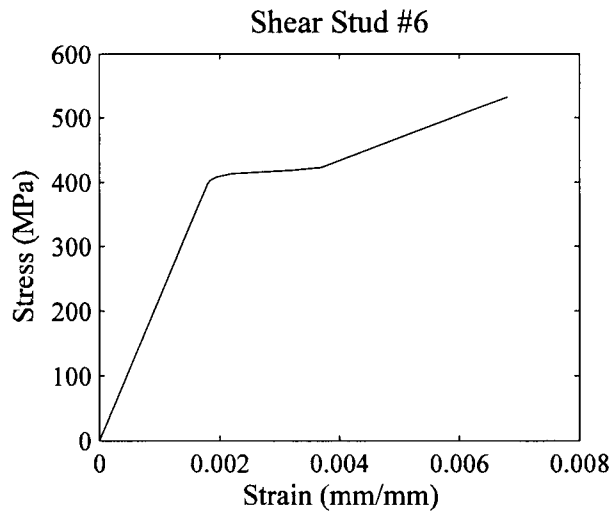
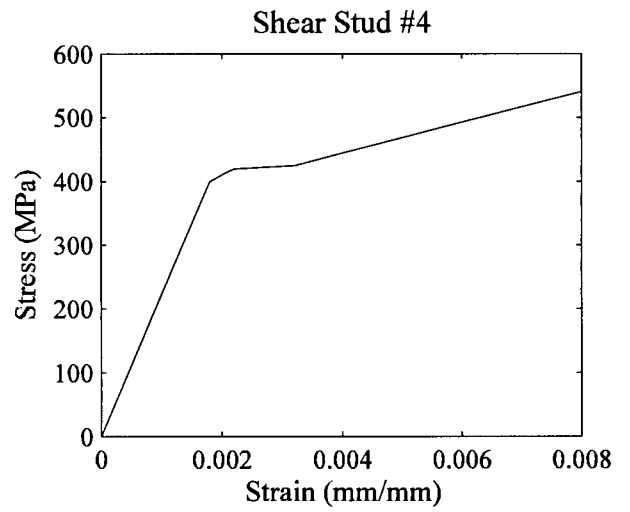
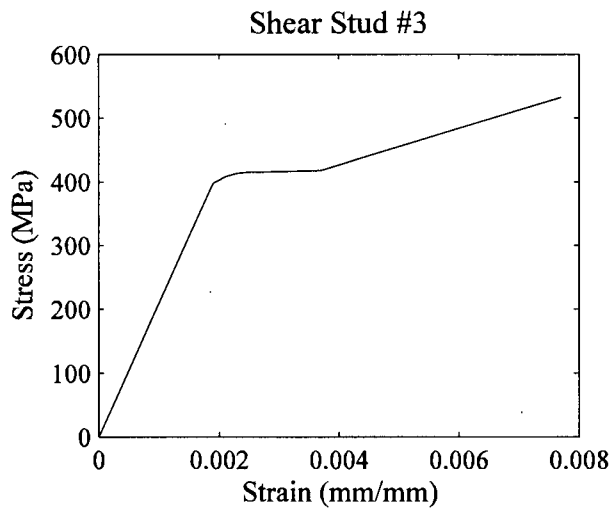
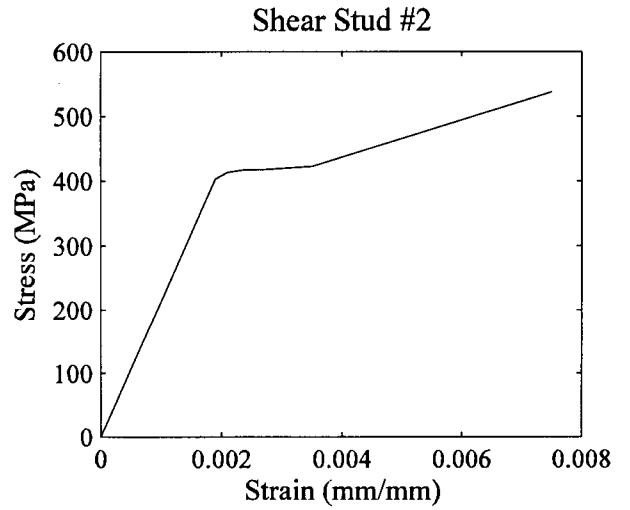
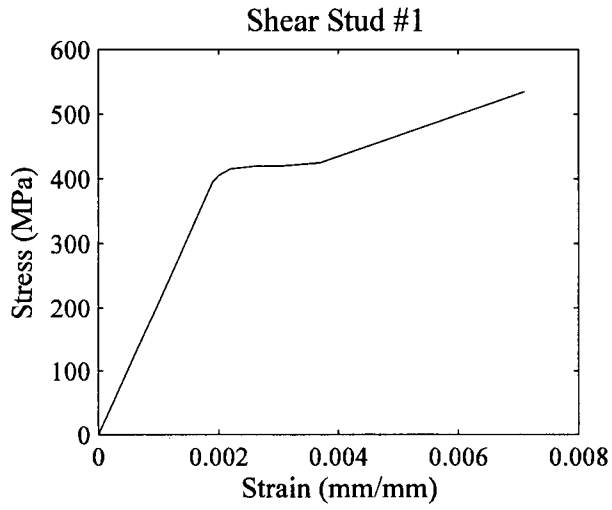
Mechanical Property	Minimum Value
Yield, 0.2% offset (MPa)	350
Ultimate tensile (MPa)	410
% Elongation	20
% Area Reduction	50

A series of four studs were machined into coupons for tensile testing to determine material properties for the monotonic tests. The body of each stud was machined and tested as per ASTM A370. The studs were loading in direct tension in the Baldwin UTM located in the materials laboratory. Table B-3 provides the results of the tensile testing used in the push tests.

Table B-3 Results of Tensile Testing Used in Monotonic Tests

Geometric Property	Coupon #						
	1	2	3	4	5	6	
Initial Diameter (mm)	8.74	8.71	8.71	8.74	8.74	8.76	
Initial Area (mm ²)	59.99	59.58	59.58	59.99	59.99	60.27	
Initial Gauge Length (mm)	35.00	35.00	35.00	35.00	35.00	35.00	
Mechanical Property							
	1	2	3	4	5	6	Average
Yield, 0.2% offset (MPa)	427.6	428.0	425.5	432.6	430.1	425.6	428.3
Ultimate Tensile (MPa)	534.6	537.1	532.0	540.9	539.2	532.1	536.0
% Elongation	24	21	23	22	24	23	22.8
% Area Reduction	68	66	69	67	68	67	67.5
Modulus of Elasticity (MPa)	207000	212000	209000	222000	210000	221000	213500

The following page contains the stress strain plots for the tensile tests conducted on the shear studs.



B.3 Monotonic Grout

The grout used for the shear pocket was “Traffic Patch – Course Mix”, produced by Target Products. This is a premixed, steel reinforced, high early strength grout, with a typical specified 28 day strength of 51.7 MPa when mixed with the maximum amount of water (3.3 L/ 25 kg). The grout was mixed in the pan mixer, located in the materials laboratory, with two bags following the manufacturer's instructions for the maximum water content. The grout was mixed until consistent, and then transported to the structures laboratory in a steel wheelbarrow. Two 25 kg bags of grout were necessary to cast two grout pockets and a minimum of three 150 mm diameter by 200 mm long cylinders, for subsequent compression testing. The grout for the monotonic loading was mixed and placed on March 16, 2004. The grout was cured with the concrete panels for 7 days under sheets of poly. Both ends of the grout cylinders were then ground flush to provide an even and parallel bearing surfaces for compression testing.

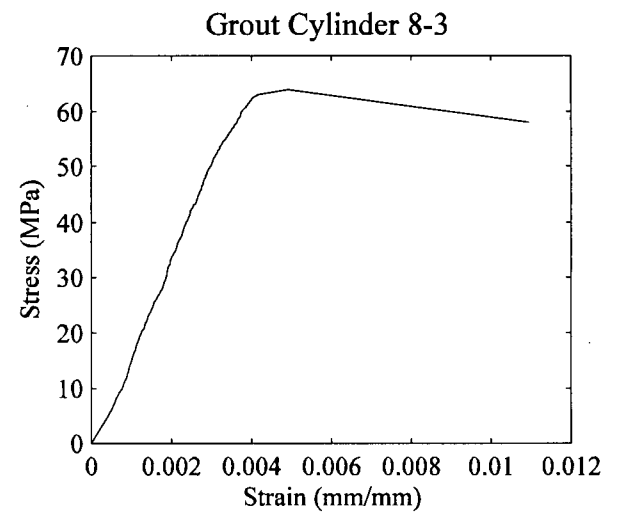
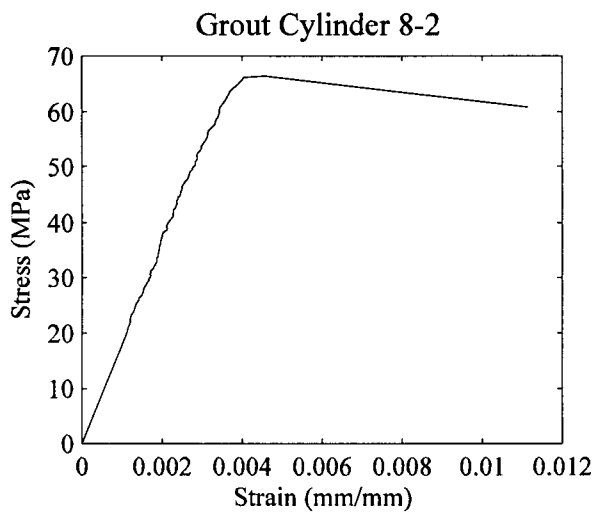
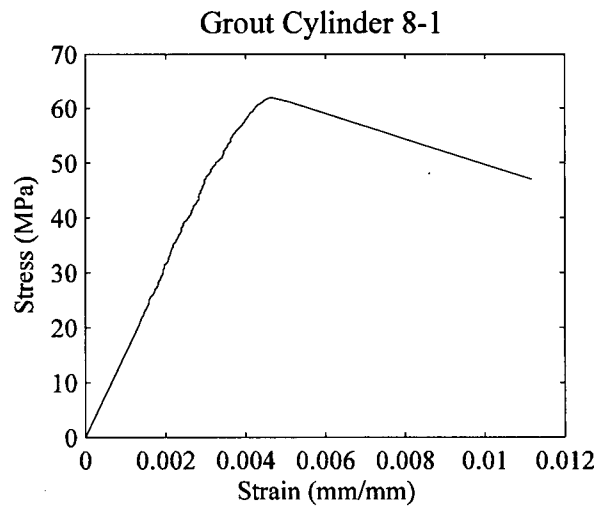
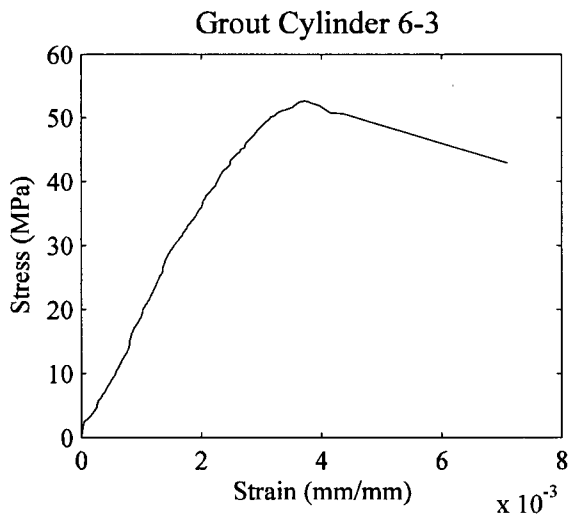
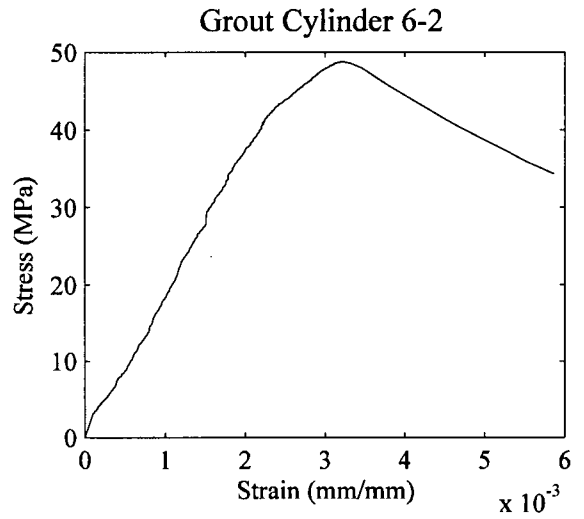
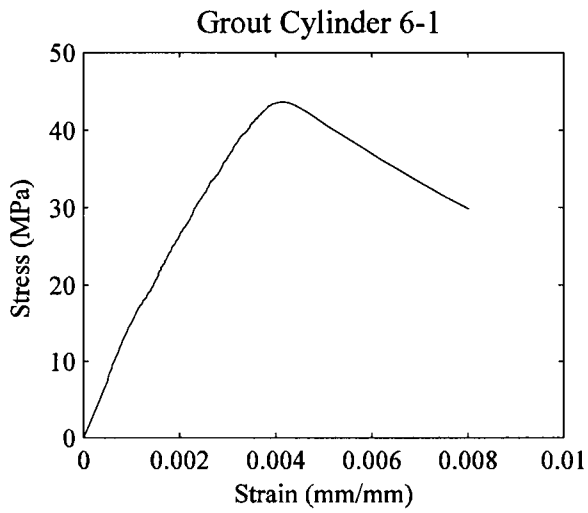
The cylinders were then labelled with a two number system; the first number related to the number of studs within the shear stud group, and the last number to identify the cylinder. The failure mode for each cylinder was consistently observed to be a 60 degree conical failure characterized by longitudinal splitting.

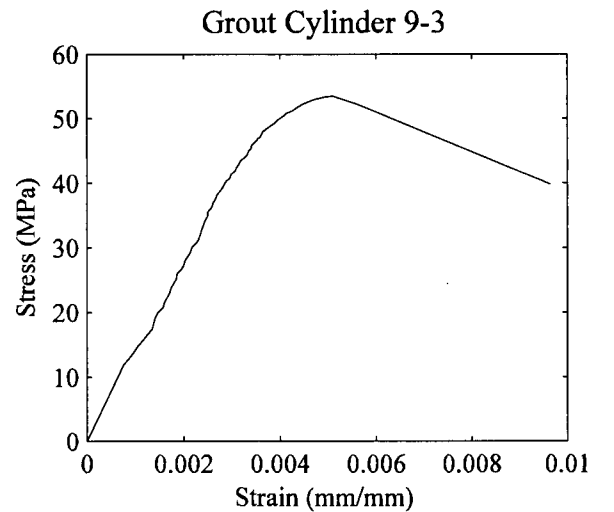
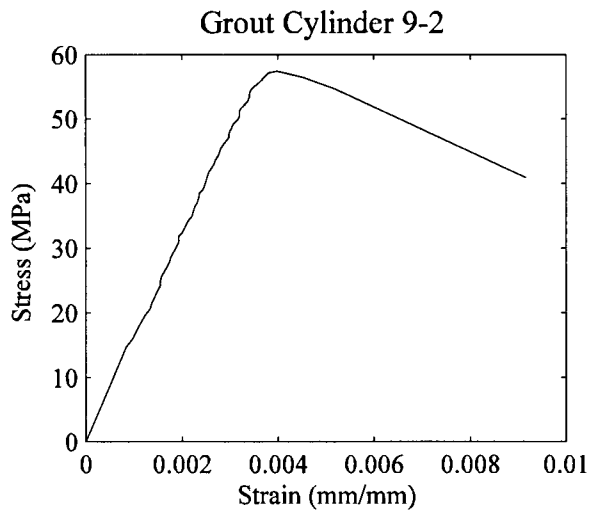
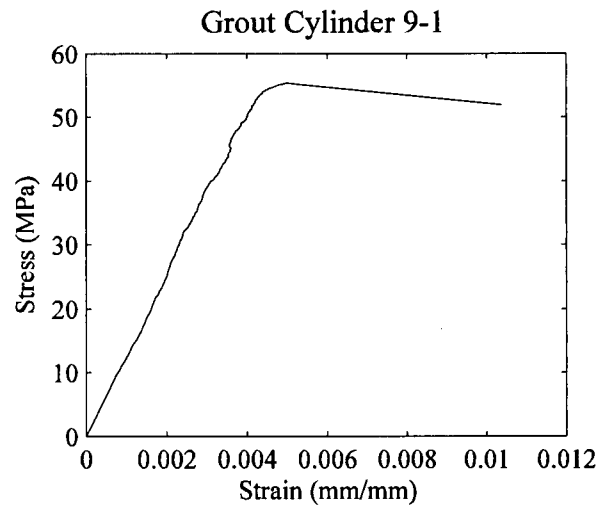
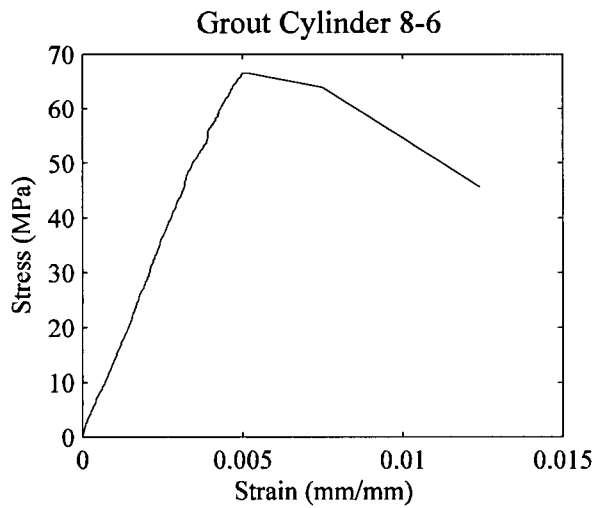
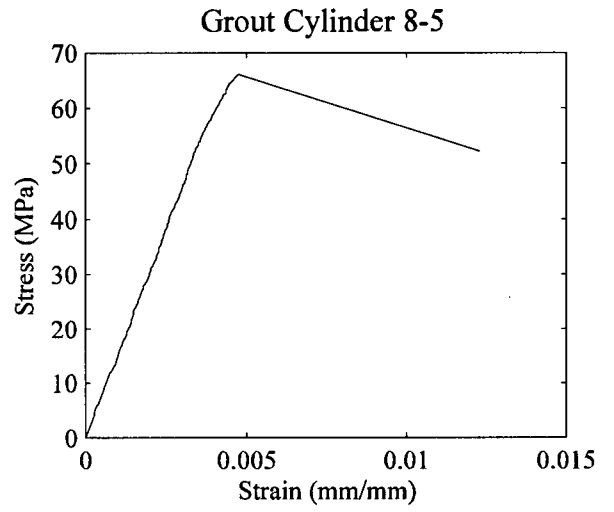
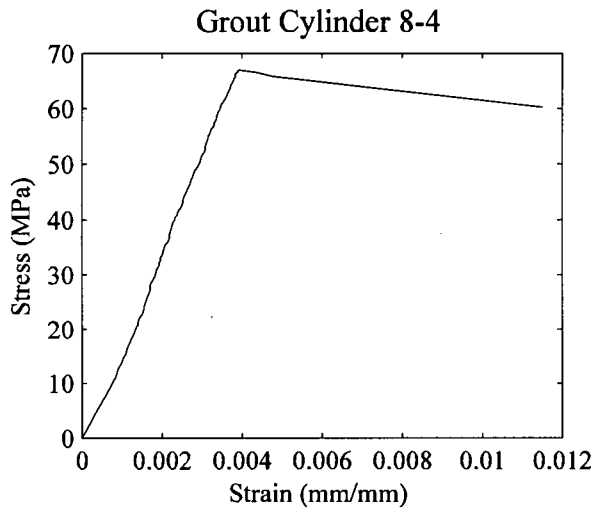
The following table summarizes the grout testing results for the monotonic tests.

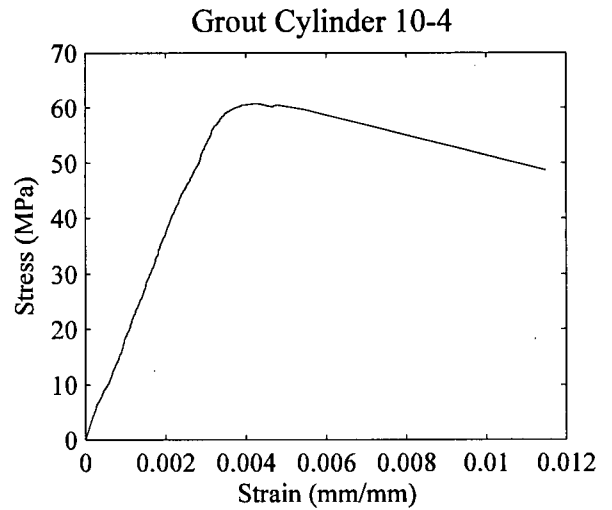
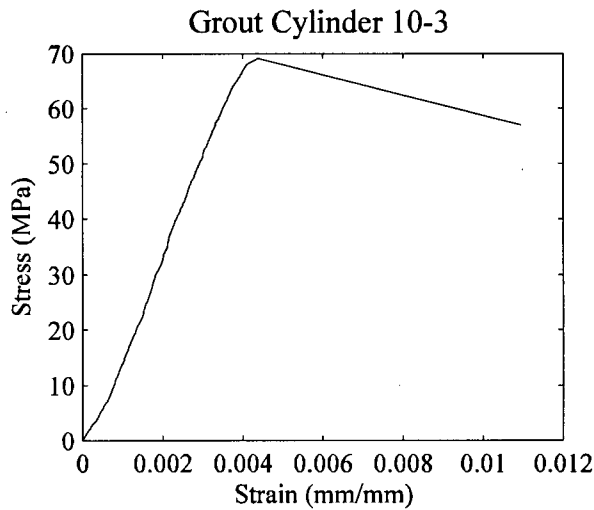
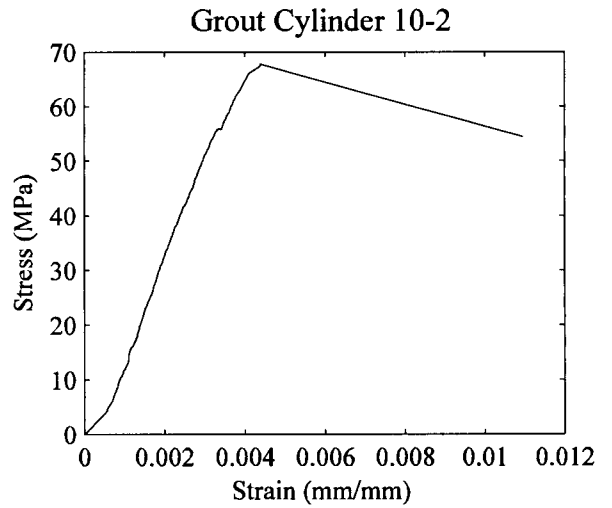
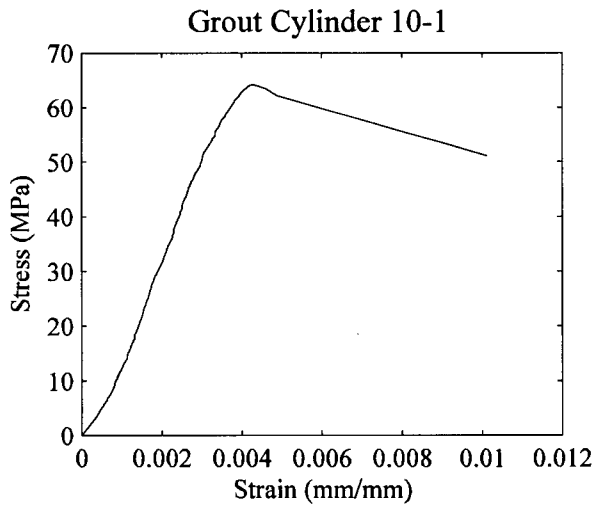
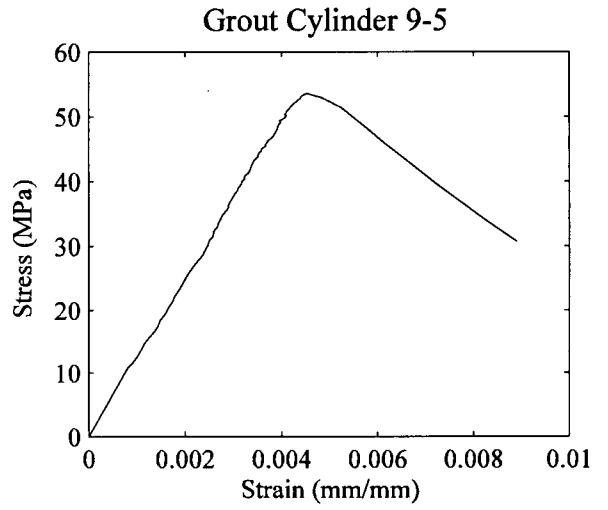
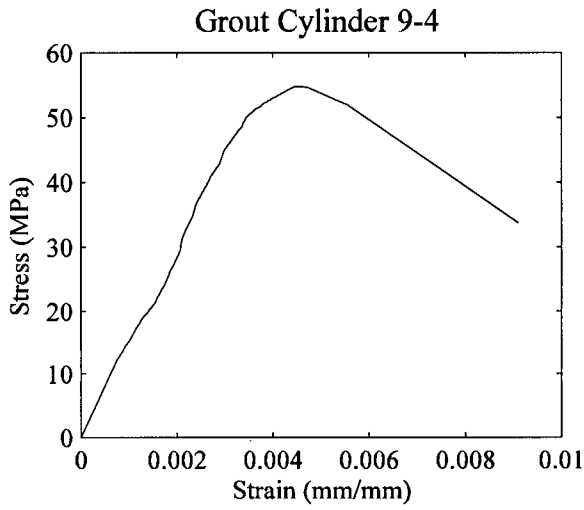
Table B-4 Grout Testing Results for Monotonic Tests

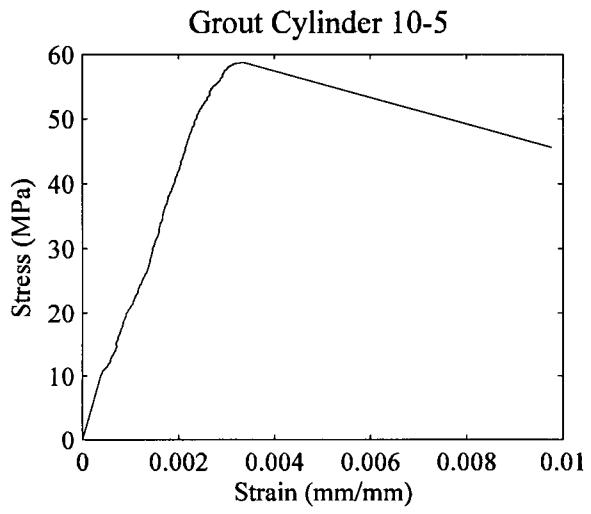
Cylinder #	Max Compressive Stress (MPa)	Average Max Compressive Stress (MPa)	Grout Age (days)
6-1	44.7	48.7	240
6-2	48.8		240
6-3	52.6		240
8-1	62.0	65.1	381
8-2	66.3		381
8-3	63.9		381
8-4	67.0		381
8-5	66.0		381
8-6	66.6		381
9-1	55.4	54.9	387
9-2	57.4		387
9-3	53.5		387
9-4	54.8		387
9-5	53.6		387
10-1	64.2	64.1	240
10-2	67.7		240
10-3	69.1		240
10-4	60.7		240
10-5	58.7		240

The following four pages contain the stress strain plots for the grout cylinders related to the monotonic push tests.









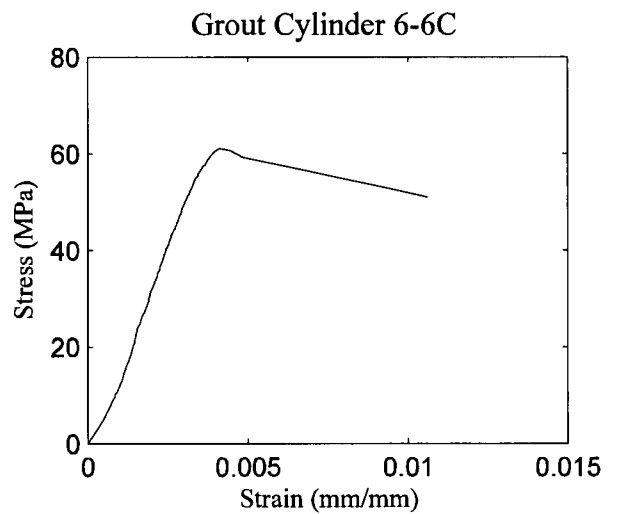
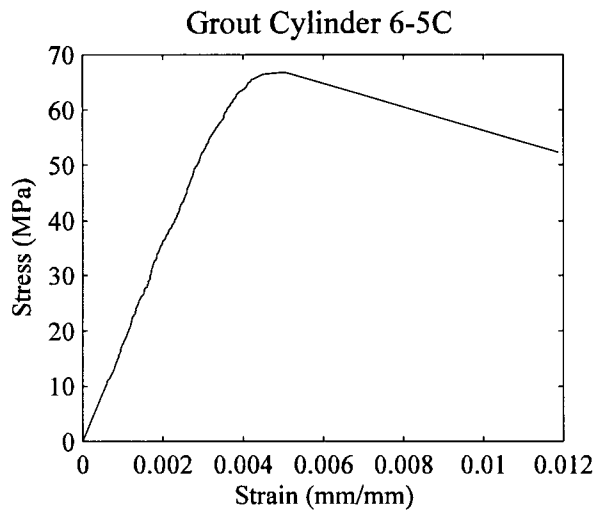
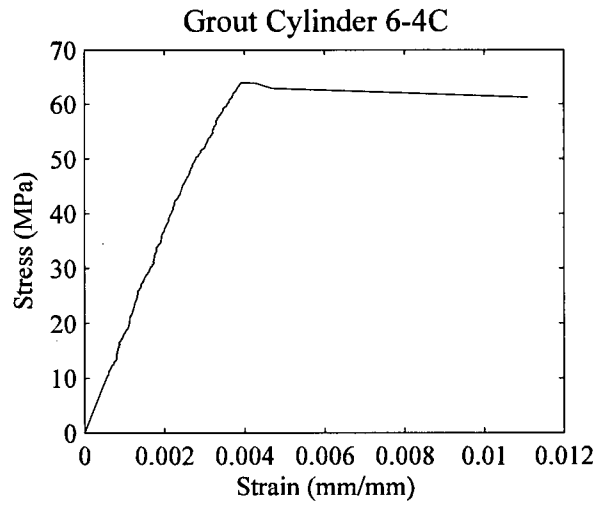
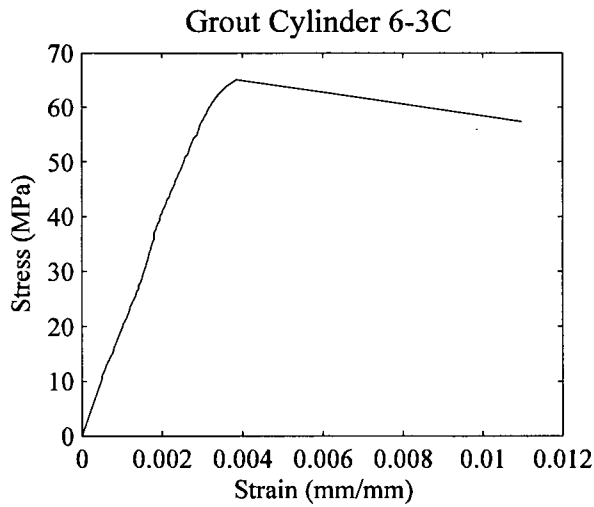
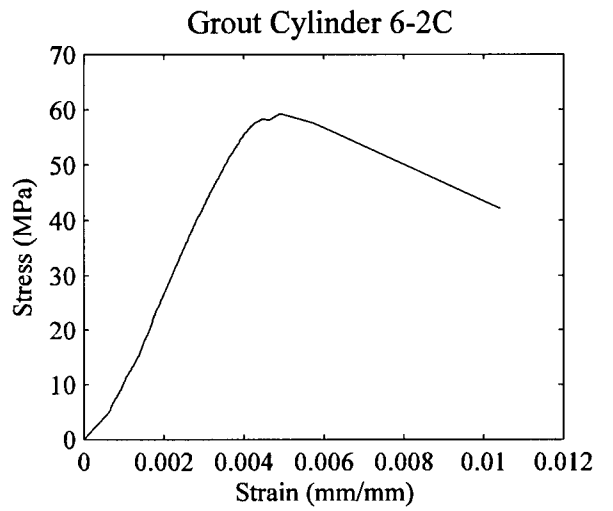
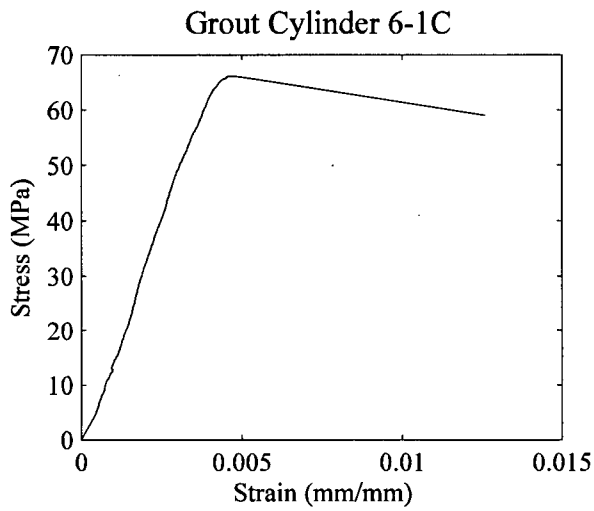
The following table summarizes the grout testing results for the cyclic tests. The grout was cast on December 22, 2004 and cured in a similar fashion to the monotonic testing.

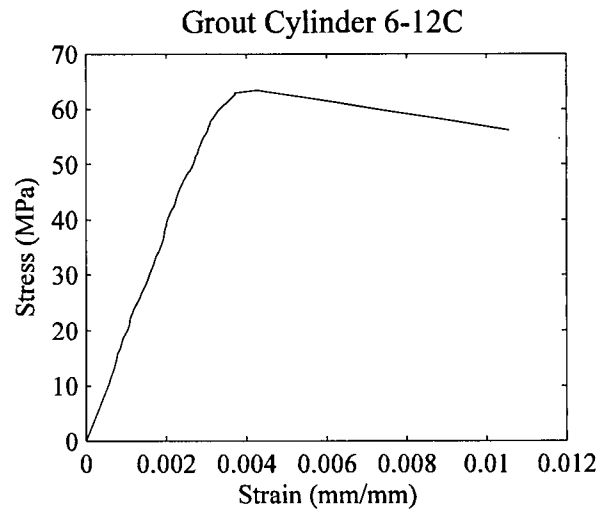
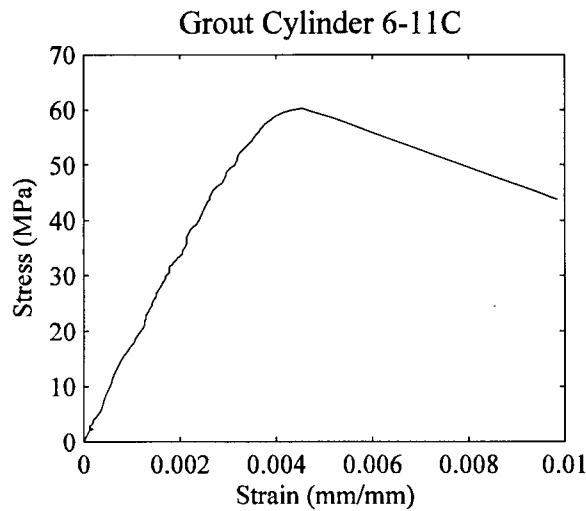
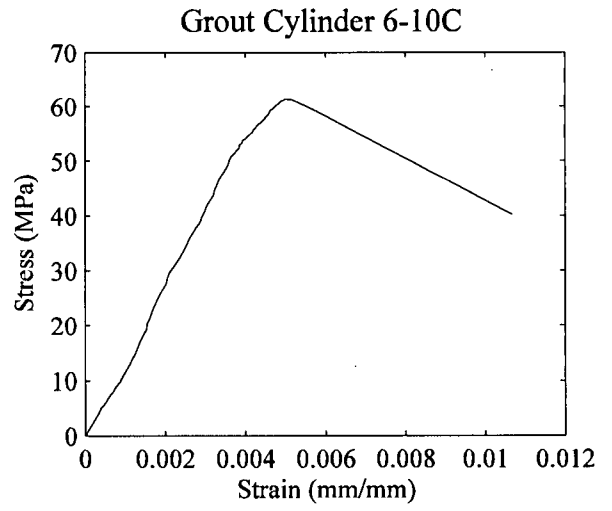
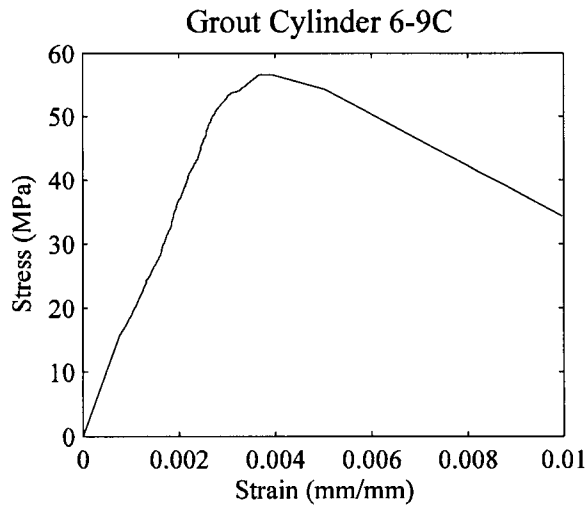
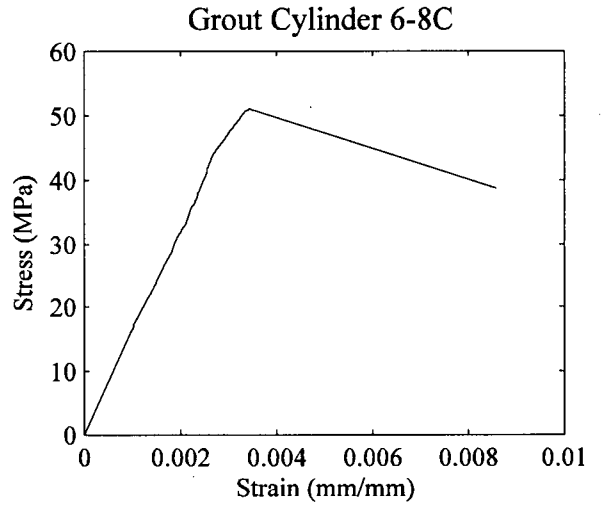
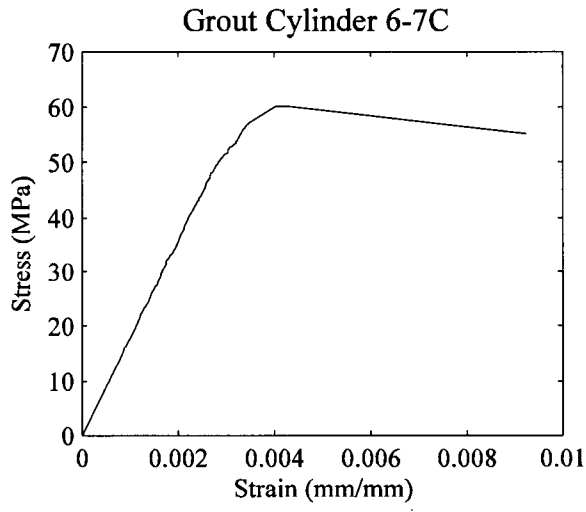
Table B-5 Grout Testing Results for Cyclic Testing

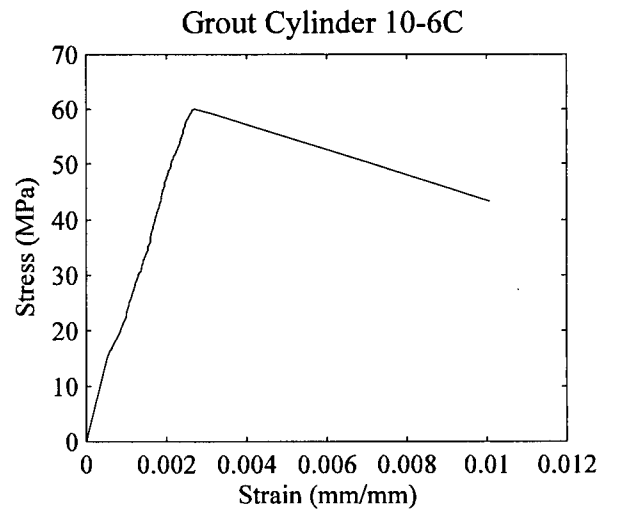
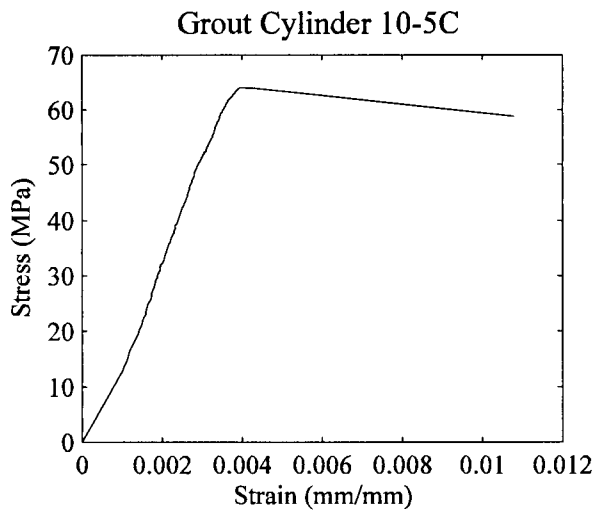
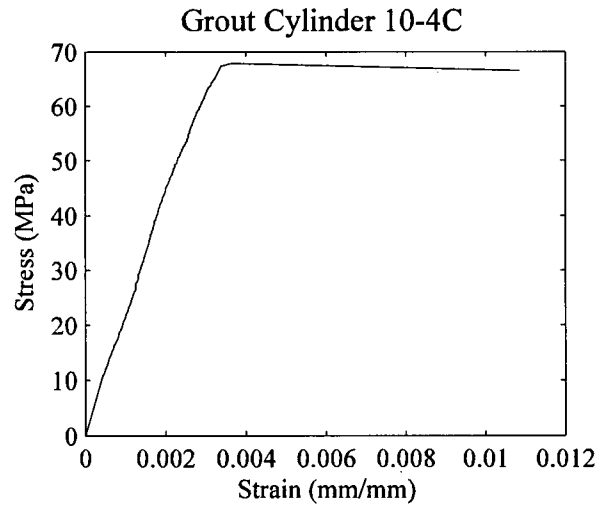
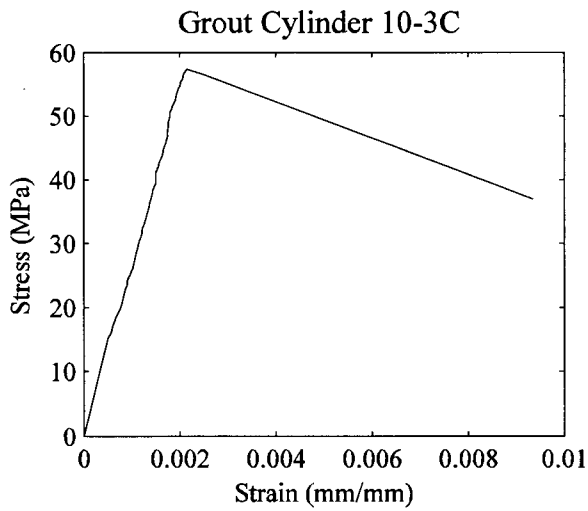
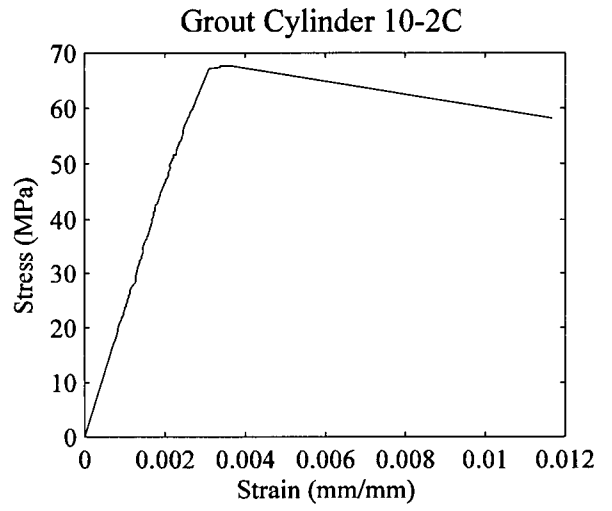
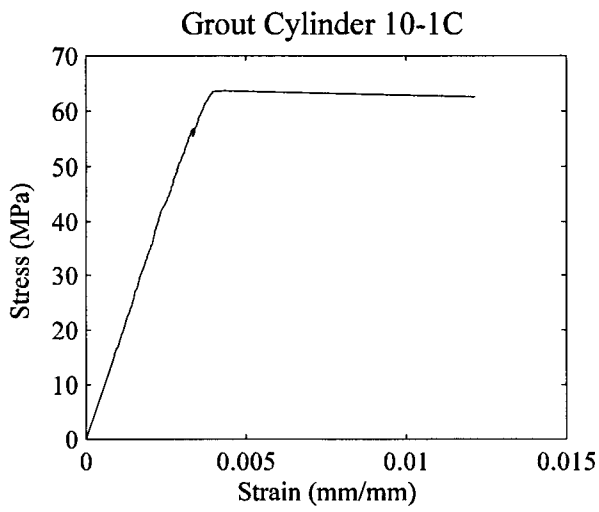
Cylinder #	Max Compressive Stress (MPa)	Average Max Compressive Stress (MPa)	Grout Age (days)
6-1C	66.1	63.6	108
6-2C	59.3		108
6-3C	65.1		108
6-4C	64.0		108
6-5C	66.8	59.8	227
6-6C	61.1		227
6-7C	60.1		227
6-8C	51.0		227
6-9C	56.5	60.4	405
6-10C	61.3		405
6-11C	60.2		405
6-12C	63.4		405
10-1C	63.7	63.8	227
10-2C	67.7		227
10-3C	57.3		227
10-4C	67.9		227
10-5C	66.3		227
10-6C	60.0		227
10-7C	67.6	68.9	405
10-8C	72.3		405
10-9C	66.7		405

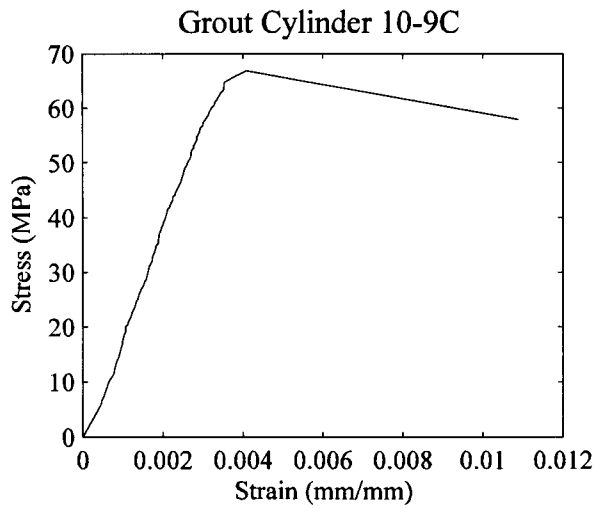
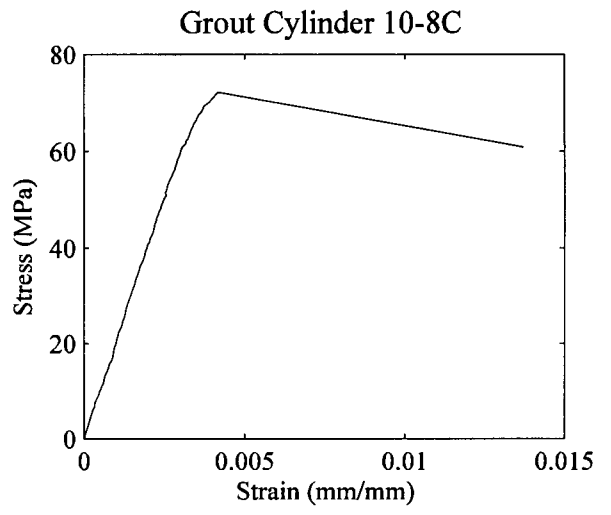
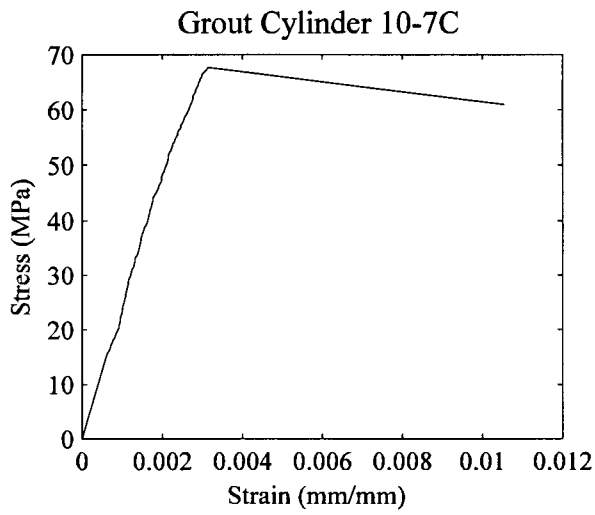
Note: Monotonic Specimen 7C used grout from the cylinders 6-1 to 6-12.

The following four pages contain the stress strain plots for the grout cylinders related to the cyclic push tests.









APPENDIX C Monotonic and Cyclic Push Test Data

C.1 Monotonic Push Tests

A series of 11 monotonic push tests were originally constructed, with two being discarded because of unreliable data. The key elements of the data that were of interest include the ultimate strength of the stud cluster, the stiffness and the slip. The following table provides the summary of the testing for the monotonic push tests.

Table C-1 Monotonic Push Test Specimen Schedule

Panel No.	Studs per Cluster	Test Date (mm-dd-yy)	Concrete Age (days)	Grout Age (days)
6A	6	10-15-04	246	213
6B	6	10-30-04	261	228
7C	7	02-13-06	732	418
8A	8	11-16-04	278	245
8B	8	11-16-04	278	245
9A	9	11-03-04	265	232
9B	9	11-04-04	266	233
10A	10	11-04-04	266	233
10B	10	11-02-04	264	231

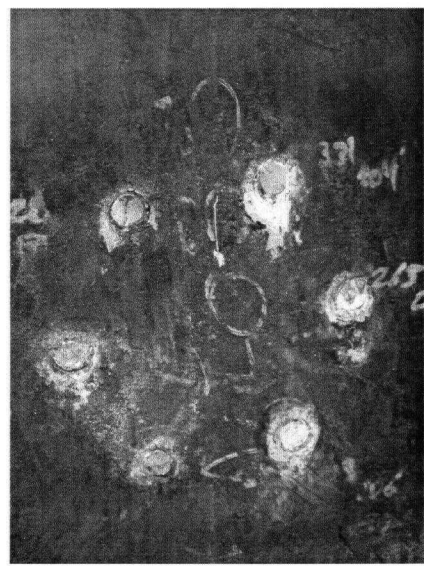
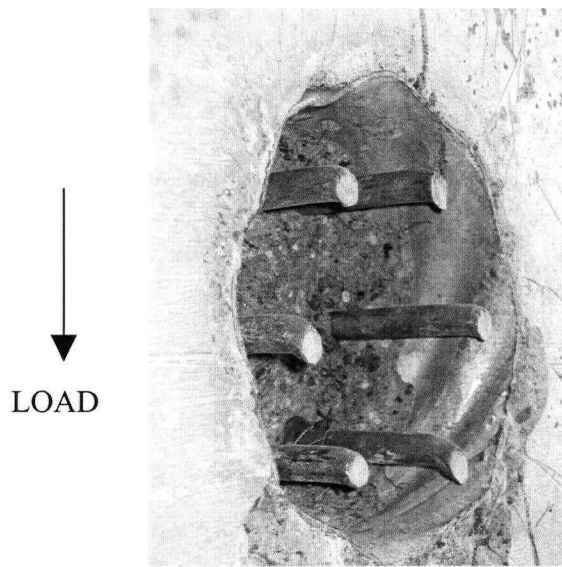
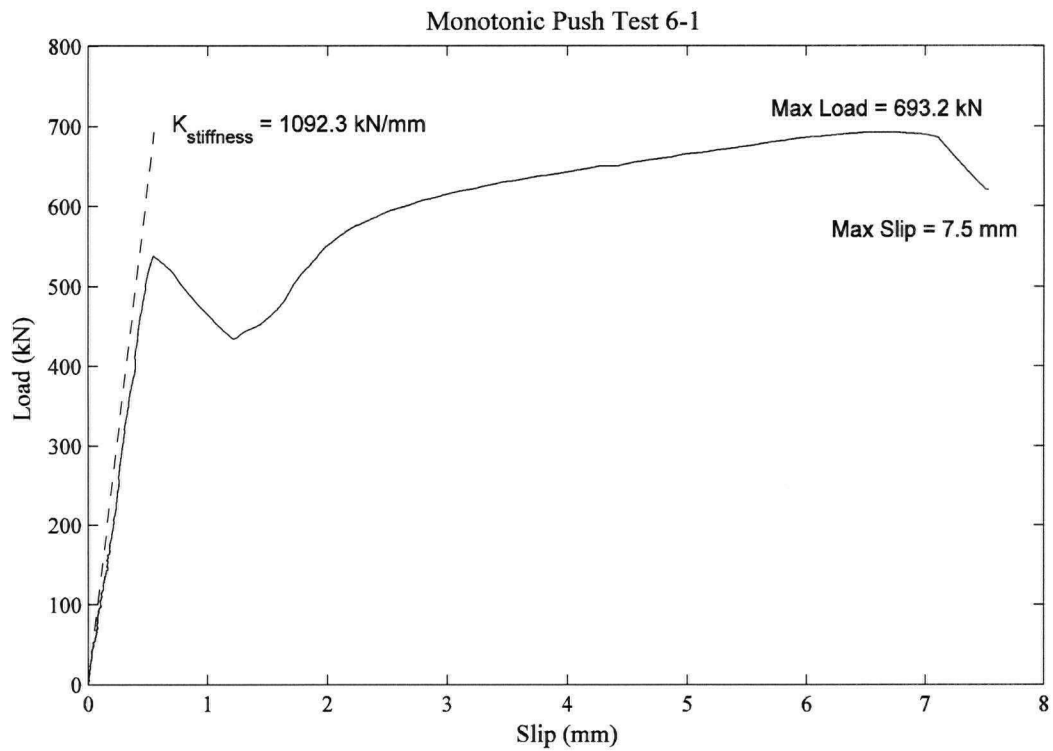
C.3 Monotonic Push Test Data

The following table provides a summary of the data processed from the monotonic push tests. The stiffness reported was taken at the load level corresponding with the allowable stress range for fatigue (9.4 kN/stud or approximately 7% of the stud strength). The maximum slip was taken at the point where the first substantial drop in load occurred.

Table C-2 Monotonic Push Test Data Summary

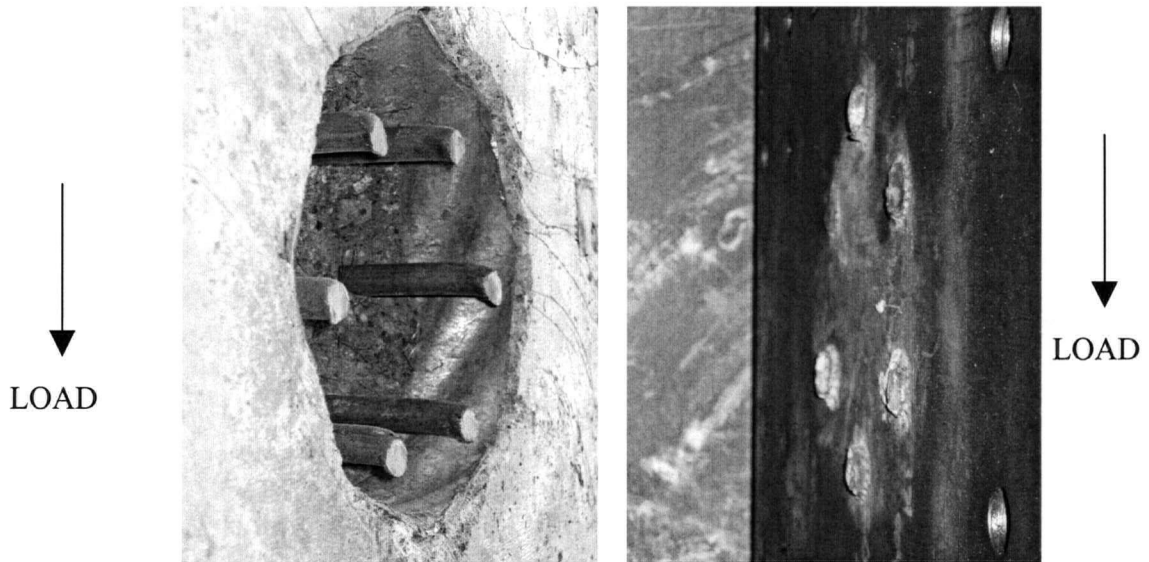
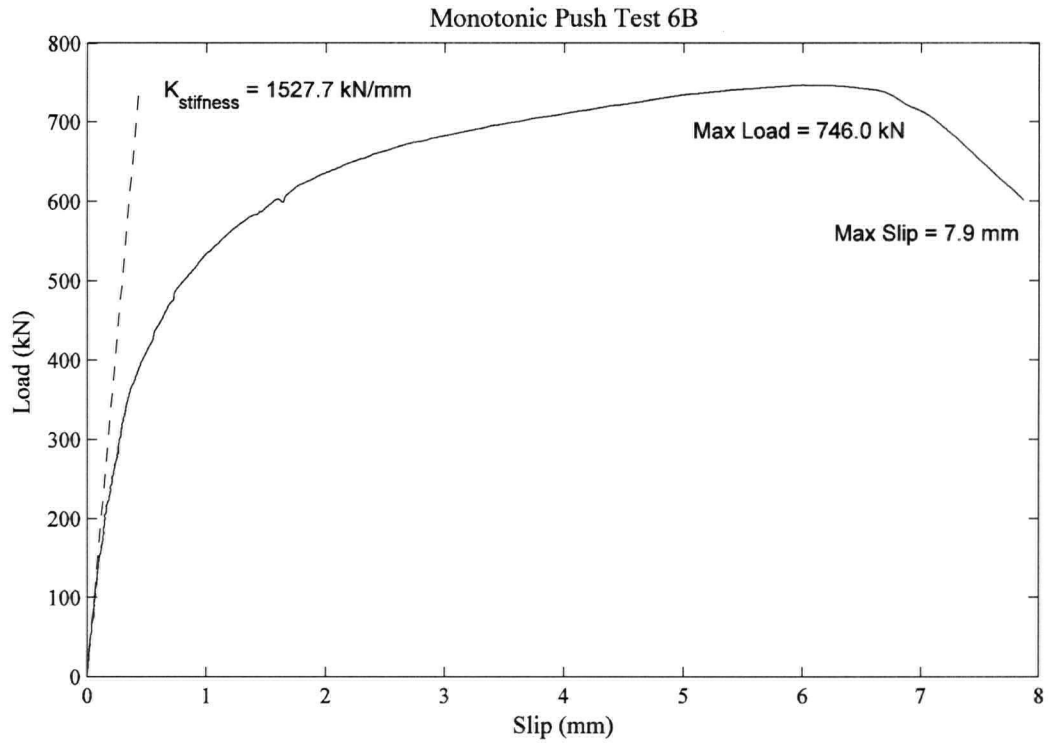
Panel No.	Ultimate Strength (kN)	Stiffness (kN/mm)	Maximum Slip (mm)
6A	693.2	1092.3	7.5
6B	746.0	1527.7	7.9
7C	836.1	909.7	9.3
8A	890.6	1280.4	9.0
8B	987.4	1213.9	8.5
9A	1036.1	1493.6	10.3
9B	1043.9	1329.8	10.7
10A	1194.3	1033.5	8.4
10B	1173.5	1288.4	9.6

The following pages contain the load slip plots for the nine monotonic tests in addition to photos and comments on the test procedures and results.



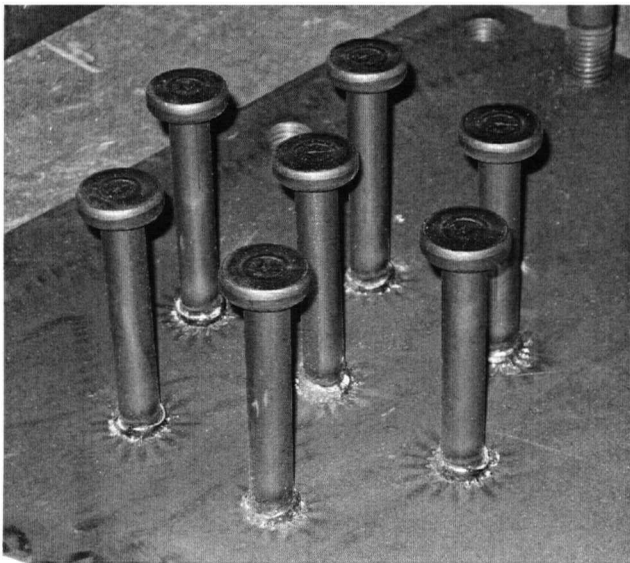
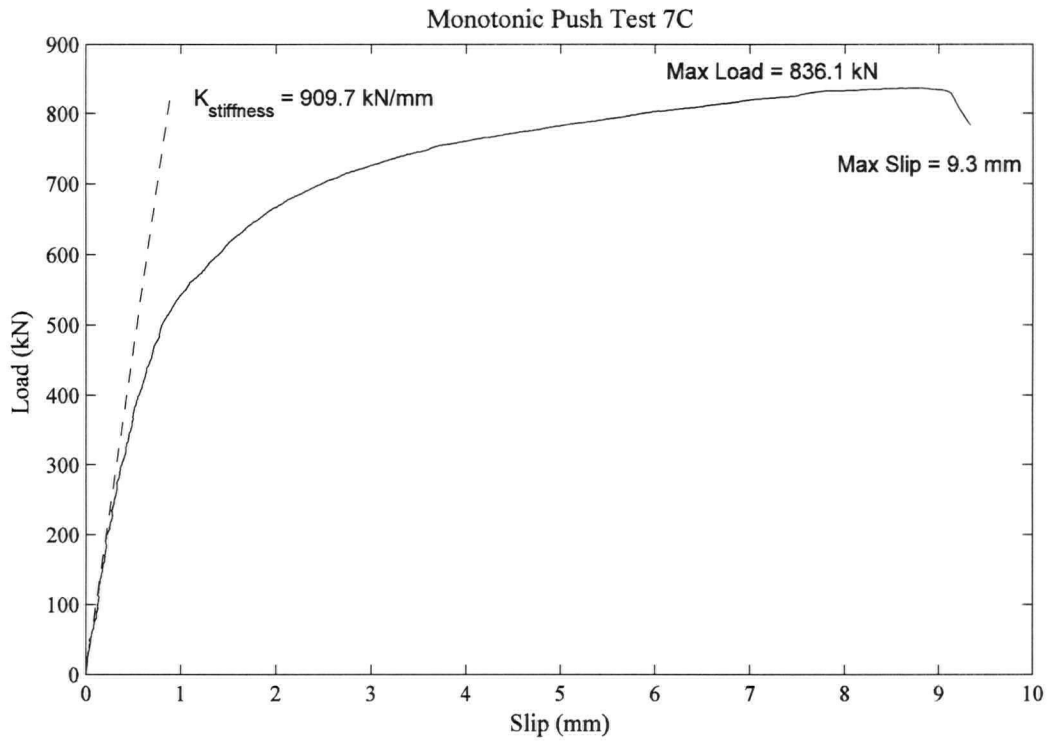
Comments: Abrupt load reduction prior to the plastic deformation region attributed to a premature stud failure. Left shows the studs in the grout, right the residual stud height.

PANEL 6A



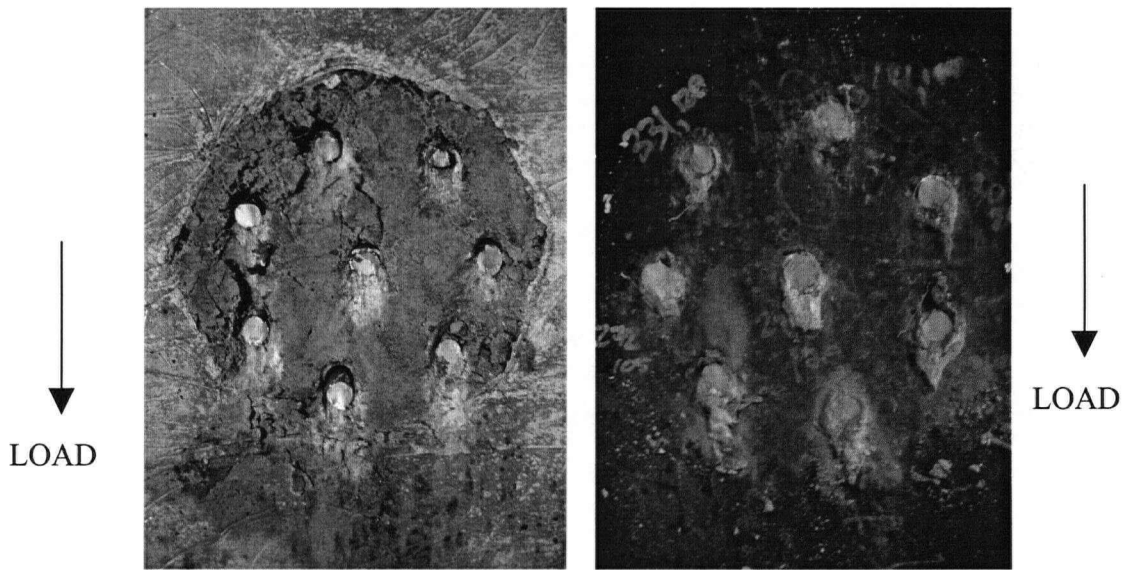
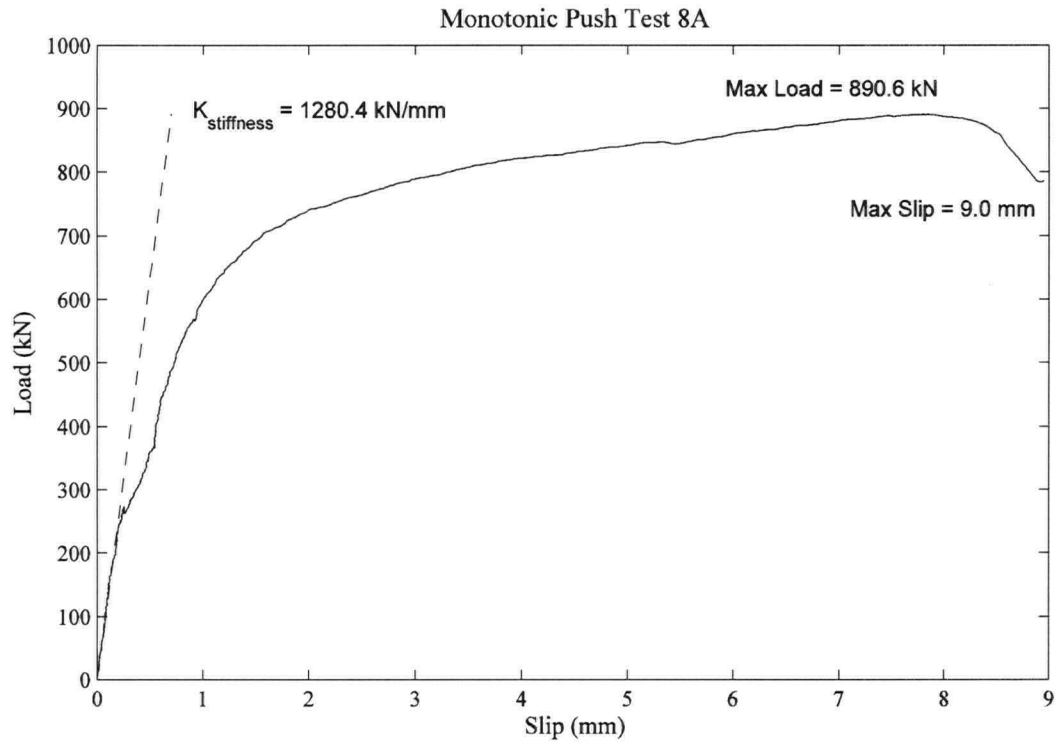
Comments: Left photo shows the studs in the grout and on the right the residual stud height on the plate.

PANEL 6B



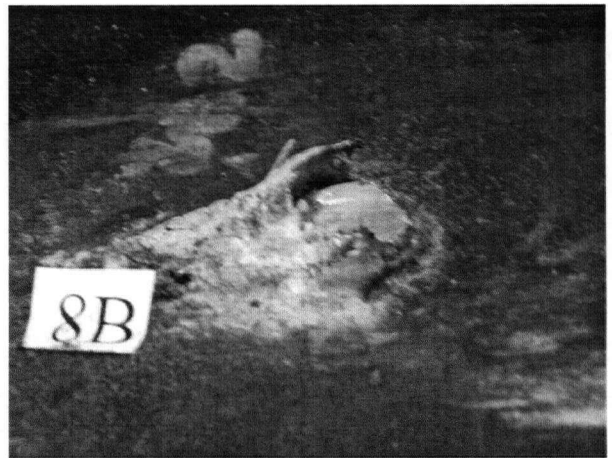
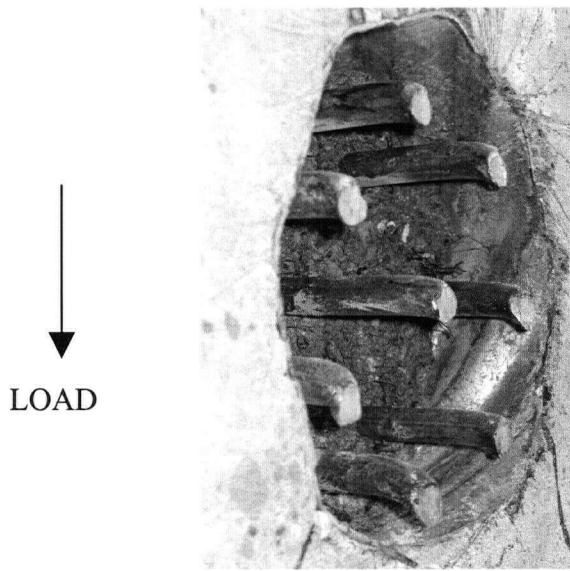
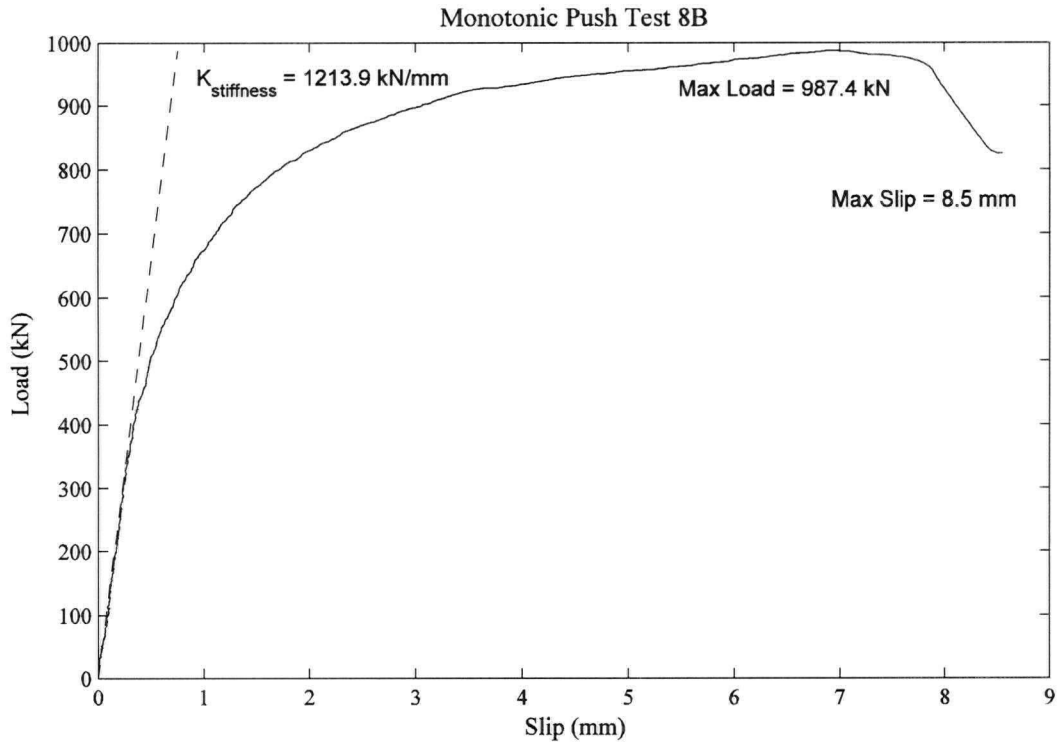
Comments: The studs were not removed from this push test. The left photo shows the studs welded on the plate and on the right the residual stud height on the plate after testing.

PANEL 7C



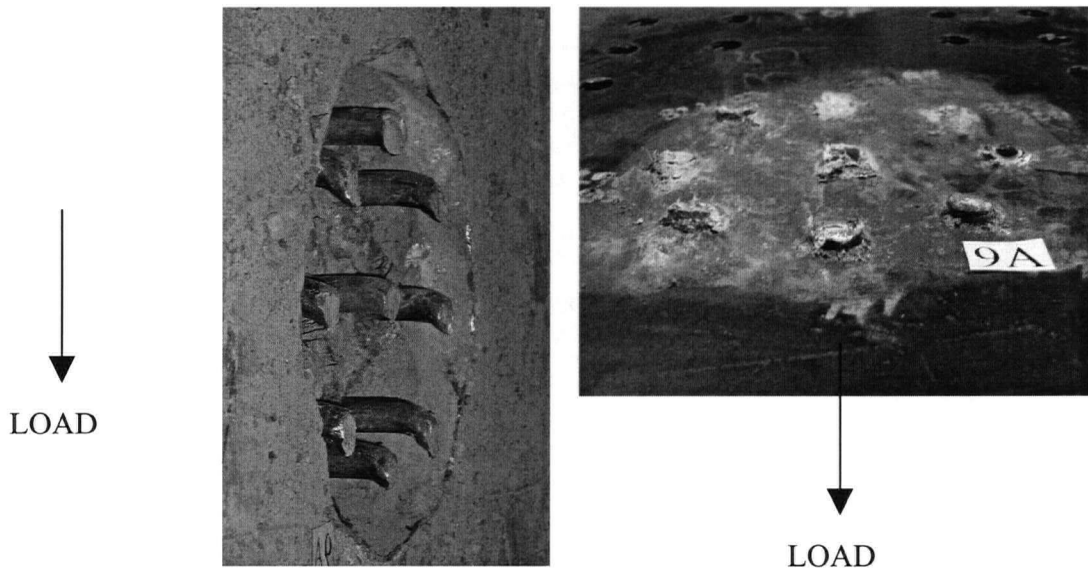
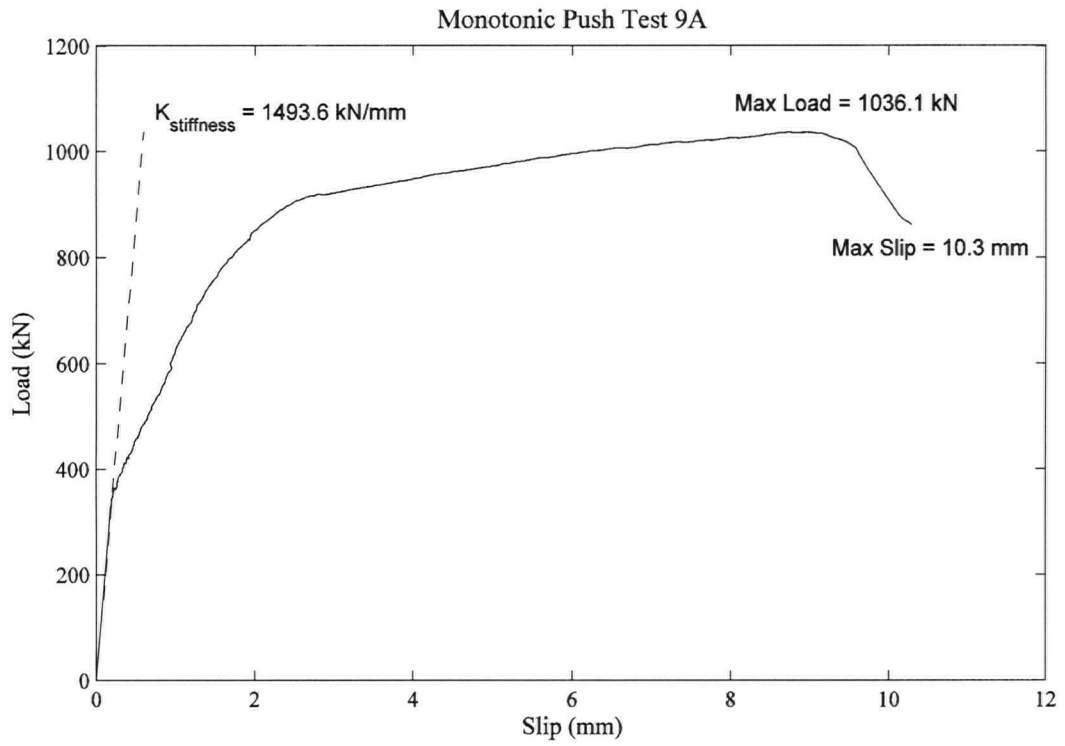
Comments: Left photo shows the studs in the grout and on the right the residual stud height on the plate.

PANEL 8A



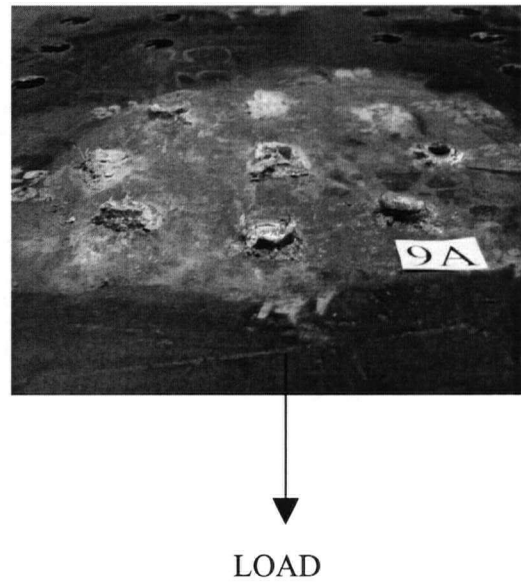
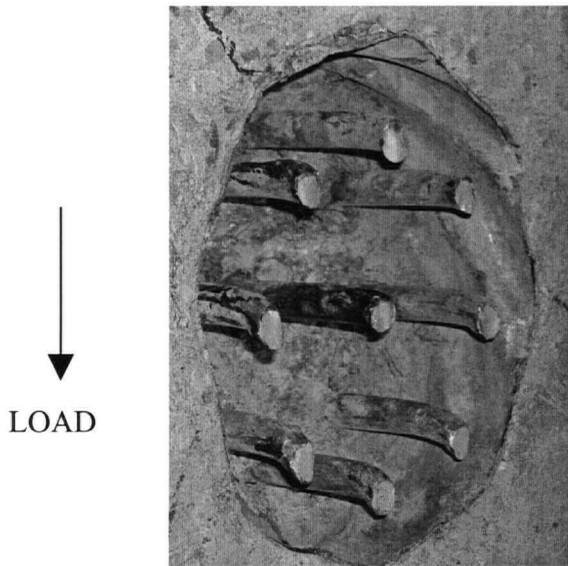
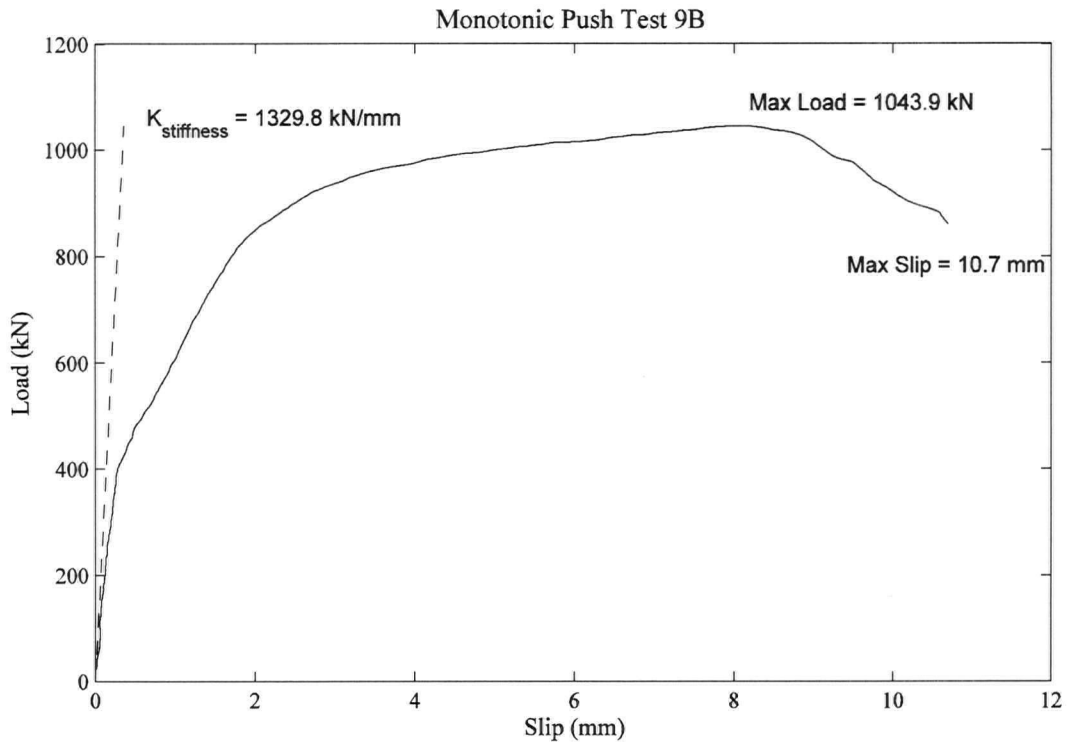
Comments: Left photo shows the studs in the grout and on the right the a close up of the residual stud height on the plate with the weld collar.

PANEL 8B



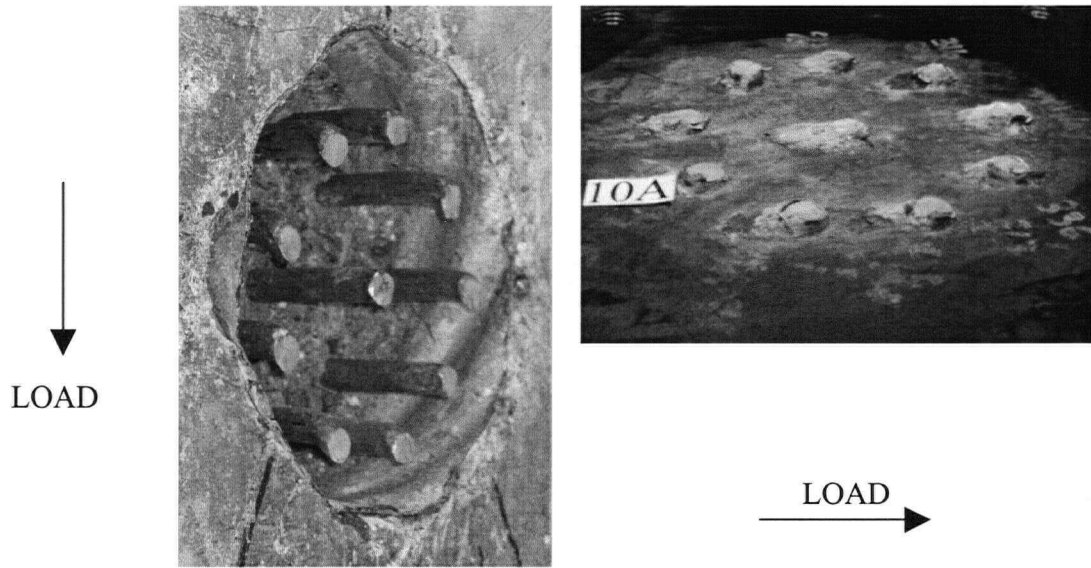
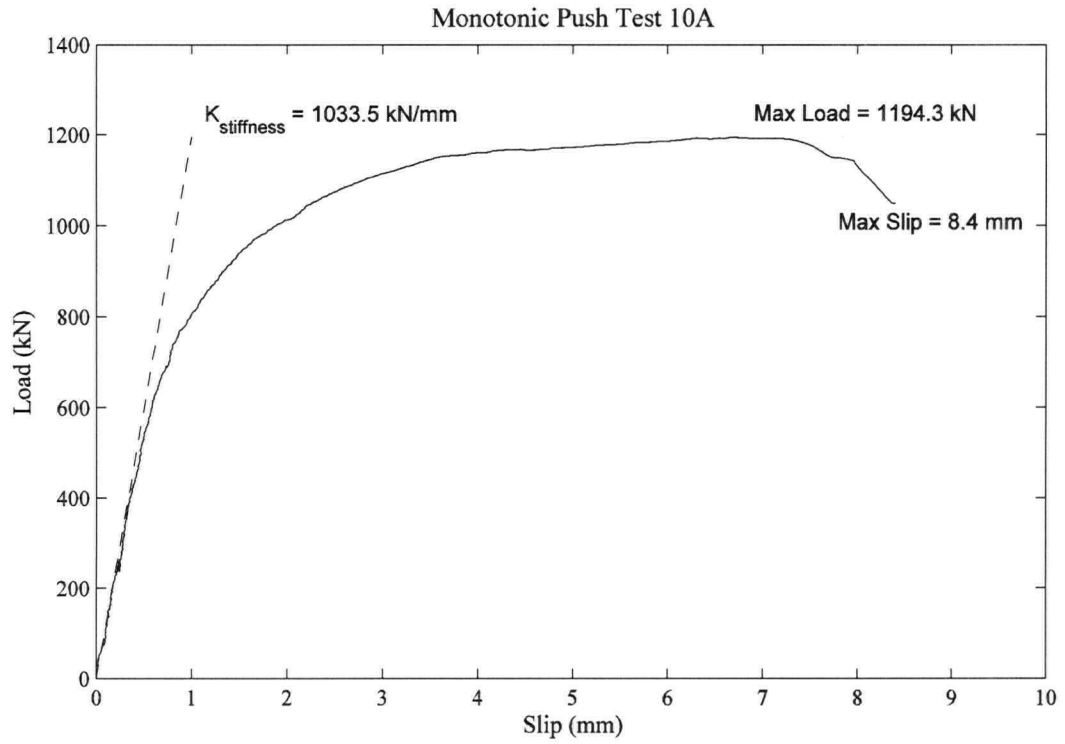
Comments: Left photo shows the studs in the grout and on the right the residual stud height on the plate.

PANEL 9A



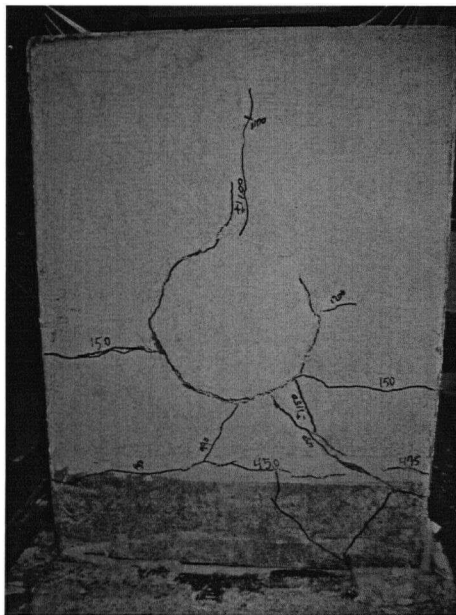
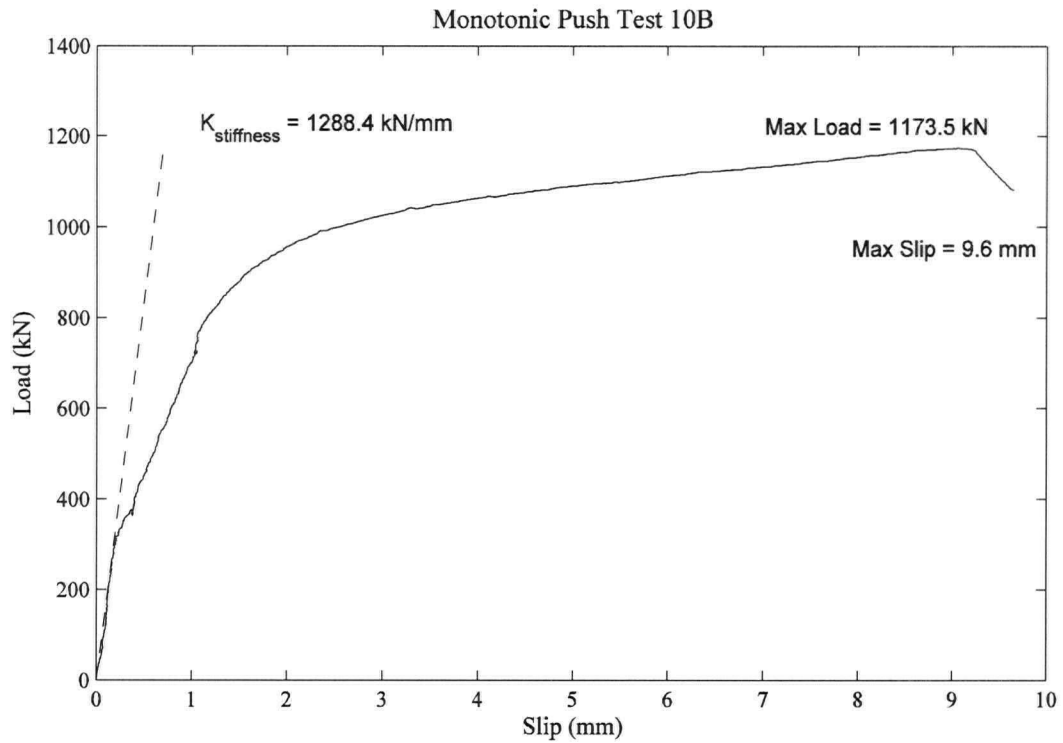
Comments: Left photo shows the studs in the grout and on the right the residual stud height on the plate.

PANEL 9B



Comments: Left photo shows the studs in the grout and on the right the residual stud height on the plate.

PANEL 10A



LOAD →

Comments: The entire grout pocket was removed from the concrete and no damage found. Left photo shows the studs typical crack pattern and on the right the residual stud height on the plate.

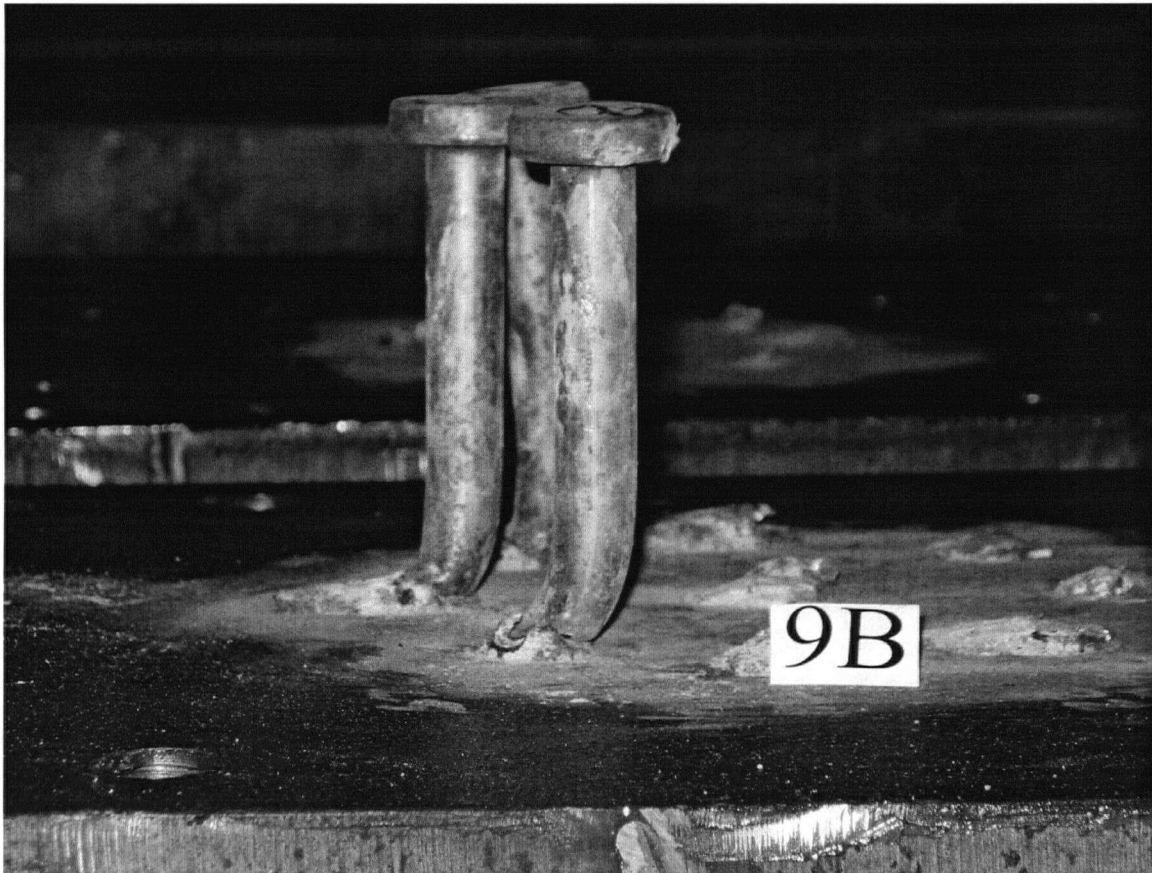
PANEL 10B

C.2 Removal of Studs from Grout Pocket

After all the data was collected from the monotonic push test specimens, the studs were removed from the grout pockets with a concrete rotary drill and jackhammer. Care was taken to minimize the stud damage. The localized crushing observed at the leading edge of the studs was estimated to be about 8mm deep, similar to the major zone of plastic deformation at the base of the studs. This was determined through feedback of the concrete rotary drill which was similar for the full length of the drill hole, except for the first 8mm which was determined to be easier to advance the drill.

The studs were removed to observe the deformation along the length of the stud and to measure the maximum displacement of the stud to compare to the average slip recorded from the push tests.

Figure C-1 Shear Studs on Plate After Removal from Grout from Specimen 9B



C.2 Cyclic Push Tests

A series of 9 cyclic push tests were originally constructed with three having a 6 stud cluster, three with an eight stud cluster and the remaining having 10 studs. Two of the eight stud cluster specimens were destroyed because of the servo valve feedback cable being inadvertently disconnected while undergoing cyclic loading in the symmetrical configuration. The final 8 stud cluster panel was discarded and not tested.

Cyclic loading of the panels with 6 studs per cluster was completed between March 19, 2005 and June 01, 2005. Cyclic loading of the panels with 10 studs per cluster was completed between June 22, 2005 and August 23, 2005.

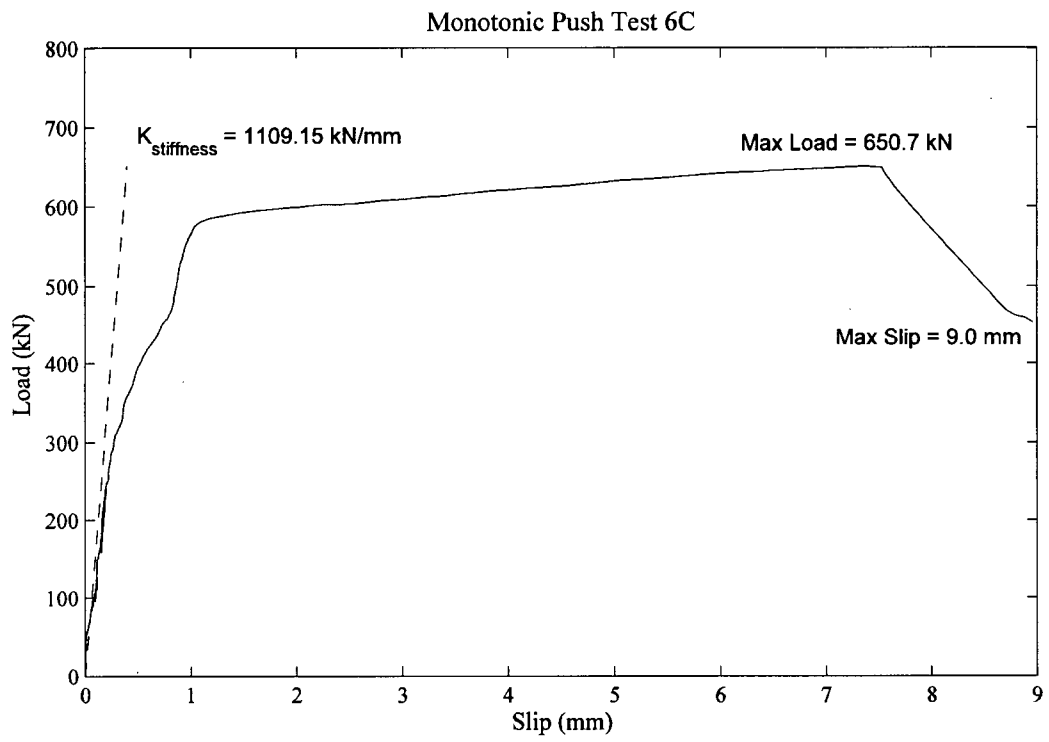
Table C-3 Cyclic Push Test Specimen Schedule

Panel No.	Studs per Cluster	No. Cycles	Test Date (mm-dd-yy)	Concrete Age (days)	Grout Age (days)
6C	6	500,000	02-11-06	731	416
6D	6	750,000	02-13-06	732	418
6E	7	250,000	02-12-06	731	417
10C	8	500,000	03-07-06	754	440
10D	8	250,000	03-07-06	754	440
10E	9	750,000	03-07-06	754	440

Table C-4 Cyclic Push Test Data Summary

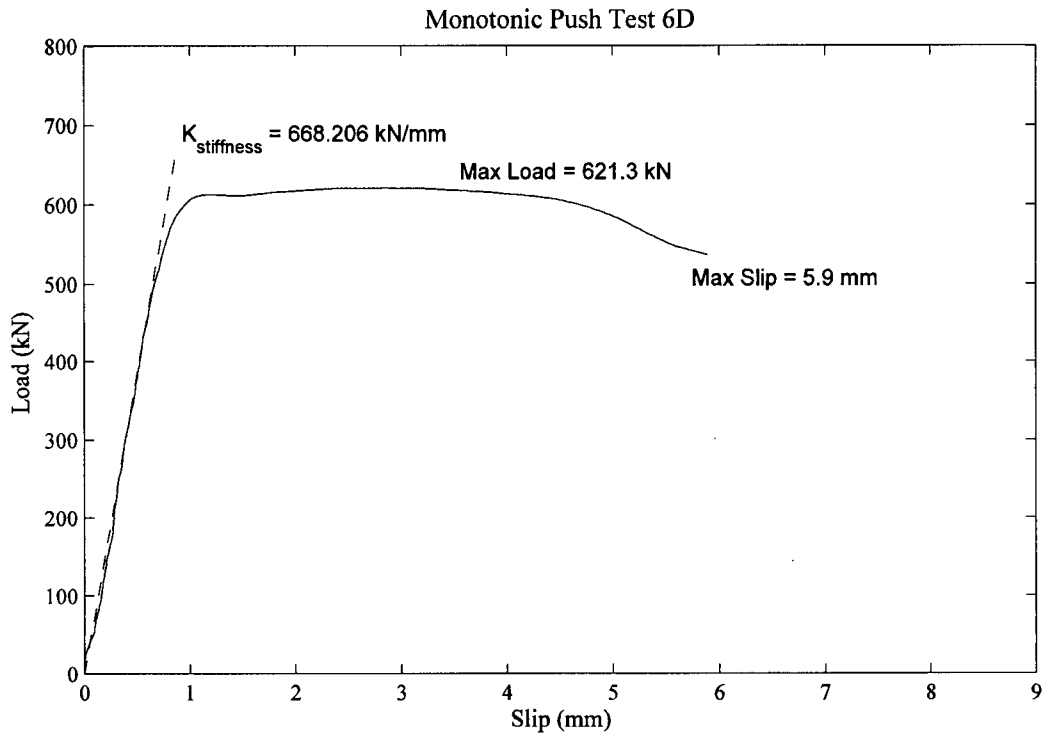
Panel No.	Ultimate Strength (kN)	Stiffness (kN/mm)	Maximum Slip (mm)
6C	6682.6	1270.2	7.2
6D	650.7	1190.2	9.0
6E	621.2	668.2	5.9
10E	1113.2	879.3	16.7
10D	1125.6	777.0	9.5
10E	1087.0	668.5	8.2

The following pages contain the load slip plots for the six cyclic.



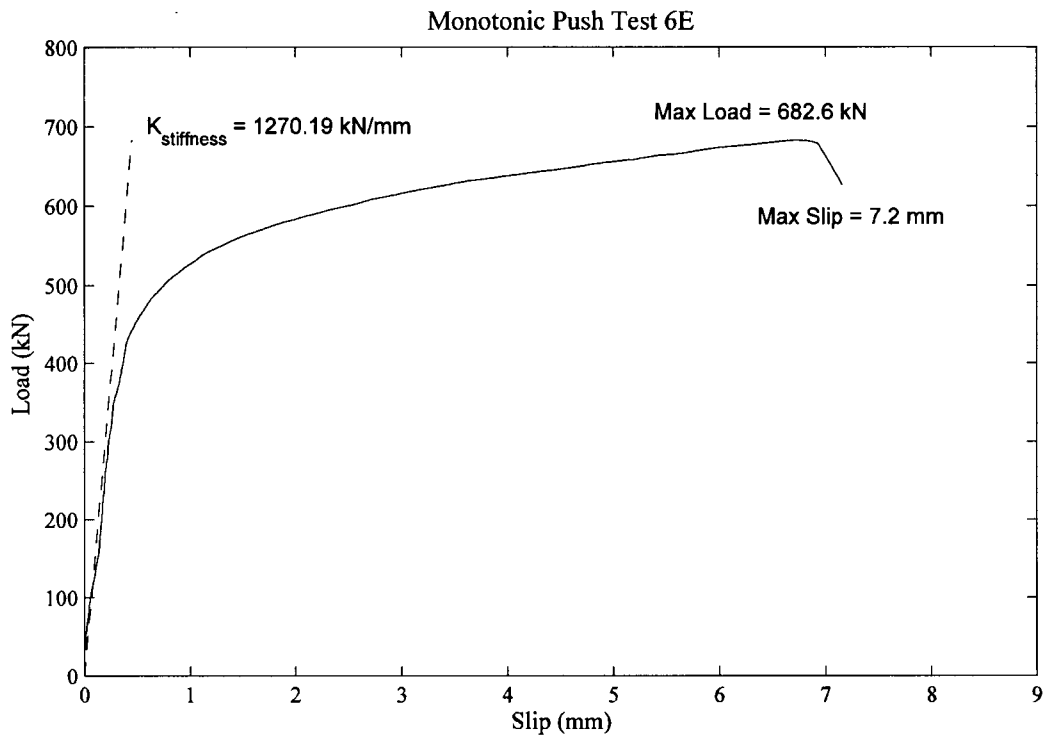
Comments: The studs were not removed from this push test.

PANEL 6C



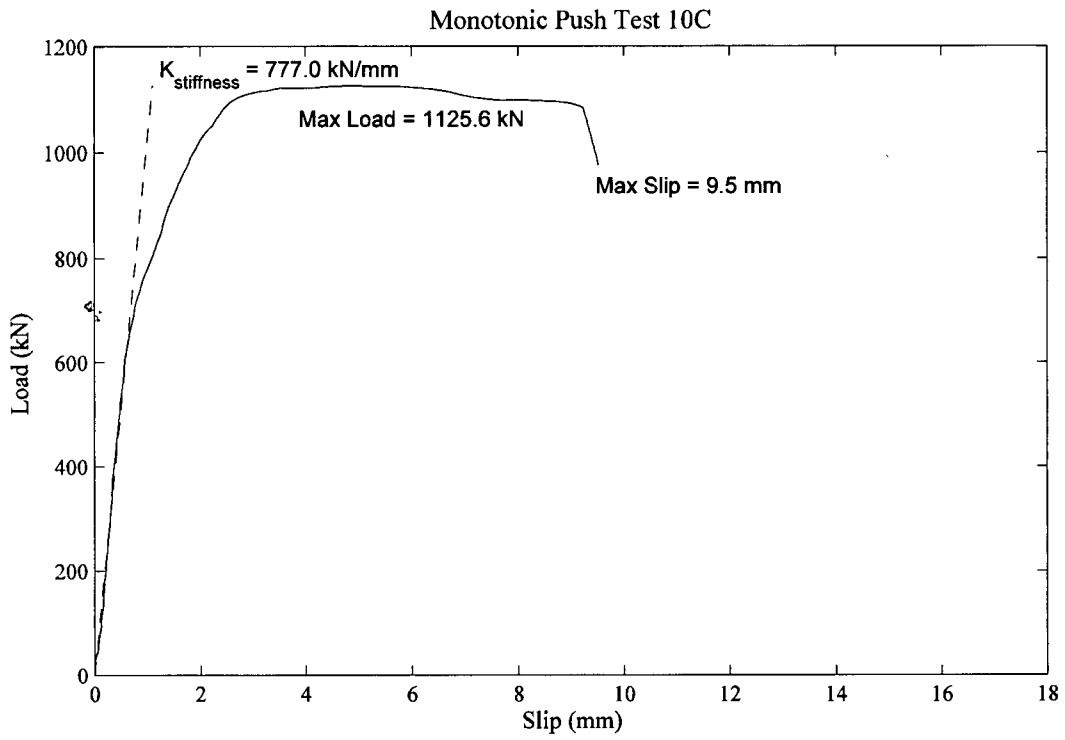
Comments: The studs were not removed from this push test.

PANEL 6D



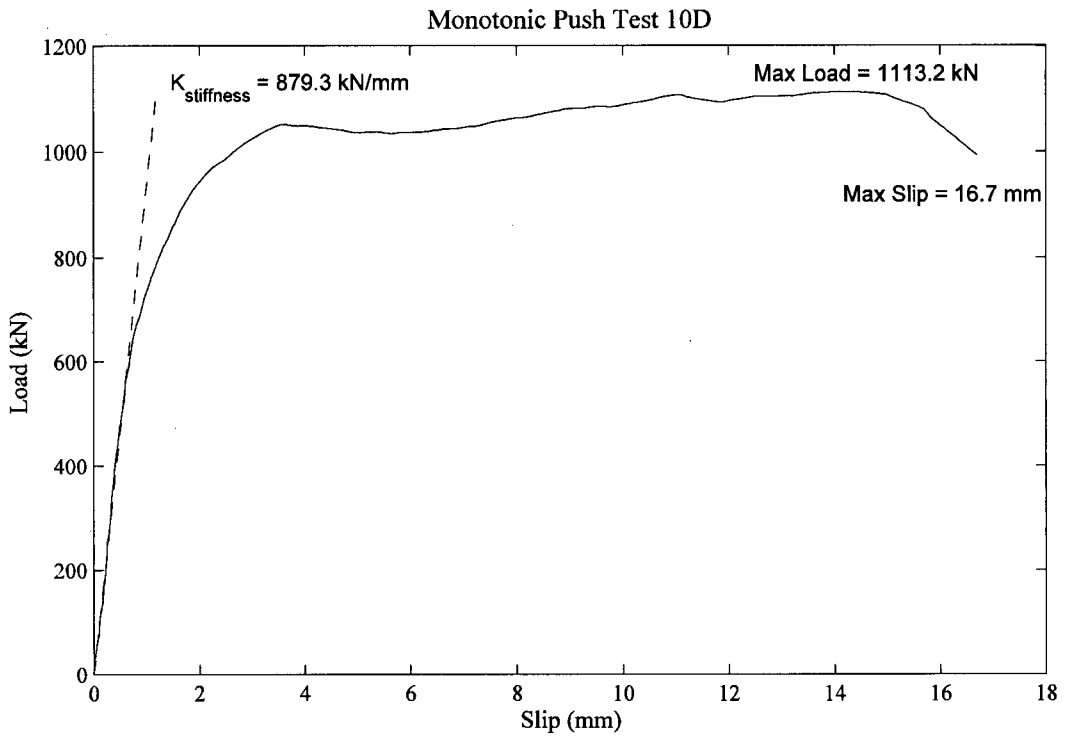
Comments: The studs were not removed from this push test.

PANEL 6E



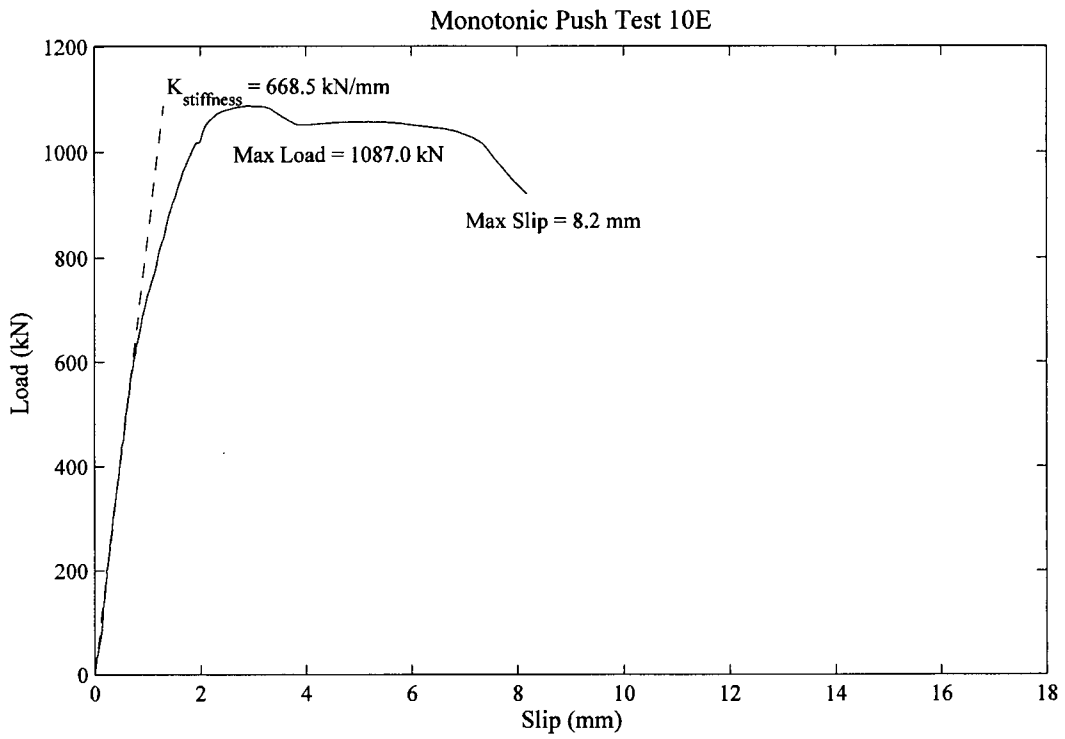
Comments: The studs were not removed from this push test.

PANEL 10C



Comments: The studs were not removed from this push test.

PANEL 10D



Comments: The studs were not removed from this push test.

PANEL 10E

APPENDIX D Bridge Analysis and Design

D.1 Introduction

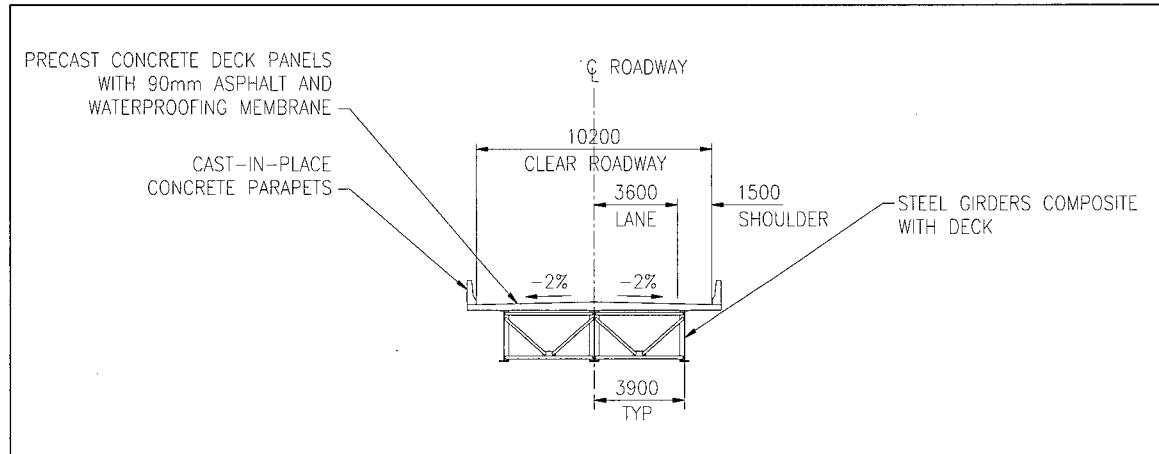
A parametric bridge study was undertaken to investigate the superstructure Serviceability Limit State response of a simply supported bridge with a 36 meter span by varying the longitudinal stud cluster spacing. Four stud cluster spacing were considered; 300 mm, 600 mm, 1200 mm and 2400 mm.

The superstructures were designed to maximize the flexibility of the superstructures, since this would have the largest impact on the serviceability limit states. The design was completed using a custom written spreadsheet implementing the “simplified methods of analysis” in CAN/CSA-S6-00. The resulting superstructure was then subsequently used to prepare a series of finite element models to study the effect of varying the stud cluster spacing and stiffness. Details of typical superstructure design, such as girder splice design, stiffeners, and etcetera were specifically not included.

D.2 Superstructure

The superstructure has a 10.98m wide deck providing a 10.2m wide driving surface. The deck was designed to a standard 810mm high MoT BC cast in place concrete parapets complete with a steel railing. An allowance was included in the design for a 90 mm deep asphalt wearing surface. A three girder superstructure system was chosen providing 3.9m center to center of girders and a 1.59m deck cantilever. This is a common bridge deck width for 2 lane roads in the province of British Columbia.

Figure D-1 Bridge Cross Section



The chosen cross-section results in a maximum of 3 design lanes according to CAN/CSA-S6-00. Code prescribed unit weights were adopted for used for the respective materials used in the design. The commercially available software STAAD.Pro 2005™ was used for the analysis of the CL-625 truck to determine bending and shear envelopes. The live load distribution factors were taken from Section 5 for the respective limit states. Dead load distribution also considered the simplified methods in CAN/CSA-S6-00. A Class 'C' highway was considered for fatigue design checks, which is consistent with the loading level chosen for the cyclic push tests. Construction loading assumed that the precast concrete deck panels would be placed by crane from the ground, thereby maximizing the flexibility of the girders. A linear varying width top and bottom flange was also incorporated into the design to increase the superstructure flexibility. For the purposes of design the shear stud clusters were assumed to be infinitely rigid. The Ultimate Limit State and Fatigue Limit State (FLS) design of the studs was completed using the design equations of CAN/CSA-S6-00. It was found that the stud cluster spacing was practical up to 1200 mm, with the 2400 mm stud cluster spacing requiring up to 26, 22 mm diameter studs per one cluster to satisfy the FLS.

A drawing of the girder design is provided in Appendix F.

D.3 Bridge Structural Analysis

The output from the commercially available STAAD.Pro 2005 analysis file and output is found on the following six pages.



STAAD.Pro Report

To: _____ From: _____
 Copy to: _____ Date: 17/08/2006 Ref: 36m beam for bridge design
 14:23:00

Job Information

	Engineer	Checked	Approved
Name:	KEL		
Date:	04-Sep-04		

Structure Type	PLANE FRAME
----------------	-------------

Number of Nodes	11	Highest Node	11
Number of Elements	10	Highest Beam	10

Number of Basic Load Cases	1
Number of Combination Load Cases	0

Included in this printout are data for:

All	The Whole Structure
-----	---------------------

Nodes

Node	X (m)	Y (m)	Z (m)
1	0.000	0.000	0.000
2	36.000	0.000	0.000
3	3.600	0.000	0.000
4	7.200	0.000	0.000
5	10.800	0.000	0.000
6	14.400	0.000	0.000
7	18.000	0.000	0.000
8	21.600	0.000	0.000
9	25.200	0.000	0.000
10	28.800	0.000	0.000
11	32.400	0.000	0.000

Beams

Beam	Node A	Node B	Length (m)	Property	β (degrees)
1	1	3	3.600	1	0
2	3	4	3.600	1	0
3	4	5	3.600	1	0
4	5	6	3.600	1	0
5	6	7	3.600	1	0
6	7	8	3.600	1	0
7	8	9	3.600	1	0
8	9	10	3.600	1	0
9	10	11	3.600	1	0
10	11	2	3.600	1	0

Materials

Mat	Name	E (kN/mm ²)	ν	Density (kg/m ³)	α (1/K)
3	STEEL	200.000	0.300	18.2E 3	6.5E -6
4	ALUMINUM	68.948	0.330	2.71E 3	23E -6
5	CONCRETE	21.718	0.170	2.4E 3	10E -6

Supports

Node	X (kN/mm)	Y (kN/mm)	Z (kN/mm)	rX (kN·m/deg)	rY (kN·m/deg)	rZ (kN·m/deg)
1	Fixed	Fixed	Fixed	-	-	-
2	-	Fixed	Fixed	Fixed	Fixed	-

Moving Load Definition : Type 1

Width (m)
-

Force (kN)	Distance (m)
-50.000	-
-125.000	3.600
-125.000	1.200
-175.000	6.600
-150.000	6.600

Moving Load Definition : Type 2

Width (m)
-

Force (kN)	Distance (m)
-150.000	-
-175.000	6.600
-125.000	6.600
-125.000	1.200
-50.000	3.600

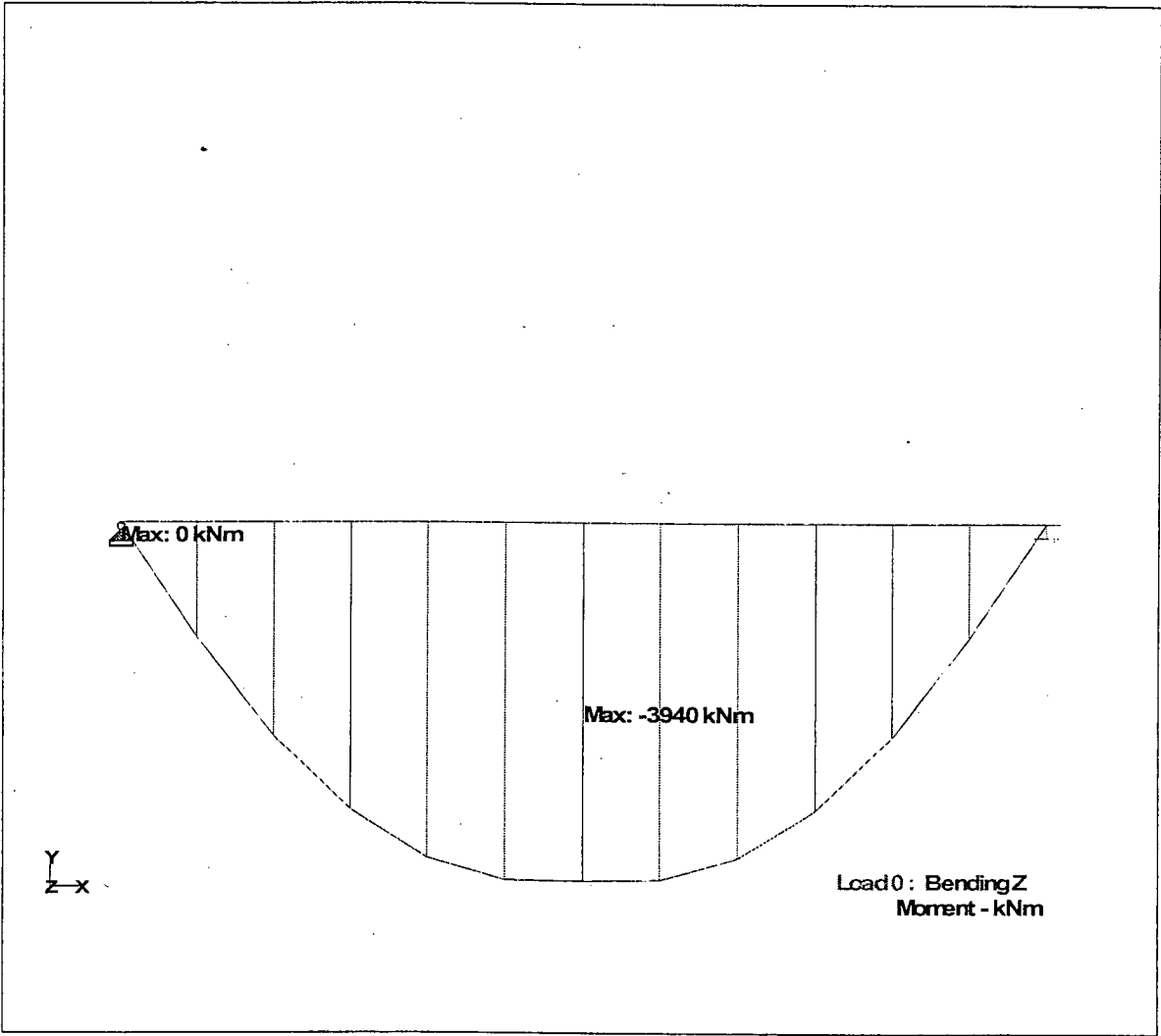
Reaction Summary

			Horizontal	Vertical	Horizontal	Moment		
	Node	L/C	FX (kN)	FY (kN)	FZ (kN)	MX (kNm)	MY (kNm)	MZ (kNm)
Max FX	1	1:LOAD	0.000	-149.999	0.000	0.000	0.000	0.000
Min FX	1	1:LOAD	0.000	-149.999	0.000	0.000	0.000	0.000
Max FY	1	110:LOAD	0.000	0.000	0.000	0.000	0.000	0.000
Min FY	1	181:LOAD	0.000	-472.084	0.000	0.000	0.000	0.000
Max FZ	1	1:LOAD	0.000	-149.999	0.000	0.000	0.000	0.000
Min FZ	1	1:LOAD	0.000	-149.999	0.000	0.000	0.000	0.000
Max MX	1	1:LOAD	0.000	-149.999	0.000	0.000	0.000	0.000
Min MX	1	1:LOAD	0.000	-149.999	0.000	0.000	0.000	0.000
Max MY	1	1:LOAD	0.000	-149.999	0.000	0.000	0.000	0.000
Min MY	1	1:LOAD	0.000	-149.999	0.000	0.000	0.000	0.000
Max MZ	1	1:LOAD	0.000	-149.999	0.000	0.000	0.000	0.000
Min MZ	1	1:LOAD	0.000	-149.999	0.000	0.000	0.000	0.000

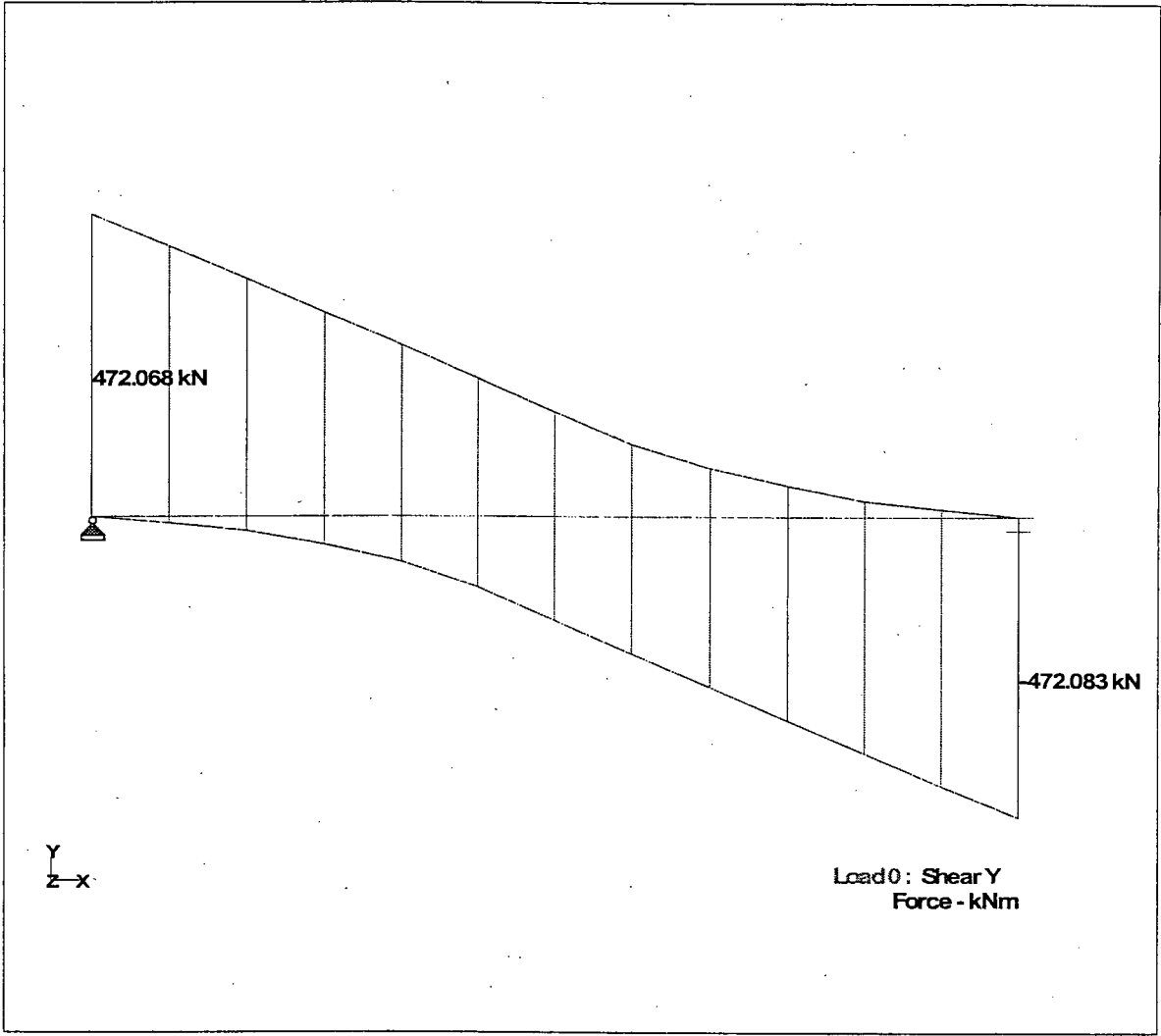
Beam Force Detail Summary

Sign convention as diagrams:- positive above line, negative below line except Fx where positive is compression. Distance d is given from beam end A.

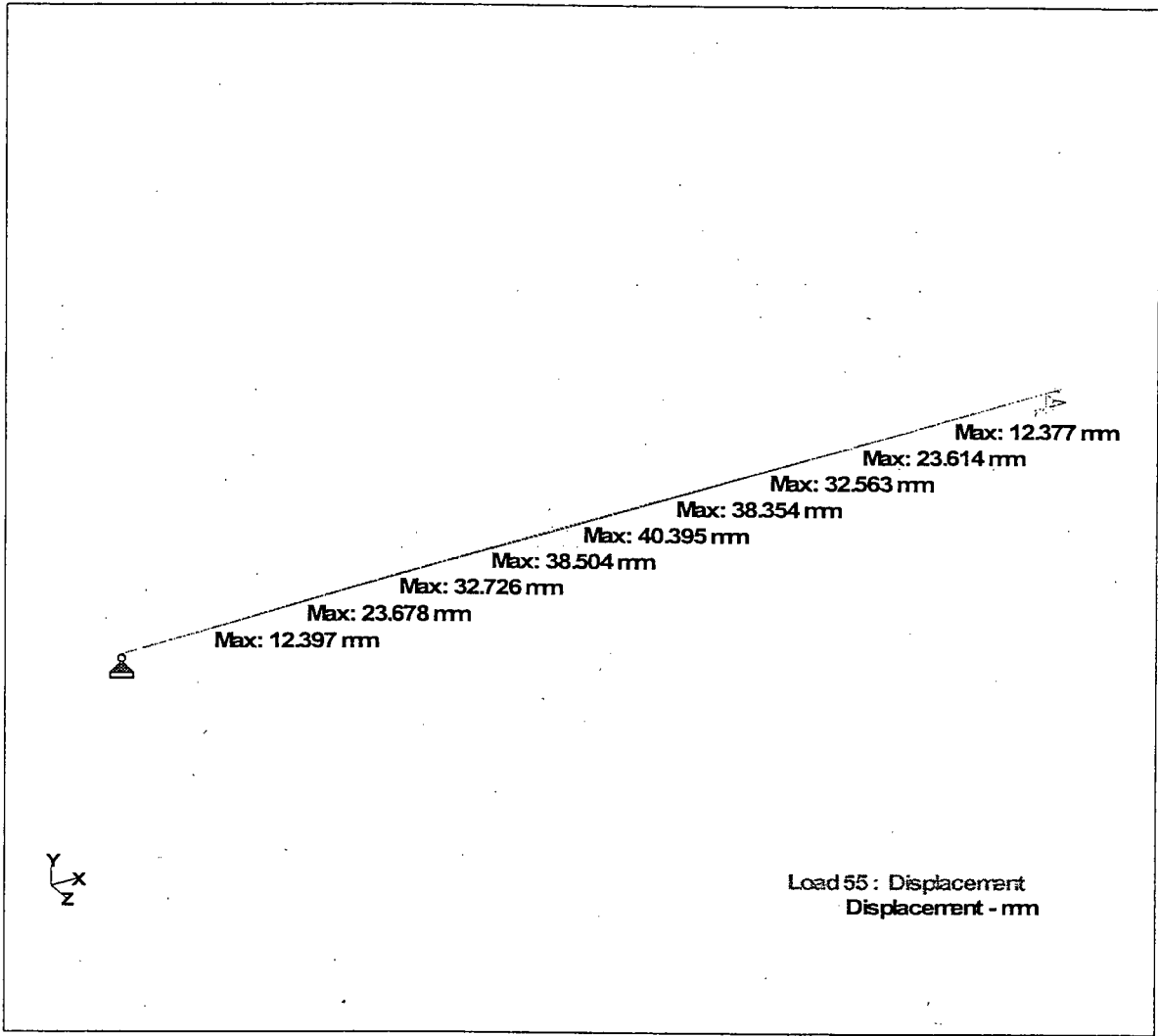
	Beam	L/C	d (m)	Axial Fx (kN)	Shear Fy (kN) Fz (kN)		Torsion Mx (kNm)	Bending My (kNm) Mz (kNm)	
Max Fx	1	1:LOAD	0.000	0.000	-149.999	0.000	0.000	0.000	0.000
Min Fx	1	1:LOAD	0.000	0.000	-149.999	0.000	0.000	0.000	0.000
Max Fy	10	73:LOAD	3.600	0.000	472.082	0.000	0.000	0.000	0.000
Min Fy	1	181:LOAD	0.000	0.000	-472.084	0.000	0.000	0.000	0.000
Max Fz	1	1:LOAD	0.000	0.000	-149.999	0.000	0.000	0.000	0.000
Min Fz	1	1:LOAD	0.000	0.000	-149.999	0.000	0.000	0.000	0.000
Max Mx	1	1:LOAD	0.000	0.000	-149.999	0.000	0.000	0.000	0.000
Min Mx	1	1:LOAD	0.000	0.000	-149.999	0.000	0.000	0.000	0.000
Max My	1	1:LOAD	0.000	0.000	-149.999	0.000	0.000	0.000	0.000
Min My	1	1:LOAD	0.000	0.000	-149.999	0.000	0.000	0.000	0.000
Max Mz	5	202:LOAD	2.880	0.000	-34.792	0.000	0.000	0.000	3.96E 3
Min Mz	10	62:LOAD	3.600	0.000	376.597	0.000	0.000	0.000	-0.000



Bending Moment Envelope, Unfactored, Undistributed, No DLA



Shear Envelope, Unfactored, Undistributed, No DLA



Displacements, Unfactored, Undistributed, No DLA for I-CL-625 Truck

D.4 Bridge Design

The design spreadsheet for the superstructure is found on the subsequent pages.

**36.0m Simple Span
Steel Girder Precast Concrete Deck Bridge Design**

Based on CSA/CAN - S6-2000 and MoT Bridge Design Standards

Kent LaRose

University of British Columbia

Table of Contents

Section	Title
A	Cover Sheet
B	Input for Geometry and Materials
C	Steel Section - Geometric Properties
D	Composite Section - Geometric Properties
E	Load Distribution, Moment and Shear Forces
F	Non-Composite Steel Section - Moment Resistance
G	Steel Section - Shear Resistance
H	Composite Section - Moment Resistance
I	Check of Moment, Shear and Code Clauses
J	Transverse Stiffener Design
K	Bearing Stiffener Design
L	Shear Studs
M	Superstructure Vibration Check
N	Flange to Web Weld Design
O	Cross Bracing Design
P	Deck Design

Input for Geometry and Materials

Bridge Dimensions	
Girder Length	36,000 mm
Span Length, L	36,000 mm
Number of Girders	3
Clearance to Stream @ Pier	0 mm
C/C of Girders	3,900 mm
C/C of CL-625 Wheels	1,800 mm
Clear Deck Width	10,200 mm

Load Factors for Analysis	
DLA	1.25 3 or more axles, except 1, 2 & 3
DLA	1.3 any 2 axles, or 1, 2 & 3
DLA	1.4 only 1 axle
DLA _{construction}	1.25 slow moving vehicle
Live Load Factor, α_{LULS1}	1.7 (Table 3.5.1 (a) - S6-2000)
Live Load Factor, α_{LULS2}	1.6 (Table 3.5.1 (a) - S6-2000)
Live Load Factor, α_{LULS3}	1.4 (Table 3.5.1 (a) - S6-2000)
Dead - CIP Concrete, α_{Dc}	1.2 (Table 3.5.1 (b) - S6-2000)
Dead - Precast Concrete, α_{Dcjp}	1.1 (Table 3.5.1 (b) - S6-2000)
Dead - Steel, α_{Dprec}	1.1 (Table 3.5.1 (b) - S6-2000)
Dead - Timber, α_{Dt}	1.2 (Table 3.5.1 (b) - S6-2000)
Dead - Wearing Surface, α_{Dws}	1.5 (Table 3.5.1 (b) - S6-2000)

* NON-COMPOSITE

Girder Only
120.6 kN
27.1 kip

Girder + Bracing
132.7 kN
29.8 kip

Geometric Properties							
Location	0	3,600	7,200	10,800	14,400	18,000	
Steel							
Symmetry	mono	mono	mono	mono	mono	mono	(mono/double)
Curvature	single	single	single	single	single	single	(single/double)
Unbraced Length	6,000	6,000	6,000	6,000	6,000	6,000	mm
Stiffener Spacing, 'a'	1,500	3,000	3,000	3,000	3,000	3,000	mm
Transverse	yes	yes	yes	yes	yes	YES	(yes/no)
Longitudinal	no	no	no	no	no	no	(yes/no)
Top Flange Thickness	25.4	25.4	25.4	25.4	25.4	25.4	mm
Top Flange Width	350.0	374.0	398.0	422.0	446.0	470.0	mm
Width of Web	12.7	12.7	12.7	12.7	12.7	12.7	mm
Height of Web	1,625.0	1,625.0	1,625.0	1,625.0	1,625.0	1,625.0	mm
Bottom Flange Thickness	31.8	31.8	31.8	31.8	31.8	31.8	mm
Bottom Flange Width	440.0	486.0	532.0	578.0	624.0	670.0	mm
Concrete Deck							
Slab Thickness	255	255	255	255	255	255	mm
Slab Width	10,980	10,980	10,980	10,980	10,980	10,980	mm
B (Clause 5.8.2.1 - S6-2000)	1,775	1,763	1,751	1,739	1,727	1,715	mm
L/B	20	20	21	21	21	21	
B _s (Clause 5.8.2.1 - S6-2000)	1,775	1,763	1,751	1,739	1,727	1,715	mm
Slab Width / Girders	3,660	3,660	3,660	3,660	3,660	3,660	mm
Effective Width, b _e	3,660	3,660	3,660	3,660	3,660	3,660	mm
Future overlay, d _s	100	100	100	100	100	100	mm
Concrete Curb							
Curb Area (one curb)	244,069	244,069	244,069	244,069	244,069	244,069	mm ²

Summary of Dead Loads from Girder and Deck (per girder)							
Dead Load - Girder	3.69	3.86	4.04	4.21	4.39	4.56	kN/m
Dead Load - Concrete Deck	22.40	22.40	22.40	22.40	22.40	22.40	kN/m
Dead Load - Overlay	7.99	7.99	7.99	7.99	7.99	7.99	kN/m
Dead Load - Concrete Curb	3.91	3.91	3.91	3.91	3.91	3.91	kN/m

Material Properties			
Steel	Concrete	Timber	
ϕ_s (shear and bending)	0.95	Unit Weight	6 kN/m ³
ϕ_b (bolts)	0.67	ϕ_s	
ϕ_w (welds)	0.67	E _c	26,199 MPa
ϕ_{sc} (shear connectors)	0.85	f' _c	35 MPa
ϕ_{ba} (bearings)	0.75	n	7.6
E _s	200,000 MPa	3n	22.9
G _s	77,000 MPa	Unit Weight 1	23.5 kN/m ³
F _y	350 MPa	Unit Weight 2	24 kN/m ³
F _u	480 MPa		
X _u	480 MPa		
Unit Weight	77 kN/m ³		

Steel Section - Geometric Properties

Location	0	3,600	7,200	10,800	14,400	18,000	mm
Summary of Section Properties							
Top Flange Area, A_f	8,890.0	9,499.6	10,109.2	10,718.8	11,328.4	11,938.0	mm ²
Centroid of Top Flange, y_f	1,669.5	1,669.5	1,669.5	1,669.5	1,669.5	1,669.5	mm
Web Area, A_{web}	20,637.5	20,637.5	20,637.5	20,637.5	20,637.5	20,637.5	mm ²
Centroid of Web, y_{web}	844.3	844.3	844.3	844.3	844.3	844.3	mm
Bottom Flange Area, A_{bf}	13,992.0	15,454.8	16,917.6	18,380.4	19,843.2	21,306.0	mm ²
Centroid of Bottom Flange, y_{bf}	15.9	15.9	15.9	15.9	15.9	15.9	mm
Total Girder Steel Area, A_{tot}	43,519.5	45,591.9	47,664.3	49,736.7	51,809.1	53,881.5	mm ²
Total Height of Girder, h	1,682.2	1,682.2	1,682.2	1,682.2	1,682.2	1,682.2	mm
Centroid of Steel Section, y_{xx}	746.5	735.4	725.3	716.0	707.5	699.6	mm
Depth of Compression of Web, d_c	935.7	946.8	956.9	966.2	974.7	982.6	mm
Moment of Inertia, I_{xx}	1.958E+10	2.085E+10	2.212E+10	2.338E+10	2.463E+10	2.587E+10	mm ⁴
Section Modulus - Top Flange, S_{top}	-2.622E+07	-2.836E+07	-3.050E+07	-3.265E+07	-3.481E+07	-3.698E+07	mm ³
Section Modulus - Bottom Flange, S_{bot}	2.092E+07	2.203E+07	2.312E+07	2.420E+07	2.527E+07	2.633E+07	mm ³
Minimum Section Modulus, S_{xmin}	2.092E+07	2.203E+07	2.312E+07	2.420E+07	2.527E+07	2.633E+07	mm ³
Radius of Gyration, r_{xx}	670.7	676.3	681.2	685.6	689.5	693.0	mm
Plastic Neutral Axis, y_{PNA}	643.4	609.8	576.3	542.7	509.1	475.5	mm
Top Flange Plastic Moment	3,192.6	3,523.2	3,868.1	4,227.4	4,601.0	4,989.0	kN-m
Top Web Plastic Moment	2,282.3	2,436.1	2,595.0	2,758.8	2,927.7	3,101.5	kN-m
Bottom Web Plastic Moment	831.4	742.6	658.8	580.0	506.3	437.5	kN-m
Bottom Flange Plastic Moment	3,073.2	3,212.7	3,317.9	3,388.7	3,425.1	3,427.1	kN-m
Total Plastic Moment, M_p	9,379.5	9,914.7	10,439.9	10,955.0	11,460.1	11,955.1	kN-m
Plastic Section Modulus, Z_{xx}	2.680E+07	2.833E+07	2.983E+07	3.130E+07	3.274E+07	3.416E+07	mm ³
Moment of Inertia, I_{yy}	3.168E+08	4.152E+08	5.327E+08	6.711E+08	8.319E+08	1.017E+09	mm ⁴
Section Modulus, S_{yy}	1.440E+06	1.709E+06	2.003E+06	2.322E+06	2.666E+06	3.036E+06	mm ³
Radius of Gyration, r_{yy}	85.3	95.4	105.7	116.2	126.7	137.4	mm
Torsional Moment of Inertia, J	7.738E+06	8.362E+06	8.986E+06	9.610E+06	1.023E+07	1.086E+07	mm ⁴
Warping Constant, C_w	1.770E+14	2.220E+14	2.734E+14	3.318E+14	3.975E+14	4.710E+14	mm ⁶
Distance Between Flanges, d_1	1,653.6	1,653.6	1,653.6	1,653.6	1,653.6	1,653.6	mm
Compression Flange Inertia, I_{yc}	9.075E+07	1.107E+08	1.334E+08	1.591E+08	1.878E+08	2.198E+08	mm ⁴
Coefficient of Monosymmetry, β_x	-635.328	-694.170	-742.223	-782.044	-815.459	-843.797	

Composite Section - Geometric Properties

1n Transformed Properties for Live Loads						
Location	0	3,600	7,200	10,800	14,400	18,000
Computation of elastic N/A relative to top of slab						
Total Depth of Composite Section	1,937.2	1,937.2	1,937.2	1,937.2	1,937.2	1,937.2 mm
Concrete Slab Depth	255.0	255.0	255.0	255.0	255.0	255.0 mm
Transformed Concrete Slab Width (1n)	479.5	479.5	479.5	479.5	479.5	479.5 mm
Transformed Concrete Area, A_{ctr} (1n)	122,259.8	122,259.8	122,259.8	122,259.8	122,259.8	122,259.8 mm ²
Total Area of Composite Section, A_{tot} (1n)	165,779.3	167,851.7	169,924.1	171,996.5	174,068.9	176,141.3 mm ²
Transformed Elastic N/A, y_{tr} (1n)	1,530.6	1,517.9	1,505.5	1,493.4	1,481.6	1,470.1 mm
Computation of moment of inertia of composite section relative to elastic N/A						
Concrete Slab Moment of Inertia, I_c (1n)	6.625E+08	6.625E+08	6.625E+08	6.625E+08	6.625E+08	6.625E+08 mm ⁴
Transformed Moment of Inertia, I_{xx} (1n)	5.652E+10	5.984E+10	6.311E+10	6.633E+10	6.950E+10	7.263E+10 mm ⁴
Computation of section modulus of composite section						
Top of Slab, S_{xxx} (1n)	-1.390E+08	-1.427E+08	-1.462E+08	-1.495E+08	-1.526E+08	-1.555E+08 mm ³
Top of Girder, S_{xxxg} (1n)	-3.728E+08	-3.642E+08	-3.572E+08	-3.514E+08	-3.465E+08	-3.424E+08 mm ³
Top of Web, S_{xxxw} (1n)	-4.478E+08	-4.308E+08	-4.172E+08	-4.060E+08	-3.968E+08	-3.890E+08 mm ³
Bottom of Web, S_{xxxw} (1n)	3.771E+07	4.027E+07	4.282E+07	4.538E+07	4.794E+07	5.049E+07 mm ³
Bottom of Girder, S_{xxxg} (1n)	3.692E+07	3.942E+07	4.192E+07	4.442E+07	4.691E+07	4.940E+07 mm ³
3n Transformed Properties for Superimposed Dead Loads						
Location	0	3,600	7,200	10,800	14,400	18,000
Computation of elastic N/A relative to top of slab						
Total Depth of Composite Section	1,937.2	1,937.2	1,937.2	1,937.2	1,937.2	1,937.2 mm
Concrete Slab Depth	255.0	255.0	255.0	255.0	255.0	255.0 mm
Transformed Concrete Slab Width (3n)	159.8	159.8	159.8	159.8	159.8	159.8 mm
Transformed Concrete Area, A_{ctr} (3n)	40,753.3	40,753.3	40,753.3	40,753.3	40,753.3	40,753.3 mm ²
Total Area of Composite Section, A_{tot} (3n)	84,272.8	86,345.2	88,417.6	90,490.0	92,562.4	94,634.8 mm ²
Transformed Elastic N/A, y_{tr} (3n)	1,260.7	1,242.5	1,225.1	1,208.6	1,192.7	1,177.6 mm
Computation of moment of inertia of composite section relative to elastic N/A						
Concrete Slab Moment of Inertia, I_c (3n)	2.208E+08	2.208E+08	2.208E+08	2.208E+08	2.208E+08	2.208E+08 mm ⁴
Transformed Moment of Inertia, I_{xx} (3n)	4.358E+10	4.591E+10	4.818E+10	5.039E+10	5.256E+10	5.469E+10 mm ⁴
Computation of section modulus of composite section						
Top of Slab, S_{xxx} (3n)	-6.442E+07	-6.608E+07	-6.766E+07	-6.916E+07	-7.061E+07	-7.200E+07 mm ³
Top of Girder, S_{xxxg} (3n)	-1.034E+08	-1.044E+08	-1.054E+08	-1.064E+08	-1.074E+08	-1.084E+08 mm ³
Top of Web, S_{xxxw} (3n)	-1.100E+08	-1.108E+08	-1.116E+08	-1.124E+08	-1.133E+08	-1.141E+08 mm ³
Bottom of Web, S_{xxxw} (3n)	3.547E+07	3.792E+07	4.037E+07	4.282E+07	4.528E+07	4.773E+07 mm ³
Bottom of Girder, S_{xxxg} (3n)	3.457E+07	3.695E+07	3.932E+07	4.170E+07	4.407E+07	4.644E+07 mm ³

Section D

Live Load Distribution - Section 5 of S6-00

Determination of Girder Loading Factors

Span, L = 36000 m
 Vehicle Edge Distance, D_{ve} = 0.99 m
 Total Moment, M_T = 1 (unity)
 Total Shear, V_T = 1 (unity)

Ultimate and Serviceability Limit States Design - Longitudinal Bending Moments

	n	R_L	N	M_{gavg}	S (m)	W_c (m)	Ω_a (m)	m	F (m)	C_r (%)	F_m	M_g
External Girder, 2 Design Lanes	2	0.9	3	0.6	3.9	10.2	5.1	1	6.799917	4.999583	1.638682	0.983209
Internal Girder, 2 Design Lanes	2	0.9	3	0.6	3.9	10.2	5.1	1	7.199611	4.999583	1.547709	0.928625
External Girder, 3 Design Lanes	3	0.8	3	0.8	3.9	10.2	3.4	0.166667	8.699889	9.999306	1.3228	1.05824
Internal Girder, 3 Design Lanes	3	0.8	3	0.8	3.9	10.2	3.4	0.166667	9.599417	9.999306	1.198845	0.959076

Fatigue Limit States Design - Longitudinal Bending Moments

	n	N	M_{gavg}	S (m)	W_c (m)	W_a (m)	μ	F (m)	C_r (%)	C_a (%)	F_m	M_g
External Girder, 2 Design Lanes	2	3	0.333333	3.9	10.2	5.1	.1	3.799944	4.999583	-0.3	2.940788	0.980263
Internal Girder, 2 Design Lanes	2	3	0.333333	3.9	10.2	5.1	1	2876.858	4.999583	0	0.003873	0.001291
External Girder, 3 Design Lanes	3	3	0.333333	3.9	10.2	3.4	0.166667	260.7714	0	-0.26	0.044984	0.014995
Internal Girder, 3 Design Lanes	3	3	0.333333	3.9	10.2	3.4	0.166667	2876.858	0	0	0.004067	0.001356

Ultimate and Serviceability Limit States Design - Longitudinal Vertical Shear

	n	R_L	N	V_{gavg}	S (m)	F (m)	F_v	V_g
External Girder, 2 Design Lanes	2	0.9	3	0.6	3.9	6.1	1.918033	1.15082
Internal Girder, 2 Design Lanes	2	0.9	3	0.6	3.9	6.1	1.918033	1.15082
External Girder, 3 Design Lanes	3	0.8	3	0.8	3.9	8.2	1.426829	1.141463
Internal Girder, 3 Design Lanes	3	0.8	3	0.8	3.9	8.2	1.426829	1.141463

Fatigue Limit States Design - Longitudinal Vertical Shear *

	n	R_L	N	V_{gavg}	S (m)	F (m)	F_v	V_g
External Girder, 2 Design Lanes	1	1	3	0.333333	3.9	3.6	3.25	1.083333
Internal Girder, 2 Design Lanes	1	1	3	0.333333	3.9	3.6	3.25	1.083333
External Girder, 3 Design Lanes	1	1	3	0.333333	3.9	3.6	3.25	1.083333
Internal Girder, 3 Design Lanes	1	1	3	0.333333	3.9	3.6	3.25	1.083333

* V_T is calculated for a single truck on the bridge in one lane only

CL-625 Truck, no DLA

DISTANCE	FY	LD	Corresponding Moment	No. Axles	MZ	LD	Corresponding No. Axles Shear	
0	MAX	472.07	181	0	4	0	115	
	MIN	0	288	0	1	0	198	
1.8	MAX	415.41	37	546.75	4			
	MIN	-14.58	8	202.5	1	-1495.66	37	223.333
3.6	MAX	345.97	45	921.126	5			
	MIN	-31.11	15	420	1	-2716	44	255.843
5.4	MAX	285.21	52	1196.5	4			
	MIN	-62.71	22	525	1	-3511.5	49	91.25
7.2	MAX	224.44	59	1303	4			
	MIN	-100.14	173	1095	3	-3907	56	64.861
9	MAX	163.68	66	1271.25	4			
	MIN	-163.68	188	1271.25	4	-3940	51	99.722
1	0	MAX	472.07	181				
		MIN	0	288			0	198
	3.6	MAX	415.41	37				
		MIN	-14.58	8		-1495.66	37	
	7.2	MAX	345.97	45				
		MIN	-31.11	15		-2716	44	
	10.8	MAX	285.21	52				
		MIN	-62.71	22		-3511.5	49	
	14.4	MAX	224.44	59				
		MIN	-100.14	173		-3907	56	
	18	MAX	163.68	66				
		MIN	-163.68	188		-3940	51	

Section E

Page 2 of 4

Moment and Shear Loading

From Staad Analysis

Location	0	3,600	7,200	10,800	14,400	18,000		
CL625 Design Loading (unfactored)								
CL625 Truck Moment (no DLA)	0.0	1,495.7	2,716.0	3,511.5	3,907.0	3,940.0	kN-m	
Load Case		37.0	44.0	49.0	56.0	51.0		
Shear Corresponding to Moment		223.3	255.8	91.3	64.9	99.7		
CL625 Pos Truck Shear (no DLA)								
Load Case	472.1	415.4	346.0	285.2	224.4	163.7	kN	
Moment Corresponding to Shear	181.0	37.0	45.0	52.0	59.0	66.0		
	0.0	546.8	921.1	1,196.5	1,303.0	1,271.3		
CL625 Neg Truck Shear (no DLA)								
Load Case	0.0	-14.6	-31.1	-62.7	-100.1	-163.7	kN	
Moment Corresponding to Shear	288.0	8.0	15.0	22.0	173.0	188.0		
	0.0	202.5	420.0	525.0	1,095.0	1,271.3		
Distributed Lane Loading	9	kN-m						
Design Truck Moment (per lane, incl. DLA)	0.0	1,869.6	3,395.0	4,389.4	4,883.8	4,925.0	kN-m	
Moment from Lane UDL	0.0	524.9	933.1	1,224.7	1,399.7	1,458.0	kN-m	
Design Lane Moment (per lane, excl. DLA)	0.0	1,721.4	3,105.9	4,033.9	4,525.3	4,610.0	kN-m	
Worst Case	0.0	1,869.6	3,395.0	4,389.4	4,883.8	4,925.0	kN-m	
Truck	Truck	Truck	Truck	Truck	Truck	Truck		
Design Truck Shear (per lane)	590.1	519.3	432.5	356.5	280.6	204.6	kN	
Shear from Lane UDL	162.0	129.6	97.2	64.8	32.4	0.0		
Design Lane Shear (per lane)	634.1	545.0	443.2	350.0	256.8	163.7	kN	
Worst Case	634.1	545.0	443.2	356.5	280.6	204.6	kN	
Lane	Lane	Lane	Truck	Truck	Truck	Truck		
Distribution for SLS and ULS Moment								
2 Design Lanes (Moment per Girder)	External	$M_g =$	0.983					
	Internal	$M_g =$	0.929					
3 Design Lanes (Moment per Girder)	External	$M_g =$	1.058					
	Internal	$M_g =$	0.959					
Distribution for SLS and ULS Shear								
2 Design Lanes (Shear per Girder)	External	$V_g =$	1.151					
	Internal	$V_g =$	1.151					
3 Design Lanes (Shear per Girder)	External	$V_g =$	1.141					
	Internal	$V_g =$	1.141					
Governing Loads - SLS and ULS								
Unfactored Moment per Girder (incl. DLA)	0.0	1978.5	3592.7	4645.0	5168.2	5211.8	kN-m	
Unfactored Shear per Girder (incl. DLA)	729.7	627.2	510.0	410.3	322.9	235.5	kN	
Distribution for FLS Moment								
2 Design Lanes (Moment per Girder)	External	$M_g =$	0.980					
	Internal	$M_g =$	0.001					
3 Design Lanes (Moment per Girder)	External	$M_g =$	0.015					
	Internal	$M_g =$	0.001					
Distribution for FLS Shear								
2 Design Lanes (Shear per Girder)	External	$V_g =$	1.083					
	Internal	$V_g =$	1.083					
3 Design Lanes (Shear per Girder)	External	$V_g =$	1.083					
	Internal	$V_g =$	1.083					
Governing Loads - FLS								
Unfactored Moment per Girder (no DLA)	0.0	1832.7	3328.0	4302.7	4787.4	4827.8	kN-m	
Unfactored Shear per Girder (no DLA)	639.3	562.5	468.5	386.2	303.9	221.7	kN	
Const Loads (per girder - unfactored, no DLA) assume that panels are erected from the ground min const. live load								
Moment	0.0	113.7	202.2	265.4	303.3	315.9		
Shear	35.1	28.1	21.1	14.0	7.0	0.0		

Location	0	3,600	7,200	10,800	14,400	18,000	
Moments (Note: Do not insert a 0 in any cell)							
Unfactored and Distributed Live Loads							
CL625 Live Load (incl DLA)	0.0	1,978.5	3,592.7	4,645.0	5,168.2	5,211.8	kN-m
Construction Live Load, M_{onst} (incl. DLA)	0.0	142.2	252.7	331.7	379.1	394.9	kN-m
Unfactored Dead Loads - Per Girder							
Girder Dead Load, $M_{DGirder}$	0.0	225.2	418.6	573.3	682.5	739.3	kN-m
Deck Dead Load, M_{DDeck}	0.0	1,306.3	2,322.3	3,048.1	3,483.5	3,628.7	kN-m
Barrier Dead Load, $M_{DBarrier}$	0.0	227.7	404.9	531.4	607.3	632.6	kN-m

Future Overlay Dead Load, M_{Over}	0.0	466.0	828.4	1,087.3	1,242.6	1,294.4	kN-m
Other Dead Loads, M_{Other}	0.0	0.0	0.0	0.0	0.0	0.0	kN-m
Construction Loading (Non-Composite Only)							
Deck Panel + Dead							
SLS1	0.0	1,659.5	2,968.4	3,919.9	4,507.2	4,723.4	kN-m
ULS1	0.0	2,057.0	3,676.9	4,852.2	5,575.4	5,839.0	kN-m
ULS2	0.0	0.0	0.0	0.0	0.0	0.0	kN-m
ULS3	0.0	0.0	0.0	0.0	0.0	0.0	kN-m
In-Service Loading							
Non-Composite Loads (Girders + Deck)							
FLS	0.0	1,531.5	2,740.9	3,621.3	4,166.0	4,368.0	kN-m
SLS1	0.0	1,531.5	2,740.9	3,621.3	4,166.0	4,368.0	kN-m
SLS2	0.0	0.0	0.0	0.0	0.0	0.0	kN-m
ULS1	0.0	1,684.7	3,015.0	3,983.5	4,582.6	4,804.8	kN-m
ULS2	0.0	1,684.7	3,015.0	3,983.5	4,582.6	4,804.8	kN-m
ULS3	0.0	1,684.7	3,015.0	3,983.5	4,582.6	4,804.8	kN-m
Composite Loads (Barrier + Overlay + Other)							
FLS	0.0	693.7	1,233.3	1,618.7	1,849.9	1,927.0	kN-m
SLS1	0.0	693.7	1,233.3	1,618.7	1,849.9	1,927.0	kN-m
SLS2	0.0	0.0	0.0	0.0	0.0	0.0	kN-m
ULS1	0.0	972.3	1,728.5	2,268.6	2,592.7	2,700.7	kN-m
ULS2	0.0	972.3	1,728.5	2,268.6	2,592.7	2,700.7	kN-m
ULS3	0.0	972.3	1,728.5	2,268.6	2,592.7	2,700.7	kN-m
Composite Loads (Live)							
FLS	0.0	1,832.7	3,328.0	4,302.7	4,787.4	4,827.8	kN-m
SLS1	0.0	1,780.6	3,233.5	4,180.5	4,651.4	4,690.6	kN-m
SLS2	0.0	1,780.6	3,233.5	4,180.5	4,651.4	4,690.6	kN-m
ULS1	0.0	3,363.4	6,107.6	7,896.5	8,785.9	8,860.1	kN-m
ULS2	0.0	3,165.5	5,748.4	7,432.0	8,269.1	8,338.9	kN-m
ULS3	0.0	2,769.8	5,029.8	6,503.0	7,235.4	7,296.6	kN-m

Number of Cross Bracing Bays	6						
Cross Bracing Spacing, l_b	6,000						
Cross Bracing Locations	0.0	6,000.0	12,000.0	18,000.0	24,000.0	30,000.0	
Construction Moments at Bracing (kN-m)	0.0	3,136.9	5,093.2	5,839.0	Sym.	Sym.	

Section E

Shear							
Location	0.0	3,600.0	7,200.0	10,800.0	14,400.0	18,000.0	
Unfactored and Undistributed Live Loads							
CL625 Live Load (incl. DLA)	729.7	627.2	510.0	410.3	322.9	235.5	kN
Construction Live Load, V_{const} (incl. DLA)	43.9	35.1	26.3	17.6	8.8	0.0	kN
Unfactored Dead Loads - Per Girder							
Girder Dead Load, V_{Girder}	66.3	55.6	43.6	30.3	15.8	0.0	kN
Deck Dead Load, V_{Deck}	403.2	322.5	241.9	161.3	80.6	0.0	kN
Barrier Dead Load, $V_{Barrier}$	70.3	56.2	42.2	28.1	14.1	0.0	kN
Future Overlay Dead Load, V_{Over}	143.8	115.1	86.3	57.5	28.8	0.0	kN
Other Dead Loads, V_{Other}	0.0	0.0	0.0	0.0	0.0	0.0	kN
Construction Loading (Non-Composite Only)							
Deck Panel + Dead							
SLS1	509.0	409.7	309.2	207.4	104.3	0.0	kN
ULS1	631.4	507.9	383.0	256.7	129.1	0.0	kN
ULS2	0.0	0.0	0.0	0.0	0.0	0.0	kN
ULS3	0.0	0.0	0.0	0.0	0.0	0.0	kN
In-Service Loading							
Non-Composite Loads (Girders + Deck)							
FLS	469.5	378.2	285.5	191.6	96.4	0.0	kN
SLS1	469.5	378.2	285.5	191.6	96.4	0.0	kN
SLS2	0.0	0.0	0.0	0.0	0.0	0.0	kN
ULS1	556.8	448.2	338.3	226.9	114.1	0.0	kN
ULS2	556.8	448.2	338.3	226.9	114.1	0.0	kN
ULS3	556.8	448.2	338.3	226.9	114.1	0.0	kN
Composite Loads (Barrier + Overlay + Other)							
FLS	214.1	171.3	128.5	85.6	42.8	0.0	kN
SLS1	214.1	171.3	128.5	85.6	42.8	0.0	kN
SLS2	0.0	0.0	0.0	0.0	0.0	0.0	kN
ULS1	300.1	240.1	180.0	120.0	60.0	0.0	kN
ULS2	300.1	240.1	180.0	120.0	60.0	0.0	kN
ULS3	300.1	240.1	180.0	120.0	60.0	0.0	kN
Composite Loads (Live)							
FLS	639.3	562.5	468.5	386.2	303.9	221.7	kN
SLS1	656.7	564.5	459.0	369.3	290.6	211.9	kN
SLS2	656.7	564.5	459.0	369.3	290.6	211.9	kN
ULS1	1,240.5	1,066.3	867.0	697.5	548.9	400.3	kN
ULS2	1,167.5	1,003.5	816.0	656.5	516.6	376.7	kN
ULS3	1,021.6	878.1	714.0	574.4	452.0	329.6	kN

Section E

Non-Composite Steel Section - Moment Resistance

Note: No b/t check of bottom flange, it is a tension member.

Location	0.0	3,600.0	7,200.0	10,800.0	14,400.0	18,000.0
Calculation of Class						
b/t - Top Flange	6.89	7.36	7.83	8.31	8.78	9.25
b/t - Class 1	7.75	7.75	7.75	7.75	7.75	7.75
b/t - Class 2	9.09	9.09	9.09	9.09	9.09	9.09
b/t - Class 3	10.69	10.69	10.69	10.69	10.69	10.69
b/t - Top Flange Class	Class 1	Class 1	Class 2	Class 2	Class 2	Class 3
Depth of Web in Comp, d_c	910.3	921.4	931.5	940.8	949.3	957.2
h/w - Web	143.35	145.10	146.69	148.16	149.50	150.75
h/w - Class 1	58.80	58.80	58.80	58.80	58.80	58.80
h/w - Class 2	90.87	90.87	90.87	90.87	90.87	90.87
h/w - Class 3	101.56	101.56	101.56	101.56	101.56	101.56
h/w - Web Class	Stiffened Plate					
Check if $h/w \leq 3150/\sqrt{F_y}$	yes	yes	yes	yes	yes	yes
Check if $h/w \leq 6000/\sqrt{F_y}$	yes	yes	yes	yes	yes	yes

mm

Non-Composite Section						
Class 1 and 2 Sections						
Clause 10.10.2.2 - Laterally Supported Members						
Moment Resistance, M_r	8,911	9,419	9,918	10,407	10,887	11,357
Clause 10.10.2.3 - Laterally Unsupported Members						
β_x	-635.328	-694.170	-742.223	-782.044	-815.459	-843.797
B_1	-1.715	-2.064	-2.411	-2.757	-3.102	-3.446
B_2	16.289	18.903	21.668	24.586	27.659	30.889
Moment Ratios, κ	0.00	0.00	-0.62	-0.62	-0.87	-0.87
ω_2	1.75	1.75	1.22	1.22	1.06	1.06
Unsupported Length, L	6,000	6,000	6,000	6,000	6,000	6,000
Critical Elastic Moment, M_u	15,665	19,107	16,009	19,076	19,651	22,994
$0.67M_p$	6,284	6,643	6,995	7,340	7,678	8,010
Moment Resistance, M_r	8,529	9,258	9,323	10,044	10,476	11,160

kN-m

mm

kN-m

kN-m

kN-m

Non-Composite Section						
Class 3 Sections						
Clause 10.10.3.2 - Laterally Supported Members						
Moment Resistance, M_r	6,956	7,324	7,686	8,046	8,402	8,755
Clause 10.10.3.3 - Laterally Unsupported Members						
β_x	-635.328	-694.170	-742.223	-782.044	-815.459	-843.797
B_1	-1.715	-2.064	-2.411	-2.757	-3.102	-3.446
B_2	16.289	18.903	21.668	24.586	27.659	30.889
Moment Ratios, κ	0.00	0.00	-0.62	-0.62	-0.87	-0.87
ω_2	1.75	1.75	1.22	1.22	1.06	1.06
Unsupported Length, L	6,000	6,000	6,000	6,000	6,000	6,000
Critical Elastic Moment, M_u	15,665	19,107	16,009	19,076	19,651	22,994
Yield Moment, M_y	7,323	7,709	8,091	8,469	8,844	9,216
$0.67M_y$	4,906	5,165	5,421	5,674	5,925	6,174
Moment Resistance, M_r	6,953	7,324	7,588	8,046	8,402	8,755

kN-m

mm

kN-m

kN-m

kN-m

kN-m

Non-Composite Section						
Stiffened Plate Girders						
Clause 10.10.4.3 - Moment Resistance						
Moment Reduction Factor	1.000	0.979	0.945	0.936	0.934	0.937
Clause 10.10.3.2 - Laterally Supported Members						
Moment Resistance, M_r	6,956	7,169	7,266	7,530	7,849	8,203
Clause 10.10.2.3 - Laterally Unsupported Members						
Moment Resistance, M_r	6,953	7,169	7,174	7,530	7,849	8,203

kN-m

kN-m

Calculated Moment Resistance						
Laterally Supported, M_r	6,956	7,169	7,266	7,530	7,849	8,203
Laterally Unsupported, M_r	6,953	7,169	7,174	7,530	7,849	8,203

kN-m

kN-m

Steel Section - Shear Resistance

$$V_r = \phi_s A_w F_s$$

$$A_w = b_w h_w$$

$$F_s = F_{cr} + F_t$$

Clause 10.10.5.1 - S6-2000

For shear, use the actual h value, not $2d_c$ (F_t at the end panel (0.0) is zero because there is no tension field anchor)

Note: End panel excludes tension field action

Location	0.0	3,600.0	7,200.0	10,800.0	14,400.0	18,000.0	
Stiffener Spacing, a	1,500	3,000	3,000	3,000	3,000	3,000	mm
a/h	0.92	1.85	1.85	1.85	1.85	1.85	
h/w	127.95	127.95	127.95	127.95	127.95	127.95	
Maximum Spacing, a _{max}	4,875	4,875	4,875	4,875	4,875	4,875	mm
Shear Buckling Coefficient, k _v	10.27	6.51	6.51	6.51	6.51	6.51	
$502\sqrt{k_v/F_y}$	85.98	68.48	68.48	68.48	68.48	68.48	
$621\sqrt{k_v/F_y}$	106.36	84.72	84.72	84.72	84.72	84.72	
F _{cr}	112.9	71.6	71.6	71.6	71.6	71.6	MPa
F _t	0.0	53.8	53.8	53.8	53.8	53.8	MPa
F _s = F _{cr} + F _t	112.9	125.4	125.4	125.4	125.4	125.4	MPa
V _r = $\phi_s F_s A_w$	2,213.1	2,459.0	2,459.0	2,459.0	2,459.0	2,459.0	kN

Section G

Page 1 of 1

Composite Section - Moment Resistance

Location	0.0	3,600.0	7,200.0	10,800.0	14,400.0	18,000.0
C _c Force in Concrete (=C ₁)	20,824	20,824	20,824	20,824	20,824	20,824
C _s Force in Steel Girder (=C ₂)	14,470	15,159	15,848	16,537	17,227	17,916

Class 1 and 2 Sections with Plastic Neutral Axis in the Concrete (and Class 3 and Stiffened Plate for < 850w/(F_y))						
Depth of Compression Block, a	177	186	194	203	211	219
C _c	14,470	15,159	15,848	16,537	17,227	17,916
Moment Arm, e _c	1,024	1,040	1,054	1,067	1,080	1,092
Moment Resistance, M _r	14,821	15,759	16,703	17,653	18,608	19,570

Class 1 and 2 Sections with Plastic Neutral Axis in the Steel (and Class 3 and Stiffened Plate for < 850w/(F_y))						
Depth of Compression Block, a	255	255	255	255	255	255
C _c	20,824	20,824	20,824	20,824	20,824	20,824
C _s	-3,177	-2,832	-2,488	-2,143	-1,799	-1,454
Plastic Neutral Axis, y _{pna}	1,709	1,705	1,701	1,697	1,694	1,692
Is y _{pna} in the Top Flange?	CONCRETE	CONCRETE	CONCRETE	CONCRETE	CONCRETE	CONCRETE
Bottom Steel Centroid, y _{sb}	CONCRETE	CONCRETE	CONCRETE	CONCRETE	CONCRETE	CONCRETE
Top Steel Centroid, y _{st}	CONCRETE	CONCRETE	CONCRETE	CONCRETE	CONCRETE	CONCRETE
Concrete Centroid, y _c	1,810	1,810	1,810	1,810	1,810	1,810
Moment Arm, e _c	CONCRETE	CONCRETE	CONCRETE	CONCRETE	CONCRETE	CONCRETE
Moment Arm, e _s	CONCRETE	CONCRETE	CONCRETE	CONCRETE	CONCRETE	CONCRETE
Moment Resistance, M _r	CONCRETE	CONCRETE	CONCRETE	CONCRETE	CONCRETE	CONCRETE

Class 3 and Stiffened Plate Sections with Depth of Compression Portion of Web Exceeding 850w/(F_y)						
Depth of Web in Compression	-53	-48	-44	-41	-38	-35
850w/(F _y)	577	577	577	577	577	577
C _c	20,824	20,824	20,824	20,824	20,824	20,824
Area of Steel in Compression, A' _{sc}	16,218	16,828	17,437	18,047	18,657	19,266
C _s	5,393	5,595	5,798	6,001	6,203	6,406
Area of Steel in Tension, A' _{st}	78,847	79,457	80,067	80,676	81,286	81,895
Bottom Steel Centroid, y _{sb}	2,129	2,058	1,989	1,922	1,856	1,792
Top Steel Centroid, y _{st}	1,533	1,538	1,543	1,547	1,551	1,555
Concrete Centroid, y _c	1,810	1,810	1,810	1,810	1,810	1,810
Moment Arm, e _c	-320	-249	-180	-112	-47	17
Moment Arm, e _s	-596	-520	-446	-375	-305	-238
Moment Resistance, M _r	-9,867	-8,088	-6,328	-4,588	-2,866	-1,163

M_r of Composite Section based on location of plastic neutral axis and class of steel member						
M _r	14,821	15,759	16,703	17,653	18,608	19,570

Check of Moment, Shear and Code Clauses

Location	0.0	3,600.0	7,200.0	10,800.0	14,400.0	18,000.0	
Ultimate Limit States - Construction Loading for Bending and Shear - Clause 10.10.5.2 - S6-2000							
Construction, M_r/M_r	0.000	0.287	0.513	0.644	0.710	0.712	
Construction, V_r/V_r	0.285	0.207	0.156	0.104	0.052	0.000	
$0.727 M_r/M_r + 0.455 V_r/V_r < 1.0$	0.130	0.303	0.443	0.516	0.540	0.518	
Note: Forces are based on moment and shear envelope for interaction check, not concurrent moments and shears.							
Composite Beams - SLS Control of Permanent Deflections - Clause 10.11.4 - S6-2000							
M_d/S Top Flange	0.0	-54.0	-89.9	-110.9	-119.7	-118.1	MPa
M_{ed}/S_{sn} Top Flange	0.0	-6.6	-11.7	-15.2	-17.2	-17.8	MPa
M_i/S_n Top Flange	0.0	-4.9	-9.1	-11.9	-13.4	-13.7	MPa
Total Stress - Top Flange	0	-66	-111	-138	-150	-150	MPa
$0.9F_y$	315	315	315	315	315	315	MPa
Check	OK	OK	OK	OK	OK	OK	
M_d/S Bottom Flange	0.0	69.5	118.6	149.7	164.9	165.9	MPa
M_{ed}/S_{sn} Bottom Flange	0.0	18.8	31.4	38.8	42.0	41.5	MPa
M_i/S_n Bottom Flange	0.0	45.2	77.1	94.1	99.2	94.9	MPa
Total Stress - Bottom Flange	0	133	227	283	306	302	MPa
$0.9F_y$	315	315	315	315	315	315	MPa
Check	OK	OK	OK	OK	OK	OK	within 0.6% - ok
Non-Composite Beams - SLS Construction Loading, Top Flange Stress Check							
M_{SL}/S_{xx} Top Flange	0	-59	-97	-120	-129	-128	MPa
$0.9F_y$	315	315	315	315	315	315	MPa
Check	OK	OK	OK	OK	OK	OK	
Non-Composite Beams - SLS Construction Loading, Bottom Flange Stress Check							
M_{SL}/S_{xx} Bottom Flange	0	75	128	162	178	179	MPa
$0.9F_y$	315	315	315	315	315	315	MPa
Check	OK	OK	OK	OK	OK	OK	
Ultimate Limit States - Full Composite Action							
ULS, M_r/M_r	0.000	0.382	0.650	0.801	0.858	0.836	
ULS, V_r/V_r	0.948	0.714	0.563	0.425	0.294	0.163	
$0.727 M_r/M_r + 0.455 V_r/V_r < 1.0$	0.431	0.602	0.729	0.776	0.757	0.682	
Note: Forces are based on moment and shear envelope for interaction check, not concurrent moments and shears.							
Serviceability Limit States - Fatigue of Bottom Flange (Detail Category 'B')							
Fatigue Life Constant, γ	3.930E+12	3.930E+12	3.930E+12	3.930E+12	3.930E+12	3.930E+12	
Constant Amplitude Threshold Stress Range, F_{sr}	110	110	110	110	110	110	MPa
Number of Cycles, N_c	15,000,000	15,000,000	15,000,000	15,000,000	15,000,000	15,000,000	cycles
Fatigue Stress Range, F_{sr}	64.0	64.0	64.0	64.0	64.0	64.0	MPa
Load Induced Fatigue, f_{sr}	0.0	46.5	79.4	96.9	102.1	97.7	MPa
Check if $0.52f_{sr} < F_{sr}$	OK	OK	OK	OK	OK	OK	

Transverse Stiffener Design

Stiffener Yield Strength, F_{ystiff} 350 MPa
 Yield Strength Ratio, $Y = F_y/F_{ystiff}$ 1.00
 Single or Double Stiffeners single
 Stiffener Type Coefficient, D 1.8

Location	0.0	3,600.0	7,200.0	10,800.0	14,400.0	18,000.0	
Stiffener Spacing, a	1,500	3,000	3,000	3,000	3,000	3,000	mm
a/h	118.11	236.22	236.22	236.22	236.22	236.22	
j	0.50	0.50	0.50	0.50	0.50	0.50	
Required Moment of Inertia, I	1,536,287	3,072,575	3,072,575	3,072,575	3,072,575	3,072,575	mm ⁴
Stiffener Thickness, t_s	12.7	12.7	12.7	12.7	12.7	12.7	mm
Minimum Stiffener Width, w_{smin}	104.17	104.17	104.17	105.50	111.50	117.50	
Maximum Stiffener Width, w_{smax}	381.0	381.0	381.0	381.0	381.0	381.0	mm
Required Stiffener Width, w_{sreq}	71.33	89.87	89.87	89.87	89.87	89.87	mm
Limiting Width/Thickness Ratio	10.69	10.69	10.69	10.69	10.69	10.69	
Check w_s/t_s	10.6	10.6	10.6	10.6	10.6	10.6	
Factored Shear, V_f	1,797	1,514	1,205	924	663	400	kN
Shear Resistance, V_r	2,213	2,459	2,459	2,459	2,459	2,459	kN
V_f / V_r	0.81	0.62	0.49	0.38	0.27	0.16	
Shear Buckling Coefficient, k_v	10.27	6.51	6.51	6.51	6.51	6.51	
Web, h/w	128.0	128.0	128.0	128.0	128.0	128.0	
C	0.44	0.65	0.65	0.65	0.65	0.65	
Required Stiffener Area, $A_{stiffreq}$	0.00	0.00	0.00	0.00	0.00	0.00	mm ²
Required Stiffener Width from A_{stiff}	0.00	0.00	0.00	0.00	0.00	0.00	mm
Provided Stiffener Width, w_s	135	135	135	135	135	135	mm

Notes:

a) At cross bracing locations, the stiffeners shall be full depth and welded to the top and bottom flanges.

b) The stiffener weld should be terminated between 4w and 6w from the flange-to-web fillet weld.

4w = 50.8 mm
 6w = 76.2 mm
 So Use: mm

c) Chamfer the corner of the stiffener at the flange-to-web fillet weld. Possibly use the value from b) above.

d) Bracing attached to connection plates shall be at least 100 mm from the face of the web.

e) Minimum design shear force for stiffener weld = $0.0001hF_y^{1.5}$ (N/mm of weld)

$0.0001hF_y^{1.5} = 1.064$ kN/mm
 Total Shear Force per Stiffener = 1,729.1 kN
 Length of Double Fillet Weld Provided = 1,525.0 mm
 New Required Shear Resistance = 1.134 kN/mm
 Strength of Weld Material, $X_w = 480$ MPa

Minimum Size of Double Fillet Weld (per fillet) = mm Fillet Provided = Ok

Bearing Stiffener Design

Bearing Design per Girder	
Vertical Reaction	
SLS1 - Permanent	613.4 kN
SLS1 - Live	512.9 kN
SLS1 - Total	1,126.3 kN
ULS - Permanent	856.9 kN
ULS - Live	1,240.5 kN
ULS - Total	2,097.4 kN

F_y of the bearing stiffener
350 MPa

Prevent local buckling of stiffener by limiting the b/t ratio to $200/\sqrt{F_y}$ (Clause 10.10.8.2 - S6-2000)

Specified Thickness	Maximum Width	
9.5	101.6	mm
12.7	135.8	mm
15.9	170.0	mm
19.0	203.1	mm
25.4	271.5	mm

Distance from Face of Web to Edge of Top Flange 169 mm
Distance from Face of Web to Edge of Bottom Flange 214 mm

Proposed bearing stiffener	
Thickness	19.7 mm
Actual Width	155 mm
Design Width	155.0 mm
Chamfer	50 mm

Check b/t : OK

Check of Web Crippling and Yielding (Clause 10.10.8.1 - S6-2000)

For end reactions, the lesser of:

- i) $B_r = \phi_{be} w (N+4t) F_y$
ii) $B_r = 0.60 \phi_{be} w^2 \sqrt{F_y E_s}$
- Length of Bearing, N #REF! mm
Thickness of Web, w 12.7 mm
Thickness of Flange, t 31.8 mm

Bearing Resistance, B_r #REF! kN #REF!

Bearing Stiffener Design (Clause 10.10.8.2 - S6-2000)

Factored Bearing Resistance, $B_r = 1.50 \phi_s A_s F_y$
Area of Stiffener in Contact with the Flange, A_s 2,069 mm²
Lesser Yield Stress of Stiffener or Flange, F_y 350 MPa

Resistance per Leg of Bearing Stiffener, B_r 1,031.7 kN
Total Resistance of Bearing and Web, B_{tot} #REF! kN

Compressive Resistance of Bearing Section (Clause 10.10.8.3 - S6-2000)

Calculate for Flexural and Flexural-Torsional Buckling (Clause 10.9.3.1 & 10.9.3.2 - S6-2000)
(Cruciform Shape - doubly symmetric cross)

The effective web length is $12w$ on either side of the stiffener element.

Width of Web Leg, $12w$	152.4 mm	
Width of Stiffener Leg	161.4 mm	
Effective Length, KL	1,218.8 mm	
Area of Cruciform, A_s	10,228.2 mm ²	
Moment of Inertia, I_{bx}	3.017E+07 mm ⁴	
Moment of Inertia, I_{by}	5.522E+07 mm ⁴	
Radius of Gyration, r	54.3 mm	
Warping Constant, C_w	1.585E+09 mm ⁶	(From Shapebuilder)
Torsion Constant, J	7.234E+05 mm ⁴	(From Shapebuilder)

Factored Axial Compressive Resistance, $C_r = \phi_s A_s F_y (1 + \lambda^{2n})^{-1/n}$

where: $\lambda = KL/r \sqrt{F_y / (\pi^2 E_s)}$ (for flexural buckling)

$\lambda = \sqrt{F_y / F_o}$ (for torsional and flexural-torsional buckling)

$F_o = (\pi^2 E_s C_w / (KL)^2 + G_s J) / (I_{bx} + I_{by})$

$n = 1.34$

Flexural, C_r 3,304.5 kN

Flexural-Torsional, C_r 2,627.3 kN

Check for Yielding of the Web and Bearing Steel

Calculate the bearing area of the web and the stiffener on the bottom flange.
(Subtract the chamfer distances)

Area, A_s	8,008.0 mm ²
Yield Force, C_{ry}	2,662.6 kN

Results

Bearing Width	155 mm	
Bearing Thickness	19.7 mm	
Bearing Chamfer	50 mm	
Minimum Distance from End of Girder	152.4 mm	
Factored Bearing Resistance, B_r	#REF! kN	#REF!

Note: The bearing stiffeners should be fitted to bear on the bottom flange OR fillet welded

Shear Studs - ULS

The number of shear connectors at the Ultimate Limit States is

$N = P/q_r$ Number of shear studs required between points of maximum and zero moment.

i) $P = \phi_s A_s F_y$ when the plastic neutral axis is in the concrete slab
 $P = 0.85 \phi_c f_c b_o t_c + \phi_s A_s f_y$ when the plastic neutral axis is in the steel section

ii) $q_r = 45 \phi_{sc} A_{sc} (f_c E_c) \leq \phi_{sc} F_u A_{sc}$

$\phi_{sc} = 0.85$
 Stud Diameter, $d = 22$ mm
 Stud Height, $h = 125$ mm
 Check $h/d \geq 4$ OK
 X-Sectional Area of One Stud, $A_{sc} = 380.1$ mm²
 Concrete Strength, $f_c = 35$ MPa
 Concrete Modulus, $E_c = 26,199$ MPa
 Ultimate Strength of Nelson Stud, $F_u = 410$ MPa
 Factored Shear Resistance of Single Stud, $q_r = 132.5$ kN
 Shear Transfer Force, $P = 17,915.6$ kN
 Number of Studs, $N = 135.2$ studs per girder from midspan to end

Maximum shear stud spacing = 600mm. (Clause 10.11.8.2 - S6-2000)

Typ. Studs per Grout Pocket =	6		
Minimum Number of Grout Pockets =	22.54 per half girder		
Actual Number of Grout Pockets =	22 per half girder	Total Studs	132

	Req'd Studs per Cluster
Cluster Spacing	No Clusters to Midspan
300	61
600	31
1200	15.5
2400	8

Shear Studs - FLS 300mm Cluster Spacing

Location	0	3600	7200	10800	14400	18000	
Shear Stud Fatigue (Detail Category: C)							
Number of Cycles, N_c	5,817,187	5,817,187	5,817,187	5,817,187	5,817,187	5,817,187	cycles
Permissible Range of Interface Shear, Z_{sr}	18.6	18.6	18.6	18.6	18.6	18.6	kN
Live Load Shear Force, V_{sr}	639	563	469	386	304	222	kN
First Moment with Respect to the Neutral Axis, Q	3.412E+07	3.567E+07	3.719E+07	3.867E+07	4.011E+07	4.152E+07	mm ³
Studs per Grout Pocket, n	4	3	3	2	2	2	
Grout Pocket Spacing, s	300	300	300	300	300	300	mm
Design Range of Interface Shear, q_{sr}	15.1	17.4	14.4	17.6	13.7	9.9	kN
Check if $q_r > q_{sr}$	OK	OK	OK	OK	OK	OK	

Shear Studs - FLS 600mm Cluster Spacing

Location	0	3600	7200	10800	14400	18000	
Shear Stud Fatigue (Detail Category: C)							
Number of Cycles, N_c	5,817,187	5,817,187	5,817,187	5,817,187	5,817,187	5,817,187	cycles
Permissible Range of Interface Shear, Z_{sr}	18.6	18.6	18.6	18.6	18.6	18.6	kN
Live Load Shear Force, V_{sr}	639	563	469	386	304	222	kN
First Moment with Respect to the Neutral Axis, Q	3.412E+07	3.567E+07	3.719E+07	3.867E+07	4.011E+07	4.152E+07	mm ³
Studs per Grout Pocket, n	7	6	5	4	4	4	
Grout Pocket Spacing, s	600	600	600	600	600	600	mm
Design Range of Interface Shear, q_{sr}	17.2	17.4	17.2	17.6	13.7	9.9	kN
Check if $q_r > q_{sr}$	OK	OK	OK	OK	OK	OK	

Shear Studs - FLS 1200mm Cluster Spacing

Location	0	3600	7200	10800	14400	18000	
Shear Stud Fatigue (Detail Category: C)							
Number of Cycles, N_c	5,817,187	5,817,187	5,817,187	5,817,187	5,817,187	5,817,187	cycles
Permissible Range of Interface Shear, Z_{sr}	18.6	18.6	18.6	18.6	18.6	18.6	kN
Live Load Shear Force, V_{sr}	639	563	469	386	304	222	kN
First Moment with Respect to the Neutral Axis, Q	3.412E+07	3.567E+07	3.719E+07	3.867E+07	4.011E+07	4.152E+07	mm ³
Studs per Grout Pocket, n	13	12	10	8	6	5	
Grout Pocket Spacing, s	1,200	1,200	1,200	1,200	1,200	1,200	mm
Design Range of Interface Shear, q_{sr}	18.5	17.4	17.2	17.6	18.2	15.8	kN
Check if $q_r > q_{sr}$	OK	OK	OK	OK	OK	OK	

Shear Studs - FLS 2400mm Cluster Spacing

Location	0	3600	7200	10800	14400	18000	
Shear Stud Fatigue (Detail Category: C)							
Number of Cycles, N_c	5,817,187	5,817,187	5,817,187	5,817,187	5,817,187	5,817,187	cycles
Permissible Range of Interface Shear, Z_{sr}	18.6	18.6	18.6	18.6	18.6	18.6	kN
Live Load Shear Force, V_{sr}	639	563	469	386	304	222	kN
First Moment with Respect to the Neutral Axis, Q	3.412E+07	3.567E+07	3.719E+07	3.867E+07	4.011E+07	4.152E+07	mm ³
Studs per Grout Pocket, n	26	24	22	16	12	10	
Grout Pocket Spacing, s	2,400	2,400	2,400	2,400	2,400	2,400	mm
Design Range of Interface Shear, q_{sr}	18.5	17.4	15.7	17.6	18.2	15.8	kN
Check if $q_r > q_{sr}$	OK	OK	OK	OK	OK	OK	

Section L

Shear Studs - ULS

The number of shear connectors at the Ultimate Limit States is

$N = P/q_r$ Number of shear studs required between points of maximum and zero moment.
 i) $P = \phi_s A_s F_y$ when the plastic neutral axis is in the concrete slab
 ii) $P = 0.85 \phi_c f_c b_s t_c + \phi_s A_s f_y$ when the plastic neutral axis is in the steel section
 $q_r = 45 \phi_{sc} A_{sc} \sqrt{f_c E_c} \leq \phi_{sc} F_u A_{sc}$

- $\phi_{sc} =$ 0.85
- Stud Diameter, $d =$ 22 mm
- Stud Height, $h =$ 125 mm
- Check $h/d \geq 4$ OK
- X-Sectional Area of One Stud, $A_{sc} =$ 380.1 mm²
- Concrete Strength, $f_c =$ 35 MPa
- Concrete Modulus, $E_c =$ 26,199 MPa
- Ultimate Strength of Nelson Stud, $F_u =$ 410 MPa
- Factored Shear Resistance of Single Stud, $q_r =$ 132.5 kN
- Shear Transfer Force, $P =$ 14,470.2 kN
- Number of Studs, $N =$ 109.2 studs per girder from midspan to end

Maximum shear stud spacing = 600mm. (Clause 10.11.8.2 - S6-2000)

Typ. Studs per Grout Pocket =	6		
Minimum Number of Grout Pockets =	18.20 per half girder	Studs Req.	109.2
Actual Number of Grout Pockets =	86.75 per half girder	Total Studs	520.5

Shear Studs - FLS

Location	0	3600	7200	10800	14400	18000	
Shear Stud Fatigue (Detail Category 'C')							
Number of Cycles, N_c	2,000,000	2,000,000	2,000,000	2,000,000	2,000,000	2,000,000	cycles
Permissible Range of Interface Shear, Z_{sr}	25	25	25	25	25	25	kN
Live Load Shear Force, V_{sr}	639	563	469	386	304	222	kN
First Moment with Respect to the Neutral Axis, Q	3.412E+07	3.567E+07	3.719E+07	3.867E+07	4.011E+07	4.152E+07	mm ³
Studs per Grout Pocket, n	6	6	6	6	6	6	
Grout Pocket Spacing, s	600	600	600	600	600	600	
Design Range of Interface Shear, q_{sr}	20.1	17.4	14.4	11.7	9.1	6.6	kN
Check if $q_r > q_{sr}$	OK	OK	OK	OK	OK	OK	

Superstructure Vibration Check -SLS

1) Simplified Natural Frequency Estimation

number of girders	3	
Average I_{xx}	6.465E+10 mm ⁴	(per girder)
Dead Load of Steel Girders	4.12 kN/m	(per girder)
Dead Load of Deck	22.40 kN/m	(per girder)
Dead Load of Wearing Surface	7.99 kN/m	(per girder)
Dead Load of Barriers	3.91 kN/m	(per girder)
Total Mass - No Wearing Surface =	3,101.9 kg/m	
Total Mass - With Wearing Surface =	3,916.3 kg/m	

First Fundamental Frequency for a Uniform, Simply Supported Beam

Angular Frequency: $\omega_1 = (n^2 \pi^2 / L^2) \sqrt{E_s I_{xx} / m}$ $n = 1$ for the first mode of vibration
Frequency: $f_1 = (\pi / (2L^2)) \sqrt{E_s I_{xx} / m}$

$f_1 =$	2.47 Hz	no wearing surface
$f_1 =$	2.20 Hz	with wearing surface

2) Bridge Vibration Serviceability Static Deflection

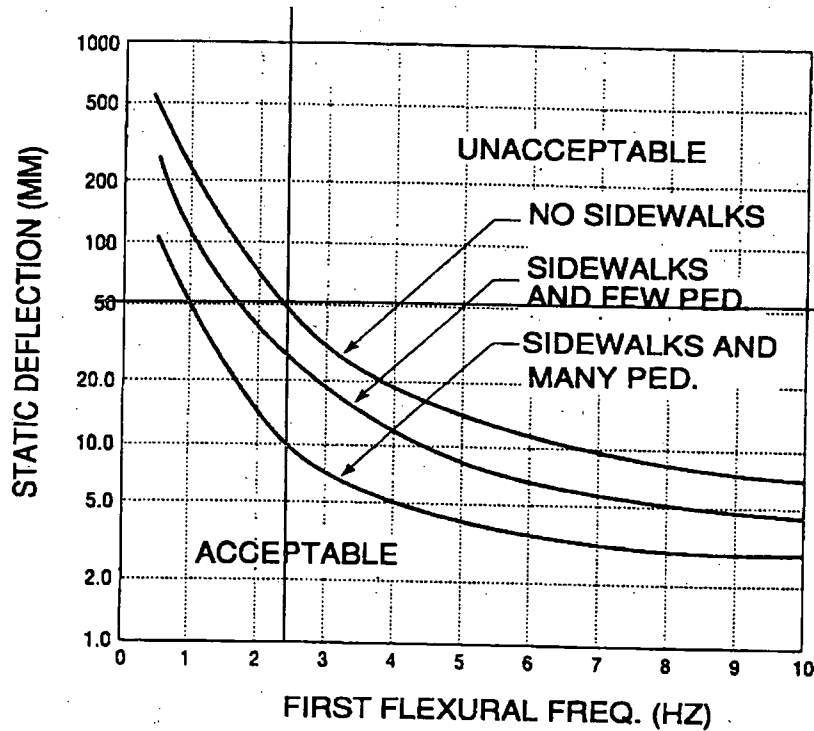
-based on single unfactored CL625 truck divided evenly across all girders
deflection = 13.5 mm (from Staad/number of girders)
-multiply by live load factor, # design lanes, and multilane reduction factor
deflection = 54.9 mm

3) Bridge Vibration Serviceability Check

Refer to Figure 3.4.4 - S6-2000 (below)

Limit from Figure \pm 52 mm **Revise** very close, say it is OK

Figure 3.4.4, Deflection Limitations for Highway Bridge Superstructure Vibration - S6-2000.



4) Check of Staad Output

Elastic deflection of a uniformly distributed beam based on unfactored loads:
Moment of Inertia is based on average I values.

$$\text{max deflection at midspan} = 5qL^4 / (384EI)$$

$$\text{max rotation at ends} = qL^3 / (24EI)$$

L = 36000 mm
 E = 200000 MPa
 $I_{xx} = 2.274E+10 \text{ mm}^4$ non-composite (average for dead loads)
 $I_{xx} (3n) = 4.922E+10 \text{ mm}^4$ composite 3n (average for superimposed dead lo:
 $I_{xx} (1n) = 6.465E+10 \text{ mm}^4$ composite 1n (average for live load)

Girder 4.1 kN/m
 Deck 22.4 kN/m
 q - non-composite = 26.5 kN/m

non-composite deflection = 127.6 mm
 non-composite rotation = 0.0113 radians 0.64963 degrees

Railing 3.9 kN/m
 Overlay 8.0 kN/m
 q - composite (3n) = 11.9 kN/m

composite (3n) deflection = 26.4 mm
 composite (3n) rotation = 0.0023 radians 0.13459 degrees

Approximate Total Dead Load Deflection = 154.0 mm

Flange to Web Weld Design

Calculate the Shear at the Flange to Web Connection

Shear Force Along Connection, $v = VQ/I$

V = shear force at section

Q = Ay' = first moment of area above connection location (non-composite)

I = moment of inertia of section (non-composite)

Shear Stress Along Connection, $\tau = v/t$

t = thickness of web (mm)

Location	0.0	3,600.0	7,200.0	10,800.0	14,400.0	18,000.0	
Top Flange, Q_{tf}	8.205E+06	8.873E+06	9.545E+06	1.022E+07	1.090E+07	1.158E+07	mm ³
Bottom Flange, Q_{bf}	1.022E+07	1.112E+07	1.200E+07	1.287E+07	1.372E+07	1.457E+07	mm ³
Moment of Inertia, I	1.958E+10	2.085E+10	2.212E+10	2.338E+10	2.463E+10	2.587E+10	mm ⁴
Thickness of Web, t	12.7	12.7	12.7	12.7	12.7	12.7	mm
Maximum ULS Shear Force, V	2,097.4	1,754.5	1,385.3	1,044.4	723.0	400.3	kN
Top Flange							
Shear Force at Top of Web, v_{tf}	0.88	0.75	0.60	0.46	0.32	0.18	kN/mm
Shear Stress at Top of Web, τ_{tf}	69.2	58.8	47.1	35.9	25.2	14.1	MPa
Required Fillet Weld Size	2.88	2.45	1.96	1.50	1.05	0.59	mm
Bottom Flange							
Shear Force at Bottom of Web, v_{bf}	1.10	0.94	0.75	0.57	0.40	0.23	kN/mm
Shear Stress at Bottom of Web, τ_b	86.2	73.7	59.2	45.3	31.7	17.7	MPa
Required Fillet Weld Size	3.59	3.07	2.47	1.89	1.32	0.74	mm

Select Top Weld Size (min. 6 mm)

Select Bottom Weld Size (min. 6 mm)

6	mm
6	mm

Fatigue Check

Location	0.0	3,600.0	7,200.0	10,800.0	14,400.0	18,000.0	
Detail Category	B	B	B	B	B	B	
Fatigue Life Constant, γ	3.930E+12	3.930E+12	3.930E+12	3.930E+12	3.930E+12	3.930E+12	
Threshold Stress Range, F_{sr}	110	110	110	110	110	110	MPa
Number of Design Cycles, N_c	2,000,000	2,000,000	2,000,000	2,000,000	2,000,000	2,000,000	
Fatigue Stress Range, F_{sr}	125.3	125.3	125.3	125.3	125.3	125.3	MPa
Live Load Shear (FLS), V_{FLS}	639.3	562.5	468.5	386.2	303.9	221.7	kN
Shear Stress at Top of Web, τ_{tf}	31.6	28.2	23.8	19.9	15.8	11.7	MPa
Shear Stress at Bottom of Web, τ_b	39.3	35.4	30.0	25.1	20.0	14.7	MPa

Section N

Page 1 of 1

Diaphragm Cross Bracing Design

1% of Compression Load = 208.2 kN
 Wind Load = 24.5 kN Langley 1:50 is 640 kPa

Unsupported Length, L = 1,950.0 mm (for bottom chord of K-bracing)

Clause 10.9.3.2 c)

For single angles (L102x102x9.5):

$$C_r = \phi_s A F_y (1 + \lambda^{2n})^{-1/n}$$

- $\phi_s = 0.95$
- $A = 1850 \text{ mm}^2$
- $F_y = 350 \text{ MPa}$
- $E_s = 200000 \text{ MPa}$
- $G = 77000 \text{ MPa}$
- $n = 1.34$
- $\lambda = \lambda_e = \sqrt{(F_y/F_e)}$
- $K_z = 1$
- $x_0 = 34.3 \text{ mm}$
- $y_0 = 0 \text{ mm}$
- $r_x = 39.7 \text{ mm}$
- $r_y = 20.1 \text{ mm}$
- $r_0^2 = 3,156.6 \text{ mm}^2$
- $H = 1$
- $K_x = 1$
- $K_y = 1$
- $C_w = 4.42E+07 \text{ mm}^6$
- $J = 5.61E+04 \text{ mm}^4$
- $F_{ex} = \pi^2 E_s / (K_x L / r_x)^2 = 818.2 \text{ MPa}$
- $F_{ey} = \pi^2 E_s / (K_y L / r_y)^2 = 209.7 \text{ MPa}$
- $F_{ez} = (\pi^2 E_s C_w / (K_z L^2) + GJ) / A r_0^2 = 743.6 \text{ MPa}$

Now Solve:

$$(F_e - F_{ex})(F_e - F_{ey})(F_e - F_{ez}) - F_e^2 (F_e - F_{ey})(x_0/r_0)^2 - F_e^2 (F_e - F_{ex})(y_0/r_0)^2 = 0$$

F_e	Equation
0	-1.28E+08
20	-1.1E+08
40	-92832534
60	-77404409
80	-63240649
100	-50311144
120	-38585784
140	-28034458
160	-18627058
180	-10333473
200	-3123592
220	3032693
240	8165493
260	12304918
280	15481078
300	17724083
320	19064042
340	19531066
360	19155265
380	17966748
400	15995626

Lowest Root:

$$F_e = 209.726 \text{ MPa}$$

$$\text{Equation} = 0$$

$$\lambda_e = 1.29$$

Compressive Resistance, $C_r = 271.9 \text{ kN}$

Total Load, $C_r = 232.8 \text{ kN}$

OK

Deck Design

Transverse Moments on Cantilever Overhang

O/O Width of Deck (Barrier to Barrier) 10.98 m
 Width of Barrier 0.39 m (0.015 m overhang)
 Location of Wheel Load w.r.t. Barrier 0.6 m
 Total Shear, $V_T =$ 1 (unity)

5.7.1.6.1

Girder Spacing S (m)	Overhang S_c (m)	S_c/S
2	3.475	1.7375
2.1	3.375	1.60714
2.2	3.275	1.48864
2.3	3.175	1.38043
2.4	3.075	1.28125
2.5	2.975	1.19
2.6	2.875	1.10577
2.7	2.775	1.02778
2.8	2.675	0.95536
2.9	2.575	0.88793
3	2.475	0.825
3.1	2.375	0.76613
3.2	2.275	0.71094
3.3	2.175	0.65909
3.4	2.075	0.61029
3.5	1.975	0.56429
3.6	1.875	0.52083
3.7	1.775	0.47973
3.8	1.675	0.44079
3.9	1.575	0.40385
4	1.475	0.36875

Red Cells Indicate Unacceptable Arrangements

Actual Values Used for Calculations:

Girder Spacing S (m)	Overhang S_c (m)	S_c/S	t_{CL} (m)	t_1 (m)	t_2 (m)	r_1 (m)	C (m)	C/ S_c	t_1/t_2
3.9	1.575	0.40385	0.31	0.2005	0.232	0.86422	0.585	0.37143	0.864224

Table 5.7.1.6.1 (a)

S_c (m)	Unstiffened Edge			Edge Stiffened w. Jersey Barrier		
	$r_1 = 1$	$r_1 = 0.833$	$r_1 = 0.667$	$r_1 = 1$	$r_1 = 0.833$	$r_1 = 0.667$
1	35.1	35.8	36.8	32.9	34.4	35.9
1.5	41.8	44.4	46.9	34.1	35.3	36.5
2	52.8	55.4	57.8	35.5	38.2	40.7
2.5	59.4	63	66.5	34.6	37.2	39.7
3	90.6	95.3	99.5	59.3	62.2	65.1
3.75	113.2	119.5	125.6	73.7	77.3	80.7

Values from Table 5.7.1.6.1 (a) (for CL625, including DLA)

$S_c =$	1.575 m					
$r_1 =$	0.86422					
	43.45	46.05	48.535	34.31	35.735	37.13
$M_y =$	45.6 kN-m/m (Unstiffened)					
$M_y =$	35.5 kN-m/m (Stiffened)					

Verify Values Using Formula from Cl. 5.7.1.6.1 (a)

$A_{unstiff} = 0.55$ from Fig. 5.7.1.6.1 (a)
 $A_{stiff} = 0.48$ from Fig. 5.7.1.6.1 (a)

CL625 - Axle 2

P (kN)	x (m)	Unstiffened M_y (kN-m/m)	Stiffened M_y (kN-m/m)
25	-3.6	0.056422	0.080773
62.5	0	21.8838	19.09859
62.5	1.2	4.236259	4.923838
87.5	7.8	0.01021	0.015187
75	14.4	0.000773	0.001159
Subtotal		26.18747	24.11955

DLA = 1.25
 Total 32.7 30.1

CL625 - Axle 3

P (kN)	x (m)	Unstiffened M_y (kN-m/m)	Stiffened M_y (kN-m/m)
25	-4.8	0.019176	0.028021
62.5	-1.2	4.236259	4.923838
62.5	0	21.8838	19.09859
87.5	6.6	0.019633	0.029073
75	13.2	0.001093	0.001637
Subtotal		26.15996	24.08116

DLA = 1.25
 Total 32.7 30.1

CL625 - Axle 4

P (kN)	x (m)	Unstiffened M_y (kN-m/m)	Stiffened M_y (kN-m/m)
25	-11.4	0.000652	0.000976
62.5	-7.8	0.007293	0.010848
62.5	-6.6	0.014023	0.020766
87.5	0	30.63733	26.73803
75	6.6	0.016828	0.02492
Subtotal		30.67612	26.79554

DLA = 1.25
 Total 38.3 33.5

CL625 - Axle 4 only

P (kN)	x (m)	Unstiffened M_y (kN-m/m)	Stiffened M_y (kN-m/m)
		0	0
		0	0
		0	0
87.5	0	30.63733	26.73803
		0	0
Subtotal		30.63733	26.73803

DLA = 1.4
 Total 42.9 37.4

35 Tonne Single (tandem) Axle Overload

P (kN)	x (m)	Unstiffened M_y (kN-m/m)	Stiffened M_y (kN-m/m)
42.9188	0	15.02761	13.115
42.9188	1.37	2.12541	2.559567
		0	0
		0	0
		0	0
Subtotal		17.15302	15.67457

DLA = 1.3
 Total 22.3 20.4

Check Deck Capacity

Dead Moment, D1 =	14.6 kN-m	
Dead Moment, D2 =	2.4 kN-m	
Live Moment, L =	35.5 kN-m	
Dead Load Factor, α_{D1} =	1.1	
Dead Load Factor, α_{D2} =	1.5	
Live Load Factor, α_L =	1.7	
Total Factored Moment, M_f =	79.9 kN-m	
Concrete Strength, f_c' =	35 MPa	
Rebar Strength, f_y =	400 MPa	
α_1 =	0.7975	
ϕ_c =	0.75	
ϕ_s =	0.9	
Bar Size =	20 M	
Bar Area =	300 mm ²	
Bar Spacing =	200 mm	
Total Steel Area, A_s =	1500 mm ²	
d_{top} =	0.162 m	60 mm clear cover at the top
a =	25.8 mm	
M_r =	80.5 kN-m/m	OK
V_r =	135.5 kN/m	59.5 kN/m
	135.5 kN/m	

Transverse Moments due to Railing Loads

Performance Level PL-2 (no DLA required)

Transverse Load =	100 kN	at 700 mm height distributed over 1050 mm
Longitudinal Load =	30 kN	
Vertical Load =	30 kN	distributed over 5500 mm
Transverse Lever =	0.94025 m	
Vertical Lever =	1.515 m	
Transverse Moment	94.0 kN-m	
Vertical Moment =	45.5 kN-m	
Live Load Factor, α_L	1.7	

Interior Deck Spans

Total Moment at Base of Parapet =	41.6 kN-m/m	(distributed over 1050 & 56°)
Total Moment at Exterior Girder =	27.4 kN-m/m	(transverse distributed over 1050 & 56° (barrier) and 55° (deck)) (vertical distributed over 5500 & 55°)
Tensile Force at Base of Parapet =	44.3 kN/m	(distributed over 1050 & 56°)
Tensile Force at Exterior Girder =	20.8 kN/m	(distributed over 1050 & 56° (barrier) and 55° (deck))

End of Bridge Deck Spans

Total Moment at Base of Parapet =	165.9 kN-m/m	(distributed over 1050/2 & 25°)
Total Moment at Exterior Girder =	128.9 kN-m/m	(transverse distributed over 1050/2 & 25° (barrier) and 20° (deck) (vertical distributed over 5500/2 & 20°)
Tensile Force at Base of Parapet =	176.4 kN/m	(distributed over 1050/2 & 25°)
Tensile Force at Exterior Girder =	112.2 kN/m	(distributed over 1050/2 & 25° (barrier) and 20° (deck))

Check Deck Capacity - at Base of Parapet - Interior Spans

Concrete Strength, f_c' =	35 MPa	
Rebar Strength, f_y =	400 MPa	
α_1 =	0.7975	
ϕ_c =	0.75	
ϕ_s =	0.9	
Bar Size =	20 M	
Bar Area =	300 mm ²	
Bar Spacing =	200 mm	
Total Steel Area, A_s =	1500 mm ²	
Steel Reduction for Tension, A_{sten} =	110.7 mm ²	
d_{top} =	0.1305 m	60 mm clear cover at the top
a =	23.9 mm	
M_f =	59.3 kN-m/m	OK

Check Deck Capacity - at Base of Parapet - End Spans

Concrete Strength, f_c' =	35 MPa	
Rebar Strength, f_y =	400 MPa	
α_1 =	0.7975	
ϕ_c =	0.75	
ϕ_s =	0.9	
Bar Size =	30 M	
Bar Area =	700 mm ²	
Bar Spacing =	100 mm	
Total Steel Area, A_s =	7000 mm ²	
Steel Reduction for Tension, A_{sten} =	441.1 mm ²	
d_{top} =	0.1255 m	60 mm clear cover at the top
a =	112.8 mm	
M_f =	163.2 kN-m/m	REVISE Close enough M_f = 165.9kN-m/m

APPENDIX E Parametric Bridge Study

The 36 m bridge designed using the simplified methods of CAN/CSA-S6-00 were modeled in three dimensions using STAAD.Pro 2005™. A total of 10 models were created, four used for the four different stud cluster spacing with infinitely rigid shear connection, and additional four to account for the experimental stud cluster stiffness, and the remaining models to assess the upper bound of the Serviceability Limit State of no shear connection. Data collected from the models included the tensile stress of the bottom flanges at midspan, deflection at midspan and the first frequency of vibration.

The model used four node plate elements to represent the deck and plate girder web. Beam elements were used for the top and bottom flanges, in addition to the diaphragms and plan bracing. The connections of the diaphragms and plan bracing were modeled with an offset from the flanges to represent a typical connection detail. The shear connection of the stud cluster was modeled with a rigid beam element with no density so as not to affect the frequency calculations, since the model with the stud clusters spaced at 300 mm had more elements than the other models. The number of plates in all the models was 4200, and the beam elements totalled 1522.

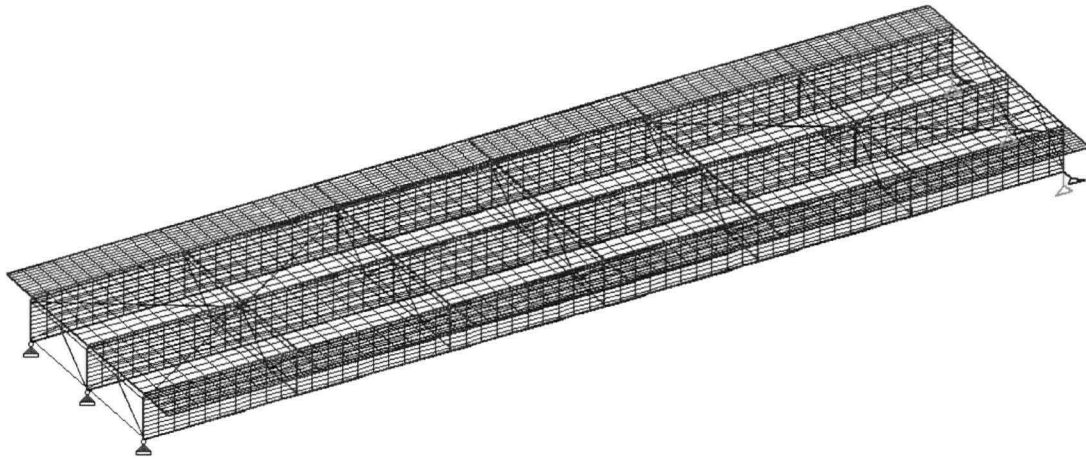
Boundary conditions were pinned at one support and expansion at the opposite end. The isotropic properties used in the model are consistent with CAN/CSA-S6-00 and are summarized in the following table.

Table E-1 Finite Element Mechanical Properties

	Elasticity (MPa)	Possion Ratio	Density (kN/m³)
Steel	200000	0.3	77
Concrete	24648	0.2	24

The following figure shows the typical finite element model layout.

Figure E-1 Typical Finite Element Bridge Model



An average stud cluster linear spring stiffness of 1100 kN/mm was chosen and used for all stud clusters in both horizontal directions, independent of their number of studs, consistent with the results from the push tests. Consistent with the requirements of CAN/CSA-S6-00, no additional stiffness from the parapets was included in the finite element models. Two three-dimensional renderings of the typical model are provided, one from above the deck and one looking at the soffit.

Figure E-2 Typical Finite Element Model Perspective from Above the Deck

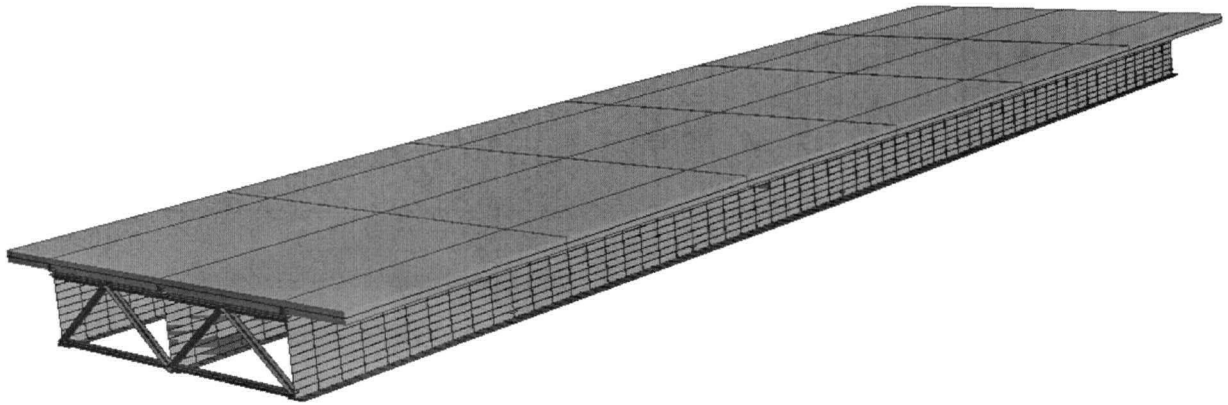
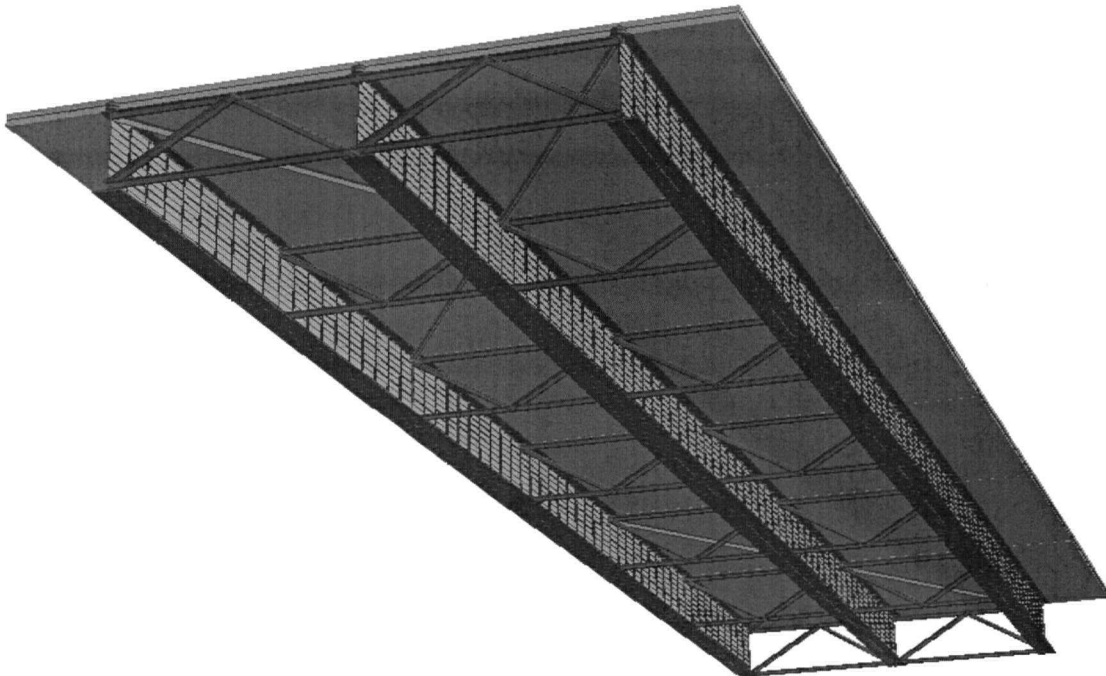


Figure E-3 Typical Finite Element Model Perspective from Below the Soffit



The superstructure was loaded in STAAD.Pro 2005, considering 2 and 3 design lanes, with the trucks orientated to produce the largest effect on the exterior girder at midspan, recognizing that other load conditions exist and that the largest force effect due to live load is not at midspan. The truck load was applied to the deck as point loads, neglecting load factors and dynamic load

allowance in the model, since they were applied after. The governing live load configuration was found to be three lanes without lane loading.

Figure E-4 Finite Element Model Two Lanes Loaded

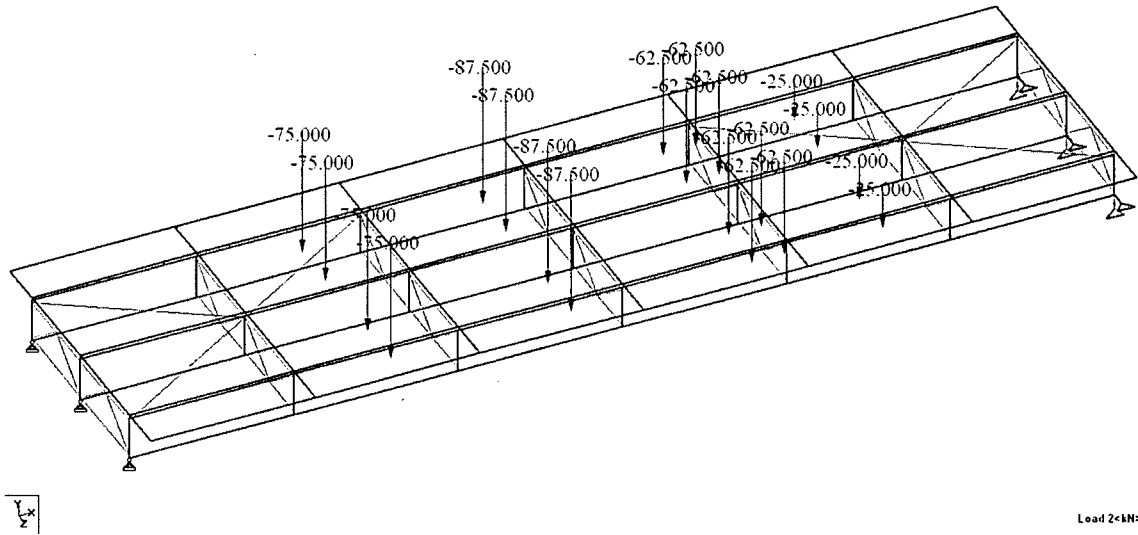
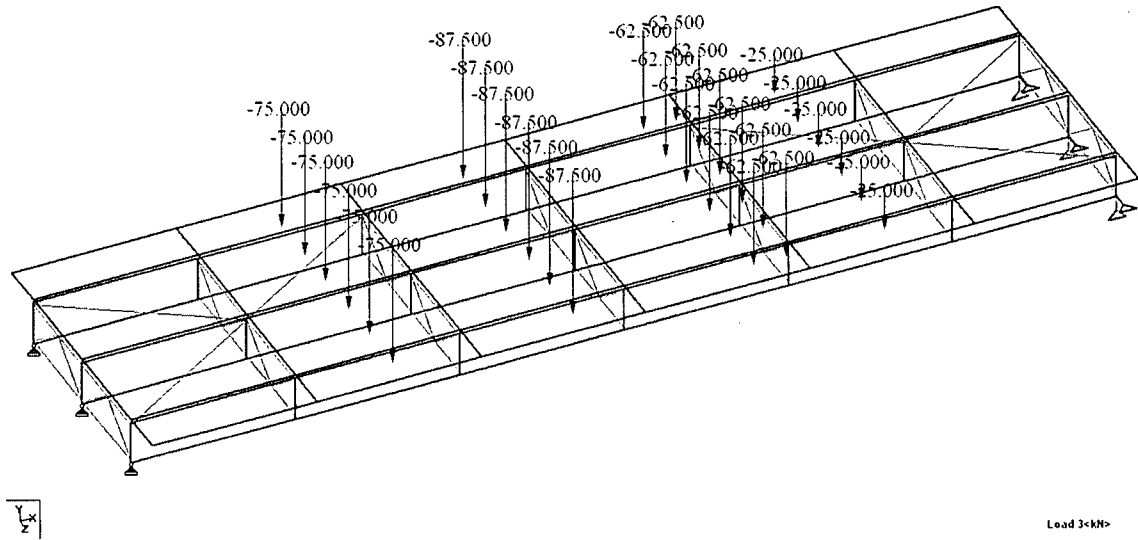
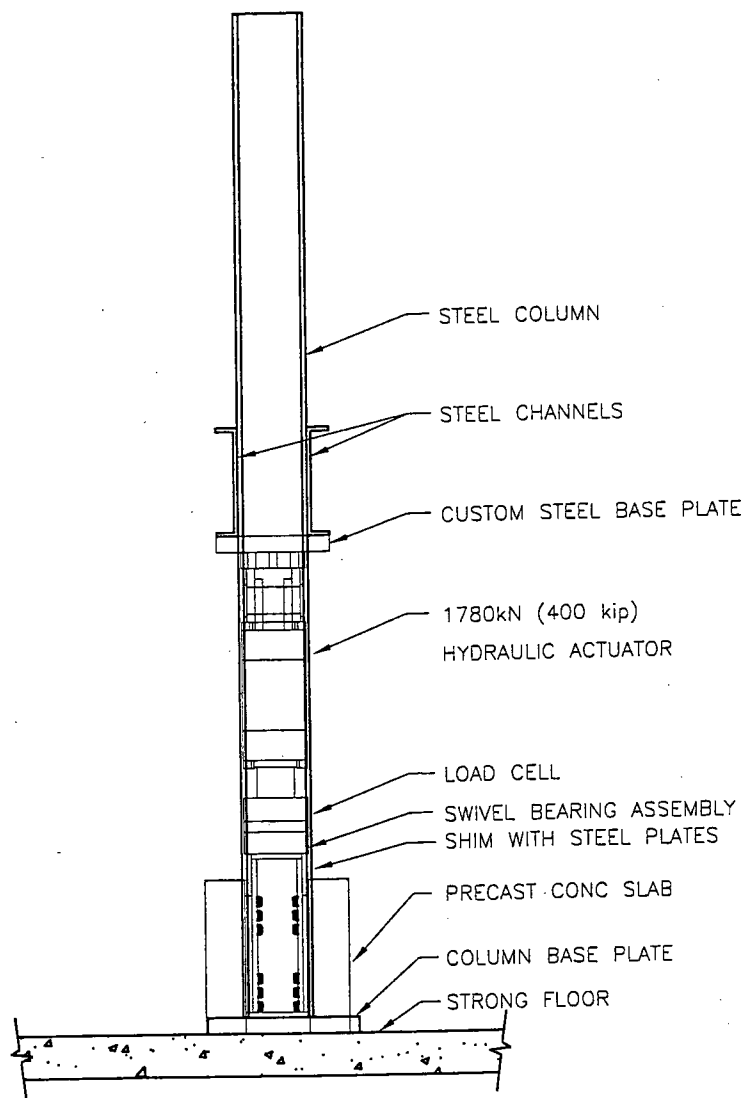


Figure E-5 Finite Element Model Three Lanes Loaded

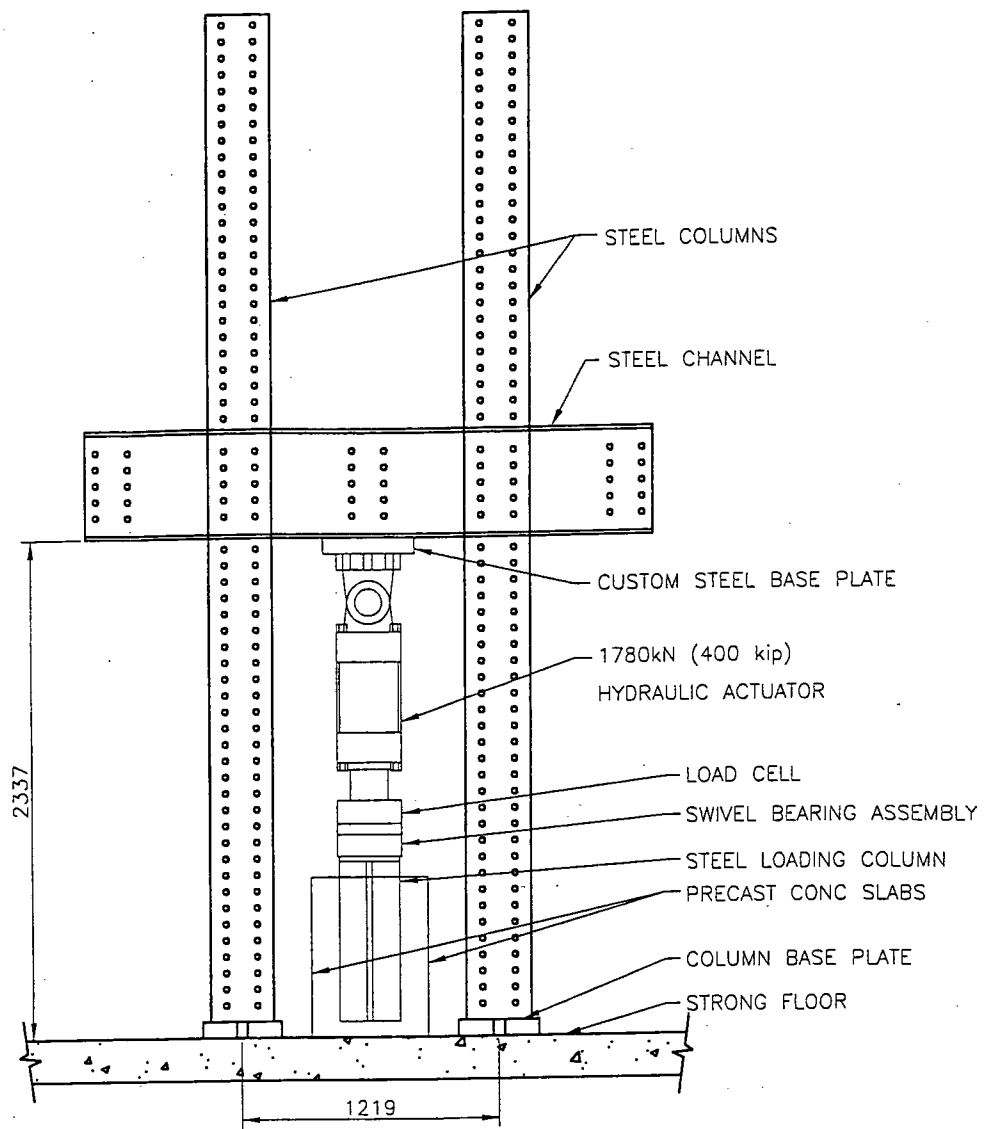


APPENDIX F Drawings

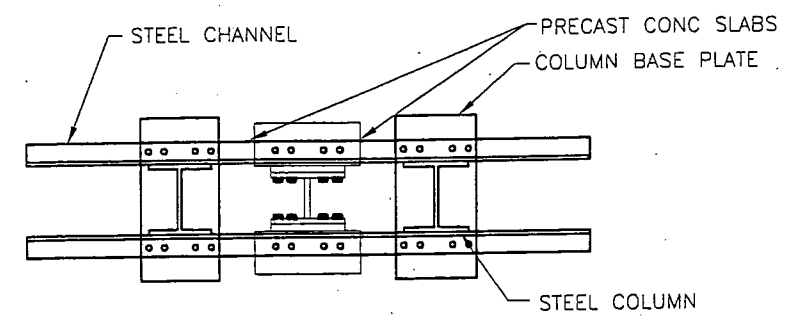
Drawings referenced throughout this document are found under cover of this Appendix.



SIDE



FRONT



TOP

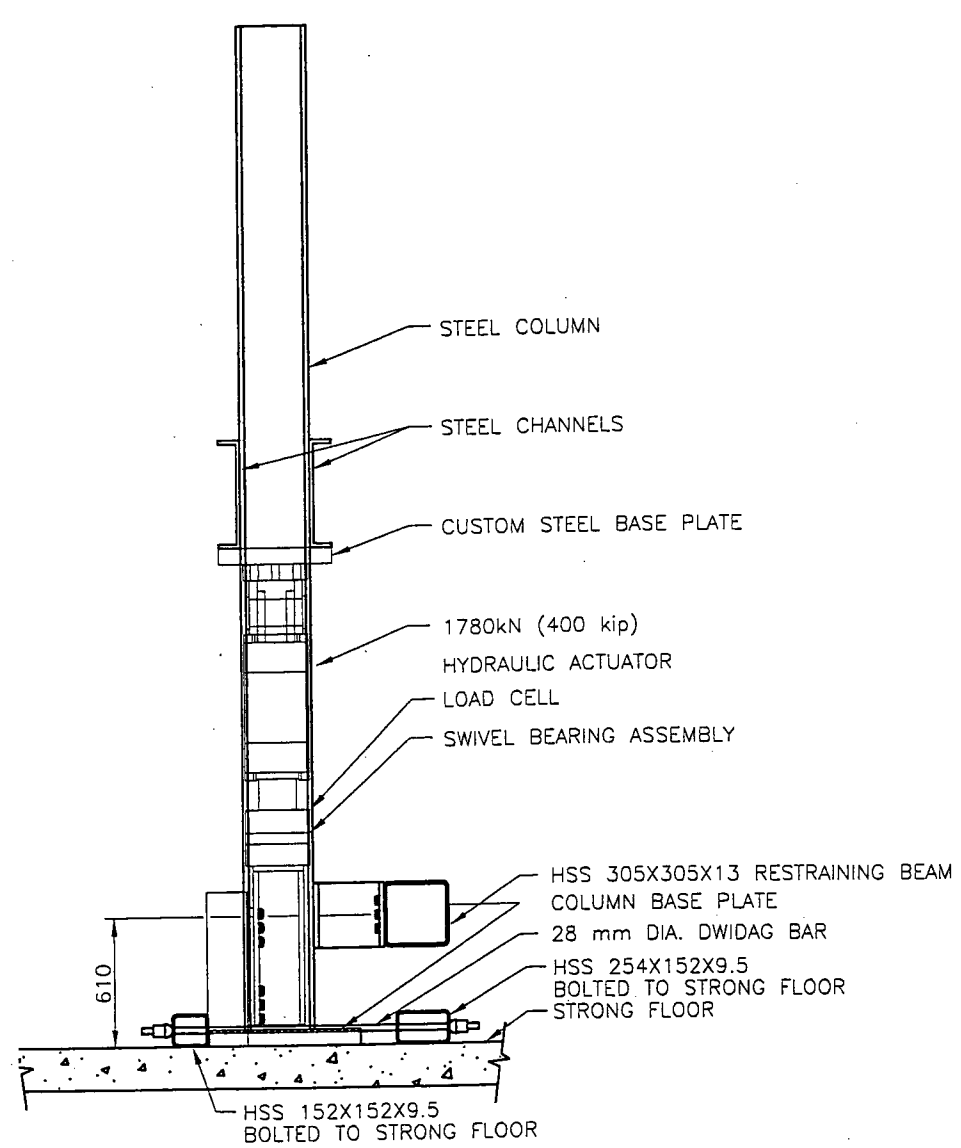
HYDRAULIC ACTUATOR NOT SHOWN FOR CLARITY

NOTES:
 INTERFACE BETWEEN STEEL SLAB AND CONCRETE PANEL TO BE GREASED WITH PETROLEUM JELLY.
 BASE OF CONCRETE PANEL TO BE BEDDED ON HYDROSTONE.

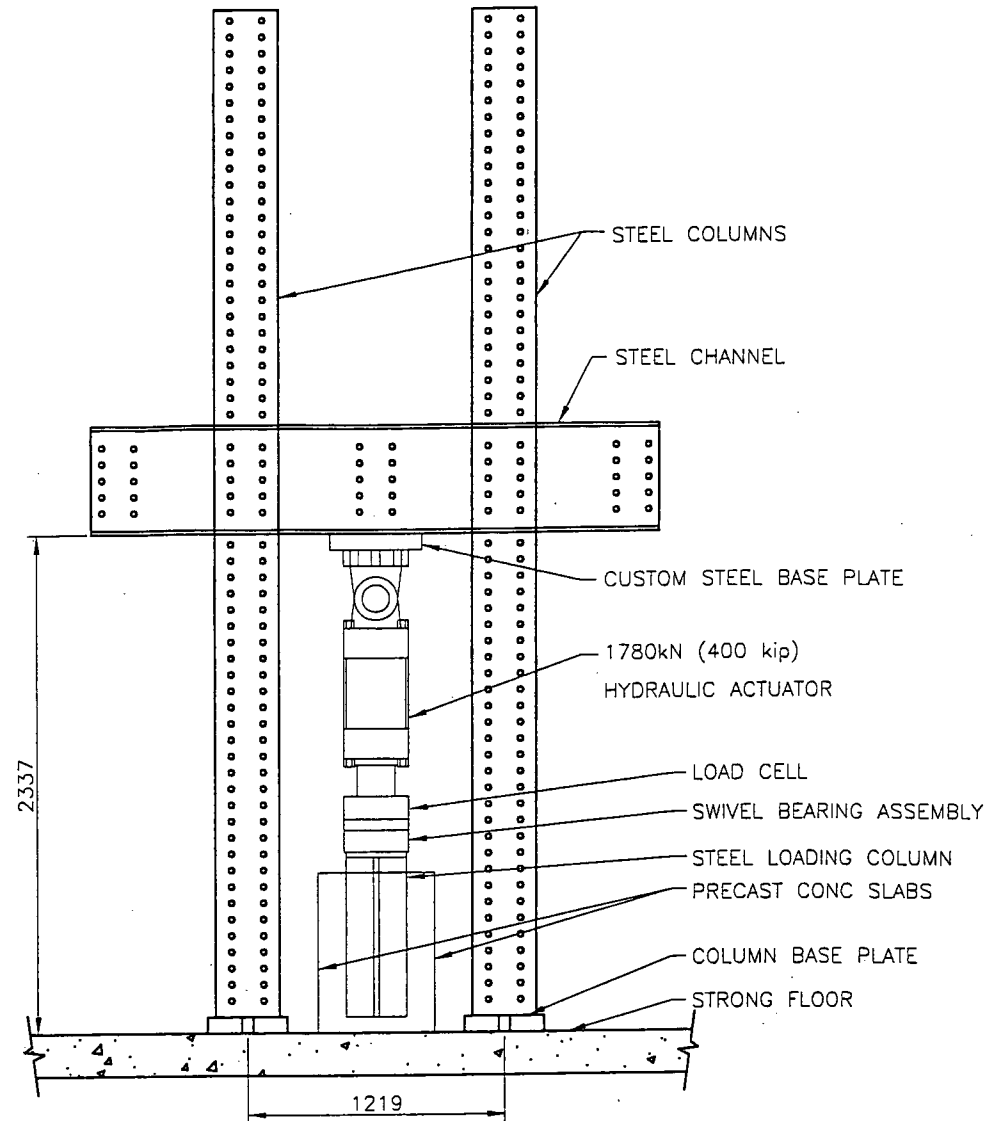
No.	Date	Revision	Dr.	Ch.

UBC
 PUSH TEST EXPERIMENT
 SYMETRICAL SETUP

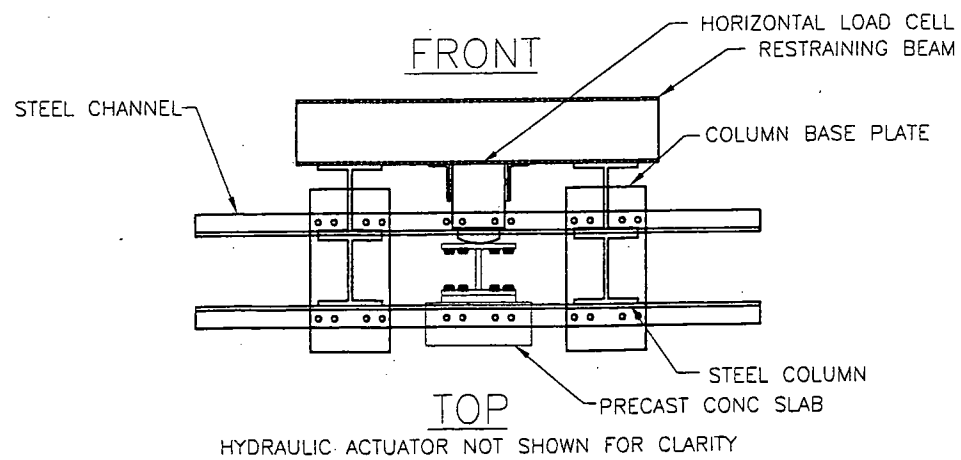
DESIGN: KEL	DATE: OCT 28/03
DRAWN: KEL	FILE:
CHECKED:	TASK:
SCALE:	DRAWING No. 1 REV.



SIDE



FRONT



TOP

NOTES:

INTERFACE BETWEEN STEEL SLAB AND CONCRETE PANEL TO BE GREASED WITH PETROLEUM JELLY.

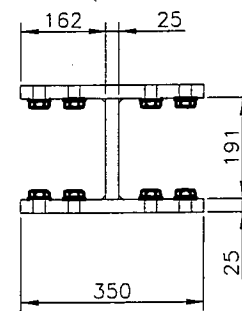
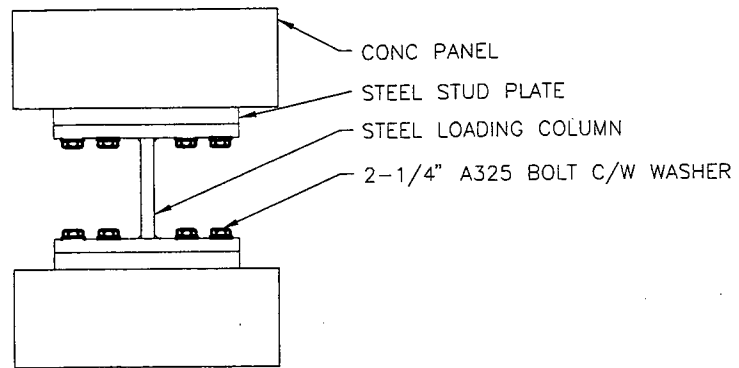
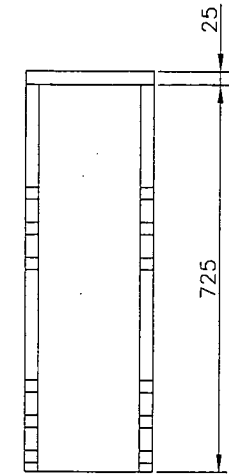
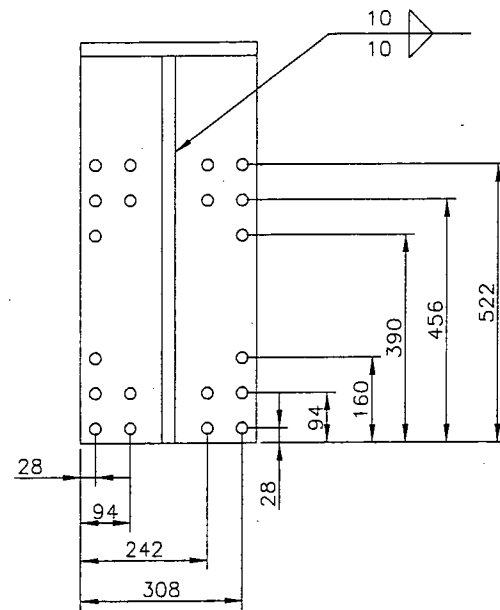
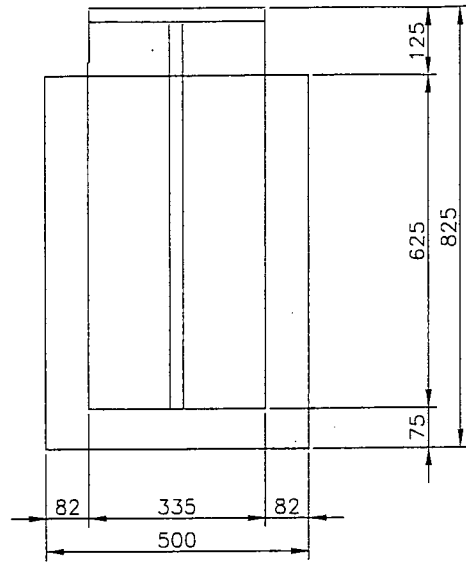
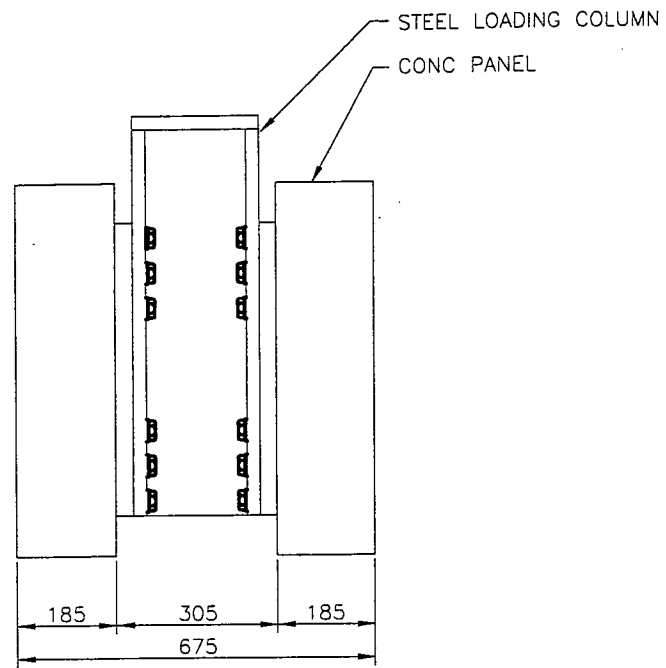
BASE OF CONCRETE PANEL TO BE BEDDED ON HYDROSTONE.

No.	Date	Revision	Dr.	Ch.

UBC

PUSH TEST EXPERIMENT
UNSYMMETRICAL SETUP

DESIGN: KEL	DATE: OCT 28/03
DRAWN: KEL	FILE:
CHECKED:	TASK:
SCALE:	DRAWING No. 2 REV.

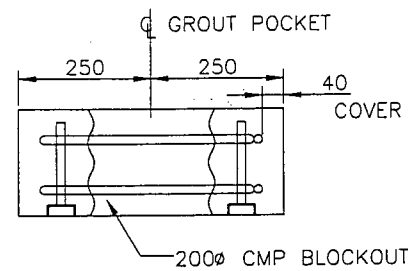
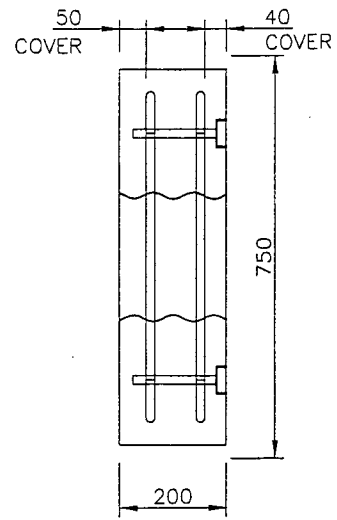
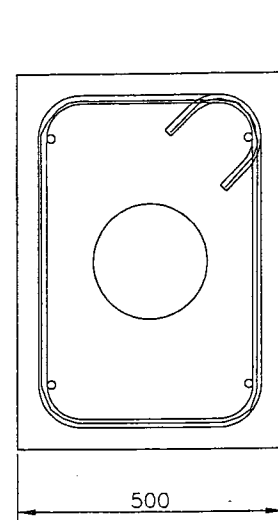


NOTES:
 CONCRETE SHALL HAVE THE FOLLOWING PROPERTIES;
 $f_c' = 35\text{MPa}$
 MAX AGG = 19mm
 AIR CONTENT = $6 \pm 1\%$
 STEEL PLATE SHALL BE GRADE 350A.

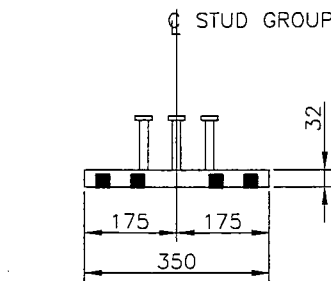
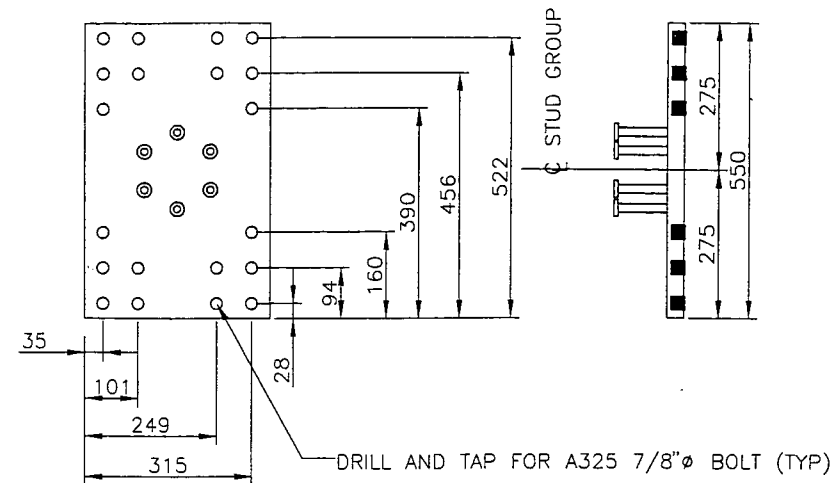
PUSH TEST SPECIMEN

STEEL LOADING COLUMN

				UBC		DESIGN: KEL	DATE: OCT 28/03	
				PUSH TEST EXPERIMENT SPECIMEN & LOADING COLUMN		DRAWN: KEL	FILE:	
						CHECKED:	TASK:	
						SCALE:	DRAWING No. 3 REV.	
No.	Date	Revision	Dr.	Ch.				



PRECAST CONCRETE PANEL



STEEL STUD PLATE

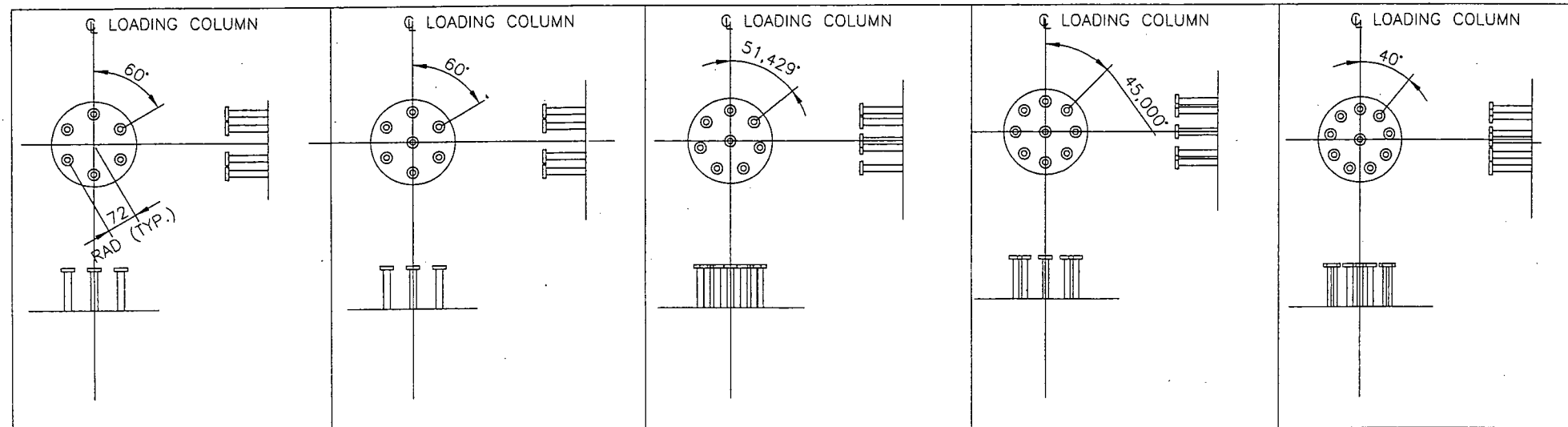
TYPICAL STUD GROUP SHOWN

NOTES:

CONCRETE SHALL HAVE THE FOLLOWING PROPERTIES;
 $f_c' = 35\text{MPa}$
 MAX AGG = 19mm
 AIR CONTENT = $6 \pm 1\%$

STEEL PLATE SHALL BE GRADE 350AT.

STUDS TO BE NELSON STUDS WITH 16 DIAMETER AND 100 LONG AND COMPOSED OF MILD STEEL.



6 STUDS

7 STUDS

8 STUDS

9 STUDS

10 STUDS

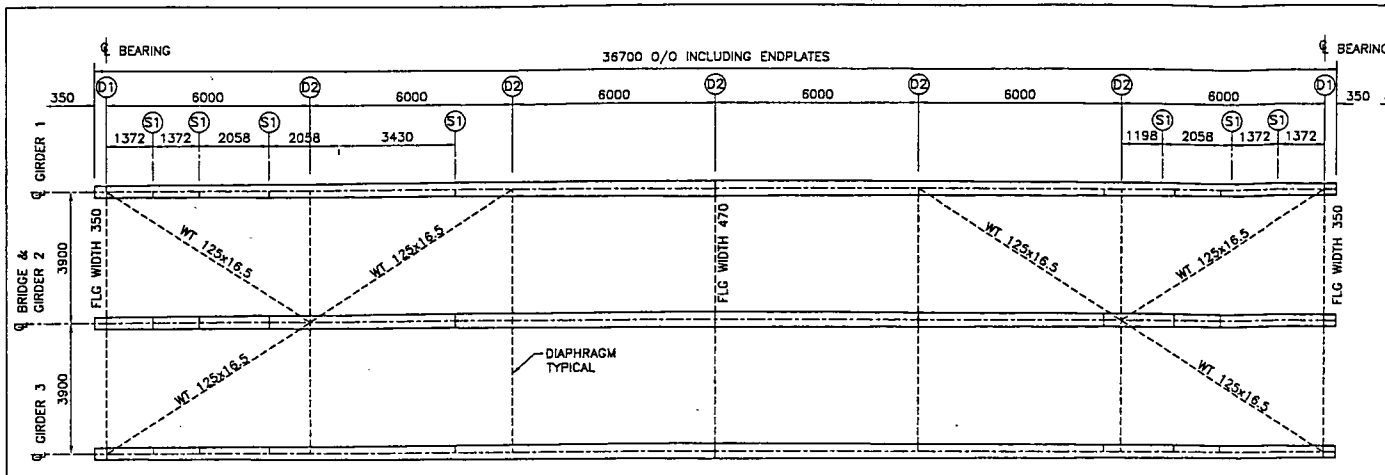
SHEAR STUD LAYOUT

No.	Date	Revision	Dr.	Ch.

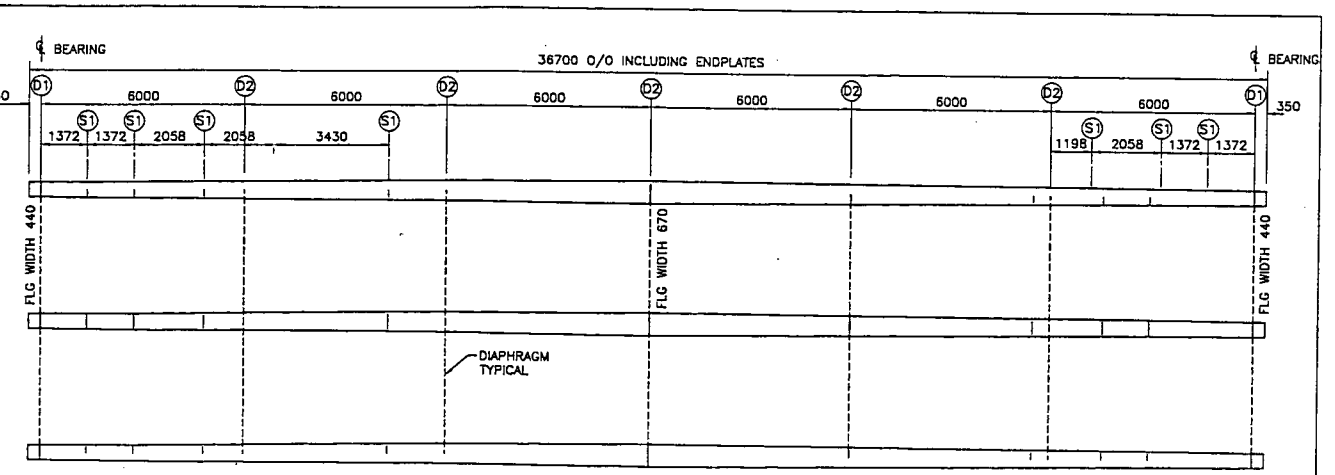
UBC

PUSH TEST EXPERIMENT
 CONCRETE PANEL & STUD PLATE

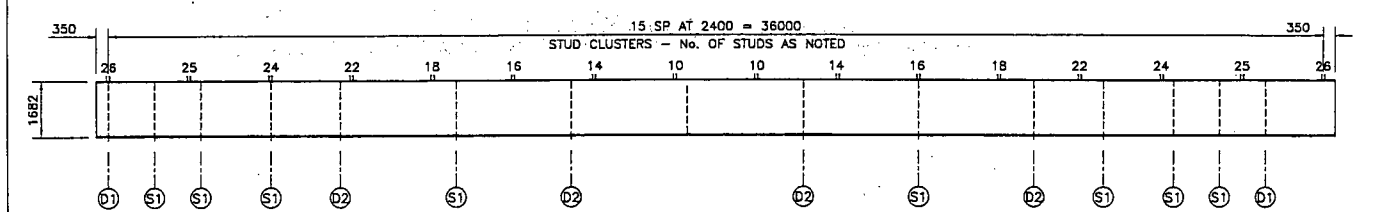
DESIGN: KEL	DATE: OCT 28/03
DRAWN: KEL	FILE:
CHECKED:	TASK:
SCALE:	DRAWING No. 4 REV.



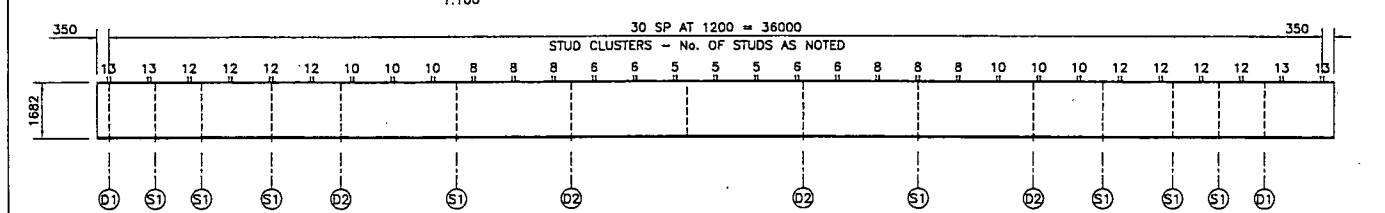
GIRDER PLAN - TOP FLANGE
1:100



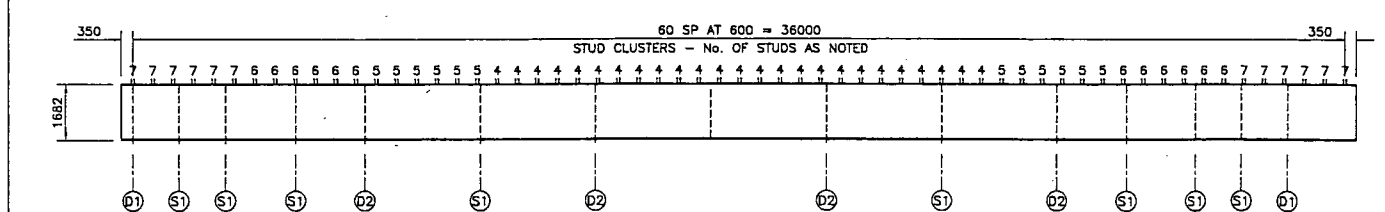
GIRDER PLAN - BOTTOM FLANGE
1:100



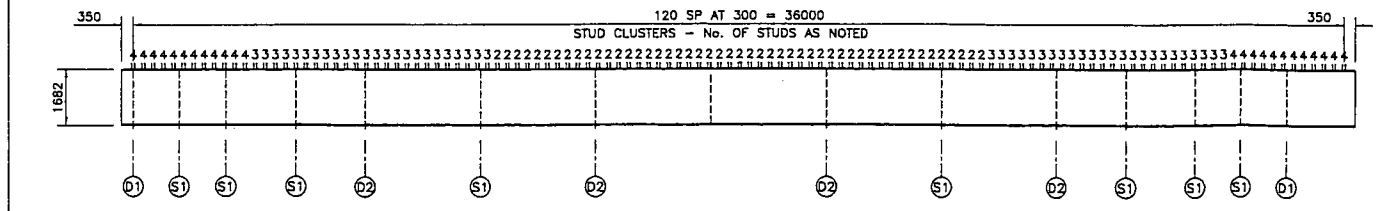
2400 mm CLUSTER SPACING GIRDER ELEVATION - 155 STUDS FROM BEARING TO MIDSPAN
1:100



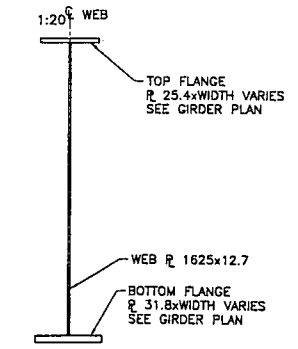
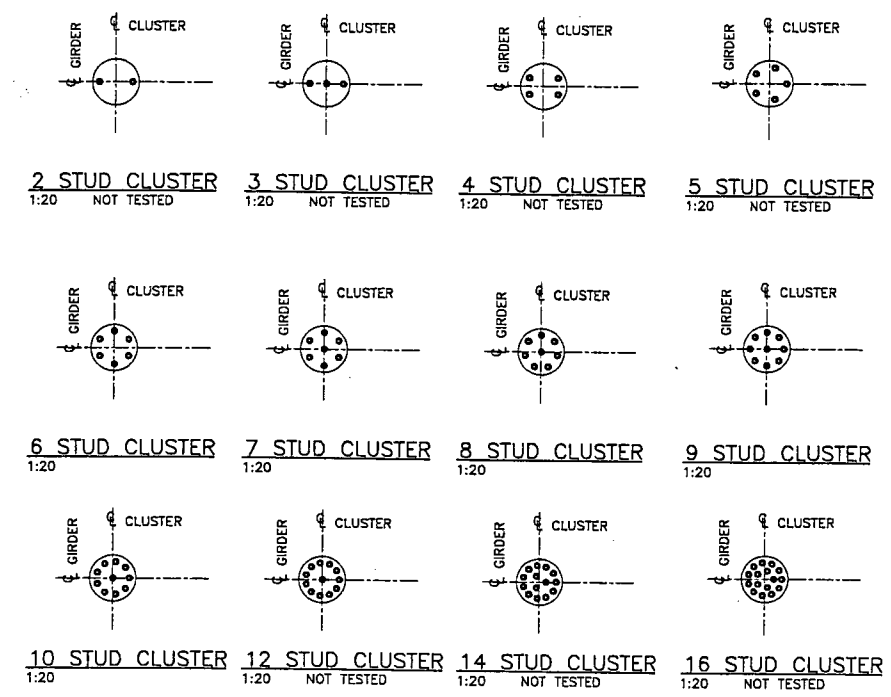
1200 mm CLUSTER SPACING GIRDER ELEVATION - 145 STUDS FROM BEARING TO MIDSPAN
1:100



600 mm CLUSTER SPACING GIRDER ELEVATION - 156 STUDS FROM BEARING TO MIDSPAN
1:100



300 mm CLUSTER SPACING GIRDER ELEVATION - 168 STUDS FROM BEARING TO MIDSPAN
1:100



GIRDER SECTION
1:20

STRUCTURAL STEEL NOTES

- ALL STEEL SHALL CONFORM TO CSA CAN3-G40.20M AND G40.21M, GRADES AS FOLLOWS:
GIRDERS - GRADE 350AT CATEGORY 3.
PLATES AND STIFFENERS - GRADE 350A.
ROLLED SECTIONS - GRADE 350A.
- SHEAR STUDS SHALL CONFORM TO ASTM A108 GRADE 1020.

No.	Date	Revision	Dr.	Ch.

UBC		DESIGN: KEL	DATE: OCT 28/03
SUPERSTRUCTURE		DRAWN: KEL	FILE:
STEEL GIRDER AND STUD CLUSTER ARRANGEMENT		CHECKED: TASK:	TASK:
SCALE:		DRAWING No.	5 REV.